Cellular and Molecular Mechanisms of Zebrafish Fin Regeneration

Stephanie McMillan

A Thesis submitted to the

Faculty of Graduate and Postdoctoral Studies

in partial fulfillment of the requirements for the

Doctorate in Philosophy degree in Cellular and Molecular Medicine

Department of Cellular and Molecular Medicine

Faculty of Medicine

University of Ottawa

Authorization for the Use of Papers that have been Previously Published in Scientific Journals.

Publication #1: Regeneration of Breeding Tubercles on Zebrafish Pectoral Fins Requires Androgens and Two Waves of Revascularization.

Hello, my name is Stephanie McMillan, I am first author on the following article published in Development:

McMillan, S. C., Xu, Z. T., Zhang, J., Teh, C., Korzh, V., Trudeau, V. L. and Akimenko, M. A. 2013. Regeneration of Breeding Tubercles on Zebrafish Pectoral Fins Requires Androgens and Two Waves of Revascularization. *Development* 140, 4323-4334.

I am writing today to ask for permission to publish this article as a part of my Ph.D. thesis. This article will be fully referenced as being already published in Development.

Thank you in advance for your time,

Sincerely,

Stephanie McMillan

Dear Stephanie,

Thank you for your permission enquiry. Requests to use figures or full paper in PhD dissertations are granted with no charge. However, since authors retain copyright of their articles, they are free to reproduce material from their own work in other publications, without the need to obtain permission from us separately.

I hope that this helps but please don't hesitate to contact us if we can be of any further assistance. We wish you the best of luck with your thesis.

Kind regards,
Sam

Samantha Arnold
Permissions | The Company of Biologists
Bidder Building, Station Road, Histon, Cambridge, CB24 9LF, UK
T: +44 (0) 1223 632867| permissions@biologists.com | www.biologists.com

Publication #2: Pectoral Fin Breeding Tubercle Clusters: A Method to Determine Zebrafish Sex.

Ballen, Karen February 5, 2016 at 5:22 PM

To: Stephanie McKay

RE: Permission to reuse article for Ph.D. thesis.

BK

Dear Stephanie:

Copyright permission is granted for this request.

Kind regards,

Karen Ballen
Manager, Reprints and Permissions

To: Ballen, Karen
Subject: Permission to reuse article for Ph.D. thesis.

To whom it may concern,

My name is Stephanie McMillan, I am writing to request permission to publish the following article in my Ph.D. Thesis:
"McMillan SC, Geraudie J, Akimenko MA. 2015. Pectoral fin breeding tubercle clusters: A method to determine zebrafish sex. Zebrafish 12(1):121-3"
This article will be fully referenced as being already being published in the journal Zebrafish.
Thank-you in advance for your time,

Sincerely,

Stephanie McMillan

Abstract

During fin regeneration, a blastema, a group of de-differentiated cells, forms underneath the wound epidermis. As regeneration proceeds, cells leave the proximal blastema and enter the differentiation zone. Adjacent to the differentiation zone, a subset of cells in the basal epidermal layer (BEL) express *sonic hedgehog a* (*shha)*. Cells that come in contact with BEL differentiate into osteoblasts and joint cells, enabling the formation of bone segments at the end of each fin ray. Generally, fin regeneration occurs similarly in males and females. However, breeding tubercles (BT), keratinized epidermal structures on the male pectoral fin, result in regenerative differences when compared to females. In this thesis, three aspects of zebrafish fin regeneration were studied: 1) Cell lineage tracing of *shha*-expressing cells in the caudal fin regenerate; 2) The differentiation of joint cells and osteoblasts in the caudal fin regenerate; 3) Regeneration of pectoral fin BTs. Studies on caudal fin regenerates suggest osteoblasts and joint cells originate from a common cell lineage, but are committed to different cell fates. Joint cells follow a genetic pathway in which *evx1* occurs downstream or parallel to *hoxa13a* and upstream of *pthrp1*. In the absence of Evx1, presumptive joint cells are committed to an osteoblast cell fate. Furthermore, joint cells do not regenerate following laser cell ablation, suggesting joint cell differentiation occurs only at specific intervals during osteoblast regeneration. Collectively, these results suggest a mechanism for joint cell differentiation during caudal fin regeneration. Studies on pectoral fins indicate androgens induce and estrogens inhibit BT formation. BT regeneration in males and androgen-treated females follows the initiation of revascularization, but occurs concomitantly with a novel second wave of angiogenesis. The inhibition of angiogenesis in androgen-treated females prevents BT formation. Altogether, these results suggest the growth and regeneration of BTs requires a

hormonal stimulus and the presence of an additional blood vessel network naturally found in males. In conclusion, these studies have increased the overall knowledge of key aspects of zebrafish fin regeneration. A gain in understanding zebrafish regeneration provides a basis in which treatments can be developed to induce regeneration in species with limited regenerative capabilities.

Table of Contents

List of Tables

List of Figures

List of Abbreviations

4-OHT	4-hydroxy-tamoxifen
AR	Androgen Receptor
B	Blastema
BAC	Bacterial Artificial Chromosome
BMP	Bone Morphogenic Protein
bp	base pairs
BF	Brightfield
BT	Breeding Tubercles
CCAC	Canadian Council on Animal Care
cmlc2	*cardiac myosin light chain 2*
col10a1a	*collagen 10a1*
CRISPRs	Clustered Regularly Interspaced Short Palindromic Repeats
cx43	*connexin43*
DAPI	4',6-diamidino-2-phenylindole
DHT	5α-dihydrotestosterone
dkk1b	*dickkopf WNT signaling pathway inhibitor 1b*
dlx5a	*distal-less homeobox 5a*
dot	days of treatment
dpa	days post amputation
dpf	days post fertilization
dpi	days post injection
dpl	days post laser ablation
dpt	days post treatment

E2	17β-estradiol
EGFP	enhanced green fluorescent protein
ENU	*N*-ethyl-*N*-nitrosourea
EtOH	Ethanol
evx1	*even skipped homeobox 1*
Fgf	Fibroblast growth factor
FISH	Fluorescence *In Situ* Hybridization
fli1a	*friend leukemia integration 1a*
fr	fin ray
GFP	Green Fluorescent Protein
Hh	Hedgehog
hox	homeobox
hpa	hours post amputation
hpf	hours post fertilization
hr	hemiray
IHH	Indian Hedgehog
ihha	*indian hedgehog a*
Ins	Insulator
ISH	*In situ* hybridization
kb	kilobases
KR	Killer Red
lef1	*lymphoid enhancer-binding factor 1*
MI	Mouse Intron

mmp9	*matrix metallopeptidase 9*
MO	Morpholino
msxb	*muscle segment homeobox b*
osc	*osteocalcin*
osn	*osteonectin*
osx	*osterix*
PAS	Periodic acid–Schiff
Pcna	Proliferating cell nuclear antigen
PCR	Polymerase Chain Reaction
ptc-1	*patched-1*
pthr	*parathyroid receptor*
pthrp	*parathyroid hormone-related protein*
qRT-PCR	Quantitative Reverse Transcription Polymerase Chain Reaction
RA	Retinoic Acid
runx2	*runt-related transcription factor 2*
Ser/Thr	Serine/Threonine
shha	*sonic hedgehog a*
T	Testosterone
Tg	Transgenic
TUNEL	Terminal Deoxynucleotidyl Transferase dUTP Nick End Labeling
ubi	*ubiquitin*

Acknowledgements

I would like to express my profound gratitude to my supervisor, Dr. Marie-Andrée Akimenko, for her supervision, encouragement, and useful suggestions throughout my project. Thank-you for accepting me into your lab; it has been a great 5 years. I am also thankful to my committee members, Dr. Catherine Tsilfidis, Dr. Valerie Wallace, and Dr. Marc Ekker for their valuable support and suggestions throughout my studies.

I would also like to thank past and present members of the Akimenko and Ekker Labs. In particular, I would like to thank Jing Zhang for her positivity and encouragement during those stressful times in the lab. I would also like to thank Robert Lalonde, Marissa Northorp, Eileen Hue-Phan, Hannah Nicholas, Samuel MacDonnell, Serina Khater, Alyssa Kositpaiboon, Yan Li, Tim Xu, Natasha Bougie, Remi Blais, Lei Huang, Alisar Alhajj, Andie Godo, Yan Li, Derek Sheppard, Qing ming Qu, Ali Khatib, Pascal Couture for being such wonderful co-workers and friends.

I would also like to send out a special thanks to my parents, Neil and Kathryn McMillan, and my sister, Victoria Robertson, for their love and support throughout my studies. Finally, I would like to express my love and gratitude to my husband, Paul McKay, and my son, Oliver McKay, for their love and support throughout my Ph.D. Without them, finishing this Ph.D. would not have been possible.

Chapter 1: General Introduction

1.1 Regeneration

Regeneration, a process in which structures that have been lost or damaged are replaced (Morgan et al., 1901; Sunderland, 2010), is highly variable among organisms. Among invertebrates, planarians and hydra can easily regenerate entire body parts (Géraudie and Ferretti, 1998; Brockes and Kumar, 2002), while C. elegans and Drosophila possess only limited regenerative capabilities (Sustar and Schubiger, 2005; Bryant, 1971; Yanik et al., 2004). Among vertebrates, amphibians and fishes easily regenerate lost appendages (for a reviews, see Poss et al., 2003; Akimenko et al., 2003; Han et al., 2005), while humans and mice possess only the restricted ability to regenerate the liver and infant digit tips (Borgens, 1982; Yokoyama et al., 1953; Hata et al. 2007; Yoshizato 2007; Han et al., 2005). The inability of humans to regenerate various body parts has resulted in a strong desire to elucidate the mechanisms underlying the regenerative abilities observed in capable organisms. Currently, several vertebrate, invertebrate, and plant model organisms are being used to study regeneration. The most extensively studied organisms being amphibian limbs, planarians, hydra, and fish fins. This study focuses on the regeneration of zebrafish fin rays.

1.2 Regeneration of Fish Fins

Since 1786 it has been known that adult fish could regenerate their fins following amputation (Broussonet, 1786; Morgan, 1901; Sunderland, 2010). Since then, fin regeneration studies have been performed on a diverse number of fishes, including goldfish (*Carassius auratus*) (Santamaria *et al.,* 1992, Santamaria *et al* ., 1996; Mari-Beffa *et al.,* 1996), tilapia (*Tilapia mossambica)* (Kemp and Park, 1970; Santamaria and Becerra, 1991;

Santamaria *et al.,* 1992; Kemp and Park, 1970), trout (*Oncorhynchus mykiss)* (Alonso *et al.,* 2000), minnows (*Fundulus*) (Nabrit, 1929; Nabrit, 1931), carp (*Cyprinus carpio*) (Böckelmann *et al.,* 2009), *Polypterus* (Cuervo *et al*., 2012), medaka (*Oryzias latipes*) (Katogi *et al*., 2004) and zebrafish (*Danio rerio*) (Géraudie *et al*., 1994; for reviews, see Poss *et al*., 2003; Akimenko *et al.,* 2003). These fish all possess the ability to regenerate their fins following amputation. However, the time required to replace the lost structure varies between species (Akimenko *et al.,* 2003). The observed variability in regeneration time is likely due to changes in temperature. For example, zebrafish caudal fin regeneration occurs nearly twice as fast at 33°C than at 25°C (Johnson and Weston, 1995). Currently, zebrafish are the most widely studied fin regeneration models (Géraudie *et al*., 1994; for reviews, see Poss *et al*., 2003; Akimenko *et al.,* 2003; Wehner and Weidinger, 2015).

1.3 Structures of the Zebrafish Fish Fins

Zebrafish exhibit two sets of paired fins, pectoral and pelvic, and three unpaired fins, dorsal, anal, and caudal. These fins all possess the same overall skeletal structure, which consists of an endoskeleton and an exoskeleton. The endoskeleton is composed of a set of endochondral bones that are not visible and set inside the body. The exoskeleton is visible and consists of intramembranous or dermal fin rays that form *via* the direct mineralization of the bone matrix, and actinotrichia, two rows of unmineralized fibrils that are located within the two most distal fin ray segments (Akimenko *et al.,* 2003). The exoskeleton of the caudal fin is composed of approximately 18 dermal bony fin rays, or lepidotrichia, that occupy a subepidermal position and are connected by interray tissue (Figure 1.1 A) (Akimenko *et al.,* 2003). Each fin ray bifurcates periodically along the proximal-distal axis, with the exception of the most lateral rays, to form two sister rays

(Figure 1.1 A) (Akimenko *et al*., 2003; Poss *et al*., 2003). Furthermore, each fin ray is made up of two opposed hemirays that are divided into segments by joints and surrounded by a monolayer of osteoblasts (Figure 1.1 A', A'') (Knopf *et al.,* 2011; Borday *et al.,* 2001). Between each ray, and in the intraray spaces, are nerve fibers, pigment cells, and fibroblast-like cells (Figure 1.1 A'') (Poss *et al*., 2003; Murciano, 2002; Mari-Beffa and Murciano, 2010). Flanking and centered in each fin ray are two veins and a single artery, respectively (Figure 1.1 A'') (Huang *et al*., 2003). The veins are connected via interray vessels and veins are connected to arteries through intervessel commissures (Huang *et al*., 2003). In zebrafish, fin ray growth and regeneration is established through the periodic distal addition of new bone segments, which are separated by joints (Johnson and Bennett, 1999; Iovine and Johnson, 2000). Interestingly, amputations that include the non-visible endoskeleton of the zebrafish caudal fins possess a reduced ability to regenerate (Shao *et al*., 2009). However, caudal amputations at the level of the dermal fin rays regenerate easily and do not display any regenerative defects, even after multiple amputations (Azevedo *et al.,* 2011). Consequently, amputations at the level of the dermal fin rays are the most widely used in caudal fin regeneration experiments.

1.4 Caudal Fin Regeneration: Wound Healing, Blastema Formation, and Regenerative Outgrowth

Following amputation, regeneration occurs through a series of three steps: wound healing, blastema formation, and regenerative outgrowth to reform the lost fin (Figure 1.1 B-B''). During wound healing, epidermal cells migrate to cover the wound (Figure 1.1 B). Subsequently, a blastema, a group of de-differentiated cells form under the wound epidermis and above each fin ray (Figure 1.1 B'). As regeneration proceeds cells leave the blastema, differentiating into the multiple cell types that will reform the lost fin (Figure 1.1

B’’). Longitudinal sections through a single fin ray enables the visualization of various structures throughout each step of fin regeneration, including the blastema, lepidotrichia, osteoblasts, and the basal epidermal layer (Figure 1.1 C-C’). Each of these three steps can be followed through the observation of a single ray (Figure 1.1 C-C’, 1.2 A).

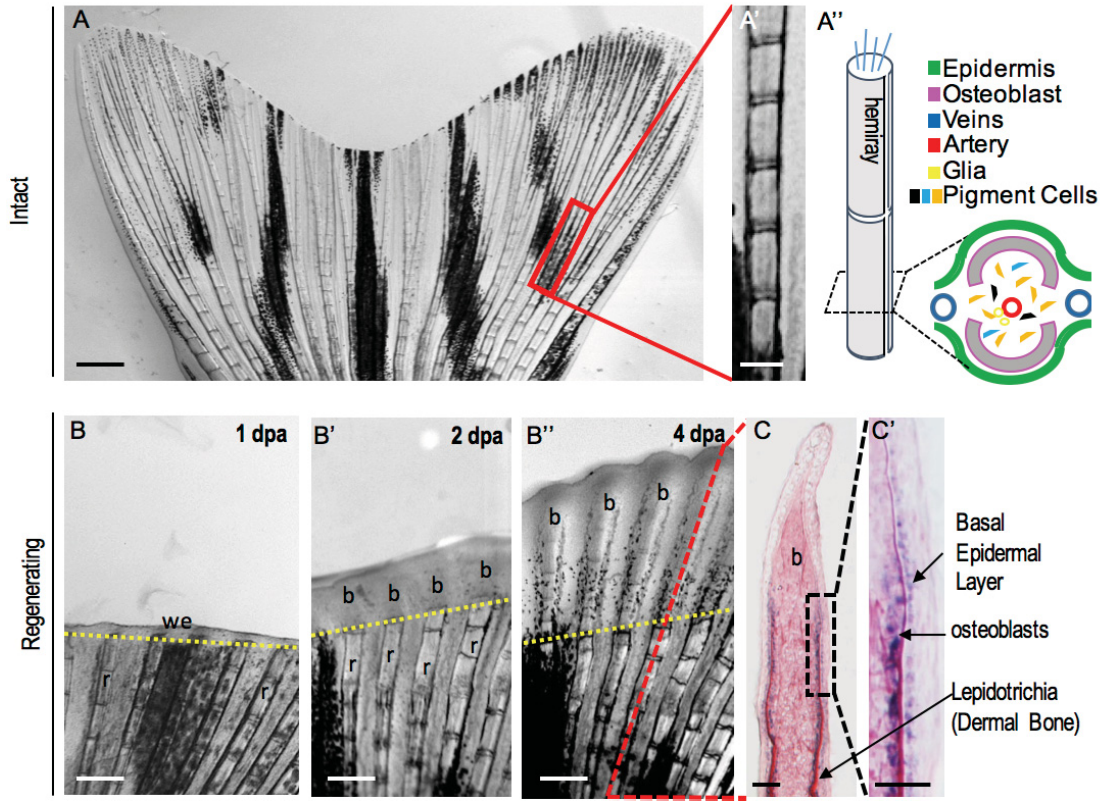

Figure 1.1: Image illustrating the intact and regenerating adult caudal fin. (A) The intact caudal fin consists of dermal fin rays that branch into two sister rays with the exception of the most lateral rays. (A') Magnification of one of those fin rays (red box) illustrates fin rays are formed of successive bone segments separated by joints. (A'') A cartoon of the two most distal fin ray segments illustrates that the dermal fin rays are comprised of two symmetrical concave hemirays. Actinotrichia, (blue lines), also appear within the two most distal fin ray segments. Cross sections of a fin ray illustrate each hemiray encloses blood vessels, nerve fibers, and a loose, vascularized connective tissue. Surrounding the hemirays is a multilayered epidermis. (B) Regeneration of the caudal fin rays (1dpa) wound healing: the epidermis covers the wound. (B') 2dpa: Blastema formation: A group of de-differentiated cells forms underneath the mature wound epidermis. (B'') Regenerative outgrowth: A group of de-differentiated/undifferentiated cells differentiate to reform the lost fin (4dpa). (C) Picrosirius red staining and *collagen, type X, alpha 1a* (*col10a1a*) *in situ* hybridization on longitudinal cryosections through the fin ray (red dotted line in B'') illustrates individual structures in the 4dpa fin regenerate. (C'). The magnification of the right hemiray (black dotted box) allows a more precise view of the basal epidermal layer and osteoblasts (stained blue for *col10a1a*), and hemirays (stained pink through Sirius red staining). Longitudinal cryosections = Jing Zhang unpublished data. b = blastema; r = ray, we = wound epidermis. Scale bars A, B-B'' = 200μm; A' = 100μm; C-C' = 50μm.

1.5 Wound Healing

During wound healing, the wound is quickly covered through the migration and rearrangement of epithelial cells, but not proliferation (Figure 1.2 A) (Poss *et al.,* 2003; Poleo *et al*., 2001; Santos-Ruiz *et al*., 2002). Following closure, the wound epidermis matures, becoming multilayered *via* continuous cell migration (Figure 1.2 A) (Poss *et al*., 2003; Poleo *et al.,* 2001; Santamaria *et al*., 1996; Nechiporuk *et al*., 2002). Once formed, the basal epidermal layer of the wound epidermis signals between itself and the underlying blastema, a process that is vital for fin regeneration (Poss *et al.* 2000; Whitehead *et al.* 2005).

1.6 Blastema Formation

During wound epidermis maturation, cells of mixed lineages up to 2 segments proximal to the amputation site migrate distally (Figure 1.2 A) (Poleo *et al*., 2001; Nechiporuk and Keating, 2002; Santos-Ruiz *et al*., 2002). These migrating cells form the blastema underneath the wound epidermis and above each fin ray (Figure 1.2 A) (Poss *et al*., 2003; Nechiporuk and Keating, 2002; Santos-Ruiz *et al.,* 2002). Several studies have shown that the pre-blastemal cells are formed through the recruitment and proliferation of de-differentiated lineage-restricted progenitor cells from the fin stump rather than multipotent stem cells. More specifically, studies using transposon-based clonal analysis have shown that the mature pigment cells, intraray glia, osteoblasts, dermal fibroblasts, endothelial cells, and epithelial cells of intact fins recapitulate their cell fates in the caudal fin regenerate (Tu and Johnson, 2011). Additional studies using transgenic reporter lines and genetic cell fate mapping have shown that following amputation osteoblasts remain lineage restricted, de-differentiating to an osteoblast progenitor-like state as they contribute

to the blastema. Subsequently, the fate restricted osteoblast progenitor cells leave the blastema, re-differentiating into the mature osteoblasts of the fin regenerate (Sousa *et al.,* 2011; Knopf *et al*., 2011). However, one study has shown that upon ablation of osteoblasts, the fin rays regenerate normally (Singh *et al.,* 2012), suggesting a transdifferentiation mechanism is triggered in an unknown cellular source. The authors propose that since intraray fibroblasts share the expression of many osteoblast markers and upregulate osteoblast commitment marker *sp7* (also known as *osterix, osx*) following osteoblast ablation, that these intraray fibroblasts represent primary candidates for an alternative source of osteoblasts (Singh *et al.,* 2012). However, the authors also suggest that there are potentially other cellular sources that are able to contribute to osteoblast regeneration (Singh *et al.,* 2012). This study contradicts the previous two studies that suggest an absence of osteoblast transdifferentiation during fin regeneration. One possibility to interpret these results is that the osteoblast ablation may not have been 100% efficient. Alternatively, transdifferentiation of osteoblasts may only occur under circumstances of extreme cell loss. For example, in mouse it has been shown that pancreatic β-cells normally regenerate via self-replication (Dor *et al*., 2004); however, following extreme loss, β-cells are replenished by duct cell or α-cell transdifferentiation (Thorel *et al.,* 2010; Xu *et al.,* 2008). To uncover the possibility of transdifferentiation under extreme cellular loss in zebrafish, cell ablations could be performed in combination with clonal analysis during caudal fin regeneration.

1.7 Molecular Regulation of Blastema Formation

During blastema formation, retinoic acid (RA) signaling is induced one to two segments proximal to the amputation plane where pre-blastemal cells proliferate and migrate distally (Blum and Begemann, 2012). At this stage, the degradation of RA, using

a transgenic line that expresses the RA degrading enzyme Cyp26a1 in a heat inducible manner, Tg(*hsp70:cyp26a1)*, inhibits proliferation of pre-blastema cells and blastema formation. Conversely, mesenchymal proliferation is increased when fish are treated with RA (Blum and Begemann, 2012). It has been suggested that the Fibroblast growth factor (Fgf) signaling pathway mediates the effects of RA signaling, as the degradation of RA results in a reduction in *fgf20a* (Blum and Begemann, 2012; Poss *et al*., 2000; Whitehead *et al.,* 2005). *fgf20a* is an Fgf family member that is initially expressed in mesenchymal cells directly underneath the wound epidermis and later expressed in the blastema (Whitehead *et al.,* 2005). Homozygous null mutants of *fgf20a* fail to form a blastema, indicating Fgf signaling is required for blastema formation. (Whitehead *et al*., 2005). Similarly, the inhibition of Fgfr1, which is expressed in pre-blastemal mesenchymal cells, inhibits mesenchymal cell proliferation and blastema formation (Poss *et al*., 2000).

Although RA signaling is required for blastema formation, it has been shown that it adversely affects osteoblast de-differentiation (Blum and Begemann, 2015). Following amputation, *aldehyde dehydrogenase 1 family member A2* (*aldh1a2*), an RA synthesizing enzyme, is excluded from osteoblasts in stump tissue (Blum and Begemann, 2012). Concurrently, mature osteoblasts one segment proximal to the amputation site upregulate Cyp26b1, an RA-degrading enzyme (Blum and Begemann, 2012). Treatments with RA have been shown to inhibit pre-osteoblast proliferation, reduce the expression of early osteoblast markers *runt domain-containing transcription factors 2a* and *2b* (*runx2a, runx2b*), and increase the expression of late osteoblast marker *osteocalcin* (*Bgp, osc*) (Blum and Begemann, 2012). In contrast, the inhibition of RA signaling through the heat shock inducible Tg(*hsp70:cyp26a1)* transgenic line, enhances *runx2a/2b* and decreases *osc*

expression (Blum and Begemann, 2012). These results indicate that the strict regulation of RA signaling is required for both osteoblast de-differentiation and proliferation during blastema formation.

1.8 Regenerative Outgrowth

Following blastema formation, regenerative outgrowth is initiated (Figure 1.2 A). During regenerative outgrowth, the blastema is subdivided into two distinct compartments: the distal blastema and the proximal blastema (Figure 1.2 A, B) (Poss *et al.,* 2003; Nechiporuk and Keating, 2002). The distal blastema, which consists of slow cycling cells, has been described as a signaling center involved in the maintenance of the highly proliferative and/or dedifferentiated state of the proximal blastema (Nechiporuk and Keating, 2002). Many signaling pathways have been elucidated that enable regenerative outgrowth during regeneration (Figure 1.2 B). For example, Fgf signaling in the distal blastema and lateral border epidermis has been shown to be required for blastema cell proliferation (Poss *et al*., 2000; Lee *et al.,* 2009). More specifically, it has been shown that the inhibition of Fgf signaling using the heat shock inducible Tg(*hsp70:dn-fgfr1*) transgenic line, inhibits blastemal proliferation in the fin regenerate (Lee *et al.,* 2005). However, the effect on proliferation is likely indirect as Fgf signaling appears inactive in the proximal blastema (Lee *et al.,* 2009). Transcriptionally dependent on Fgfr activation, *sonic hedgehog a* (*shha)* is also expressed in the lateral border epidermis, and hedgehog (Hh) signaling is required for blastemal proliferation (Laforest *et al*., 1998; Poss *et al*., 2000; Quint *et al.,* 2002). Therefore, it has been suggested that Hh signaling may mediate the effects of Fgf signaling in the proximal blastema (Figure 1.2 B) (Lee *et al.,* 2009). Similarly, Wnt/β-catenin signaling, from the distal blastema acts to positively regulate

proliferation indirectly in the proximal blastema (Figure 1.2 B) (Wehner *et al*., 2014). Through the investigation of various pathways that may mediate the effects observed in the proximal blastema, it was discovered that Hh ligands (*shha* and *indian hedgehog a* (*ihha*)) and RA synthesizing enzyme *aldh1a2* are transcriptionally regulated by Wnt signaling (Wehner *et al.,* 2014). Furthermore, the pharmacological induction of Hh signaling or RA signaling, rescues blastemal proliferation following the inhibition of the Wnt/β-catenin signaling pathway (Blum and Begemann, 2012; Stoick-Cooper *et al.,* 2007; Wehner *et al.,* 2014). In contrast, the activation of Wnt/β-catenin signaling did not rescue blastemal proliferation following the inhibition of Hh signaling using cyclopamine (Wehner *et al.,* 2014). Together, these data strongly suggest that RA signaling and Hh signaling mediate the effects of Wnt/β-catenin signaling to regulate blastemal proliferation (Figure 1.2 B). Similar to Wnt/β-catenin signaling pathways, Notch signaling has been shown to promote blastema proliferation indirectly through RA signaling (Münch *et al.,* 2013). Furthermore, the inhibition and induction of Notch signaling reduces and increases blastemal proliferation in the fin regenerate, respectively (Münch *et al.,* 2013). In addition to promoting blastemal proliferation, studies have shown that Notch gain of function results in the expansion of early osteoblast markers, a decrease in intermediate osteoblast markers, and the prevention of bone regeneration. These results indicate Notch signaling promotes the proliferation of de-differentiated blastemal cells and prevents osteoblast differentiation (Münch *et al.,* 2013).

As pre-osteoblasts leave the proximal blastema and enter the differentiation zone, it has been shown that RA levels and Notch activity decrease, enabling osteoblast differentiation (Figure 1.2 B) (Münch *et al.,* 2013). Differentiating osteoblasts have been

shown to align adjacent to the basal epidermal layer. Cells medial to the osteoblasts differentiate into actinotrichia forming cells (Zhang *et al.,* 2010) or fibroblast cells (Tu and Johnson, 2011).

1.9 Basal Epidermal Layer

Located at the border between the proximal blastema and differentiation zone, is a subset of basal epidermal cells that express *sonic hedgehog a* (*shha*), a Hh signaling ligand, its receptor, *patched-1 (ptc-1)*, *bone morphogenetic protein 2b* (*bmp2b*), and *lymphoid enhancer-binding factor 1 (lef1),* a downstream effector of Wnt/β-catenin signaling (Poss *et al*., 2000) (Figure 1.2 B). Previously, it has been shown that the *lef1* and *shha* expression domains are positioned by the opposing action of two distinct Fgf signaling branches from the basal epidermal layer (Figure 1.2 B) (Lee *et al.,* 2009; Wehner *et al*., 2014). Proximally, Fgf signaling induces *shha* and *lef1* expression; however, distally Fgf signaling induces the expression of *wnt5b*, which acts to restrict the *shha* expression domain to the border between the proximal blastema and the differentiation zone (Figure 1.2 B) (Lee *et al*., 2009). Shha signaling in the basal epidermal cell layer has been implicated in branching morphogenesis of the regenerating fin rays (Poss *et al*., 2000. Quint *et al*., 2002; Zhang *et al*., 2012). The Hh signaling pathway and branching morphogenesis are discussed in the following two sections (1.10 and 1.11, respectively).

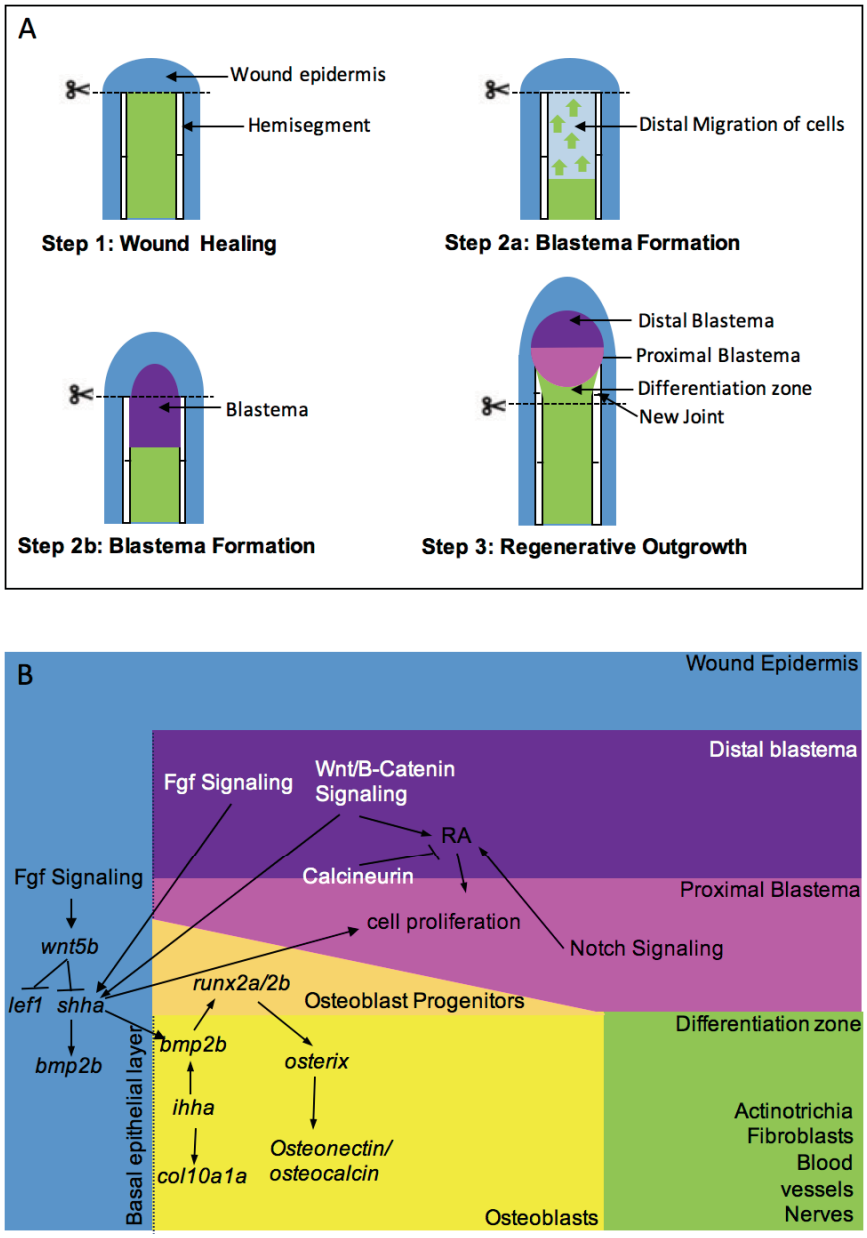

Figure 1.2: Fin ray regeneration occurs as a series of steps. Step 1 - Wound Healing: the wound is quickly covered through the migration and rearrangement of epithelial cells. Step 2a/2b - Blastema formation: the wound epidermis matures, becoming multilayered *via* continuous cell migration. Cells proximal to the amputation site de-differentiate, migrate distally, and proliferate, forming the blastema underneath the wound epidermis. Step 3: Regenerative outgrowth: the blastema is subdivided into two distinct compartments: the distal blastema and the proximal blastema. Cells leaving the proximal blastema and enter the differentiation zone, where they differentiate into the multiple cell types that reform the lost fin. B) Signaling Pathways involved in the regenerative outgrowth of a single fin ray. Signals from the epidermis (blue), distal blastema (purple), proximal blastema (pink), and differentiation zone (yellow and green) enable the successful regeneration of the fin ray. (Image A adapted from Poss *et al.,* 2003).

1.10 The Hedgehog Signaling Pathway

The Hh signaling pathway plays a major role in fin regeneration, and has been a major focus in two of the projects outlined in this thesis (See Section 1.16 Objectives 1 and 2; Chapters 2 and 3). Consequently, current knowledge on the Hh signaling pathway in vertebrate species has been summarized in this section.

The Hh signaling pathway requires the regulated expression, processing, release and binding of Hh ligands. In zebrafish, because of the additional genome duplication following the divergence of the teleost lineage from the tetrapod lineage, ligands include Sonic hedgehog a (Shha), Sonic hedgehog b (Shhb), Indian hedgehog a (Ihha), Indian hedgehog b (Ihhb), and Desert hedgehog (Dhh) (Roelink *et al.,* 1994; Ekker *et al.,* 1995; Currie and Ingham, 1996; Avaron *et al*., 2006). Hh ligands are synthesized as full length precursor proteins that subsequently undergo autoproteolytic cleavage in the endoplasmic reticulum, generating a C-terminal and a N-terminal fragment (Figure 1.3) (Varjosalo and Taipale, 2008; Porter *et al.* 1996). The C-terminal fragment aids in the addition of a cholesterol at the C-terminus of the N-terminal fragment, and is subsequently translocated out of the ER and undergoes proteasomal degradation (Porter *et al.* 1996; Chamoun *et al.* 2001). The cholesterol addition allows the association of the N-terminal fragment with membranes, facilitating the addition of a palmitic acid moiety to the N-terminus (Pepinsky *et al.* 1998; Varjosalo and Taipale, 2008). Subsequently, the N-terminal fragment is released by one of four key mechanisms: 1) The fragment is released through the action of Dispatched (Disp), a multi-transmembrane protein (Burke *et al*. 1999; Ma *et al*. 2002), 2) The fragment can self-associate and is released as a large soluble multimer (Chen *et al*., 2004), 3) Multiple fragments can interact with heparan sulphate chains of glypicans, recruit

apolipoproteins, and are released as lipoproteins (Han et al., 2004; Eugster et al.,2007; Panakova *et al.,* 2005), 4) Multiple fragments can be released at the surface of exovesicles (Figure 1.3) (Therond, 2012; Briscoe and Thérond, 2013).

In vertebrates, released Hh proteins bind to the 12-transmembrane protein Patched1 (Ptc1) and its co-receptors: growth arrest-specific 1 (Gas1), CAM-related/downregulated by oncogenes Cdo, and brother of Cdo (Boc) (Figure 1.3) (Briscoe and Thérond, 2013; Tenzen *et al*. 2006). Binding of Hh to Ptc1 results in its internalization and subsequent degradation by lysosomes (Chen and Struhl, 1996; Incardona *et al*. 2000; Gallet and Therond 2005). The internalization acts to restrict the spreading of the Hh ligand, and allows the ciliary accumulation and activation of Smoothened (Smo), a member of the G protein-coupled receptor superfamily (Ho and Alman 2010; Briscoe and Thérond, 2013). The activation of Smo results in a signaling cascade that enables the transport of the full length versions of Gli family zinc finger transcription factors (Gli1, Gli2 and Gli3) to the nucleus. These transcriptional activators lead to the expression of specific target genes such as *Ptc1*, *Gli1*, and *Hedgehog interacting protein 1* (*Hip1*, or *hhip* in zebrafish) (Karlstrom *et al*., 2003; Jeong and McMahon 2005; Hammond and Whitfield, 2009). Hip1 acts to bind and sequester Hh ligands, limiting their diffusion (Chuang and McMahon 1999; Jeong and McMahon 2005). In the absence of Hh, Ptc1 inhibits Smo activity. When Smo is inhibited, Suppressor of Fused (SuFu) binds Gli transcription factors, sequestering them in the cytoplasm (Figure 1.3) (Cheng and Bishop 2002; Kogerman *et al.,* 1999; Paces-Fessy *et al*., 2004). Retention in the cytoplasm results in the phosphorylation of Gli2 and Gli3 by factors such as Protein Kinase A (PKA), Casein kinase 1 (CKI) and Glycogen synthase kinase 3β (GSK3β) (Tuson *et al.,* 2011; Fumoto *et al.,* 2006; Sillibourne *et al.,* 2002).

Phosphorylation results in the proteolytic processing of these factors, generating the transcriptional repressor forms of Gli2 and Gli3 (Briscoe and Thérond, 2013). Gli1 lacks a proteolytic cleavage site and acts only as a transcriptional activator (Hynes *et al.,* 1997; Aza-Blanc *et al*., 2000). However, differential phosphorylation events act to inhibit or induce the ability of Gli1 to function as an activator (Kaesler *et al*, 2000; Atwood *et al*., 2014).

Studies specifically in zebrafish have shown that Gli1 is similarly a major activator of the Hh-signaling pathway (Karlstrom *et al*., 2003; Vanderlaan *et al.,* 2005). Furthermore, Gli2a/b (due to the additional genome duplication event) and Gli3 have been shown to repress or activate the Hh signaling pathway, depending on the cellular context (Karlstrom *et al*., 2003; Ke *et al.,* 2005; Tyurina *et al*., 2005).

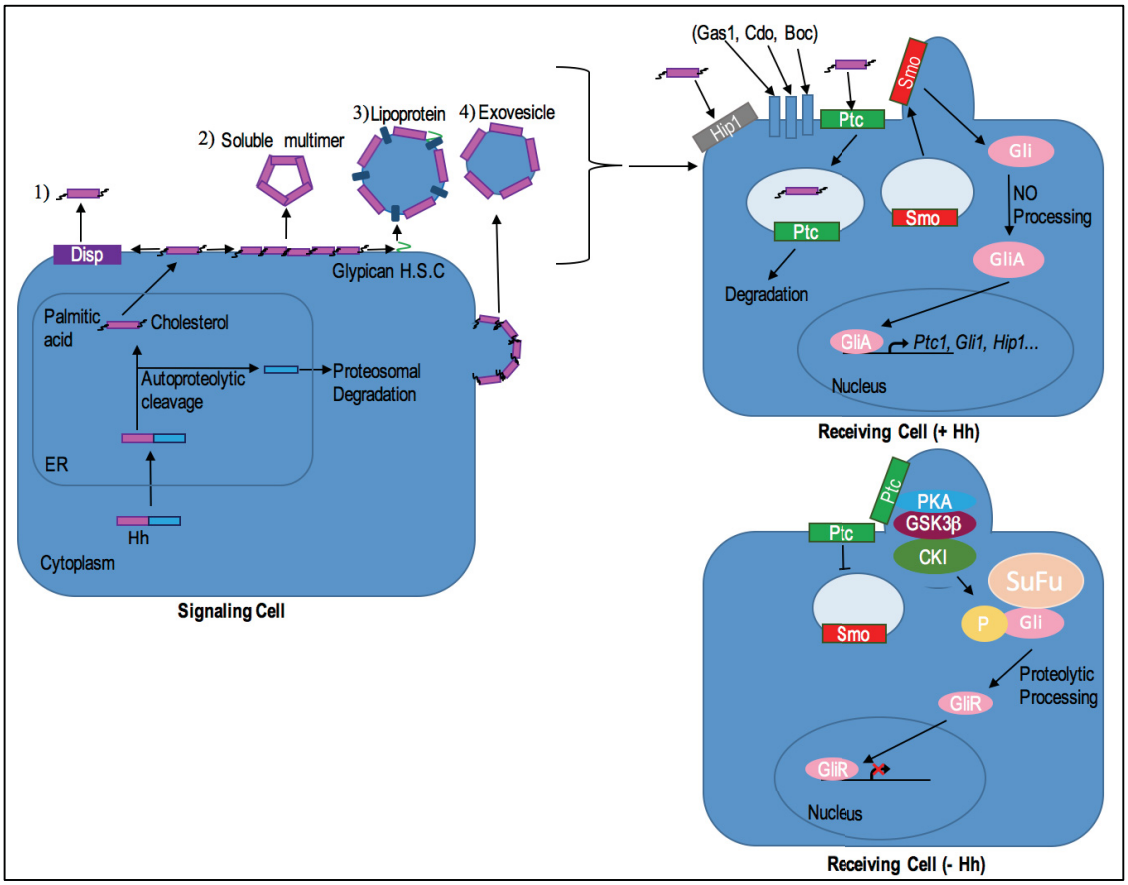

Figure 1.3: The Hedgehog Signaling Pathway. In the signaling cell: Full length Hedgehog (Hh) ligands (combined blue and pink) undergo autoproteolytic cleavage in the endoplasmic reticulum (ER), generating a C-terminal (blue) and a N-terminal (pink) fragment. The C-terminal fragment is translocated out of the ER and is degraded. The N-terminal fragment undergoes cholesterol modification and palmitoylation. The N-terminal fragment is released through one of four mechanisms: 1) Dispatched (Disp), 2) a soluble multimer, 3) a lipoprotein, 4) an exovesicle. In the receiving cell (+ Hh): Co-receptors growth arrest-specific 1 (Gas1), CAM-related/downregulated by oncogenes Cdo, and brother of Cdo (Boc) promote Hh binding to Patched 1 (Ptc 1). Upon binding, Hh proteins inhibit Ptc1, resulting in the internalization and degradation of Hh and Ptc1, and the accumulation/activation of Smoothened (Smo), in cilia. Smo activation results in the inhibition of proteolytic processing, enabling the transport of Gli transcriptional activators (GliA) to the nucleus where multiple target genes are expressed such as *Ptc1, Gli1* and *Hip1*. Hip1 binds and sequesters Hh ligands, limiting their diffusion. In the Receiving Cell (- Hh): Ptc1 inhibits Smo activity. When Smo is inhibited, SuFu binds to Gli transcription factors sequestering them in the cytoplasm. These factors are subsequently phosphorylated by PKA, CKI and GSK3β, leading to their proteolytic cleavage into transcriptional repressors (GliR).

1.11 Branching Morphogenesis – Involvement of Hh Signaling

During regeneration the fin rays branch, forming two sister rays in a process termed branching morphogenesis. Prior to fin ray branching, a single group of *shha*-expressing cells is detected at the center of the hemiray (Figure 1.4 A) (Zhang *et al.,* 2012). As regeneration proceeds, the expression domain of *shha* separates into two except for the two most lateral rays that never bifurcate (Figure 1.4 A, B) (Laforest *et al*., 1998). Following the splitting of the *shha* expression domains, the fin rays bifurcate, and a single group of *shha*-expressing cells is maintained at the distal tip of each sister ray until the second bifurcation event (Figure 1.4 A, B) (Zhang *et al*., 2012).

To investigate the role of *shha*-expressing cells during branching morphogenesis, cell ablation experiments were performed (Zhang *et al*., 2012). To laser ablate *shha*-expressing cells, our lab acquired the zebrafish *Tg(2.4shha:GFP:ABC)* transgenic line, which expresses *gfp* under the control of *shha cis*-acting regulatory elements: a 2.4kb genomic fragment containing the *shha* promoter and the *ar-A*, *ar-B*, and *ar-C* enhancers from the first and second introns (Ertzer *et al.,* 2007). GFP expression in this transgenic line recapitulates endogenous s*hha* expression during fin regeneration (Figure 1.4 B-C') (Zhang *et al*., 2012). The transient deletion of GFP positive *shha*-expressing cells in the caudal fin regenerates of *Tg(2.4shha:GFP:ABC)* fish, through laser ablation, delays the bifurcation process (Zhang *et al*., 2012). More specifically, in many rays branching occurred more than 2 segments distal to the corresponding non-ablated internal controls (Zhang *et al.,* 2012). In addition, using gain of function analysis, it has been shown that the *in vivo* transfection of *shha* between sister rays leads to ectopic bone formation (Quint *et al*., 2002). Overall, these studies show that *shha*-expressing cells may act as a signaling center, interacting with adjacent mesenchymal cells for the proper patterning or positioning

of osteoblasts that form the fin rays.

Although the role of Shha signaling in branching morphogenesis has been outlined here, it is possible that other factors that are co-expressed in the basal epidermal layer also regulate branching morphogenesis. Previously, it has been shown that treatments with RA or a Fgfr1 inhibitor (SU5402) down-regulates both *shha* and *lef1* expression in the basal epidermal layer (Poss *et al*., 2000). Furthermore, in mouse and chick it has been shown that Lef1 is required for the formation of organs that depend on epithelial–mesenchymal tissue interactions (Boras-Granic *et al*., 2006, Fujimori *et al.,* 2010, van Genderen *et al*., 1994, Widelitz *et al*., 2000). Therefore, Lef1 may play a role in branching morphogenesis analogous to that proposed for Shha.

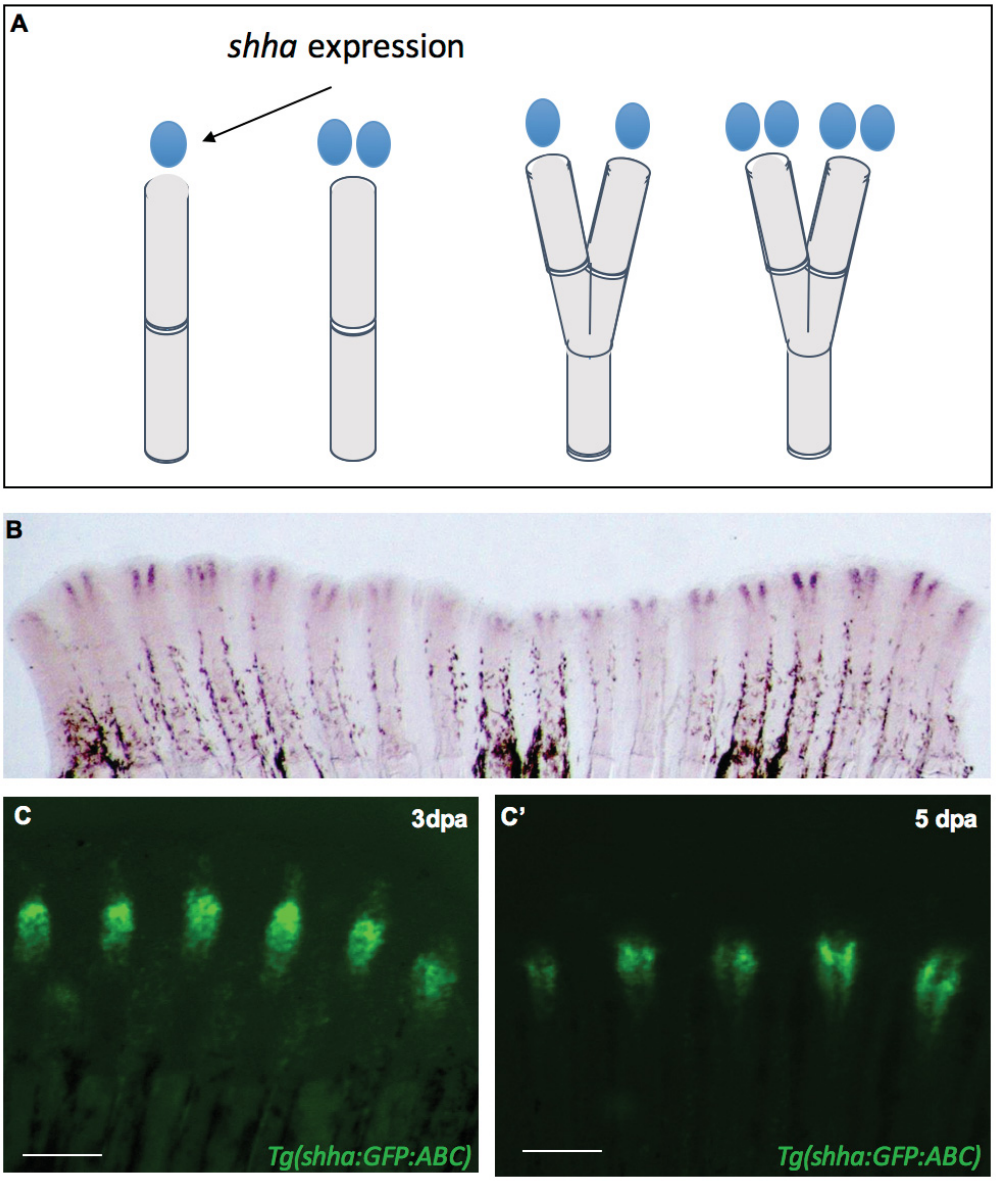

Figure 1.4: *shha* expression patterns of the regenerating zebrafish caudal fin. A) *shha* is expressed at the distal tip of the fin regenerate. Prior to the branching, the expression domain of *shha* splits into two. Following branching, only a single domain is observed until the next bifurcation event. B) Wholemount *in situ* hybridization shows two distinct domains of endogenous *shha* expression in the fin regenerate 4dpa, with the exception of the most lateral rays, which consistently possess a single *shha* domain. C) Tg(*shha:GFP:ABC#15)* transgenic line recapitulates endogenous expression of *shha*. 3dpa a single domain of Gfp positive *shha* expressing cells is observed in the regenerating fin rays. C') 5dpa the GFP positive domain is split into two. All scale bars = 200μm.

1.12 Intramembranous versus Endochondral Ossification

Bone formation can occur in two distinct ways: intramembranous ossification or endochondral ossification. During intramembranous ossification mesenchymal cells compact into sheets or membranes and commit to an osteoblast progenitor cell fate (Figure 1.5 A) (Komori *et al*., 1997; Nakashima *et al.,* 2002). Upon commitment to an osteoblast cell fate, cells further differentiate into osteoblasts, which deposit the bone matrix (Figure 1.5 A) (Bruder and Caplan, 1989). In mammals, osteoblasts become embedded in the secreted matrix, further differentiating into osteocytes (Figure 1.5 A) (Ornitz and Marie, 2002). However, in more basal teleosts (i.e. zebrafish) osteocytes are present in some bones, but absent from others, such as the dermal fin rays (Apschner *et al*., 2011; Meunier, 1989; Mackay *et al.,* 2014; Santamaria *et al.,* 1992). Osteocytes are absent from the fin rays because osteoblast secrete the bone matrix in a polarized fashion (Figure 1.5 B). As the bone matrix is secreted, osteoblasts retract from the bone surface and are not incorporated into the matrix (Huysseune, 2000).

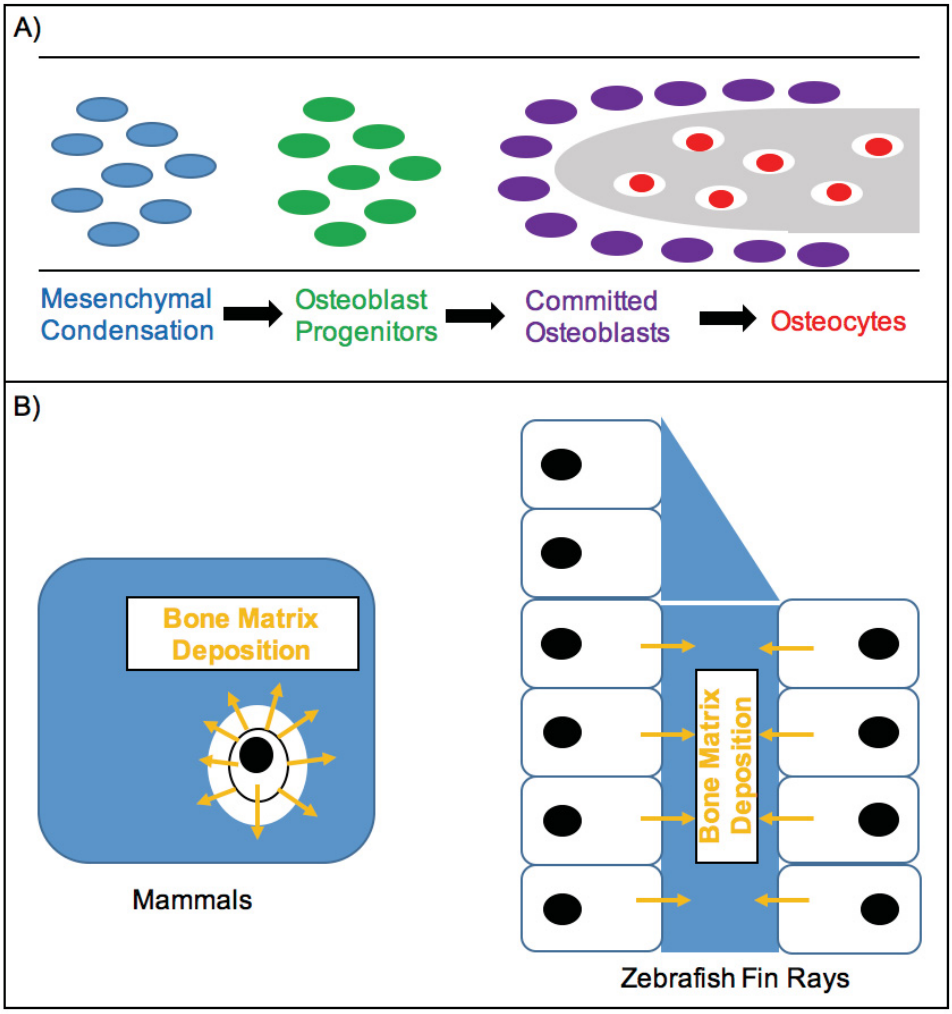

Figure 1.5 Intramembranous ossification. A) During intramembranous ossification mesenchymal cells condensate (blue cells) and commit to an osteoblast progenitor cell fate (green cells). Once committed osteoblast progenitors differentiate into osteoblasts (purple cells). Osteoblasts secrete the bone matrix (gray). A, B) In mammals, osteoblasts get trapped within the secreted bone matrix, and further differentiate into osteocytes. B) In zebrafish, bone matrix deposition is polarized and osteoblasts do not differentiate into osteocytes.

During endochondral ossification, mesenchymal cells condense and commit to a chondrocyte cell fate, undergoing differentiation in a sequential manner to form the cartilage anlagen (Figure 1.6) (Mak *et al.,* 2008a). Concurrently, mesenchymal cells lining the surface of the cartilage anlagen flatten and elongate, forming the perichondrium (Figure 1.6). Mesenchymal cells of the perichondrium differentiate into osteoblasts, generating a layer of bone called the periosteum (Figure 1.6) (Eames *et al*., 2003; Hall and Miyake, 2000). During chondrocyte differentiation, periarticular chondrocytes differentiate into highly proliferative chondrocytes (Figure 1.6) (Abad *et al*., 2002). Subsequently, the proliferating chondrocytes differentiate into pre-hypertrophic chondrocytes. These cells then undergo hypertrophy, secreting extracellular matrix, which is eventually mineralized (Figure 1.6) (Howlett, 1979; Hunziker, 1994; Karp *et al*., 2000). Hypertrophic chondrocytes then undergo apoptosis, which induces vascular invasion, allowing bone marrow cells, osteoclasts, and osteoblasts into the cartilaginous matrix (Figure 1.6) (Mackie *et al.,* 2008; Colnot *et al*., 2012; Kronenberg, 2003). The osteoclasts assist in the removal of the calcified cartilage matrix, and the differentiating osteoblasts deposit of bone matrix, which is subsequently mineralized (Mackie *et al.,* 2008; Knowles *et al.,* 2012).

Compared to endochondral ossification, much less is known about the genetic regulation of intramembranous bone. The simple structure, limited cell types, rapid regeneration time, and ease of accessibility makes the dermal caudal fin rays an excellent model for the study of intramembranous ossification.

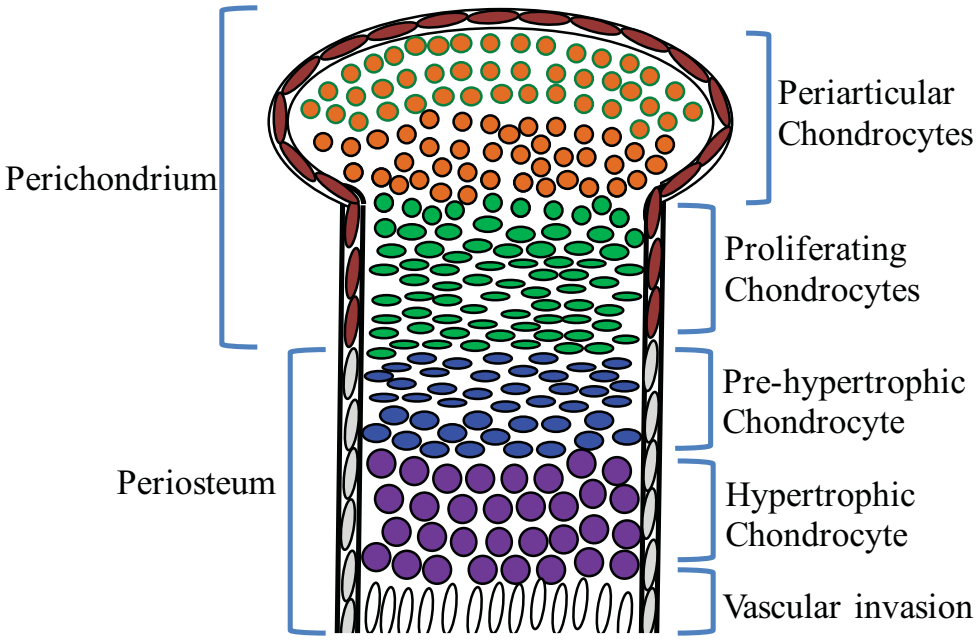

Figure 1.6: Endochondral ossification. mesenchymal cells lining the bone, form the perichondrium. Cells of the perichondrium differentiate into osteoblasts, generating the periosteum. During chondrocyte differentiation, periarticular chondrocytes differentiate into proliferative chondrocytes. These cells differentiate into pre-hypertrophic chondrocytes, then become hypertrophic chondrocytes that undergo apoptosis, inducing vascular invasion, allowing bone marrow cells, osteoclasts, and osteoblasts into the cartilaginous matrix.

1.13 Intramembranous Ossification of the Fin Rays

The regenerating zebrafish dermal fin rays regenerate *via* intramembranous ossification. Following amputation of the dermal fin rays, mature osteoblasts de-differentiate, proliferate, and migrate to accumulate in the lateral regions of the proximal blastema (Knopf *et al*., 2011). In the proximal blastema, pre-osteoblasts express *runx2a* and *runx2b* (Figure 1.2 B) (Brown *et al.,* 2009; Poss *et al*., 2000; Nechiporuk and Keating, 2002; Santos-Ruiz *et al.,* 2002). As pre-osteoblasts undergo maturation along the proximal distal axis, cells enter the differentiation zone where *runx2a* and *runx2b* may directly regulate the expression of *osx* (Figure 1.2 B) (Komori *et al*., 1997; Nakashima *et al*., 2002; Nishio *et al*., 2006; Brown *et al*., 2009). Upon expression of *osx* cells are committed to an osteoblast cell fate (Nakashima *et al*., 2002), and subsequently express intermediate stage markers *collagen, type X, alpha 1a* (*col10a1a*) (Figure 1.2 B) (Avaron *et al*., 2006). As osteoblasts mature and become even more proximal, late differentiation markers, *osteonectin* (*sparc, osn*) and *osc*, are expressed (Figure 1.2 B) (Gavaia *et al.,* 2006; Sousa *et al*., 2011). Osteoblasts expressing late stage differentiation markers synthesize and release bone matrix into the subepidermal space. The bone matrix then mineralizes, forming the lepidotrichia, which make up the fin rays (Becerra *et al*., 1996; Marí-Beffa *et al*., 1996; Santamaría *et al*., 1996; Akimenko *et al*., 2003).

Differentiating osteoblasts adjacent to the expression domain of *shha* in the basal epidermal layer have also been shown to express *indian hedgehog a* (*ihha*), another member of the Hh gene family (Figure 1.2 B), and *patched-1*, a Hedgehog receptor (Avaron *et al*., 2006). Currently, the specific role of *ihha* is unknown. However, based on its expression pattern, it is likely that Ihha is involved in osteoblast differentiation. Bmp2b, a downstream target of Hh signaling, is expressed in the same cells as *shha* and in adjacent

osx positive osteoblasts and likely plays a role in osteoblast differentiation (Figure 1.2 B) (Quint *et al*., 2002; Stewart *et al.,* 2014). Previously, it has been shown that the ectopic expression of *bmp2b* between regenerating fin rays induces ectopic bone matrix deposition leading to the fusion of adjacent sister rays (Quint *et al.,* 2002). In contrast, the inhibition of BMP signaling through the ectopic expression of *chordin*, a BMP antagonist, in the blastema results in a delay in bone matrix deposition due to the downregulation of early and late bone markers (Smith *et al*., 2006). In contrast, treatment using the BMP receptor inhibitor (LDN193189) (Cuny *et al*., 2008), resulted in an increase in *runx2*-positive pre-osteoblast cells and a decrease in *osx* and *col10a1a* – positive osteoblasts (Stewart *et al*., 2014). Nonetheless, these results both indicate that BMP signaling acts to promote osteoblast differentiation (Figure 1.2 B) (Stewart *et al*., 2014). Furthermore, LDN193189 treatments have been shown to result in a decrease in *dkk1b* expression, a secreted Wnt antagonist, in osteoblasts. Consequently, Wnt/β-catenin signaling expands proximally from *runx2*-positive pre-osteoblasts to include the more proximal *osx*-positive osteoblasts. These results indicate BMP signaling induces secreted Wnt antagonists in proximal osteoblasts to restrain Wnt activity to the distal pre-osteoblast pool (Stewart *et al.,* 2014).

Interestingly, following RA treatments, it has been shown that the expression of both *dkk1b* and *bmp2b* are downregulated. These data imply that RA signaling may inhibit pre-osteoblast differentiation by negatively interfering with BMP and promoting Wnt/β-catenin signaling (Blum and Begemann, 2015). Currently, due to the activation of this pathway in various blastemal compartments including *runx2* positive pre-osteoblasts and adjacently located actinotrichia-forming cells, the specific roles of Wnt/β-catenin signaling in the pre-osteoblasts are unclear (Wehner *et al*., 2014).

1.14 Joint Regeneration

During regeneration the fin rays become segmented through the periodic addition of new joints to the distal end of each fin ray (Johnson and Bennett, 1999; Iovine and Johnson 2000). The formation of caudal fin ray joints is a multistep process that begins with condensation of a discrete band of cells located in the presumptive joint regions of the distal fin regenerate (Figure 1.7) (Pacifici *et al*., 2006). Initially, these joint regions have been observed as a group of elongated cells, which then become round and/or appear pinched at one end. As the joints mature, these cells form two distinct rows that eventually separate, forming a physical joint in the bone matrix (Figure 1.7) (Sims *et al*., 2009).

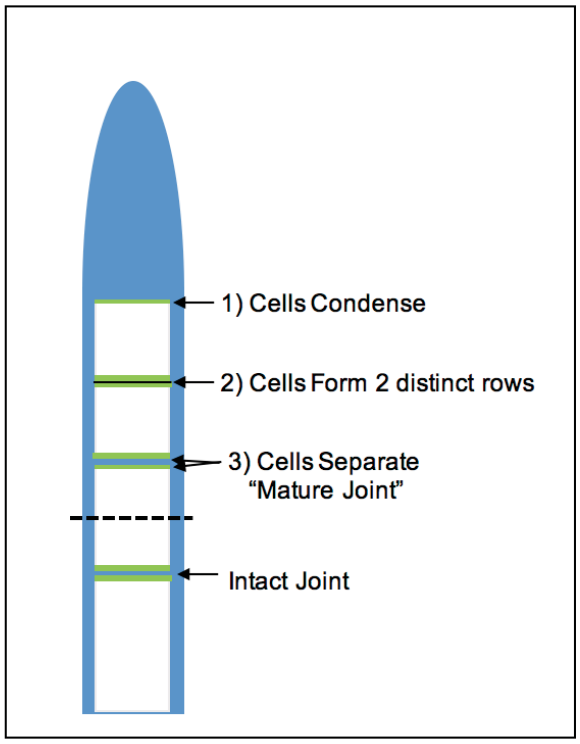

Figure 1.7: Fin ray segments are established through the periodic distal addition and maturation of new joints to each fin ray. (1) At the location of the future joint, a discrete band of joint forming cells (green) form a cluster. (2) As joints mature, clustered joint cells are rearranged, forming two distinct rows (green). (3) Further maturation allows the two rows to separate, forming a physical joint in the bone matrix (green). Once separated, joints appear similar to those of the intact stump (green lines). Dotted line = amputation plane.

Currently, the mechanisms controlling joint formation are largely unknown. However, it has been suggested that these joint regions express a unique set of genes that are involved in joint formation. The *even-skipped homeobox 1* (*evx1*) gene, which encodes for a transcription factor that belongs to a family of vertebrate *eve-related homeobox* genes (Faiella *et al*., 1991), is expressed at the level of the joints (Borday *et al*., 2001). Furthermore, homozygous *evx1*$^{-/-}$ null mutants, possessing a point mutation that produces a stop codon at the beginning of the DNA-binding homeodomain, lack fin ray joints (Schulte *et al*., 2011) suggesting that Evx1 is required for joint formation during development and regeneration (Schulte *et al*., 2011; Sims *et al*., 2009). Currently, the exact mechanism with which Evx1 controls joint formation is unknown. However, it has been shown that *dlx5a* and *mmp9* are downstream targets of *evx1* and contribute to joint formation (Ton and Iovine, 2013).

Furthermore, *connexin43 (cx43*), a gap junction protein that is expressed in the blastema and a subpopulation of osteoblasts surrounding both newly formed and mature joints, has been shown to suppress joint formation (Iovine *et al.*, 2005). Indeed, previous studies have identified four zebrafish mutants that are associated with *cx43* and are characterized by a reduction in fin ray segment length and a short fin phenotype (Iovine *et al*., 2005). More specifically, *N*-ethyl-*N*-nitrosourea (ENU) -induced *short fin* mutants (*sof*^{j7e1}, *sof*^{j7e2}, *sof*^{j7e3}) possess missense mutations in the *cx43* coding sequence (Iovine *et al*., 2005). The spontaneous *short fin* (*sof*^{b123}) mutant maps to the *cx43* gene, and *cx43* expression is reduced, but no mutations were found in the coding sequence (Iovine *et al.,* 2005). More in-depth studies using the *sof*^{b123} mutants, suggest that a decrease in *cx43* leads to reduced proliferation and the premature expression of joint genes such as *evx1*.

Consequently, *sof*^{b123} mutants develop both short segments and short fin lengths (Iovine *et al.,* 2005; Hoptak-Solga *et al.,* 2008; Ton and Iovine, 2013). In contrast to the *short fin* phenotype, a null mutation in *kcnk5b* (*another long fin* , *alf*^{dty86}), a gene coding for a potassium channel, results in increased fin length and inconsistent/longer segment lengths (Ton and Iovine, 2013; Perathoner *et al*., 2014). Analysis of the *alf*^{dty86} mutant indicates the inconsistent/longer segment lengths are associated with irregular expression of *evx1* (Perathoner *et al.,* 2014; Ton and Iovine, 2013). Furthermore, the observed increase in fin length is due to an increase in cell proliferation. However, how this potassium channel regulates cell proliferation to establish fin length remains unclear.

Overall, there is a correlation between fin length and segment length in the *sof* and *alf* mutants. These results indicate the mechanisms controlling fin growth and joint formation may be linked. However, the *long fin* (*lof*) and *rapunzel* (*rpz*) mutants possess longer fins, but do not have altered segment lengths (Goldsmith *et al.,* 2003; Iovine *et al.,* 2000). Furthermore, *evx1* mutants have normal fin lengths (Schulte *et al.,* 2011). These results indicate that growth and joint formation may also occur via independent processes.

1.15 Regulation of Growth Rate and Positional Information during Regeneration

During regeneration, growth rate is dependent on the proximal-distal position of the amputation site (Lee *et al*., 2005). More specifically, fins regenerate more quickly following proximal amputations than distal amputations (Akimenko *et al*, 1995; Lee *et al.,* 2005). However, they fully regenerate in similar amounts of time (Iovine, 2007). A similar overall regeneration time for both proximal and distal amputations occurs because there is an initial increase in growth rate (allometric growth) following proximal amputations but as the regenerate approaches the size of the original fin the growth rate decreases

(isometric, proportionate growth) (Lee *et al*., 2005). The initial accelerated growth rates correlate with higher expression of growth factors such as Fgf (Lee *et al.,* 2005), indicating that the rate of regeneration is molecularly linked to the proximal-distal identity of cells at the amputation site. However, the precise mechanisms involved in coordinating these factors to re-establish the appropriate fin size during regeneration are unclear.

Recently, calcineurin, a Ser/Thr phosphatase, was identified as an inhibitor of regenerative outgrowth and regulator of proximal distal patterning (Kujawski *et al.,* 2014). Kujawski *et al.* (2014) showed that Calcineurin phosphatase activity increases as regenerates recover the final size and shape of the fin. Calcineurin functions through its binding to FK506-binding proteins (FKBPs), which are induced in the blastemas of fin regenerates (Kujawski *et al.,* 2014). Treatment of fish with the Calcineurin inhibitor Tacrolimus (FK506), which binds to FKBP and subsequently blocks the phosphatase activity of Calcineurin (Thomson *et al.,* 1995), results in increased blastemal cell proliferation and enhanced fin ray outgrowth in regenerating fins (Kujawski *et al.,* 2014). Furthermore, distal gene expression domains involved in regeneration were expanded in FK506 treated fish, appearing similar to more proximal gene expression domains in control fish. FK506 treated fish also demonstrated a distal shift in fin ray bifurcation sites compared to vehicle and non-treated controls. Overall, this data suggests that treatment with FK506 results in a change in positional information along the proximal-distal axis (Kujawski *et al.,* 2014). Currently, the exact mechanism in which calcineurin regulates growth and proximal-distal patterning in the fin regenerate is unknown. However, the authors suggest calcineurin acts upstream of RA signaling during zebrafish fin regeneration (Figure 1.2 B) (Kujawski *et al.,* 2014). Studies in tetrapods indicate that RA regulates

proximal-distal patterning of regenerating appendages (Maden, 1982). During regeneration, increases in RA result in the duplication of proximal structures, resulting in the extended outgrowth of limbs (Maden, 1982; Niazi and Saxena, 1978; Thoms and Stocum, 1984). In teleosts, treatment with RA has been shown to lead to a distalization of ray bifurcations (Géraudie *et al*., 1994; White *et al.,* 1994; Laforest *et al*., 1998), indicating RA may play a similar role in proximal-distal patterning in the caudal fin. However, the mechanisms of branching are unclear. Consequently, branch points may not be a reliable readout for proximal-distal patterning (Blum and Begemann, 2012).

As mentioned previously, various joint mutants have indicated that there is a correlation between growth and segment formation. Considering the overgrowth phenotype of FK506 treated fins, it would be of interest to investigate whether calcineurin plays a role in joint formation (see Chapter 3).

1.16 Caudal Fin Vascular Regeneration

The vasculature of the fin can be easily visualized throughout development and regeneration using a transgenic zebrafish line *Tg(fli1a-EGFP)* that expresses EGFP under the control of the promoter of the *fli1a* gene, an endothelial marker (Lawson and Weinstein, 2002). Each fin ray possesses a centrally located artery connected through intervessel commissures to two flanking veins (Huang *et al*., 2003). Veins of two adjacent rays are then connected *via* interray vessels (Huang *et al*., 2003). Following caudal fin amputation, blood vessels heal their ends by 24 hours post amputation (hpa) (Figure 1.8 A) (Huang *et al*., 2003). Afterwards, blood vessels reconnect, allowing the restoration of blood flow at the amputation site (Figure 1.8 B). These truncated vessels then grow distally, forming a cluster of blood vessels called plexuses (Figure 1.8 C-D). These plexuses are remodeled in

a proximal to distal fashion until the original vasculature pattern is re-established (Figure 1.8 E) (Huang *et al*., 2003). Once established, blood vessel growth continues through active sprouting until the fin has fully reformed (Figure 1.8 F-G) (Huang *et al*., 2003). Treatments with PTK787, an inhibitor of vascular endothelial growth factor receptor tyrosine kinases, effectively inhibits angiogenesis in the caudal fin regenerate (Wood *et al.,* 2000; Bayliss *et al.,* 2006). However, caudal fin regeneration proceeds up to 1mm from an intact blood supply (Bayliss *et al*., 2006). These results indicate that regeneration can occur at a distance from a blood supply; however, blood vessels are necessary for complete regeneration.

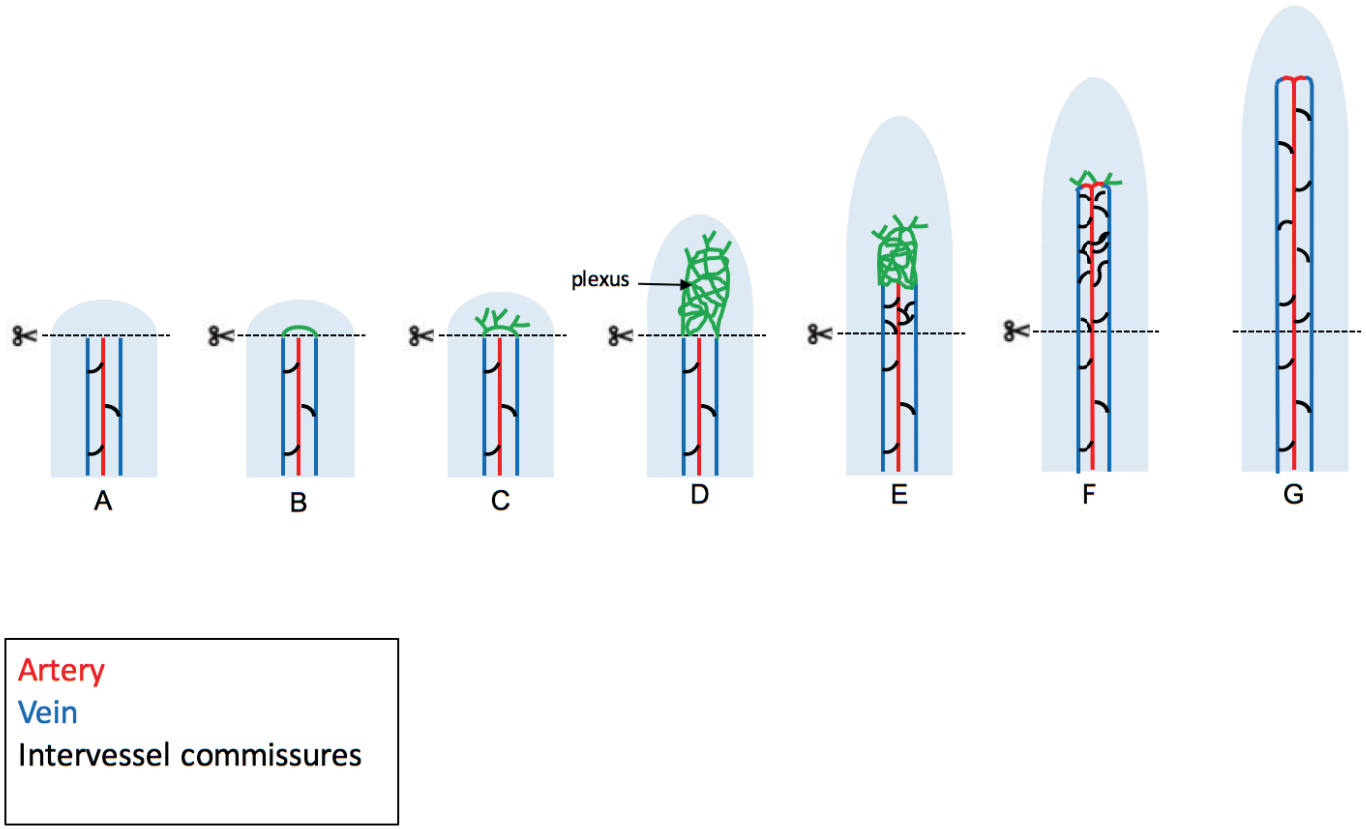

Figure 1.8: Vascular regeneration in the caudal fin. (A) Following caudal fin amputations (black dotted line), blood vessels heal their ends concurrently with the formation of the wound epidermis. (B) Blood vessels then start to reconnect (green vessels), allowing the restoration of blood flow to the amputation site. (C) Blood vessels then sprout outwards, forming plexuses (green blood vessel clusters) (D). (E) These plexuses continue to grow outward and are remodeled to form veins (blue), arteries (red), and intervessel commissures (black). (F) Excess intervessel commissures are removed in a proximal to distal fashion until the original vasculature pattern is re-established. Blood vessel growth continues through active sprouting until the fin has fully regenerated (G).

1.17 Pectoral Fin Regeneration

Although zebrafish possess the ability to regenerate all five sets of their fins, approximately half of wildtype (EK and AB strains) adult male zebrafish have been known to display defects in the anteromedial rays of regenerating pectoral fins (Nachtrab *et al.,* 2011). Males with defective anterior fin ray regenerates displayed impaired blastema proliferation and were significantly shorter than the corresponding female fin rays (Figure 1.9) (Nachtrab *et al*., 2011). The observed regenerative defect in males is caused by androgen-regulated gene expression in the anteromedial pectoral fins of males, or the region of breeding tubercle (BT) clusters (Nachtrab *et al*., 2011). These BT clusters, multicellular keratinized epidermal structures that play a role in spawning (Figure 1.9), have been shown to be stimulated *de novo* by androgens (Wiley and Collette, 1970; McMillan *et al.,* 2013; Kang *et al*., 2013).

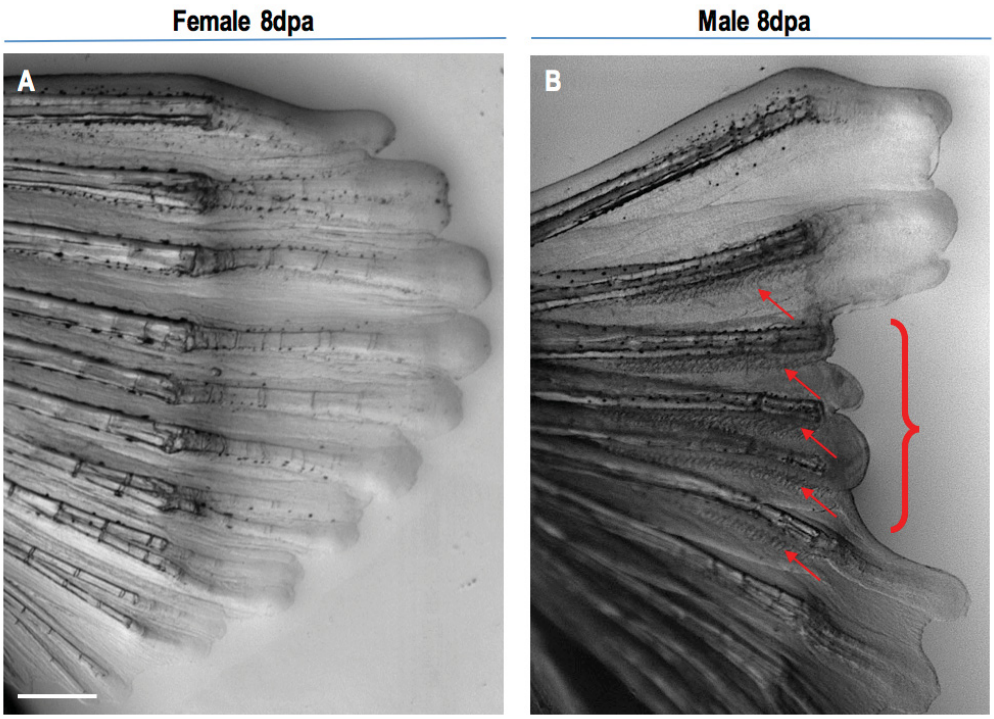

Figure 1.9: Pectoral fin regeneration in male and females. (A) Brightfield image of an adult regenerating female pectoral fin 8dpa. (B) Brightfield image of a regenerating adult male pectoral fin 8dpa. Regeneration defects, a lack of proper fin ray outgrowth (red bracket), is observed in the region containing breeding tubercles (red arrows). Scale bar for both images on A = 200μm.

The androgen-induced formation and maintenance of these clusters involves the strict regulation of Wnt/β-catenin signaling (Kang *et al*., 2013). More specifically, in androgen treated females, it has been shown that Wnt signaling predominates in immature epidermal cells in the putative regions of BT formation. The ectopic expression of *dkk1b*, a secreted Wnt/β-catenin antagonist, inhibits *de novo* formation of BTs in juvenile males and androgen-treated females (Kang *et al.,* 2013). In contrast, increasing Wnt signaling resulted in a significant increase in *de novo* BT formation in androgen treated females (Kang *et al*., 2013). These results indicate Wnt signaling plays a positive role in *de novo* formation of BTs of juvenile males and androgen treated females. However, as formation progresses, *dkk1b* is expressed in discreet units within individual BTs of males and androgen-treated females. The presence of *dkk1b* indicates it is involved in epidermal differentiation of BT clusters.

In most fins, *dkk1b* expression is excluded from the fin regenerate, enabling Wnt signaling during blastema formation (Moro *et al.,* 2012; Stoick-Cooper *et al.,* 2007). However, it has been shown that an amputation within the field of BT clusters results in *dkk1b* expression in the wound epidermis, a decrease in Wnt target genes in the blastemas, and limited blastemal mesenchymal proliferation (Kang *et al*., 2013). Therefore, it has been suggested that the male-specific regenerative defects result, at least in part, due to deficient Wnt signaling in fin rays covered with BTs (Kang *et al.,* 2013). The regeneration of pectoral fin breeding tubercles will be discussed in greater detail in Chapter 4.

1.18 Objectives

Regenerative medicine is a branch of medical research that works towards restoring structure and function to damaged tissues following injury or illness (reviewed in

Andersson and Lendahl, 2009). Presently, the field of regenerative medicine is highly successful, but is also limited to structures that can regenerate well in mammals, including bone marrow transplantation (Clift *et al.*, 2004), partial liver transplantation (Vagefi *et al*., 2011), and skin grafting (Markeson *et al.,* 2015). Therefore, a significant effort is being put forward to develop methods, drugs or tools to induce regeneration in structures that do not possess the innate ability to do so. In order to develop such abilities, one must first understand the fundamental mechanisms underlying regeneration. Consequently, several vertebrate, invertebrate, and plant model organisms are being used to study regeneration. The focus of this thesis is centered on the cellular and molecular mechanisms underlying fin regeneration in *Danio rerio,* or zebrafish. More specifically, three aspects of zebrafish fin regeneration were studied:

1. During caudal fin regeneration Sonic hedgehog a (Shha), expressed in a subset of basal epidermal cells at the level of new bone matrix deposition, has been implicated in the patterning of the regenerating fin rays (Zhang *et al*., 2012; Quint *et al.,* 2002). However, the mechanism by which the expression domain of *shha* splits and is maintained at the same proximal-distal location in the fin regenerate is unknown. Therefore, in Chapter 2, an inducible genetic fate-mapping approach was used in an attempt to identify the contributions of the derivatives of *shha*-expressing cells to the epidermis of fin regenerates.

2. Adjacent to the *shha*-expressing cells, *ihha* is expressed in differentiating osteoblasts. Currently, the role of *ihha* in osteoblast differentiation is unknown. However, in other species, Ihh signaling has been shown to play a role in both endochondral and intramembranous ossification (Kobayashi *et al.* 2002;

Kronenberg 2003; Vortkamp *et al.,*1996; Abzhanov *et al*., 2007; Lenton *et al*., 2011). Therefore, we sought to investigate whether Ihha plays a similar role and interacts with similar factors during dermal fin ray regeneration. This investigation unraveled the potential role of *pthrp1* (a factor that is known to interact with Ihh to regulate endochondral ossification (Lanske *et al*., 1996; St-Jacques *et al.,* 1999; Kronenberg 2003; Vortkamp *et al*. 1996)) in joint formation. Consequently, Chapter 3 focuses on the use of the regenerating dermal fin rays as a model to elucidate the mechanisms underlying intramembranous ossification and joint formation.

3. In an attempt to further elucidate the roles of Hh signaling during fin regeneration, gene expression analysis was performed for *shha* during the formation and regeneration of pectoral fin breeding tubercle clusters. Although no differences in *shha* expression were observed, differences in regenerative capabilities and vascularization were highlighted between male and female pectoral fins. These observations led to a detailed analysis of Breeding Tubercles on developing and regenerating pectoral fins. Chapter 4 outlines the results of this detailed analysis and consists of two publications.
    a) The first publication characterizes these BT clusters on male pectoral fins, and subsequently describes the requirement of androgens and two waves of vascularization for their formation and regeneration.
    b) The second publication discusses the use of Breeding tubercles on male pectoral fins in determining zebrafish sex.

Chapter 2: Determining Cell Fate of *shha*-Expressing Cells During Zebrafish Caudal Fin Regeneration.

2.1 Summary:

During growth and regeneration, the zebrafish fin rays bifurcate, or split into two sister ray branches, except the most lateral rays, using a process termed branching morphogenesis (Akimenko *et al*., 2003; Laforest *et al.,* 1998; Zhang *et al*., 2012). Sonic hedgehog a (Shha), expressed in a subset of cells in the basal epidermal layer, plays an essential role in branching morphogenesis of the regenerating zebrafish fin rays (Zhang *et al*., 2012; Quint *et al.,* 2002). In mammals, Shh has been shown to play a critical role in branching of the developing lungs (Affolter *et al.,* 2009; Chuang and McMahon*,* 2003; Gjorevski and Nelson, 2010; Miller *et al*., 2004; Pepicelli *et al.,* 1998), prostate (Freestone *et al*., 2003; Pu *et al.,* 2004; Thomson and Marker, 2006) and salivary glands (Harunaga *et al.,* 2011; Jaskoll *et al*., 2004). Therefore, it is of interest to gain a greater understanding of the roles of Shh during branching morphogenesis. The zebrafish fin offers a simple model system to better understand the various mechanisms controlling branching morphogenesis. In this chapter, an inducible genetic fate-mapping approach was used in an attempt to identify the contributions of the derivatives of *shha*-expressing cells to the epidermis of fin regenerates. These experiments attempt to provide a greater understanding of epidermal regeneration and how the expression pattern of *shha* is maintained. These experiments were performed by Stephanie McMillan. Eileen Hue-Phan (4th year Honor's student) helped perform some of the tamoxifen treatments under the supervision of Stephanie McMillan.

2.2 Introduction:

During fin regeneration, a blastema, a group of undifferentiated mesenchymal cells,

forms underneath the wound epidermis. As regeneration proceeds, cells in the proximal blastema differentiate, giving rise to the multiple cell types that will reform the lost fin (Akimenko *et al*., 2003). Differentiated osteoblasts secrete a matrix that reforms the lost bones of the fin rays. Sonic hedgehog a (Shha), a signaling molecule that is expressed in a subset of basal epidermal cells at the border between the proximal blastema and the differentiation zone, has been implicated in the patterning of the regenerating fin rays (Laforest *et al.,* 1998; Zhang *et al.,* 2012; Quint *et al*., 2002). Live imaging of the *Tg(2.4shha:gfp:ABC)* transgenic line*,* which expresses *gfp* under the control of *shha cis*-acting regulatory elements, has enabled the dynamic expression pattern of *shha* to be visualized in the caudal fin regenerate. Two days post amputation (dpa), a single group of *shha*-expressing cells is detected at the center of the hemiray in the differentiation zone (Zhang *et al.,* 2012). However, as regeneration proceeds, two domains of *shha*-expressing cells are observed at the lateral limits of the hemiray. The separation of the *shha*-expressing cells into two domains precedes fin ray bifurcation. Following fin ray bifurcation, a single group of *shha*-expressing cells is maintained at each sister ray until the second bifurcation event (Zhang *et al*., 2012). The transient deletion, through laser ablation, of GFP positive *shha*-expressing cells in *Tg(2.4shha:gfp:ABC*) caudal fin regenerates delays the bifurcation process (Zhang *et al*., 2012). In contrast, gain-of-function analysis *via* the *in vivo* transfection of *shha*-expressing constructs between sister rays leads to ectopic bone formation at the site of injection inducing the fusion of the sister rays (Quint *et al.,* 2002). Overall, these studies show that *shha*-expressing cells may act as a signaling center, interacting with adjacent mesenchymal cells for the proper growth and patterning of the fin rays. The mechanism by which the expression domain of *shha* splits and is maintained at

the same proximal-distal location in the fin throughout regeneration is unknown.

The maintenance of the *shha* domain in the differentiation zone indicates that basal epidermal cells are either moving distally or that *shha* expression is activated in more distal cells and downregulated in more proximal cells in the fin regenerate. Similarly, the lateral separation of the *shha* expression domain during branching morphogenesis (Laforest *et al*., 1998; Zhang *et al*., 2012), could be the result of a lateral movement of *shha*-expressing cells or changes in *shha*-expression in central and lateral epithelial cells of the basal layer (Figure 2.1 A). Furthermore, it has yet to be determined whether *shha* expressing cells give rise to epithelial cells in the upper layers of the fin epidermis. If *shha*-expressing cells do contribute to upper epidermal layers, the extent to which the descendants of the *shha*-expressing cells contribute to the epidermis of the regenerate is unknown (Figure 2.1 B).

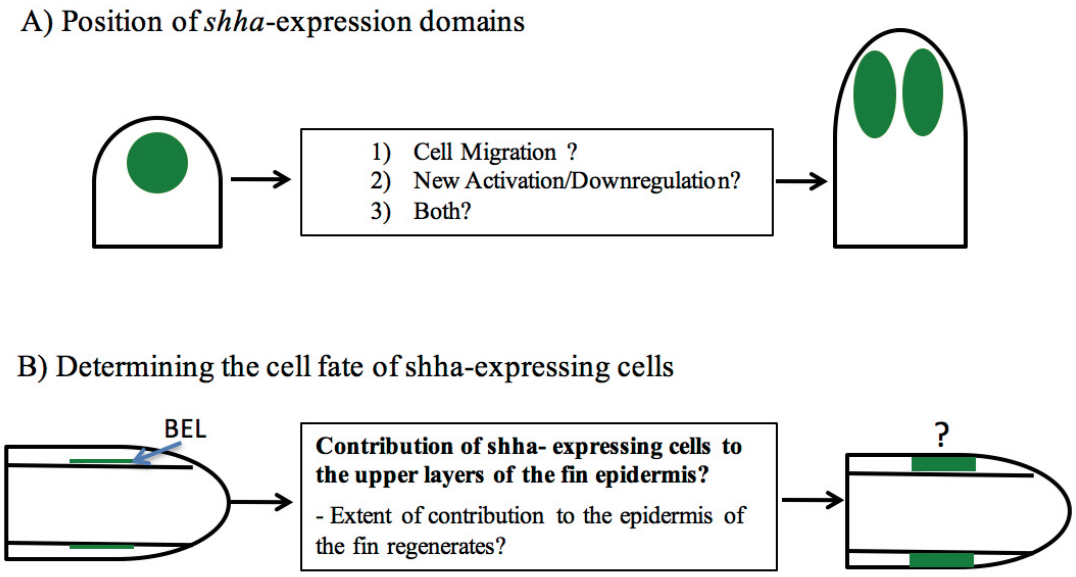

Figure 2.1: Determining the cell fate of *shha*-expressing cells in the regenerating adult caudal fin. A) The expression domain of *shha* splits into two prior to the bifurcation of the two fin rays and remains in the differentiation zone, or distal tip, of the fin regenerate. The dynamic expression patterns of *shha* during fin regeneration indicates that the cells of the basal epidermal layer are undergoing cell migration and/or that *shha* expression is being activated/downregulated as the fin regenerates. B) the extent of contribution of *shha*-expressing basal cells to the upper epidermal layers of the fin regenerate remain to be determined. BEL = Basal Epidermal Layer.

In this study, an inducible genetic fate-mapping approach was attempted to identify the contributions of the derivatives of *shha*-expressing cells to the epidermis of fin regenerates. In this approach, a transgenic line was generated that expresses er^{t2}-*cre*-er^{t2} under the control of *shha cis*-acting regulatory elements *Tg(shha: $ER^{T2}CreER^{T2}$:ABC)* (Figure 2.2). In this line, Cre recombinase is temporally controlled through the use of two modified estrogen receptor ligand binding domains (ER^{T2}) fused to Cre (Feil *et al.* 1997; Indra *et al.* 1999). In the absence of 4-hydroxy-tamoxifen (4-OHT), Heat-shock protein 90 (Hsp90) associates with the modified estrogen receptors and effectively retains Cre in the cytosol (Feil *et al*. 1996; Hayashi and McMahon 2002; Reviewed in Cox *et al*., 2012). However, upon 4-OHT treatment, 4-OHT binds to the ER^{T2} and Hsp90 is released, enabling the translocation of the ER^{T2}-Cre-ER^{T2} protein to the nucleus where it catalyzes a recombination event between two loxP sites (Feil *et al*. 1996; Hayashi and McMahon 2002; Reviewed in Cox *et al*., 2012). In many cases only a single estrogen receptor moiety is used. However, $ER^{T2}CreER^{T2}$, which has two 4-OHT binding domains (ER^{T2}), was chosen in lieu of $CreER^{T2}$ because it is more tightly regulated and has been shown to possess no basal activity when used in other zebrafish transgenic lines (Matsuda and Cepko, 2007; Boniface *et al.,* 2009). These transgenic lines also possess a screening tool, EGFP under the control of the promoter of the heart specific *cmlc2* gene (Figure 2.2) (Mosimann *et al*., 2011). Once generated, the *Tg(shha: $ER^{T2}CreER^{T2}$:ABC; cmlc2-EGFP)* line was crossed to *Tg*(*ubi:loxP-GFP-loxP-mCherry*), a reporter line that uses the ubiquitin promoter (*ubi*) to ubiquitously expresses GFP, but switches to express mCherry permanently following the Cre catalyzed excision of GFP at the LoxP sites (Mosimann *et al*., 2011)(Figure 2.3). Therefore, treatment of the double transgenic fish *Tg(shha:*

ER^{T2}CreER^{T2}:ABC; ubi:loxP-GFP-loxP-mCherry) with 4-OHT leads to the permanent loss of the EGFP reporter in *shha* expressing cells, resulting in the activation of mCherry expression (Figure 2.3). The permanent activation of mCherry should allow *shha*-expressing cells and their descendants to be traced throughout caudal fin regeneration. However, determining the cell fate of *shha* expressing cells was unsuccessful due to insufficient *cre* expression in *shha*-expressing cells. Subsequent to these results, a new transgenic line was made that included a gene insulator (HS4), which has been used successfully in other zebrafish labs (Bessa *et al.,* 2009; Zhu *et al*., 2007), downstream of the *ar-C* enhancer fragment. The HS4 insulator was used to block any suppressive effects that may have been associated with the presence of the heart marker *cmlc2-EGFP* (Figure 2.2 B). Although strong switching was observed in *shha* expressing cells of *Tg(shha: ER^{T2}CreER^{T2}:ABC; insulator; cmlc2:EGFP; ubi:loxP-GFP-loxP-mCherry*) embryos, *cre* expression continued to be insufficient in adult caudal fin regenerates. Potential factors that may have lead to insufficient *cre* expression in adult caudal fins compared to embryos is discussed at the end of this chapter.

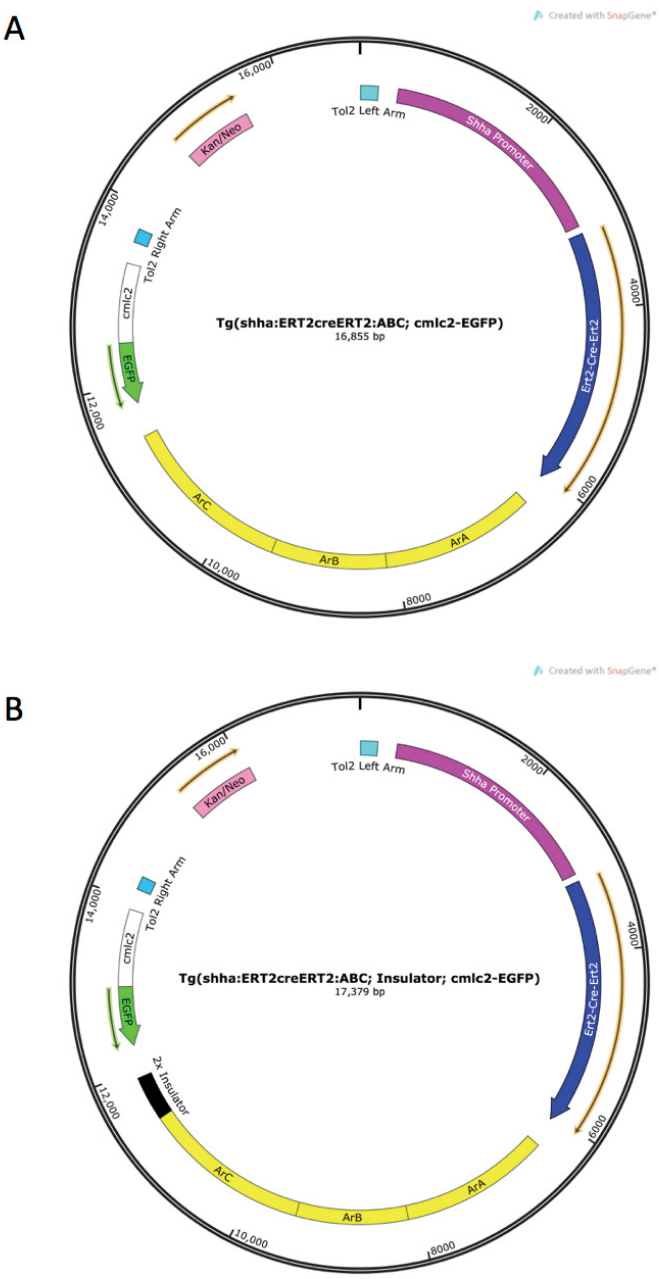

Figure 2.2: Cloning of *(shha: $ER^{T2}CreER^{T2}$:ABC)* constructs. (A) *(shha: $ER^{T2}CreER^{T2}$:ABC; cmlc2:EGFP)* construct expresses *cre* under the control of *shha cis*-acting regulatory elements: a 2.4kb genomic fragment containing the *shha* promoter (upstream of $ER^{T2}CreER^{T2}$) and the *ar-A*, *ar-B*, and *ar-C* enhancers from the first and second introns (downstream of $ER^{T2}CreER^{T2}$). This construct also possesses an EGFP under the control of a heart specific *cmlc2* promoter *(cmlc2-EGFP)*. *cmlc2-EGFP is in* reverse transcriptional orientation to the *shha* regulatory modules. (B) *(shha: $ER^{T2}CreER^{T2}$:ABC; Insulator*; *cmlc2:EGFP)* is the same as (A) with the addition of a 2x HS4 insulator downstream of the *ar-C* fragment.

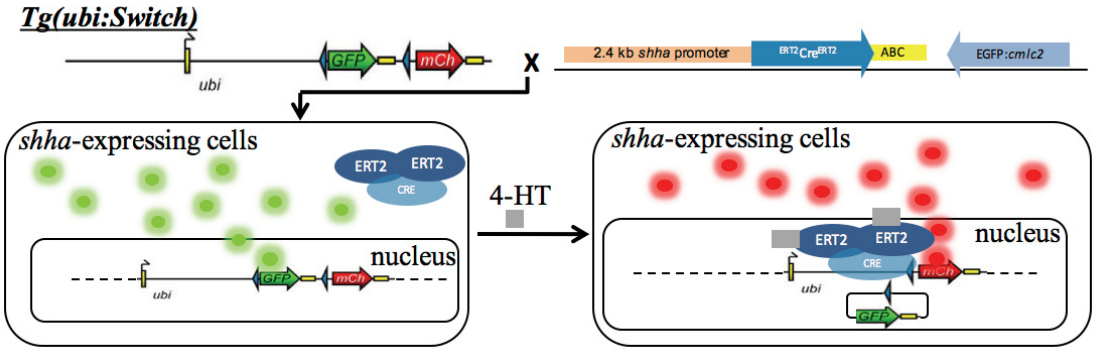

Figure 2.3: Using the Cre-LoxP system to permanently label *shha*-expressing cells. Treatment of double transgenic embryos: *Tg(shha: $ER^{T2}CreER^{T2}$:ABC; cmlc2:EGFP; ubi:loxP-EGFP-loxP-mCherry* with tamoxifen results in $ER^{T2}CreER^{T2}$ mediated excision of the GFP reporter through recombination of loxP sites (blue) and activation of mcherry expression wherever *shha* is expressed. Consequently, only cells expressing *shha* and their descendants will be permanently labelled with mCherry.

2.3 Materials and Methods

2.3.1 Animal Maintenance

All fish used in the experiments were maintained at 28°C with a photoperiod of 14 hours of light and 10 hours of darkness. Fish were fed regularly (Westerfield, 1995). The *Tg(-2.4shha:gfp:ABC)* line was a gift from Dr. Uwe Strahle (Shkumatava *et al.,* 2004). All experiments were performed according to the CCAC guidelines.

2.3.2 Molecular Cloning

To generate the (*shha:ER^{T2}CreER^{T2}:ABC; cmlc2:EGFP*) construct: *ert2-cre-ert2* (Boniface *et al.,* 2009) replaced the *gfp* from the the *Tg(-2.4shha:gfp:ABC)* plasmid (Shkumatava *et al.,* 2004). Subsequently, the entire (*shha:ER^{T2}CreER^{T2}:ABC*) was subcloned into a Tol2 vector that had a *cmlc2-EGFP* cloned downstream and in opposite orientation to the ABC enhancers. To generate the (*shha: ER^{T2}CreER^{T2}:ABC; Insulator; cmlc2:EGFP*) construct: the chicken HS4 Insulator fragment was amplified from the pBT268_(pCA-ATG-tTA2-iiTRE-tdTii) plasmid (Addgene), and cloned downstream of the ArC enhancer of the (*shha: ER^{T2}CreER^{T2}:ABC; cmlc2:EGFP*) construct (Figure 2.2).

2.3.3 Generation of Transgenic Lines

Upon completion of the above constructs, the Tol2 transposon system was used to integrate the transgenes into the zebrafish genome (Kawakami, 2007). Briefly, the Tol2 constructs were injected into one-cell stage embryos along with *tol2* transposase mRNA. 3dpf, embryos were screened for the presence of Egfp in the heart (*cmlc2-EGFP*). Embryos that expressed *egfp* in the heart were collected and raised to adulthood. These primary injected adults were then outcrossed to wildtypes to screen for transmission of the

transgene. Embryos from these outcrosses that express *gfp* in the heart are raised and maintained as transgenic lines.

2.3.4 Fin Amputations

Zebrafish were anesthetized by immersion in system water containing 0.17mg/ml tricaine (Westerfield, 1995). Caudal fins were amputated 2 segments proximal from the first branch point of the lepidotrichia. Fish were then returned to fresh system water to recover.

2.3.5 Tamoxifen Treatments

4-hydroxy-tamoxifen (4-OHT; H7904, Sigma) was dissolved in ethanol at a stock concentration of 10mM. To induce recombination embryos, treatments were performed overnight with 5μM 4-OHT in embryo medium starting at 8hpf. 5μM 4-OHT treatments were chosen as this concentration was proven effective in our lab and previous publications (Mosimann *et al*., 2011). Embryos were then washed 3x with fresh embryo medium to remove any residual 4-OHT. To induce recombination in adults, 4-OHT was added to system water at a final concentration of 5μM or 2μM 2 and 3 days post amputation (dpa) and left overnight. 5μM 4-OHT was initially chosen as this concentration was proven effective in a previous publication (Singh *et al.,* 2012). However, this dosage was reduced to 2μM as it has also been shown to be equally effective and reduced any potential damage to the fin regenerate (Personal Communication, Poss Lab). Adults were washed 3x with system water to remove any residual 4-OHT. All 4-OHT treatments were accompanied by two controls. These control tanks contained either the same percentage of ethanol that was used in 4-OHT treatments or system water alone.

2.3.6 Live Imaging

Fish were anesthetized and placed either on a 1% agarose plate with the fins spread out naturally (adults) or placed on an embryo plate (larvae). Embryo plates are 1.5% agarose plates that possess 1mm depressions, stabilizing embryos or larvae for microinjections or imaging. The plates were placed under a Leica MZ FLIII dissection microscope and images were taken using an AxioCam HSM digital camera and AxioVision AC software (Carl Zeiss). All images were processed using ImageJ (NIH).

2.3.7 *In situ* hybridizations

In situ hybridizations (ISH) on longitudinal cryosections of adult fin regenerates were performed as previously described (Smith *et al*., 2008). Whole-mount ISH were performed as previously described (Thisse and Thisse, 2008). Antisense RNA probes for *shha* (Smith *et al.,* 2006), and *gfp* (Zhang *et al*., 2012) were synthesized as previously described. For the *cre* antisense RNA probe, *cre* cDNA in pBS (Cynthia Soleck, Ekker Lab) was linearized with XhoI and transcribed *in vitro* with T7 RNA polymerase.

2.3.8 RT-PCR

Total RNA was extracted from ten adult caudal fins or 50 embryos (1 dpf) using Trizol according to manufacturers protocol. Total RNA was checked for purity (Nanodrop) and integrity (agarose gel). Total RNA (1µg) was reverse transcribed with the QuantiTect Reverse Transcription Kit (Qiagen) according to manufacturers instructions. PCR was performed using the primers listed in table 2.1. “No reverse transcription” controls and “No template” controls were run in parallel to ensure there was no contamination.

Table 2.1: Primers used for RT-PCR Analysis

Method	Primer Name	Primer Sequence 5'-3'
RT-PCR: Gene Expression Analysis	*cre* forward	TGTCTGGTGTGGCTGATGAC
	cre reverse	CTCTCATGTCTCCAGCGTCC
	β-actin forward	ATGGATGAGGAAATCGCTGCCCTGGTC
	β-actin reverse	CTCCCTGATGTCTGGGTCGTCCAAC

2.4 Results: Cell fate of *shha*-expressing cells in the adult fin regenerate

To elucidate the mechanisms involved in the observed *shha* expression patterns, 4 transgenic lines (numbered #3, #9, #15, and #17) in which the regulatory modules of *shha* drives a 4-OHT inducible ER^{T2}-CRE-ER^{T2} and a screening tool, EGFP under the control of the promoter of the heart specific *cmlc2* gene, were generated (Figure 2.2 A, 2.3). Once created, the 4 *Tg(shha: $ER^{T2}CreER^{T2}$:ABC; cmlc2:EGFP)* lines were outcrossed to *Tg(ubi:loxP-EGFP-loxP-mCherry)*. 8 hpf, double transgenic *Tg(shha: $ER^{T2}CreER^{T2}$:ABC; cmlc2:EGFP ; ubi:loxP-EGFP-loxP-mCherry)* embryos were treated overnight with 5μM of 4-OHT to test that the *cre-loxP* system was functional prior to raising adults for fin regenerate studies (Figure 2.4). 5μM 4-OHT treatments were chosen as this concentration was proven effective in our lab and previous publications (Mosimann *et al*., 2011). During development *shha*, is expressed initially in the presumptive notochord cells of the axial chordal mesoderm at 75% epiboly, or 8.0-9 hours post fertilization (hpf) (Hammerschmidt *et al.*, 1996). Subsequently, *shha* expression continues in the notochord and appears in the floor plate cells of the neural tube at 11.6 hpf, or the 5-9 somite stage (Ekker *et al*., 1995). 24hpf, *shha* is also expressed in the ventral forebrain (Krauss *et al.,* 1993). *shha* expression is then progressively lost in the notochord in a rostral to caudal manner, but is maintained in the floor plate (Krauss *et al*., 1993). Therefore, 4-OHT treatment of the double transgenic fish from 8-24hpf would activate the *$ER^{T2}CreER^{T2}$* in *shha*-expressing cells, leading to the permanent loss of EGFP and the activation of *mCherry* in the notochord, floorplate, and ventral forebrain. In line #3, 3 days post treatment (3dpt) or 3dpf, live imaging indicates a small number of cells in the notochord, floorplate, and brain had switched from EGFP to mCherry-expressing cells, in a pattern that is consistent with endogenous *shha* expression

(n = 20) (Figure 2.4 Aa-Ac). However, in the remaining 3 lines, switching was observed 4dpf or 4dpt in only a few cells of the floor plate (data not shown). No switching was observed in untreated or ethanol (EtOH) vehicle control groups (Figure 2.4 Ba-Bc, Ca-Cc).

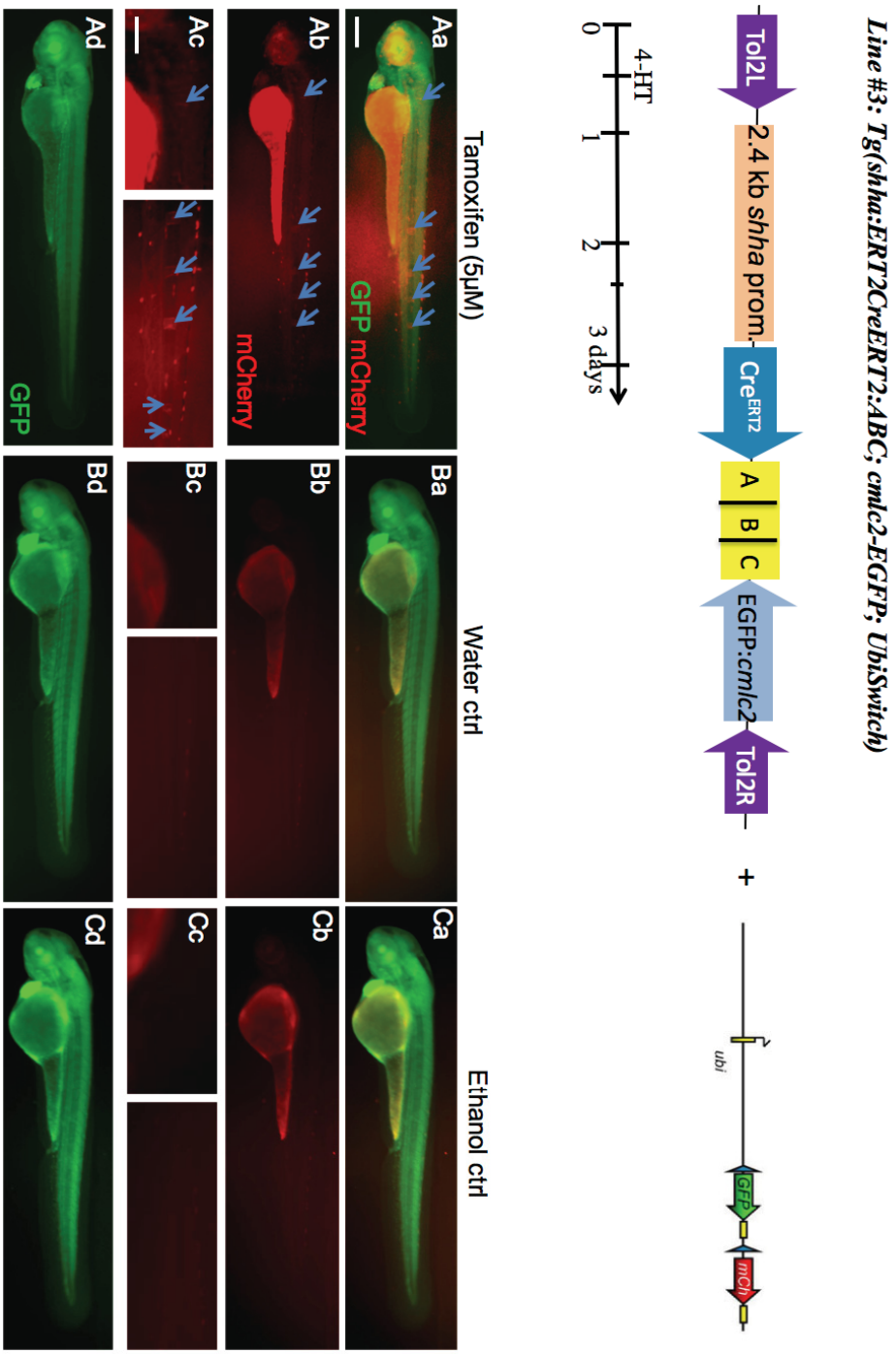

Figure 2.4: Switching of double transgenic *Tg(shha: ER^{T2}CreER^{T2}:ABC; cmlc2:EGFP; ubi:loxP-EGFP-loxP-mCherry)* embryos. (Aa-Ad) 8hpf Embryos were treated overnight with 5μM of tamoxifen and imaged daily. 3dpf/3dpt: mCherry positive cells were observed in the notochord and brain (blue arrows). (Ac) Magnified image of the notochord and brain illustrate individual mCherry positive cells. (Ba-Bd, Ca-Cd) No mCherry positive cells were observed in untreated controls (Ba-Bd) or treatment with ethanol alone controls (Ca-Cd). Scale bar for Aa-Ca, Ab-Cb, Ad-Cd = 200μm (shown in Aa); Scale bar for Ac-Cc = 200μm (shown in Ac).

Since reduced/absent switching could be from low *cre* expression, *in situ* hybridizations were performed on 2dpf *Tg(shha: ER^{T2}CreER^{T2}:ABC; cmlc2:EGFP ; ubi:loxP-EGFP-loxP-mCherry)* embryos. Out of the four lines, 2 displayed faint and patchy *cre* expression when compared to endogenous *shha* expression and *gfp* expression in the *Tg(shha:GFP:ABC#15)* line that uses the same regulatory elements (Figure 2.5). The other two lines did not display any *cre* expression (data not shown).

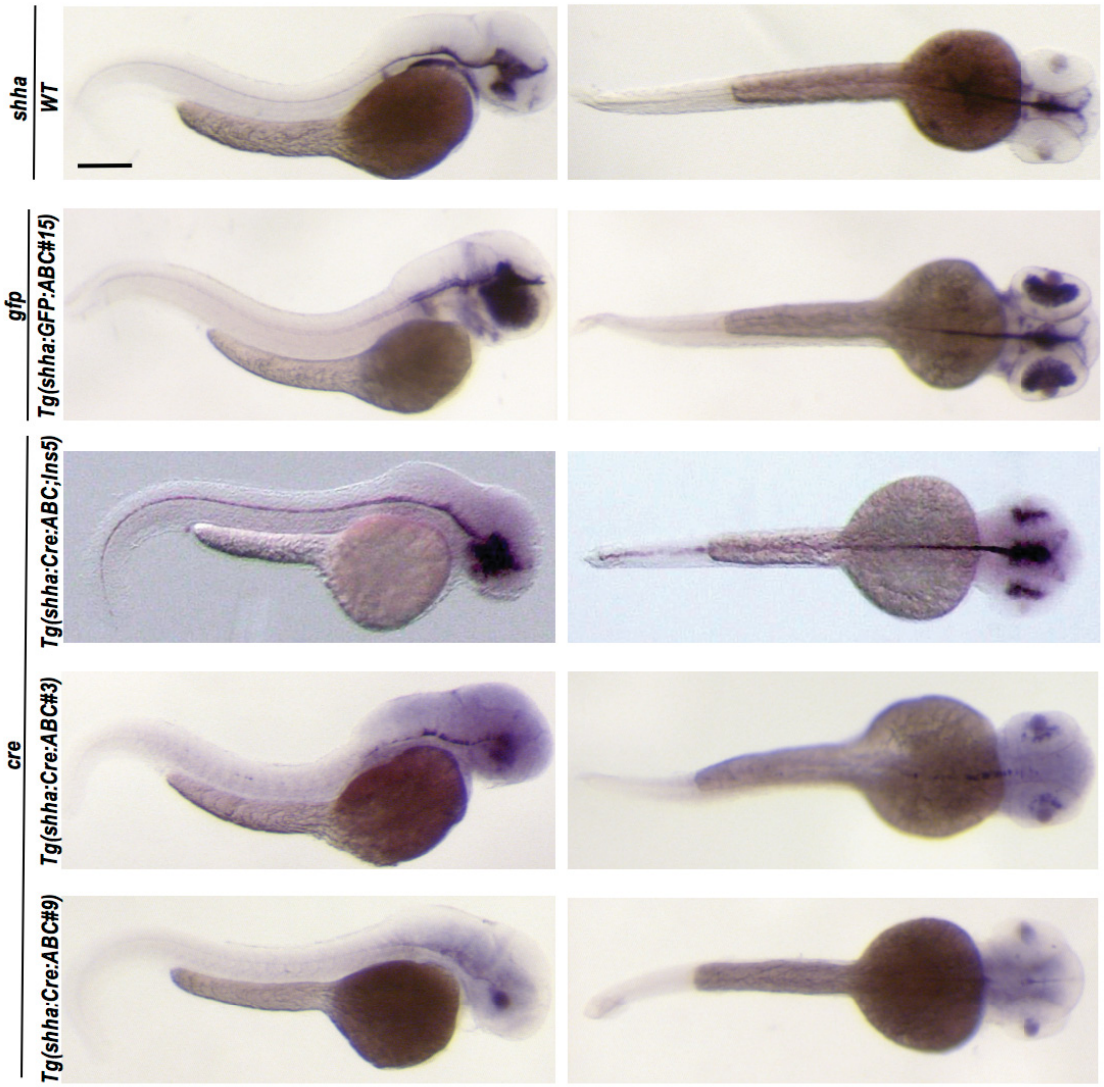

Figure 2.5: *In situ* hybridizations comparing *cre* expression with endogenous *shha* expression and *gfp* expression of *Tg(shha:GFP:ABC#15)*, in 2dpf embryos. *cre* expression in the first two lines *Tg((shha: ER^{T2}CreER^{T2}:ABC; cmlc2:EGFP #9)* and *Tg((shha: ER^{T2}CreER^{T2}:ABC; cmlc2:EGFP #3)* is patchy and faint. The addition of an insulator downstream of *ar-C*, *Tg(shha: ER^{T2}CreER^{T2}:ABC; Insulator; cmlc2:EGFP)*, strongly increased *cre* expression in a pattern similar to endogenous *shha* and mimicked the *gfp* expression pattern of *Tg(shha:GFP;ABC#15)* embryos. Scale bar for all figures = 50μm.

Although *cre* expression was faint or absent, all four *Tg(shha: ER^{T2}CreER^{T2}:ABC; cmlc2:EGFP ; ubi:loxP-EGFP-loxP-mCherry)* lines were grown to adulthood to determine the fate of *shha*-expressing cells in caudal fin regenerates. Three months post fertilization (mpf), the fins of all four *Tg(shha: ER^{T2}CreER^{T2}:ABC; cmlc2:EGFP ; ubi:loxP-EGFP-loxP-mCherry)* lines were amputated and allowed to regenerate for 2 days. At the end of the second and third days post amputation (dpa), fish were treated with 5μM of 4-OHT overnight (Figure 2.6). 3dpa/1dpt, fish were imaged daily for 5 days to observe whether there were any mCherry positive cell populations in the fin regenerate compared to untreated or equivalent ethanol treated controls (Figure 2.6). Unfortunately, mCherry-expressing cells were not observed in the fin regenerate of any lines (Lines #3, #9, #15, and #17) 7dpa/5dpt (n = 20). An example of a lack of mCherry positive cells in Line #3 can be observed on Figure 2.6 Aa-Ac.

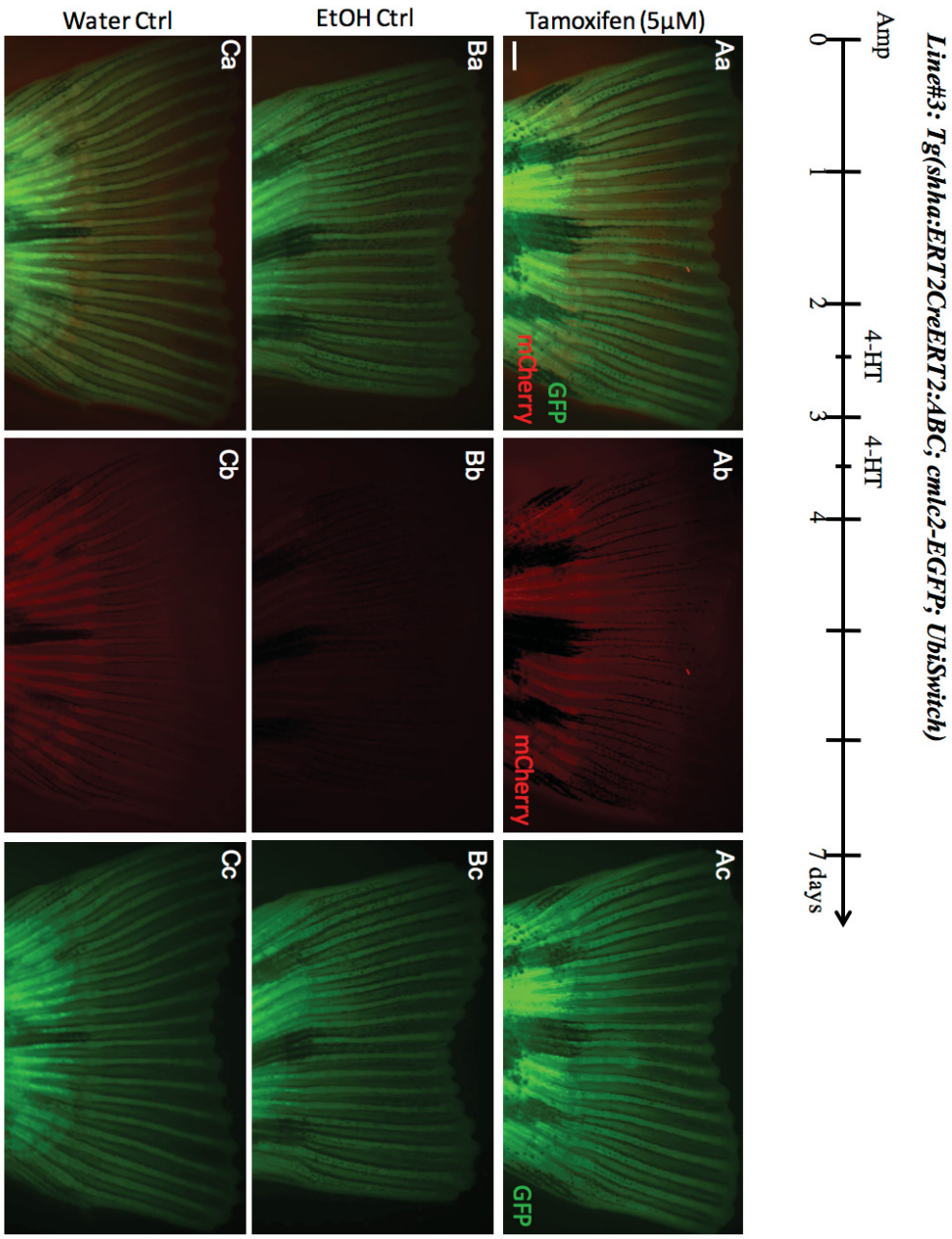

Figure 2.6: Switching of double transgenic *Tg(shha: $ER^{T2}CreER^{T2}$:ABC; cmlc2:EGFP; ubi:loxP-EGFP-loxP-mCherry)* adult caudal fin regenerates. The adult caudal fin was amputated and allowed to regenerate for two days. At the end of day 2 and day 3 adults were treated with 5µM of tamoxifen and imaged daily from 3dpa/1dpt to 7dpa/5dpt. (Aa-Ac) 7dpa/5dpt: Tamoxifen treated fin regenerates were compared to the fin regenerates of *Tg(shha: $ER^{T2}CreER^{T2}$:ABC; cmlc2:EGFP; ubi:loxP-EGFP-loxP-mCherry)* ethanol vehicle control (Ba-Bc) or untreated control fish (Ca-Cc). When compared to controls, no switching was observed in the fin regenerates of tamoxifen treated *Tg(shha: $ER^{T2}CreER^{T2}$:ABC; cmlc2:EGFP; ubi:loxP-EGFP-loxP-mCherry)* fish. Scale bar for all figures = 200µm.

Furthermore, *cre* expression could not be detected in adult caudal fin regenerates through *in situ* hybridization of all four lines (data not shown). The reduced/absent expression of *cre* in the embryos and adults led to an investigation into the details of the *(shha: $ER^{T2}CreER^{T2}$:ABC; cmlc2:EGFP)* construct used to create these four lines. The *(shha: $ER^{T2}CreER^{T2}$:ABC; cmlc2:EGFP)* construct was compared to *(shha:GFP:ABC#15)*, a construct used to make a transgenic line, which successfully expresses GFP strongly in *shha*-expressing cells of the larvae and regenerating adult caudal fin (Ertzer *et al*., 2007; Zhang *et al*., 2012). One of the differences between the two constructs was the addition of a heart marker, *cmlc2*:*EGFP*, which has recently been shown to drive GFP expression in the heart, but also suggested to suppress expression of adjacent transgenes (Figure 2.7 A-C, Chien, 2007). Furthermore, other lines created in our hands with *cmlc2*:*EGFP* resulted in lines with either a reduction or absence in transgene expression when compared to the same construct without *cmlc2:EGFP* (Figure 2.7 A, B, data not shown).

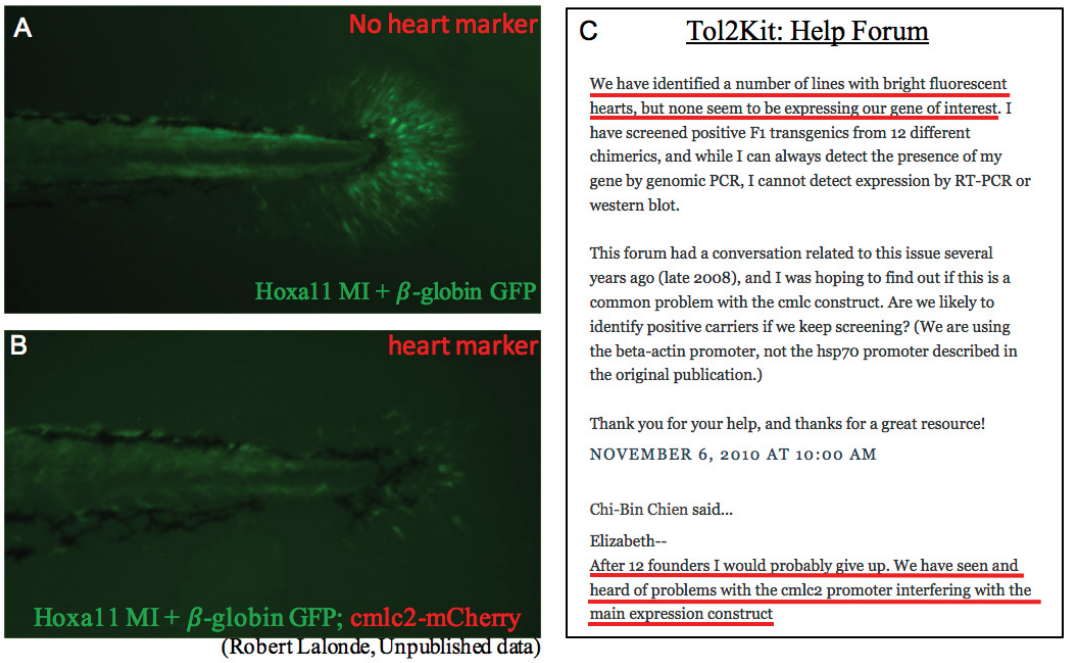

(Robert Lalonde, Unpublished data)

Figure 2.7: Evidence indicating *cmlc2-EGFP* interferes with main expression construct. (A) *Tg(Hoxa11 MI β-globin: egfp)* without any heart marker illustrates strong expression in the mesenchyme of the larval median fin fold. (B) This expression pattern is greatly reduced with the addition of *cmlc2-EGFP, Tg(Hoxa11 MI β-globin: egfp; cmlc2-EGFP*) (Robert Lalonde, unpublished data). (C) Screenshot of the Tol2Kit:Help Forum indicating other scientists have had similar problems with *cmlc2-EGFP*. Here it is suggested that *cmlc2* expresses GFP in the heart, but also interferes with the expression of the main construct (Chien *et al.,* 2007).

To resolve this potential issue, a second construct was created that included a gene insulator (HS4) from chicken downstream of the *ar-C* enhancer fragment to block any suppressive effects associated with the presence of the heart marker (Figure 2.2 B). This HS4 chicken insulator has been successfully used in other zebrafish labs (Bessa *et al.,* 2009; Zhu *et al*., 2007). Using this construct, another transgenic line *Tg(shha: $ER^{T2}CreER^{T2}$:ABC; Insulator; cmlc2:EGFP)* was created and crossed with *Tg(ubi:loxP-EGFP-loxP-mCherry)*. Double transgenic *Tg(shha: $ER^{T2}CreER^{T2}$:ABC; Insulator; cmlc2:EGFP; ubi:loxP-EGFP-loxP-mCherry)* embryos were treated 8 hours post fertilization (hpf) with 5μM of 4-OHT overnight (n = 30) (Figure 2.8). 1dpf/1dpt, strong switching was observed in the majority of cells of the notochord, floorplate and brain in 4-OHT treated double transgenic larvae (Figure 2.8 Aa-Ac). The observed switching pattern is consistent with the endogenous expression pattern of *shha* (Krauss *et al*., 1993; Ekker *et al*., 1995; Hammerschmidt *et al.*, 1996). No switching was observed in the control groups that were untreated or treated with equivalent ethanol vehicle control (Figure 2.8 Ba-Bc, Ca-Cc).

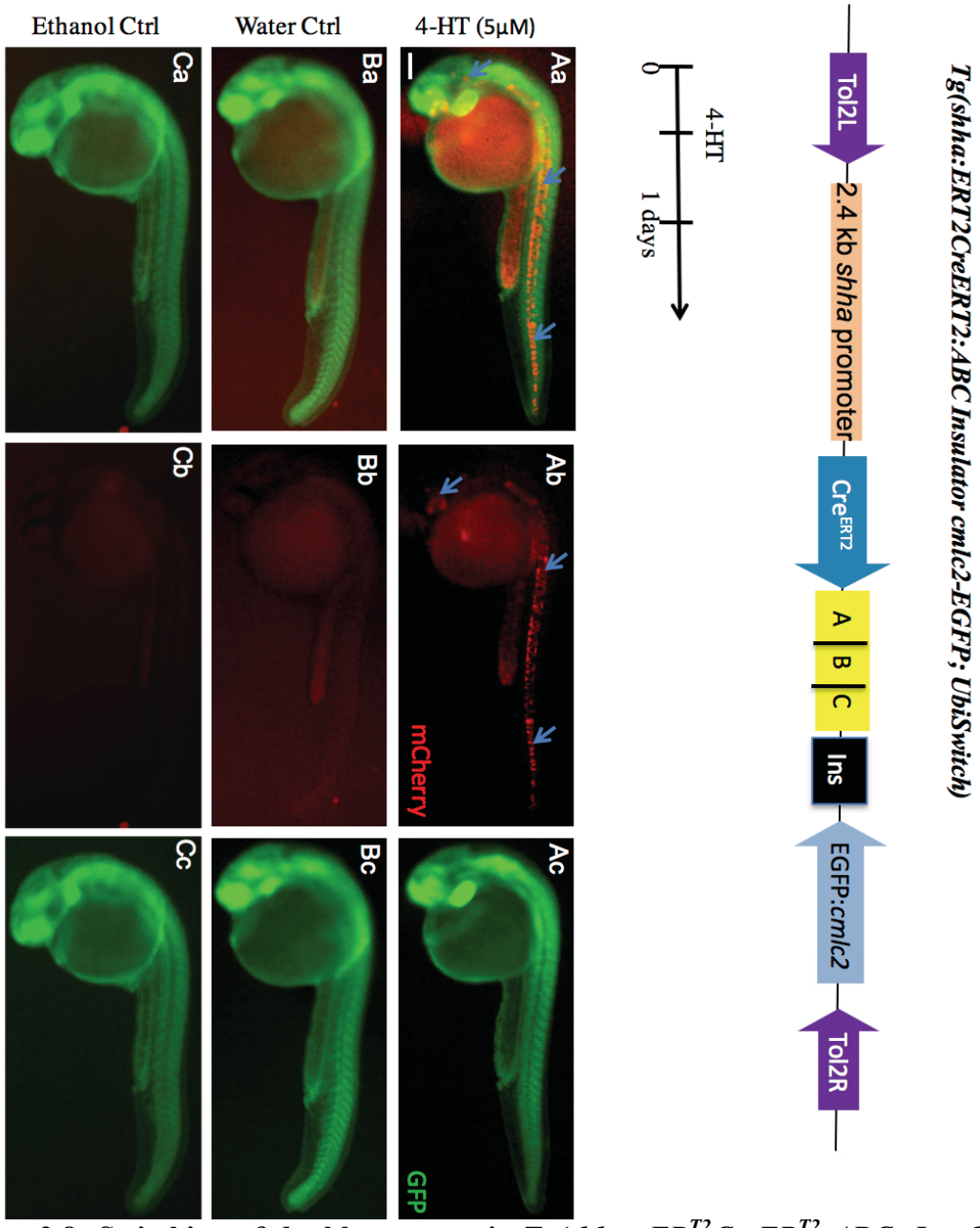

Figure 2.8: Switching of double transgenic *Tg(shha: ER^{T2}CreER^{T2}:ABC; Insulator*; *cmlc2:EGFP; ubi:loxP-EGFP-loxP-mCherry)* embryos. (Aa-Ac) Embryos treated at 8hpf with 5µM of tamoxifen overnight illustrate strong mCherry expression in the notochord and brain (blue arrows) 1dpf/1dpt. mCherry is not observed in control *Tg(shha: ER^{T2}CreER^{T2}:ABC; Insulator*; *cmlc2:EGFP; ubi:loxP-EGFP-loxP-mCherry)* embryos that were untreated (Ba-Bc) or ethanol treated controls (Ca-Cc). Scale bar for all figures = 200µm.

Furthermore, *in situ* hybridizations of 2dpf *Tg(shha: ER^{T2}CreER^{T2}:ABC; Insulator; cmlc2:EGFP)* larvae illustrate strong *cre* expression in a similar pattern to *shha*-expressing cells and *gfp*-expressing cells of the *Tg(shha:GFP:ABC#15)* line (Figure 2.5). Consequently, this line was raised to adulthood to determine the fate of *shha*-expressing cells in caudal fin regenerates. Similar to previous experiments, fins were amputated and allowed to regenerate for 2 days. 2 and 3dpa, fish were treated overnight with 2μM of 4-OHT (Figure 2.9). Previously, a dose of 5μM 4-OHT was chosen due to its effectiveness in a previous publication (Singh *et al.,* 2012). However, this dosage was reduced to 2μM as it has also been shown to be equally effective and reduced any potential damage to the fin regenerate (Personal Communication, Valerie Tornini, K. Poss Lab). Subsequent to 4-OHT treatments, caudal fin regenerates were imaged daily from 3-7dpa and compared to untreated or treated with equivalent ethanol vehicle controls (Figure 2.9). Unfortunately, no switching was observed in the caudal fin regenerates (n = 14) (Figure 2.9).

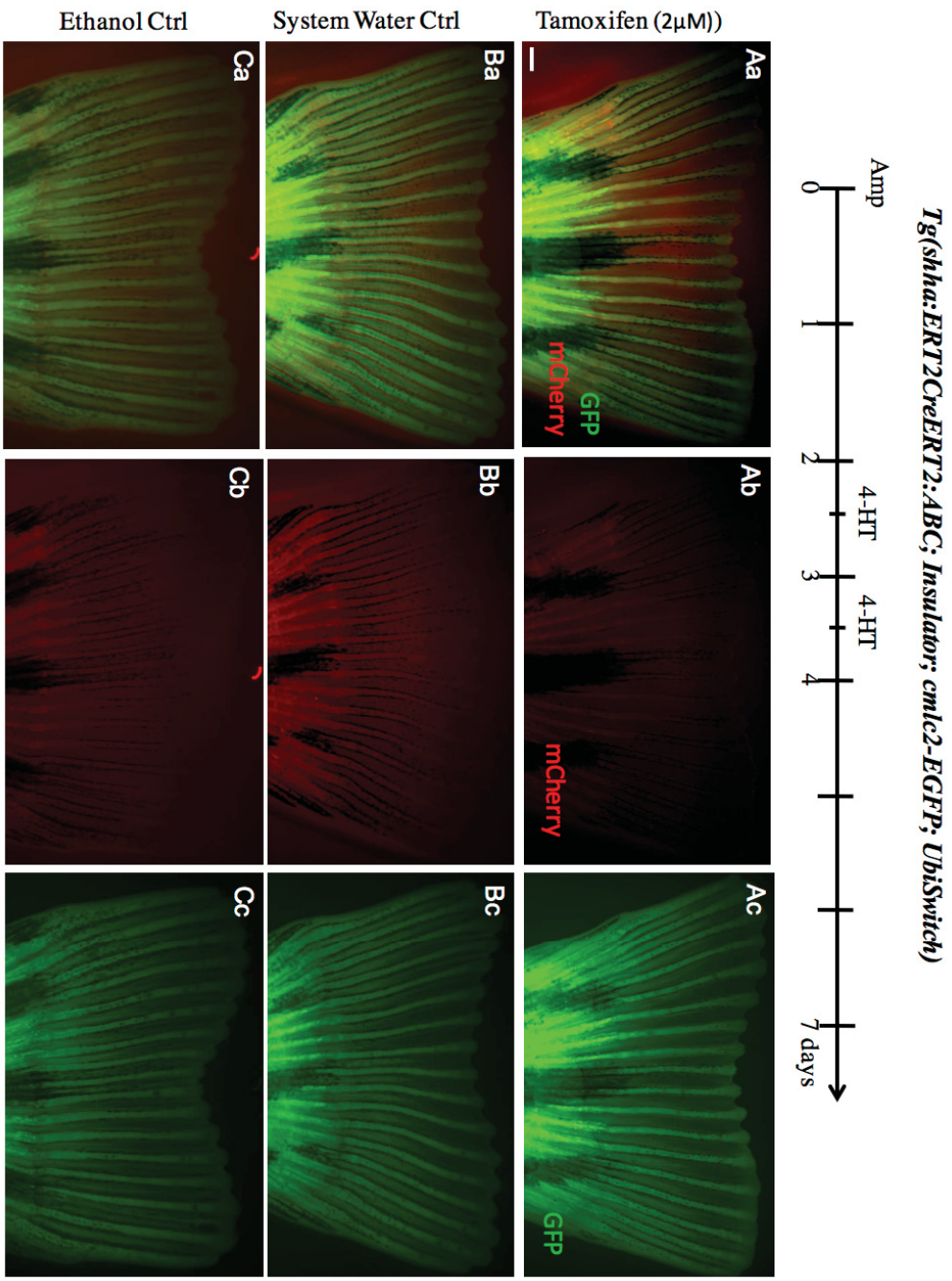

Figure 2.9: Switching of double transgenic *Tg(shha: ER^{T2}CreER^{T2}:ABC; Insulator; cmlc2:EGFP; ubi:loxP-EGFP-loxP-mCherry)* adult caudal fin regenerates. The adult caudal fin was amputated and allowed to regenerate for two days. 2dpa and 3dpa, adults were treated with 2μM of tamoxifen. Fins were imaged daily from 3dpa/1dpt to 7dpa/5dpt. (Aa-Ca) 7dpa/5dpt fin regenerates were compared to the fin regenerates of *Tg(shha: ER^{T2}CreER^{T2}:ABC; cmlc2:EGFP; ubi:loxP-EGFP-loxP-mCherry)* untreated control fish (Ba-Bc) or ethanol vehicle control fish (Ca-Cc). When compared to controls, no switching was observed in the fin regenerates of tamoxifen treated *Tg(shha: ER^{T2}CreER^{T2}:ABC; cmlc2:EGFP; ubi:loxP-EGFP-loxP-mCherry)* fish. Scale bar for all figures = 200μm.

Furthermore, *in situ* hybridizations indicate no clear *cre* expression in the caudal fin of 4dpa regenerates when compared to *shha* positive controls (Figure 2.10 A, B). However, RT-PCR indicates *cre* is expressed in the caudal fin of 4dpa regenerates (Figure 2.10 C). No *cre* expression was observed in wildtype control 4dpa regenerates. Furthermore, assays containing no cDNA and no reverse transcription controls were performed to ensure there was no genomic contamination (Figure 2.10 C). Overall, these results indicate *cre* expression was present, but too low to allow successful switching in the *Tg(shha: $ER^{T2}CreER^{T2}$:ABC; Insulator; cmlc2:EGFP; ubi:loxP-EGFP-loxP-mCherry)* adult caudal fin regenerates.

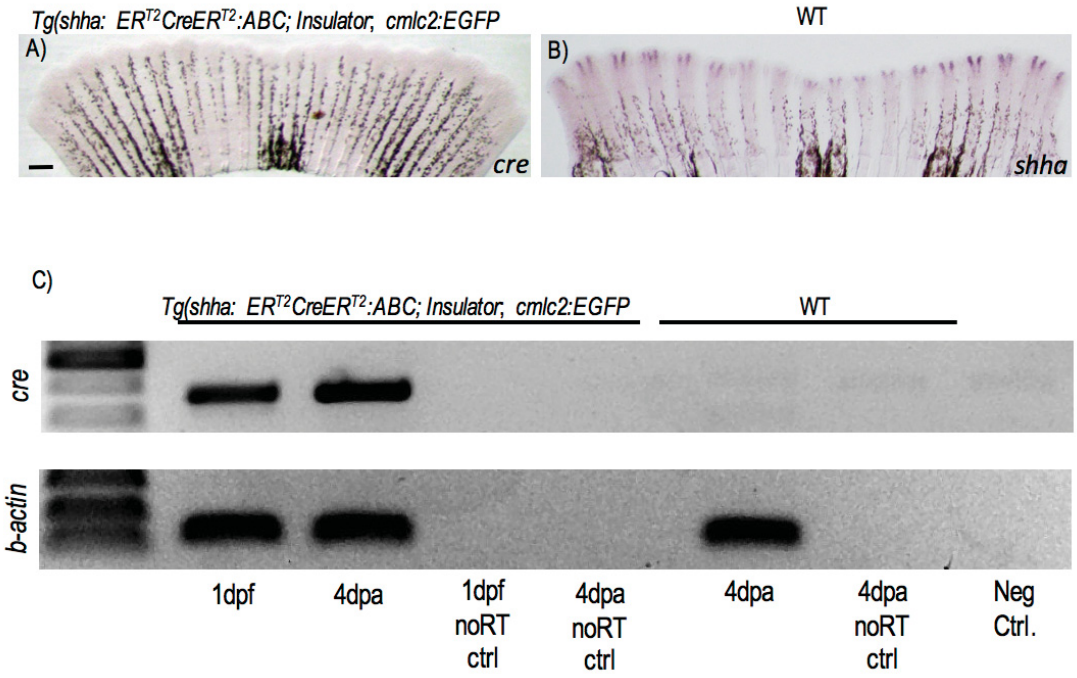

Figure 2.10: Examining *cre* expression in adult *Tg(shha: ER^{T2}CreER^{T2}:ABC; Insulator*; *cmlc2:EGFP; ubi:loxP-EGFP-loxP-mCherry)* 4dpa fin regenerates. A) *In situ* hybridization for *cre* in 4dpa fin regenerates show no visible *cre* expression where endogenous *shha* is expressed when compared to WT controls (B). C) RT-PCR indicates *cre* is expressed in the caudal fin 4dpa regenerates. No expression was observed in WT control 4dpa regenerates (WT 4dpa), No reverse transcription controls (no RT ctrl) and No template controls (Neg Ctrl). β-actin was used as housekeeping control. Scale bar for *in situ* figures = 200μm.

2.5 Discussion and Future Work:

During fin regeneration, *shha* is expressed at the level of the differentiation zone and its domain of expression splits into two prior to fin ray branching. The dynamic expression pattern implies that *shha*-expressing cells migrate or that *shha*-expression is being actively upregulated/downregulated in response to various unknown cues. Furthermore, we currently do not know to what extent the descendants of the *shha*-expressing cells contribute to the epidermis of the regenerate. To answer these questions, an inducible genetic fate-mapping approach was attempted to identify the contributions of the *shha*-expressing cell derivatives to the epidermis of fin regenerates. However, determining the fate of *shha*-expressing cells was unsuccessful due to a lack of sufficient *cre* expression in *shha*-expressing cells of the *Tg(shha: $ER^{T2}CreER^{T2}$:ABC; Insulator; cmlc2:EGFP; ; ubi:loxP-EGFP-loxP-mCherry)* line during caudal fin regeneration.

Often the first problem encountered during transgenesis is the variability of expression due to "position effects". The term position effect is used to describe the influence of the surrounding regulatory environment on the expression of a transgene following genomic integration (Jaenisch *et al*., 1981; Wilson *et al.,* 1990; Rossant *et al.*, 2011; Roberts *et al.,* 2014). This influence can be ectopic enhancement or silencing. Creating multiple transgenic lines can alleviate problems associated with position effects. In this study, 5 lines have been created, all showing a lack of sufficient *cre* expression in the adult caudal fin. Additionally, another student in the lab was unsuccessful in recapitulating *shha* expression patterns in other lines (n = 11) using the same regulatory elements (Minshuo Lin, M.Sc. Thesis, 2013). Therefore, it is unlikely that the lack of *cre* expression is due to silencing as a result of position effects. Nonetheless, in future constructs, an insulator will be added, upstream of the *shha* promoter, to the *Tg(shha:*

ER^{T2}CreER^{T2}:ABC; insulator cmlc2:EGFP ; ubi:loxP-EGFP-loxP-mCherry) construct to limit any potential position effects (Figure 2.11 B). The use of insulators has been successfully used to limit position effects (Bessa *et al*., 2009; Zhu *et al*., 2007). However, caution should be used as in some cases insulators have been unsuccessful at removing the variability associated with position effects (Grajevskaja *et al.,* 2013).

Another problem encountered during transgenesis is ensuring that all regulatory modules are included in the construct. The strong expression of *gfp* in *shha*-expressing cells of caudal fin regenerates in the *Tg(shha:GFP:ABC#15)* line indicates that the corresponding construct possesses the regulatory elements required for *cre*-expression in caudal fin regenerates. However, it is possible that the construct used to make the *Tg(shha:GFP:ABC#15)* line does not contain all the appropriate regulatory fin modules, but was coincidentally integrated within range of endogenous enhancers that boost GFP expression in *shha*-expressing cells of the developing and regenerating caudal fin. Published research on the elements associated with the *Tg(shha:GFP:ABC#15)* line focuses only on midline expression in the embryo, and suggests a lack of embryonic pectoral fin regulatory modules (Ertzer *et al*., 2007). In mouse, a *cis*-acting regulatory element that controls *Shh* expression in the limb bud has been identified 1Mb upstream from the *Shh* promoter (Lettice *et al.,* 2002). This mouse regulatory module confers expression in the zebrafish pectoral fin in a similar pattern to endogenous *shha* (Bhatia *et al.,* 2015). Therefore, it has been suggested that a similar regulatory element is potentially responsible for the expression of *shha* observed in the posterior of the developing fin bud. These results indicate that there are likely additional *shha* regulatory modules that are not present in the *Tg(shha:GFP:ABC#15)* line. However, it is unknown which regulatory

modules are required for expression in the fin rays of the adult caudal fin. Due to their large size, BAC clones often contain all, or most, of the *cis*-regulatory elements for mimicking expression of various genes (Jessen *et al.,* 1998). Furthermore, BAC transgenes tend to be more resistant to position-mediated effects from the surrounding genome (Beil *et al*., 2012). Currently, libraries of BAC clones that contain zebrafish genomic DNA have been constructed and a BAC clone containing the genomic locus of the zebrafish *shha* (CH211-105D1), is available via BAC PAC Resources. Therefore, future work could focus on creating a new transgenic line with the CH211-105D1 BAC clone using the recE, recT recombination system (ET cloning) (Zhang *et al*., 1998). The ET cloning system uses phage derived protein pairs RecE/RecT to catalyze homologous recombination between a transgene flanked by short homology arms to the region of interest and a target, in this case on a BAC clone (Muyrers *et al.,* 2001, Zhang *et al.,* 1998). Since homology arms can be used to target any sequence, any region on the BAC clone can be altered (Muyrers *et al*., 2000). Therefore, the $ER^{T2}CreER^{T2}$, Tol2 arms, an insulator, and heart marker can also be added to the BAC clone easily using ET cloning. Once generated, the BAC construct could be injected using the Tol2 System (Suster *et al*., 2009).

In this chapter, the Tol2 system was used to generate the transgenic lines. The Tol2 System involves the injection of transposase mRNA with a transgene of interest flanked with Tol2 arms, 200 and 150 base pairs of DNA from the left and right ends of the Tol2 sequence, into a one cell stage embryo (Suster *et al*., 2009). Once injected, the transposase catalyzes the transposition of a single copy of a transgene into the genome through a cut and paste mechanism (Suster *et al*., 2009). Recently there has been some speculation that the Tol2 system used to create our transgenic lines, in an as of yet unknown mechanism,

may silence expression of genes of interest following morphogenesis into adulthood (Personal communication, Dr. Hammerschmidt and Dr Bally-Cuif, 2015). Therefore, future work will include creating new constructs in which the Tol2 arms are replaced with *I-SceI* arms to employ the meganuclease system (Grabher and Wittbrodt, 2007; Thermes *et al*., 2002) (Figure 2.11 C). Transgenesis using the meganuclease system involves the injection of the *I-SceI* meganuclease, an endonuclease that recognizes an 18bp sequence not observed in the zebrafish genome, with a transgene of interest flanked at both ends by the two *I-SceI* recognition sites (Grabher and Wittbrodt*,* 2007). Once injected into the cytoplasm of one cell-staged embryos, the *I-SceI* meganuclease causes double strand breaks at the recognition sites flanking the transgene (Grabher and Wittbrodt*,* 2007). Although the exact function of the meganuclease in transgenesis is unclear, it has been suggested that the *I-SceI* endonuclease also cleaves concatamers and protects cleaved ends from degradation/ligation (Thermes *et al.,* 2002). It is suggested that these functions allow transgene integration at a higher frequency than DNA injections alone (Thermes *et al*., 2002). The *Tg(shha:GFP:ABC#15)* transgenic line, which strongly expresses GFP in the caudal fin regenerate, was created using meganuclease technology (Ertzer *et al.,* 2007). Therefore, if Tol2 was negatively impacting *cre* expression, a new Cre line made with meganucleases instead of Tol2 should also be successful. Once an adult transgenic line has been created, we will re-perform switching experiments to determine the cell fate of *shha*-expressing cells in the fin regenerate.

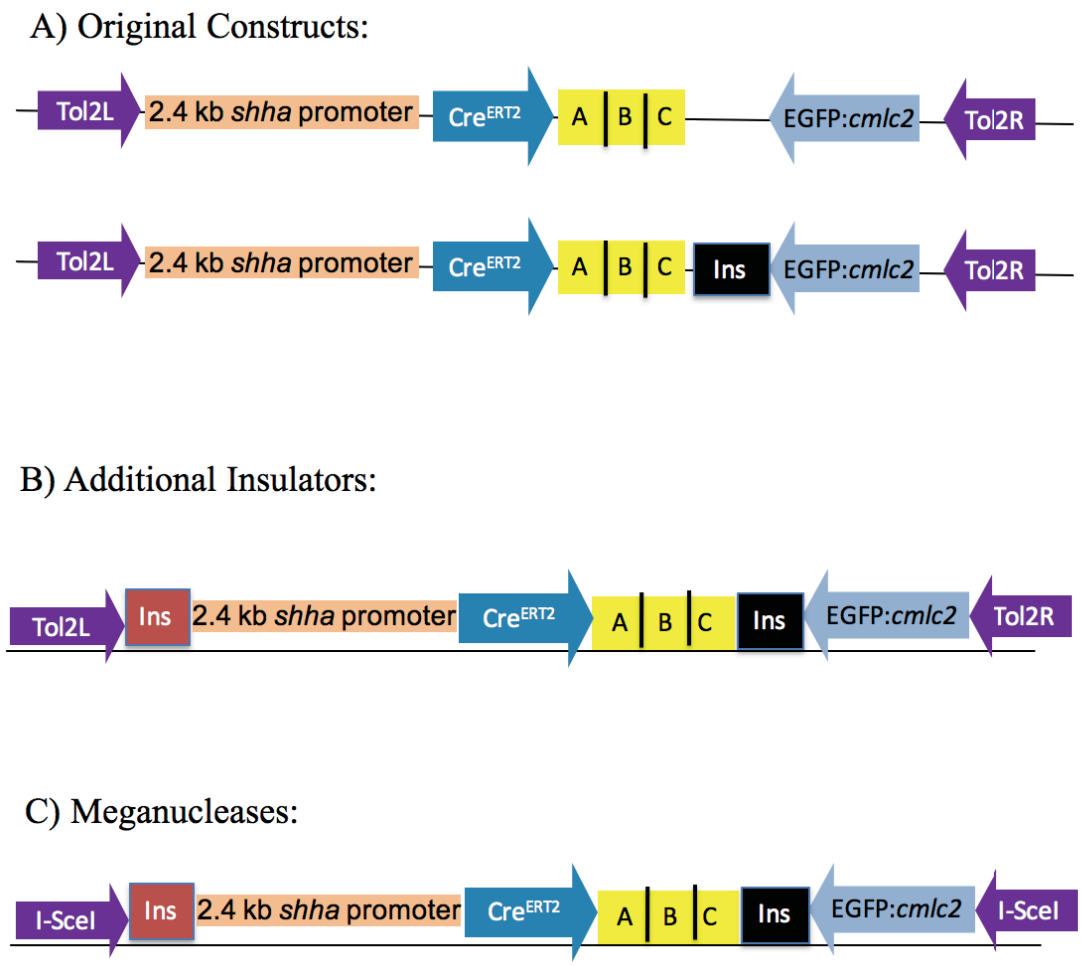

Figure 2.11: Schematic of current and future constructs that will be used to create a successful *Tg(shha: ER^{T2}CreER^{T2}:ABC; Insulator; cmlc2:EGFP)* transgenic line. A) Illustration of the original *Tg(shha: ER^{T2}CreER^{T2}:ABC; cmlc2:EGFP)* and *Tg(shha: ER^{T2}CreER^{T2}:ABC; Insulator; cmlc2:EGFP)* constructs. B) An additional insulator will be placed upstream of the *shha* promoter (red "Ins" box). C) Subsequent constructs will replace the Tol2 arms with the *I-SceI* arms (purple arrows), enabling the use of the meganuclease system.

Overall, future work will entail creating a successful line, which expresses *cre* more strongly in *shha*-expressing cells of the caudal fin regenerate. The creation of a successful line will provide evidence toward how the dynamic expression pattern of *shha*-expressing cells is maintained in the caudal fin regenerate. Furthermore, it will elucidate the ability of *shha*-expressing cells of the basal epidermal layer to contribute to upper, more differentiated layers of the epidermis.

Previous studies have shown that disruptions in the correct expression patterns through the transient deletion of *shha*-expressing cells or the *in vivo* transfection of *shha* between sister rays disrupts proper fin ray branching (Zhang *et al.,* 2012; Quint *et al*., 2002). Therefore, the dynamic expression pattern of *shha*-expressing cells is integral to the correct patterning and regeneration of the caudal fin. The above-mentioned experiments will provide a greater understanding on how these dynamic expression patterns are maintained throughout regeneration. Determining the ability of these cells to contribute to upper layers of the epidermis will provide a greater understanding of epidermal growth and regeneration.

Chapter 3: Regulation of Joint Cell Differentiation During the Regeneration of Fin Ray Bone Segments

3.1 Summary

In the first study, we sought to elucidate the cell fates of *shha*-expressing cells in the caudal fin regenerates. However, since our lab studies Hedgehog signaling, it was also discovered that *ihha* is expressed in differentiating osteoblasts of the regenerating intramembranous fin rays (Avaron *et al.,* 2006). Currently, very little is known about the roles of *Ihh* in intramembranous ossification. However, *Ihh* has been well described as a major factor regulating endochondral ossification in tetrapods (Bitgood and McMahon,1995; Vortkamp *et al.,*1996). More specifically, it has been shown that a negative feedback mechanism occurs between Ihh and PTHrP to allow the precise control over the amount of chondrocyte proliferation and differentiation during endochondral ossification in long bones (Long *et al.,* 2004). Gene expression analysis indicated that *pthrp1,* the homolog of the mammalian *Pthrp* was expressed in joint cells of the caudal fin regenerate. Consequently, the regenerating dermal fin rays were used as a model to elucidate the mechanisms underlying intramembranous ossification and joint formation. Currently, this chapter is a manuscript in preparation; however, more experiments will be added to clarify some conclusions prior to submission.

Regulation of Joint Cell Differentiation During the Regeneration of Caudal Fin Ray Bone Segments

Stephanie C. McMillan[ab*], Jing Zhang[b*], Leona Probst[b], Marie-Andrée Akimenko[bc].

[a] Department of Cellular and Molecular Medicine, University of Ottawa, ON, K1N 6N5 Canada

[b] CAREG, 30 Marie Curie, University of Ottawa, ON, K1N 6N5 Canada

[c] Department of Biology, 30 Marie Curie, University of Ottawa, ON, K1N 6N5 Canada

* Both authors contributed equally to this work.

Corresponding author:

Marie-Andrée Akimenko Department of Biology University of Ottawa 30, Marie Curie, Ottawa, ON, K1N 6N5, Canada

Fax: 613 562 5486 Tel: 613 562 5800 #7399

Key Words: Zebrafish, Caudal Fin, Regeneration, Joints, Osteoblasts, Proximal-Distal Patterning, *hox* genes.

3.2 Contribution of Authors

Stephanie McMillan: Performed all experiments related to Evx1 loss of function mutants (Figures 3.6), FK506 experiments (Figures 3.9; 3.10), and the morpholino knockdowns published in Appendix I. Additional experiments include *in situ* hybridizations (Figure 3.2 *osteocalcin, col10a1a, ihha*; 3.3 C), double fluorescence *in situ* hybridizations (Figures 3.4 A-A", C-C", D-D"; 3.5; 3.8 A', B'), qRT-PCR (Figure 3.7), and RT-PCR (Figure 3.3 D). The manuscript was also written by Stephanie McMillan.

Jing Zhang: Performed the initial experiments for this manuscript which include the initial *in situ* hybridizations (Figures 3.2 *runx2a/2b, osterix*), some of the double fluorescence *in situ* hybridizations (Figures 3.4 B-B"; 3.8 A, B, C, D-D'), laser ablation experiments (Figure 3.11; 3.12), Pcna immunohistochemistry, and Zns5 immunohistochemistry (Figure 3.1).

Leona Probst: Performed initial *in situ* hybridization studies showing *pthrp1* and *evx1* were expressed at the level of joints on consecutive sections (Figure 3.3 A, B). Additional experiments include some initial morpholino knockdowns for *ihha* and *pthrp1* (not published in this thesis).

Marie-Andrée Akimenko: Supervised the project and provided critical reading of the manuscript.

3.3 Abstract

The outgrowth of the dermal zebrafish fin rays occurs through the periodic distal addition of bone segments which are separated by joints. The present study on caudal fin regenerates suggests that osteoblasts and joint cells originate from a common cell lineage, but are committed to different cell fates. Joint cell differentiation can be separated into three distinct cell types: Presumptive joint cells, joint-forming cells, and mature joint cells. Using the *evx1* homozygous loss of function mutant and chemical inhibitor FK506, a pathway has been elucidated in which calcineurin activity regulates the position of *hoxa13a*-expressing presumptive joint cells in the fin regenerate. As differentiation progresses towards joint-forming cells, *evx1* is expressed downstream or parallel to *hoxa13a,* but upstream of *pthrp1*. The expression of all three of these factors is maintained in mature joint cells of the fin regenerate. In the absence of Evx1, *hoxa13a*-expressing presumptive joint cells are committed to an osteoblast cell fate. Furthermore, laser ablation of newly forming joint cells leads to the fusion of bone segments with no sign of joint cell regeneration. The fusion of bone segments indicates that joint cells can only regenerate in the context of the normal process of regeneration.

3.4 Introduction

In zebrafish, fin regeneration occurs as a series of three steps. These steps include wound healing, blastema formation, and regenerative outgrowth (Akimenko *et al*., 2003; Poss *et al*., 2003). During wound healing, the injured site is quickly covered through the migration and rearrangement of surrounding epithelial cells to form the wound epidermis (Poss *et al*., 2003; Santos-Ruiz *et al*., 2002; Poleo *et al*., 2001). Subsequently, cells proximal to the amputation site migrate distally (Poleo *et al.,* 2001; Nechiporuk and

Keating, 2002; Santos-Ruiz *et al*., 2002; Poss *et al*., 2003). These lineage-restricted migrating cells concurrently proliferate and de-differentiate, forming the blastema underneath the wound epidermis (Tu and Johnson, 2011; Knopf *et al*., 2011). Once the blastema has formed, the regenerative outgrowth phase is initiated. During regenerative outgrowth, the blastema is subdivided into two distinct compartments: the distal blastema and the proximal blastema (Poss *et al.,* 2003; Nechiporuk and Keating, 2002). As regeneration proceeds, cells leave the proximal blastema and enter the differentiation zone where they differentiate into the multiple cell types that reform the lost fin.

Osteoblast-derived blastema cells entering the differentiation zone come in contact with *sonic hedgehog a* (*shha*) - expressing basal epidermal cells and differentiate into osteoblast progenitors expressing *indian hedgehog a* (*ihha*)*, patched-1* (*ptc-1*)*,* and *bone morphogenetic protein 2b* (*bmp2b*) (Avaron *et al*., 2006; Laforest *et al*., 1998; Knopf *et al.,* 2011). Currently, the molecular mechanisms underlying osteoblast differentiation are unclear. However, previously, it was shown that Bmp2b, a downstream target of Hedgehog signaling, mediates osteoblast differentiation through the induction of early osteoblast markers *runt-related transcription factor 2a* and *2b* (*runx2a* and *runx2b*) (Smith *et al.,* 2006). Upon commitment to an osteoblast fate, cells express *sp7 (*also named *osterix, osx*), and further differentiation results in the expression of bone matrix genes *osteocalcin* (*Bgp, osc*) and *collagen, type X, alpha 1a* (*col10a1a*) (Sousa *et al*., 2011; Avaron *et al*., 2006; Gavaia *et al.,* 2006). These mature osteoblasts synthesize and release bone matrix into the subepidermal space to form the dermal fin rays (Marí-Beffa *et al*., 1996; Akimenko *et al*., 2003). Currently, the specific role of Ihha during osteoblast differentiation in the dermal fin rays is unclear.

However, Ihha has been shown to play a role in the formation of craniofacial intramembranous bones in zebrafish larvae (Huycke *et al.,* 2012). More specifically, it has been shown that *ihha* is expressed in the growing edge of the opercle, one of the bones that make up the craniofacial skeleton (Huycke *et al*., 2012). Furthermore, analysis of *ihha* and *ptc-1* mutants indicate that Hh signaling is required for the recruitment and proliferation, but not differentiation of *runx2a/2b* expressing pre-osteoblasts to the growing edge (Huycke *et al*., 2012). Later in development, *ihha* mutants display fusions between opercular dermal bones that normally form functional articulations, suggesting that Ihha also plays a role in maintaining joint identity (Hulsey *et al.,* 2005; Huycke *et al.,* 2012). Other studies in mouse and chick have revealed conflicting mechanisms by which Ihh signaling at osteogenic fronts may regulate intramembranous bone ossification during cranial suture formation (Abzhanov *et al*., 2007; Lenton *et al*., 2011). During mouse cranial suture formation, it has been shown that in the absence of Ihh, osteoblast differentiation was significantly reduced, leading to widened sutures (Lenton *et al*., 2011). Therefore, it was suggested that Ihh promotes osteoblast differentiation (Lenton *et al.,* 2011). In contrast, other studies in chick and mouse indicate that a loss in Ihh results in premature differentiation of osteoblasts in the suture region, resulting in widened sutures (Abzanov *et al.,* 2007). These results indicate that *Ihh* inhibits differentiation of osteoblasts into mature osteoblasts (Abzhanov *et al.,* 2007). Interestingly, it has been shown that *parathyroid hormone related protein* (*Pthrp*), expressed in cells of osteogenic fronts during cranial suture formation, similarly prevents the differentiation of preosteoblasts to an osteoblast cell fate (Abzhanov *et al*., 2007). Whether Ihh and PthrP interact during intramembranous ossification is unclear, but they have been suggested to act in parallel

pathways (Abzhanov *et al.,* 2007). Overall, the mechanisms underlying intramembranous ossification are controversial and unclear. However, the roles of PthrP and Ihh during endochondral ossification, a process in which a cartilage template is replaced by a bony matrix (Erlebacher *et al.,* 1995), have been well established.

During early endochondral ossification in the long bones, PTHrP signals from the periarticular perichondrium, through its receptor, *parathyroid hormone related receptor 1* (*Pthr1*), keeping growth plate cells in a proliferating state and suppressing *Ihh* expression (Lanske *et al*., 1996; St-Jacques *et al.,* 1999; Kronenberg 2003; Vortkamp *et al*. 1996). Since PTHrP is secreted to exert its effect on surrounding cells, the extent of the domain of proliferating chondrocytes in the growth plate is limited by the distance of the cells from the site of PTHrP production. In cells at a great enough distance, PTHrP cannot exert its effects, allowing chondrocytes to stop proliferating and begin hypertrophy (Zhao *et al*. 2002). Ihh signaling, from early hypertrophic cells, then stimulates the production of PTHrP and proliferation in the perichondrium (Kobayashi *et al.* 2002; Kronenberg 2003; Vortkamp *et al*. 1996). The feedback mechanism between Ihh and PTHrP allows the precise control over the amount of chondrocyte proliferation and differentiation (Long *et al.,* 2004). Independent of PTHrP signaling, Ihh has also been shown to promote chondrocyte hypertrophy (Mak *et al.,* 2008), and stimulate osteoblast differentiation of the mesenchymal cells surrounding the cartilage model (Karp *et al*., 2000; Long *et al.,* 2004; St-Jacques *et al.,* 1999).

Duplicated Pthrp paralogs, *pthlha* (*pthrp1*) and *pthlhb* (*pthrp2*) are expressed in larval zebrafish tissues (Yan *et al.,* 2012). Similar to tetrapods, *pthlha* (*pthrp1*), which has been shown to be the most similar to human PTHLH, inhibits differentiation in both

intramembranous and endochondral ossification through the suppression of *runx2a* and *runx2b* (Yan *et al.,* 2012). However, the exact mechanism in which this occurs is unknown.

The zebrafish dermal caudal fin rays are periodically segmented along the proximal distal axis. Between each segment are non-moveable, collagen rich, joints that are comparable to fibrous joints that are typically found between skull bones, or cranial sutures (Borday *et al*., 2001). The regeneration of joints appears initially as a condensation of a discrete band of cells in the distal fin regenerate (Pacifici *et al*., 2006). As the joints mature and become more proximal, two distinct rows of cells form that eventually separate, leaving a space in the bone matrix (Sims *et al*., 2009).

Currently, the mechanisms controlling joint formation during growth and regeneration of the fin rays are largely unknown. However, it has been suggested that the presumptive joint regions express a unique set of genes that are involved in joint formation. The *even-skipped homeobox 1* (*evx1*) gene, which belongs to a family of vertebrate *eve-related homeobox* genes (Faiella *et al*., 1991), and encoding for a transcription factor, is expressed in at the level of joints and has been shown to be required for joint formation during development and regeneration (Schulte *et al*., 2010; Borday *et al*., 2001; Sims *et al*., 2009). More specifically, homozygous *evx1*$^{-/-}$ null mutants lack fin ray joints (Schulte *et al*., 2011). Currently, the exact mechanism by which Evx1 controls joint formation is unknown. However, mutations in *cx43* (*sof*^{b123}) and *kcnk5b* (*alf*^{dty86}) have been shown to alter *evx1* expression, resulting in shorter and longer fin ray segments, respectively (Sims *et al.,* 2009). In addition, *sof*^{b123} mutants possess short fin lengths (Iovine *et al.,* 2005; Hoptak-Solga *et al.,* 2008; Ton and Iovine, 2013), while *alf*^{dty86} mutants possess inconsistent/longer segment lengths (Ton and Iovine, 2013; Perathoner *et al*., 2014). The

correlation between segment length and fin size indicates that the mechanisms controlling fin growth and joint formation may be linked. However, the *long fin* (*lof*) and *rapunzel* (*rpz*) overgrowth mutants do not have altered segment lengths (Goldsmith *et al.,* 2003; Iovine and Johnson*.,* 2000). Additionally, *evx1* mutants that lack joints have normal fin lengths (Schulte *et al.,* 2011). Therefore, joint formation may also occur independently from growth.

Recently, calcineurin, a Ser/Thr phosphatase, was identified as an inhibitor of regenerative outgrowth and regulator of proximal distal patterning (Kujawski *et al*., 2014). The role of calcineurin in regulating growth and proximal-distal patterning indicates that it may also regulate joint formation. Currently, the exact mechanism in which calcineurin regulates growth and proximal-distal patterning in the fin regenerate is unknown. However, it has been suggested that calcineurin acts through the inhibition of retinoic acid signaling (Kujawski *et al.,* 2014).

Overall, the mechanisms underlying intramembranous ossification and joint formation in the caudal fin rays must be clarified. In this report, we have characterized a morphologically distinct group of non-proliferating cells that emerge along the proximal-distal axis that correspond to the locations of joint formation. Based on gene expression analysis, cells expressing *runx2a, runx2b* and *hoxa13a* are specified to become joint cells, but possess the ability to commit to an osteoblast cell fate. As regeneration progresses, presumptive joint cells commit to the joint cell lineage and express *evx1*, *hoxa13a*, and *pthrp1*. During joint cell differentiation a regulatory pathway leading to joint cell formation is emerging where *hoxa13a* acts upstream or parallel to *evx1,* which regulates *pthrp1.* In the absence of *evx1*, *pthrp1* expression is lost and *hoxa13a* expressing presumptive joint

cells are committed to an osteoblast cell fate. Furthermore, laser ablation of joint cells in the fin regenerate leads to the fusion of bone segments, suggesting joint cell differentiation occurs only at specific intervals during osteoblast regeneration. Collectively, these results suggest a mechanism for joint cell differentiation during caudal fin regeneration.

3.5 Materials and Methods

3.5.1 Animal Maintenance

All fish used in the experiments were maintained at 28°C with a photoperiod of 14 hours of light and 10 hours of darkness. Fish were fed regularly (Westerfield, 1995). Homozygous *evx1*$^{-/-}$ mutant fish were a gift from Dr Katherine E. Lewis (Schulte *et al*., 2011). The *Tg(Hoxa11 MI β-globin: egfp)* transgenic line, was generated by Robert Lalonde (Akimenko lab). All experiments were performed according to the CCAC guidelines.

3.5.2 Fin Amputations

Zebrafish were anesthetized by immersion in system water containing 0.17mg/ml tricaine (Westerfield, 1995). Caudal fins were amputated 2 segments proximal from the first branch point of the lepidotrichia. Fish were then returned to fresh system water to recover.

3.5.3 Live Imaging

Fish were anesthetized and placed on a 1% agarose plate with the caudal fins spread out naturally (adults). The plate was placed under a Leica MZ FLIII dissection microscope and images were taken using an AxioCam HSM digital camera and AxioVision AC software (Carl Zeiss). All images were processed using ImageJ (NIH).

3.5.4 *In situ* hybridizations

In situ hybridizations (ISH) on longitudinal cryosections of adult fin regenerates were performed as previously described (Smith *et al*., 2008). Antisense RNA probes for *evx1* (Thaëron *et al*., 2000), *ihha* (Avaron *et al*., 2006), *hoxa13a* (Ahn and Ho, 2008), *col10a1a* (Padhi *et al*., 2004), *bmp2b* (Nikaido *et al.,* 1996), *ptc-1* (Condordet *et al*., 1996),

and *osx* (Li *et al.,* 2009) were synthesized as previously described. *pthrp1* (693bp) was amplified using *pthrp1* forward 5'-ggggacatcatcatcatcatc-3' and *pthrp1* reverse 5'-agcatttaggcgtcacaagtcctc-3' primers and inserted into pDrive, linearized with XhoI, and transcribed *in vitro* with T7 RNA polymerase. *pth1R* (654bp) was amplified using *pth1R* forward 5'-ggcctggaacagaaggactc-3' and *pth1R* reverse 5' -ATTCACGTCCCCACAATGCT-3' primers and cloned into pDrive. *pth1R* was then linearized with BamHI and transcribed *in vitro* with Sp6 RNA polymerase.

3.5.5 Double Fluorescence *in situ* hybridizations on Sections

Double fluorescence ISH on longitudinal cryosections of adult fin regenerates was adapted from protocols that were previously described (Welten *et al.,* 2006; Perkin-Elmer Manufacturers protocol). Briefly, 4dpa adult caudal fin regenerates were fixed and sectioned as previously described (Smith *et al*., 2008). Hybridization and post-hybridization washes on sections were also performed as previously described (Smith *et al*., 2008). Slides were incubated for 10min in 2% H2O2 in TBST, washed (4 x 5 min) in TNT (0.1 M Tris-Hcl pH 7.5; 0.15 M NaCl; 0.5% Tween20), blocked for 4 hours in TBSTB (TNT with 0.5% Perkin-Elmer blocking powder), and incubated overnight in anti-DIG-POD (1:100) (Perkin-Elmer) in TBSTB at 4°C. Slides were then washed in TNT (3 x 30 min), stained with Tyr-Cy3 (1:100) in amplification diluent (Perkin-Elmer), and washed in TNT (3 x 5 min). Steps were then repeated from the "2% H2O2 in TBST" step until the "blocking step". Slides were then incubated overnight with anti-DNP-POD (1:100)(Perkin-Elmer) at 4°C. Slides were then washed in TNT (3 x 30 min), stained with Tyr-Fluorescein (1:100) in amplification diluent (Perkin-Elmer), and washed in TNT (3 x 5 min). Slides were then incubated in DAPI stock solution (5mg/ml) diluted to 1:10000 with TNT (1 x 5

min), washed in TNT (3 x 5 minutes), washed briefly with water, and mounted with AquaPolymount.

3.5.6 FK506 Treatments

FK506 (Tacrolimus) (Sigma) was dissolved in ethanol and added to system water at 0.1μg/L; this concentration was chosen based on published data (Kujawski *et al*., 2014). Fish were treated with FK506 for two days prior to fin amputation to ensure the chemical had time to take effect. 2 days post treatment (dpt), fins were amputated and allowed to regenerate for 4-8 days depending on the study. Every two days, the water was changed with fresh drug. Zebrafish were fed and kept in glass tanks throughout treatments. Control tanks contained either the same percentage of ethanol or system water alone. Each experiment was performed in triplicate (4 fish/tank/experiment).

3.5.7 Laser Ablation Experiments

Fish were anesthetized in tricaine and placed under an upright Nikon FN1 Microscope. Using a 25x water immersion lens, the most immature joints were chosen on three adjacent regenerating fin rays. Laser settings were as follows: 100% laser power, wavelength of 700nm, stimulation speed of 4lines/s, and a stimulation time of 10 seconds. Following laser ablations, fish were flipped over and laser ablations were performed again to ablate joint cells on adjacent hemirays. Following laser ablations, fish were returned to system water for recovery. Live imaging was performed daily following laser ablations to observe the effect on joint formation.

3.5.8 Immunohistochemistry

Fin regenerates were fixed in 4% paraformaldehyde overnight at 4°C and cryosectioned as previously described (Smith *et al*., 2006). PCNA immunohistochemistry

was performed as previously described (McMillan *et al*., 2013). Zns5 immunohistochemistry was adapted from a protocol that was previously described (Smith *et al*., 2006). Longitudinal cryosections of 4dpa fin regenerates were incubated with ZNS5 monoclonal antibody (1:200) alone or in conjunction with a rabbit anti-GFP (Molecular Probes) at 1:500. Fluorescently labeled secondary antibodies Alexa Fluor 488 goat anti-mouse IgG (H+L) (Invitrogen A11001) were used at 1:500. Slides were counterstained with DAPI and mounted.

3.5.9 RT-PCR

Total RNA was extracted from ten adult caudal fins or 50 embryos (1 dpf) using Trizol according to manufacturers protocol. Total RNA was checked for purity (Nanodrop) and integrity (agarose gel). Total RNA (1µg) was reverse transcribed with the QuantiTect Reverse Transcription Kit (Qiagen) according to manufacturers instructions. PCR was performed using the primers listed in Table 3.1.

3.5.10 qRT-PCR

Total RNA was extracted from 10 zebrafish fin regenerates using TRIZOL according to the manufacturer's protocol (Invitrogen). Tissue incorporating all the fin regenerate distal to the amputation site was extracted. 1µg of total RNA from each sample was reverse transcribed with the QuantiTect Reverse Transcription Kit as per the manufacturer's protocol (Qiagen). Quantitative PCR reactions were carried out in triplicate with four different biological samples using the CFX96 Touch™ Real-Time PCR Detection System (BioRad). The specificity of the reactions was confirmed by using melting curve and gel electrophoresis analysis. Assays containing no cDNA and no reverse transcription controls were also performed for each primer set to ensure there was no

contamination. The relative amount of each transcript (*bmp2b, ihha, ptc1, and col10a1a*) was normalized to the level of the housekeeping genes (*β-actin, gapdh, eef1a1l1, and 18srna*). The target stability of each housekeeping gene was calculated using the geNorm method (Hellemans *et al.* 2007), which has been integrated into the CFX Manager 3.1 Software (BioRad). All housekeeping genes were determined to be stable between *evx1*$^{-/-}$ mutant and wildtype fin regenerates using the geNorm method. Graphics and statistical significance ($p<0.001$) were analyzed using the CFX Manager 3.1 Software. Primers used for qRT-PCR were designed using the software PrimerBlast (NCBI) and Multiple primer analyzer (ThermoScientific) and are indicated in Table 3.2.

Table 3.1: Primers used for RT-PCR Analysis.

Method	Primer Name	Primer Sequence 5'-3'
RT-PCR	*β-actin* forward	ATGGATGAGGAAATCGCTGCCCTGGTC
	β-actin reverse	CTCCCTGATGTCTGGGTCGTCCAAC
	pthrp1 forward	CGTAATGCTGAGCCGGACA
	pthrp1 reverse	TCACTGAACGCTTCATTCGGCT
	pthrp2 forward	AGCAGACAACGGCGTTCAGT
	pthrp2 reverse	GCATTTGGAAGGCACACGCT
	pth1R forward	TGTGCCAAATTCTTCCCCCA
	pth1R reverse	GAGCCGTCGAAAGTATCCGA
	pth2R forward	CTTCTGTTCTCCGCGTCAGT
	pth2R reverse	ATGCATGTGCTGCATGGTTG
	pth3R forward	AAGCATGGTGTCAGTGGAGG
	pth3R reverse	ACGCGTATCCTCTGTGGTTG
RT-PCR: Splice Blocking Efficiency	*pthrp1* forward	AGGACGTAATGCTGAGCCGGACAC
	pthrp1 reverse	GGTTTGTGCCCTCCTCATCTTCCAG
	ihha forward	TCTCCATGACTGGCTTTGCGTAAAGC
	ihha reverse	GCGTAGCAGGAGGAAACAATGCCA

Table 3.2: **Primers used for qRT-PCR Analysis**

Method	Primer Name	Primer Sequence 5'-3'
qRT-PCR:	*bmp2b* forward:	CGAGGAGCACTATGGGAAAACAT
	bmp2b reverse	TTTTCCTTTCAGGCTGGACAGTG
	eef1α forward	CTGGAGGCCAGCTCAAACAT
	eef1α reverse	ATCAAGAAGAGTAGTACCGCTAGCATTAC
	col10a1 forward	CAGTACCAGCCTTACTCCGTG
	col10a1a reverse	GGCAGACCTTCACCATCTTGT
	patched1 forward	TTGGCCCTTATCCTGAGGTATC
	patched1 reverse	GTCGTGTGACTTGGACGCAT
	gapdh forward	CGCTGGCATCTCCCTCAA
	gapdh reverse	TCAGCAACACGATGGCTGTAG
	β-actin forward	CGAGCTGTCTTCCCATCCA
	β-actin reverse	TCACCAACGTAGCTGTCTTTCTG
	18srna forward	GGCGGCGTTATTCCCATGACC
	18srna reverse	GGTGGTGCCCTTCCGTCAATTC
	ihha forward	GGGCAAGATCACCAGGAACT
	ihha reverse	GAGTGCTCTGACTTGACGCTG

3.6 Results:

During regeneration, the fin rays are established through the periodic distal addition of new lepidotrichial segments separated by joints (Johnson and Bennett, 1999; Iovine and Johnson 2000). Analysis of brightfield images illustrate the periodic addition of joints to the distal fin rays (Figure 3.1 A, A'). Measurements between the first two formed joints indicate that the first segment formed during regeneration is approximately 200-300μm in length depending on the observed fin ray and proximal distal location on the fin (n = 12). Following 4',6-diamidino-2-phenylindole (DAPI) stains on longitudinal cryosections of 4dpa fin regenerates, a small cluster of cells aligned with the osteoblast layer was observed approximately 200-300μm from the last formed joint (n = 12) (Figure 3.1 B, B'). Considering the location of the cell cluster in relation to the last formed joint, it appears that these cells are the newly forming distal joints that were observed on the wholemount brightfield images (Figure 3.1 A, A'). Analysis of cell proliferation using Pcna immunohistochemistry on 4dpa fin regenerates indicates strong proliferation in the blastema, but no proliferation in the joint cell cluster outlined by a DAPI counterstain (Figure 3.1 C-C'').

3.6.1 Zns5 Positive Joint Cells Express Only Early Osteoblast Differentiation Markers

Previously, Zns5, an antibody directed against osteoblasts of all differentiation stages (Johnson and Weston, 1995), has been used to observe joint formation in fin regenerates (Sims *et al*., 2009). As expected, the Zns5 antibody labels joint cell clusters and the adjacent osteoblasts in the fin regenerate (Figure 3.1 D, D'). Since joint-forming cells are labelled with Zns5, osteoblast differentiation markers were analyzed.

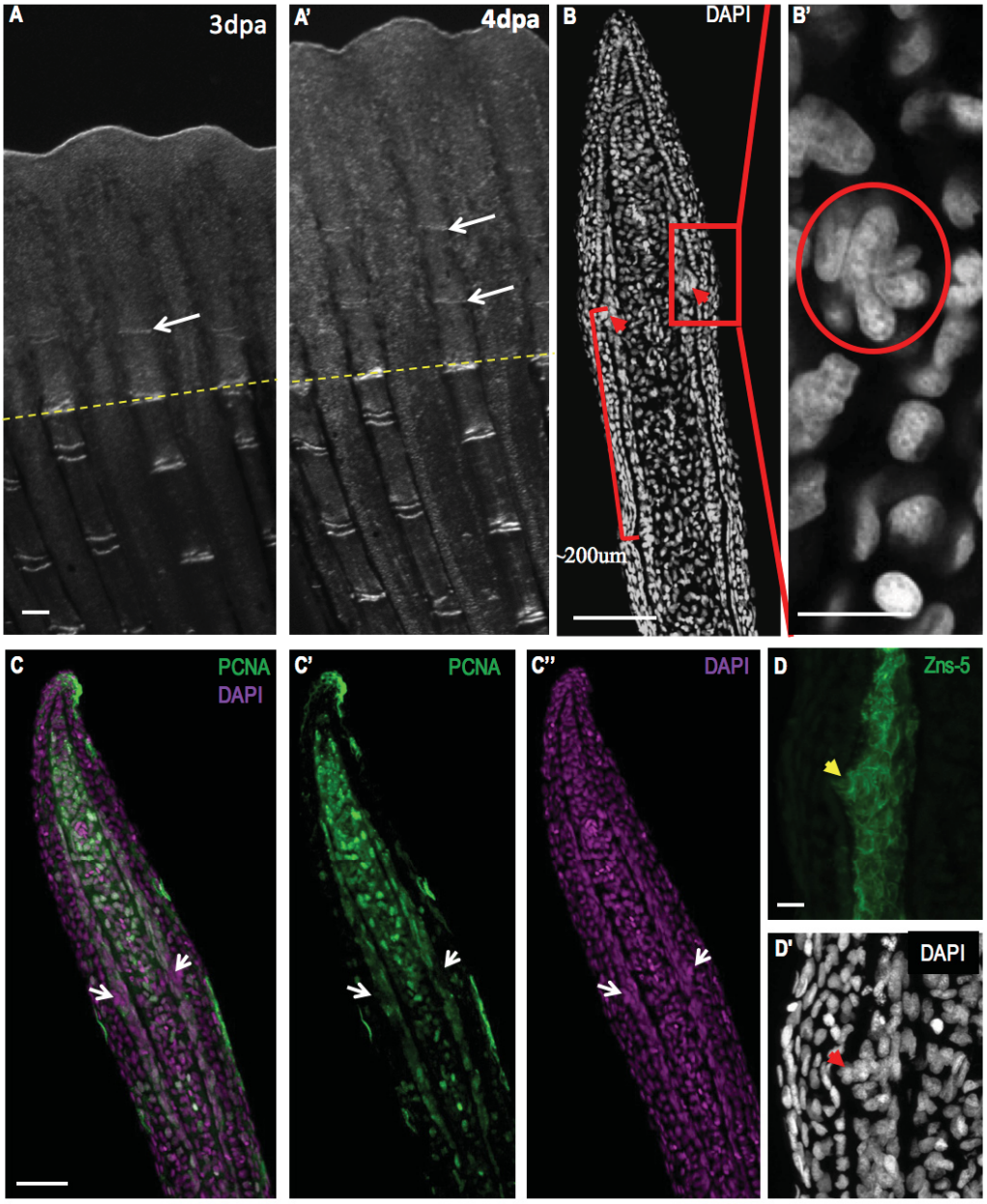

Figure 3.1: Analysis of joint cell clusters on wholemount and longitudinal sections of fin regenerates. (A-A') Brightfield images of the 3dpa (A) and 4dpa (A') fin regenerate illustrates the periodic addition of joints (white arrows) to the distal end of fin rays. (B) DAPI stains on a longitudinal cryosection illustrates a single cluster of nuclei approximately 200μm from a joint in the osteoblast layer of each hemiray on a 4dpa fin regenerate (red arrows). (B') Magnified image of the nuclei cluster (red circle). (C-C'') PCNA immunohistochemistry counterstained with DAPI illustrates the cell clusters (white arrows) are not proliferating. (D) The osteoblast marker Zns5 labels the cell cluster and adjacent osteoblasts. (D') DAPI counterstain to identify cell clusters of Zns5 immunohistochemistry. (C-C'') Merged PCNA and DAPI (C), PCNA image alone (C') and DAPI image alone (C''). Scale Bars = A-A' , B-B', C-C'' = 100μm; D-D' = 10μm.

Gene expression analysis using ISH indicates *runx2a* and *runx2b*, pre-osteoblast markers (Smith *et al.,* 2006; Nakashima *et al*., 2002), are expressed in osteoblasts including in the cells forming a "bump" that corresponds to the joint cell cluster (Figure 3.2). However, the joint cell cluster does not express subsequent lineage-commitment osteoblast marker *osx* or late osteoblast marker *col10a1a*, as there is a gap of expression corresponding to the "bump" or joint cell cluster (Figure 3.2). Late osteoblast marker, *osc* remains proximal on the fin regenerate compared to other osteoblast markers and is not expressed in joint cell clusters or joints (Figure 3.2; Sousa *et al*., 2011). Furthermore, *ihha* is not expressed in the joint cell clusters, although this must be confirmed by RT-PCR (Figure 3.2). Overall, this data indicates that the joint cells and osteoblast cells may originate from a common cell lineage, but are later committed to different cell fates.

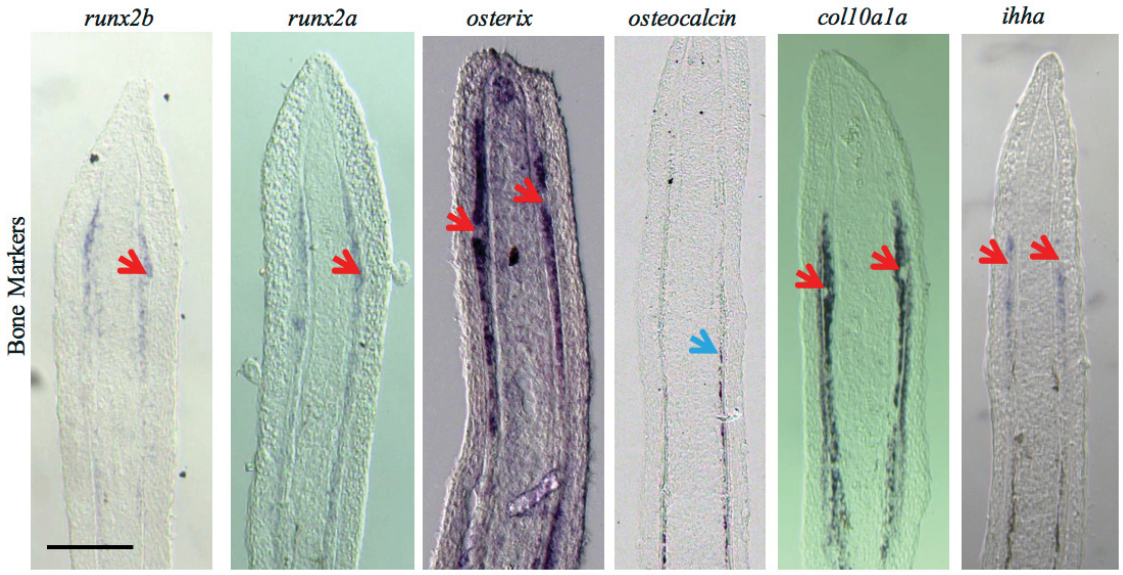

Figure 3.2: Gene expression analysis of osteoblast markers using *in situ* hybridization. Early osteoblast markers, *runx2a/runx2b* are expressed in a "bump" associated with the joint cell cluster (red arrows). A gap in the expression of lineage-commitment osteoblast marker *osx,* indicates a lack of expression in the joint cell cluster. The expression of late osteoblast marker, *osteocalcin* remains proximal (blue arrow) on the fin regenerate compared to other osteoblast markers and is not expressed in joint cell clusters. A gap in expression is also observed with other osteoblast markers *col10a1a* and *ihha*, illustrating an absence of expression in joint cell clusters. Scale Bars = 100μm.

3.6.2 Joint Cells Express *pthrp1:* A Potential inhibitor of Osteoblast Differentiation

In other models, it has been shown that Ihh interacts with PthrP, playing a role in regulating both intramembranous and endochondral ossification (Abzhanov *et al*., 2007; Lanske *et al*., 1996; St-Jacques *et al.,* 1999; Vortkamp *et al*., 1996). Consequently, the expression of *pthrp1,* an ortholog of the mammalian PTHrP (Yan *et al*., 2012), was analyzed. ISH for *pthrp1* and *evx1*, a joint cell marker, on consecutive sections of 4dpa fin regenerates indicate that the identified cell clusters are joint-forming cells and that these cells express *pthrp1* (Figure 3.3 A, B).

Since *pthrp1* was expressed in joint cells, we examined the expression of other *pthrps* and/or *pthrp-receptors* in 4dpa fin regenerates. *parathyroid receptor 1R* (*pth1R*) is expressed in differentiating osteoblasts; however, the stain was too faint to determine the presence or absence of this factor in joint cells (Figure 3.3 C). Furthermore, expression of *pthrp2* and *pth2R* was not visible (data not shown). However, non-quantitative RT-PCR indicates that *pthrp2,* and the *pthrp* receptor, *pth2R,* are expressed in 4dpa wildtype fin regenerates. *pth3R* is not expressed in 4dpa fin regenerates (Figure 3.3 D).

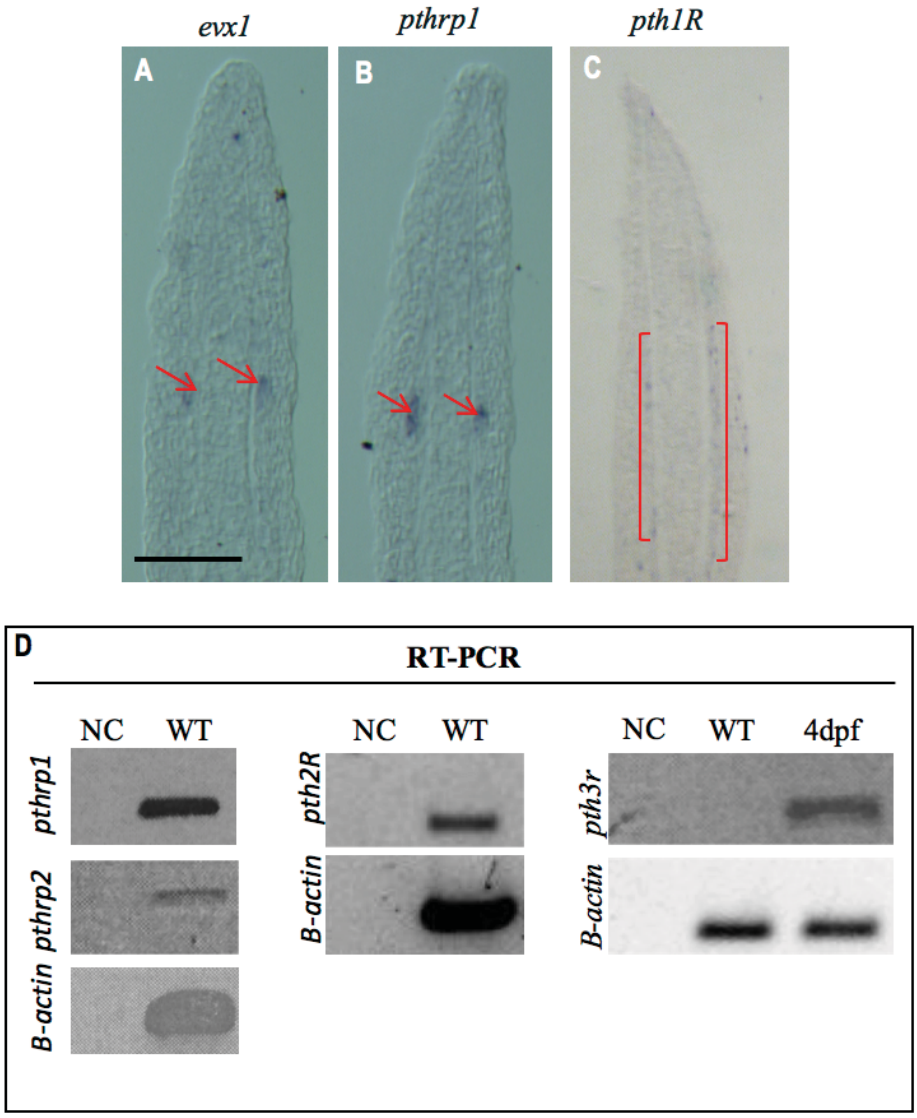

Figure 3.3: Gene expression analysis of *pthrps and pthrp*-receptors in wildtype 4dpa regenerates. (A) consecutive sections indicate *evx1* is expressed in joint cells that also express *pthrp1* (B). (C) *pth1R* is expressed faintly in differentiating osteoblasts (red brackets). (D) RT-PCR indicates *pthrp1, pthrp2,* and *pth2r* are expressed in the 4dpa fin regenerates. *pth3r* is not expressed in 4dpa wildtype fin regenerates, but is expressed in 4 days post fertilization (dpf) larvae. *β-actin* was used as the housekeeping control. NC = Negative Control. WT = wildtype. Scale bar = 100μm.

Double FISH on 4dpa fin regenerates confirmed *pthrp1* is co-expressed with *evx1* in joint cell clusters (Figure 3.4 A-A''). The *pthrp1* positive joint-forming cells do not appear to express *col10a1a* or *ihha*, although this must be confirmed by RT-PCR (Figure 3.4 B-B'', C-C''). However, *pthrp1* expressing joint cells do express *patched-1 (ptc-1)* (Figure 3.4 D-D''). Overall, the expression patterns of *ihha, pthrp1*, and their receptors indicate that these factors potentially interact. To determine the specific role of *pthrp1* and *ihha,* morpholino (MO) knockdowns were performed to elucidate the roles of these factors in joint formation and bone growth (Appendix I). However, the specificity of the MO knockdowns was unable to be determined.

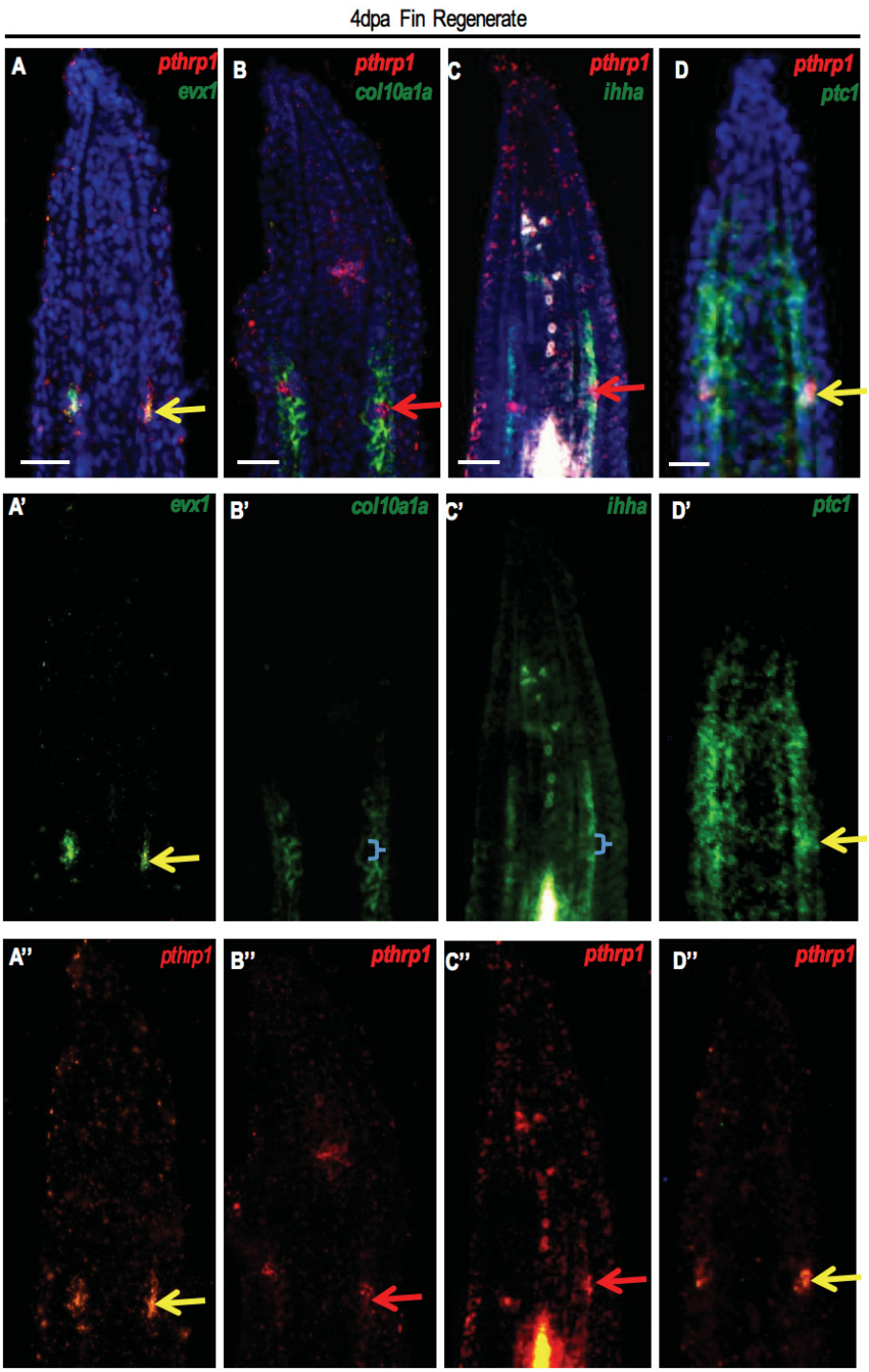

Figure 3.4: Double fluorescence ISH for joint and osteoblast markers. (A-A'') *pthrp1* and *evx1,* are expressed in joint-forming cells (yellow arrows). (B-B'') *pthrp1*-expressing cells (red arrows) do not express *col10a1a* (blue brackets) or *ihha* (blue brackets) (C-C''), but do express *ptc-1* (yellow arrows) (D-D''). (A-D) merged cy3 (red) and fluorescein (green) images. (A'-D') fluorescein (green) images only. (A''-D'') cy3 (red) images only. (A''-D'') Cy3 (red) images only. All scale bars = 100μm.

3.6.3 hoxa13a is Expressed in Presumptive Joint-Forming Cells Prior to *evx1* and *pthrp1*

evx1 is localized approximately 9.4kb upstream and in reverse transcriptional orientation of *homeobox A13a* (*hoxa13a*) in the zebrafish genome (Yates *et al*., 2016; Ensembl Database Version 83.10). Previous studies have observed common regulatory elements in intergenic regions that influence flanking factors (Zerucha *et al*., 2000; Moreau and Jeannotte, 2002). Furthermore, *hoxa13a* is expressed in a similar pattern to *evx1* during pectoral fin development (Ahn and Ho, 2008). Overall, these data suggest that it is possible that the intergenic region may contain similar regulatory modules that influence both of these factors, resulting in similar expression patterns. Double fluorescence ISH with *hoxa13a* and *pthrp1* confirmed that *hoxa13a* is expressed in joint-forming cells of fin regenerates (Figure 3.5 A-C). Furthermore, *hoxa13a* is expressed in a more distal domain than *pthrp1*(Figure 3.5 A-C). Since fins regenerate *via* the periodic addition of new joints to the distal fin rays, the most distal *hoxa13a* expression domain may correlate with presumptive joint-forming cells. As these presumptive joint cells mature and become more proximal on the fin regenerate, *pthrp1* is activated in *hoxa13a* expressing joint-forming cells. The expression of both factors (*hoxa13a, pthrp1*) continues as joint cells are observed on both internal and external sides of the lepidotrichia (Figure 3.5 A, C). As maturation progresses, the joint cells separate, forming the mature joint.

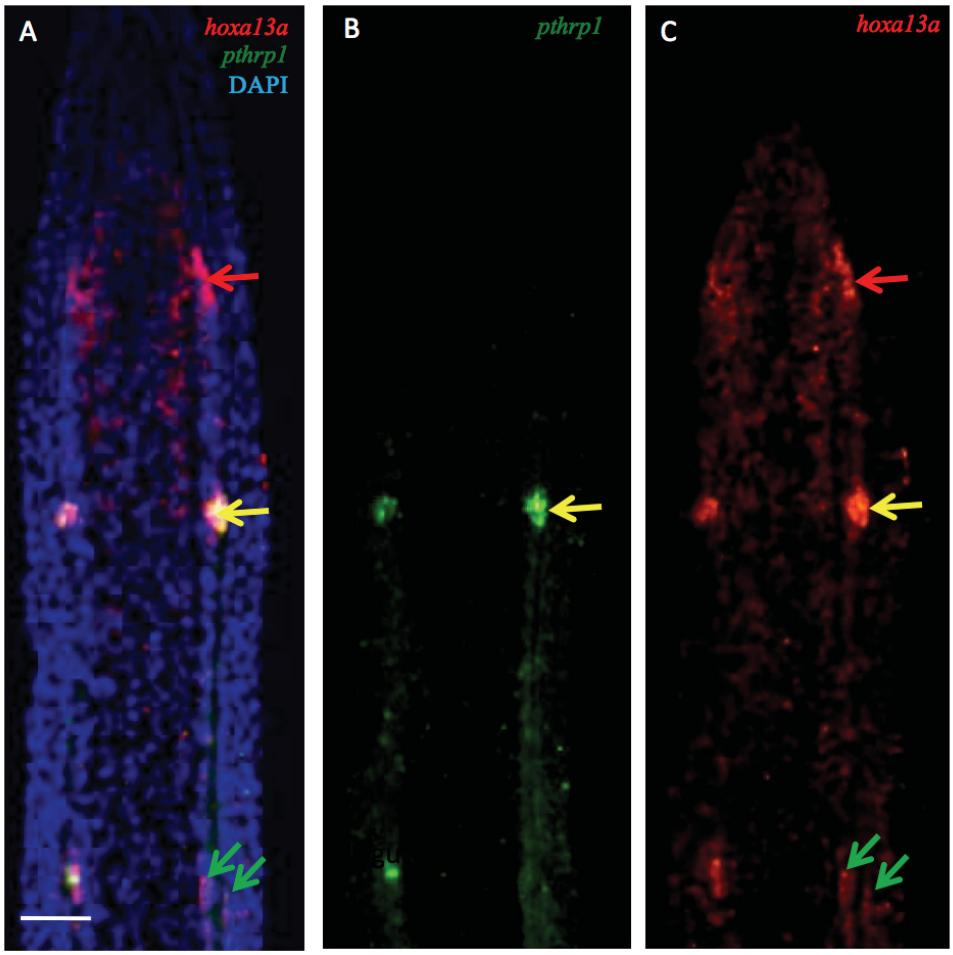

Figure 3.5: Double fluorescence ISH for *hoxa13a* and *pthrp1*. Gene expression analysis indicates an expression domain of *hoxa13a* distal to *pthrp1* (red arrows in A and C). As joint forming cells mature proximally *pthrp1* is co-expressed with *hoxa13a* (yellow arrows in A-C). The expression of both factors (*hoxa13a, pthrp1*) continues as joint cells are observed on both internal and external sides of the lepidotrichia (green arrows in A and C). (A) Merged cy3 (red, *hoxa13a*) and fluorescein (green, *pthrp1*) images. (B, C) Single color images indicate *pthrp1* (green) (B) and *hoxa13a* (red) (C) expression. Scale bar = 50μm.

Overall, the data acquired from the expression of *hoxa13a, evx1,* and *pthrp1,* indicates that joint cell differentiation can be divided into three separate cell types: Presumptive joint cells, joint-forming cells, and mature joint cells. Presumptive joint cells correspond to the distal-most domain where *hoxa13a* is expressed alone. The joint-forming cells correspond to the cell clusters that co-express all three factors: *hoxa13a, evx1,* and *pthrp1*. The mature joint cells correspond to any group of joint cells proximal to the 2nd distalmost domain that co-expresses all three factors. In contrast to the joint forming cells, the more mature joint cells are located on both internal and external sides of the lepidotrichia.

3.6.4 Joint Cells Commit to an Osteoblast Cell Fate in *evx1*$^{-/-}$ Mutants.

To further elucidate the genetic pathways associated with joint formation, gene expression analysis was performed on 4dpa regenerates from wildtype and *evx1*$^{-/-}$ loss of function mutants (Figure 3.6) (Schulte *et al*., 2011). In *evx1*$^{-/-}$ homozygous loss of function mutants, *pthrp1* expression is lost, but not *pth1r* (Figure 3.6). These data indicate that *pthrp1* lies downstream of *evx1* during joint formation. Interestingly, *hoxa13a* expression, is observed in presumptive joint cells of *evx1*$^{-/-}$ mutants, confirming that it is likely upstream or parallel to *evx1* and is potentially one of the first factors expressed in the presumptive joint-forming cells (Figure 3.6).

Since *pthrp1* has been implicated in intramembranous ossification and endochondral ossification and is absent in joint-forming cells of *evx1*$^{-/-}$ mutants, we also examined the expression of osteoblast markers in *evx1*$^{-/-}$ mutants (Figure 3.6). The expression of *ihha, ptc-1, col10a1a,* and *bmp2b* in osteoblasts appears unchanged in wildtype and *evx1*$^{-/-}$ mutants (Figure 3.6).

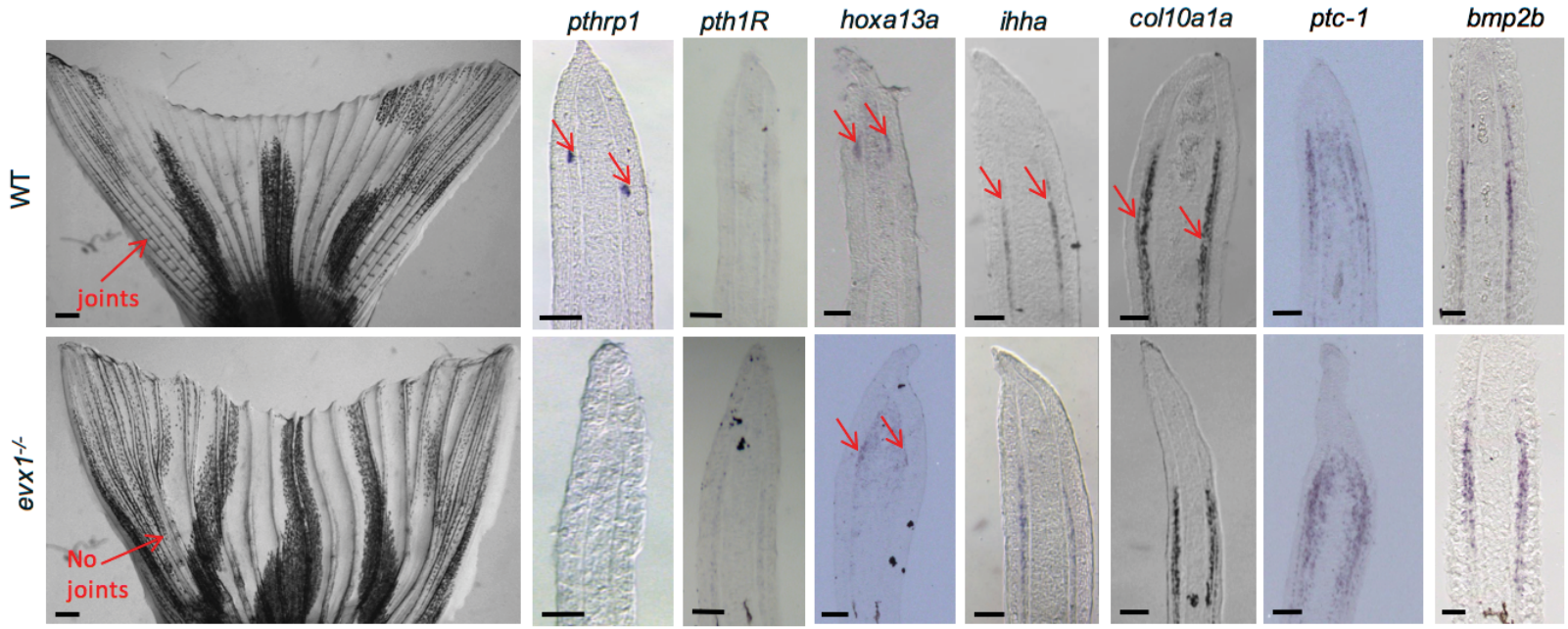

Figure 3.6: Morphological and gene expression analyses in wildtype and *evx1*$^{-/-}$ loss of function mutants. Brightfield images illustrate the lack of joints in *evx1*$^{-/-}$ mutants when compared to wildtype (red arrows). Comparison of 4dpa longitudinal sections of fin regenerates indicate the expression of *pthrp1,* but not *pth1R,* is lost in *evx1*$^{-/-}$ homozygous loss of function mutants. The expression of *hoxa13a* in joint cells remains in *evx1*$^{-/-}$ mutants. Expression of *ihha, col10a1a, ptc-1* and *bmp2b* appear similar in wildtype and *evx1*$^{-/-}$ mutants. However, *col10a1a* and *ihha no* longer possess gaps where *pthrp1* expressing cells are usually observed. Red arrows in wildtype and *evx1*$^{-/-}$ mutants indicates expression or lack of expression (gaps) in joint cells. Upper row = wildtypes and Lower row = *evx1*$^{-/-}$ mutants. Scale bars: brightfield images = 500μm; *pthrp1, hoxa13a,* and *ptc-1* = 100μm; *col10a1a, bmp2b, ihha*, and *pth1R* = 50μm.

However, qRT-PCR analysis reveals that the expression of these factors is significantly increased in *evx1*$^{-/-}$ mutant 4dpa fin regenerates when compared to wildtype controls ($p \leq 0.01$) (Figure 3.7). The upregulation of osteoblast markers in *evx1*$^{-/-}$ mutants suggests that wildtype joint-forming cells signal, potentially through Pthrp1, to surrounding Pth1r-expressing osteoblasts to suppress osteoblast differentiation markers. However, this hypothesis must be tested following the specific loss of *pthrp1* in joint cells.

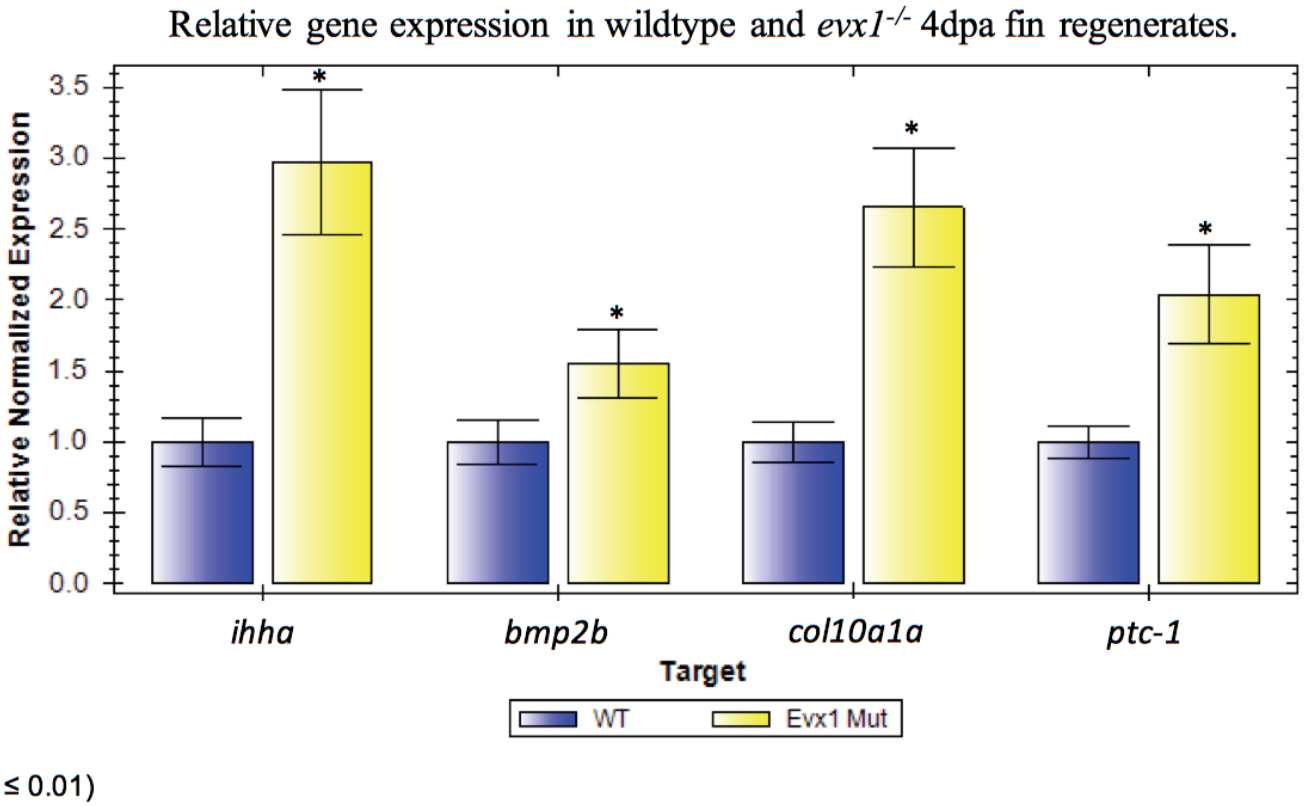

Figure 3.7: Relative gene expression analysis of wildtype and *evx1*$^{-/-}$ 4dpa fin regenerates. qRT-PCR demonstrates significant increases in *ihha*, *bmp2b, col10a1a,* and *ptc1* expression in 4dpa *evx1*$^{-/-}$ mutants relative to wildtype ($p \leq 0.001$). Significance is indicated by an asterisk. Error bars indicate standard deviation from the mean. Wildtype is indicated as blue bars, and *evx1*$^{-/-}$ mutants are indicated as yellow bars.

Interestingly, although the presumptive joint cells are specified, as indicated through the expression of *hoxa13a,* the gap of *ihha* and *col10a1a* expression corresponding to the joint cells is absent in *evx1*$^{-/-}$ mutant fin regenerates (n = 24 rays) (Figure 3.6). To determine whether presumptive joint cells are initially specified, but take on an osteoblast cell fate in the absence of Evx1, double fluorescence ISH for *hoxa13a* and *osx* (a marker of lineage-committed early osteoblasts) was performed on 4dpa wildtype and *evx1*$^{-/-}$ mutant fin regenerates (Figure 3.8). In wildtype, two distinct expression patterns was observed in the 4dpa fin regenerate depending on the presence or absence of a presumptive joint. When a presumptive joint is present, *hoxa13a* is expressed distal to the domain of *osx* expressing osteoblasts (Figure 3.8 A, A'). In fin rays lacking a presumptive joint, *hoxa13a* is expressed in the more proximal joint-forming cells on the fin regenerate, which are surrounded by *osx*-expressing osteoblasts (Figure 3.8 B, B'). In all cases, *hoxa13a* is never co-expressed with *osx* (n = 8). In *evx1* mutants, two distinct patterns of *hoxa13a* and *osx* are also observed in the fin regenerate. Similar to wildtypes, some fin rays express *hoxa13a* in presumptive joint cells distal to the domain of *osx* expressing osteoblasts in *evx1*$^{-/-}$ mutants (Figure 3.8 C). However, in contrast to wildtypes, some fin rays possess *hoxa13a*-expressing cells that co-express *osx* (n = 8) (Figure 3.8 D, D'). These results indicate that the presumptive joint cells are initially specified, but in the absence of Evx1, are committed to an osteoblast cell fate.

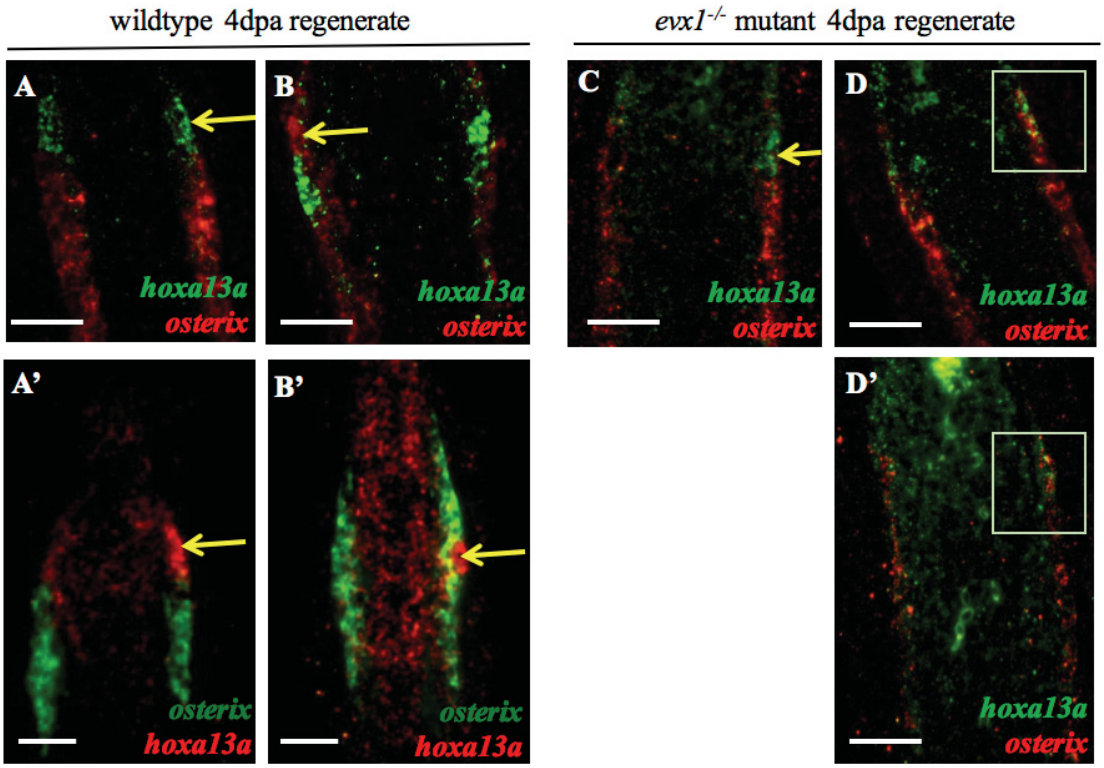

Figure 3.8: Double fluorescence ISH for *hoxa13a* and *osterix* expression on longitudinal sections of 4dpa wildtype and *evx1*$^{-/-}$ mutant fin regenerates. (A, A') Two examples indicating *hoxa13a* (yellow arrows) is expressed in presumptive joint forming cells in a domain distal to *osterix* expressing osteoblasts. (B, B') Two examples illustrating that maturing joint forming cells (yellow arrows) do not express *osterix*, but are surrounded by *osterix* expressing osteoblast cells. (C) In *evx1*$^{-/-}$ mutants, *hoxa13a* is expressed in presumptive joint forming cells in a domain distal to *osterix* expressing osteoblasts (yellow arrow). (D, D') Two examples illustrating that presumptive joint forming cells of *evx1*$^{-/-}$ mutants in some rays co-express *osterix* and *hoxa13a* (white boxes). (A,B,C,D) Merged confocal images illustrating *hoxa13a* (green) and *osterix* (red). (A', B', D') Merged fluorescence microscope images illustrating *osterix* (green) and *hoxa13a* (red). All scale bars: = 50μm.

3.6.5 A Disruption of Positional Information Inhibits Joint Formation and Increases Expression of Osteoblast Markers.

Calcineurin, a Ser/Thr protein phosphatase (Klee and Haiech, 1980), has been shown to regulate tissue growth and has been suggested to provide positional information through regulation of RA signaling during caudal fin regeneration (Kujawski *et al*. 2014). Previous studies indicate that the mechanisms controlling fin growth and joint formation may be linked (Ton and Iovine, 2013). To determine whether Calcineurin may be involved in positioning new joints, fish were treated with 0.1 μg/mL of FK506, a concentration that was proven effective in a previous publication (Kujawski *et al.,* 2014), for two days prior to fin amputation to ensure the chemical had time to take effect. 2 days post initiation of treatment (dpt), fins were amputated and allowed to regenerate while treatments continued for 8 days (Figure 3.9 A). Every two days, live imaging was performed followed by change of the water with fresh drug. 8dpa/10dpt, live imaging indicates that fish treated with FK506 do not form joints in the regenerate; however, joints remain intact in the stump (n = 12) (Figure 3.9 B). Untreated fish (n = 12) or equivalent ethanol treated control fish (n = 12) all formed joints in the caudal fin regenerate at 8dpa (Figure 3.9 C, D). Overall, this data indicates that calcineurin affects joint formation, but not joint maintenance in the adult caudal fin.

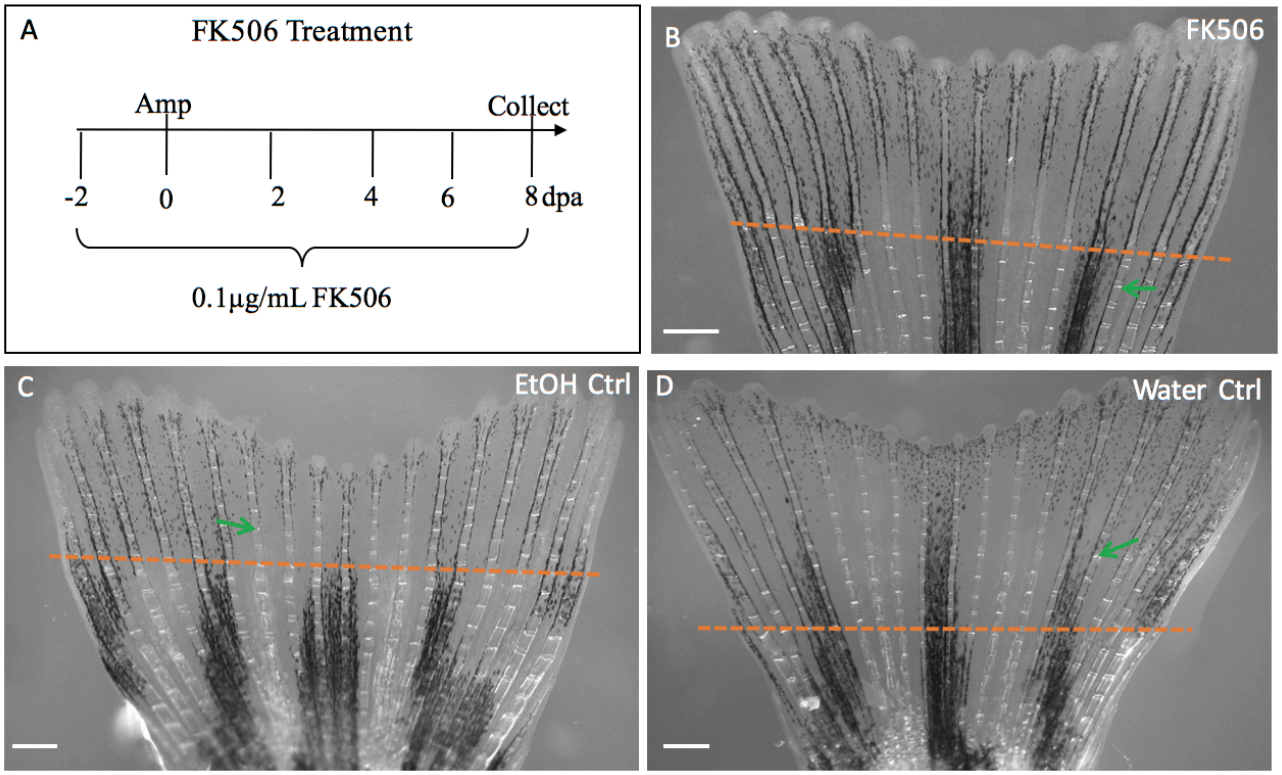

Figure 3.9: FK506 treatments during adult caudal fin regeneration. (A) Experimental setup for FK506 treatments. Fish were treated with 0.1 µg/mL of FK506 for 2 days. 0dpa/2dpt, caudal fins were cut and allowed to regenerate. Every two days, live imaging was performed followed by change of the water with fresh drug. (B) 8dpa/10dpt, caudal fin regenerates of FK506 treated fish do not form joints in the fin regenerate, but joints remain intact in the stump (green arrow). (C, D) Fish treated with equivalent amounts of ethanol (C) and untreated controls (D) illustrate the presence of joints (green arrows) 8dpa/10dpt. Dashed orange line indicates amputation plane. Scale bar for all images = 250µm.

Since FK506 treatment affects segment formation, it was of interest to examine the effect of a loss of calcineurin activity on joint and bone markers. ISH on regenerating fins 4dpa/6dpt indicate that FK506 inhibits the expression of all joint markers (*evx1, pthrp1,* and *hoxa13a*) (Figure 3.10). However, *hoxa13a* expression is maintained in the blastema (Figure 3.10). The loss of *hoxa13a* expression indicates that calcineurin activity may regulate the position of *hoxa13a* expressing presumptive joint cells in the fin regenerate. The expression of *ihha* and *ptc-1* appear unchanged (Figure 3.10). However, qRT-PCR should be performed to quantify these results.

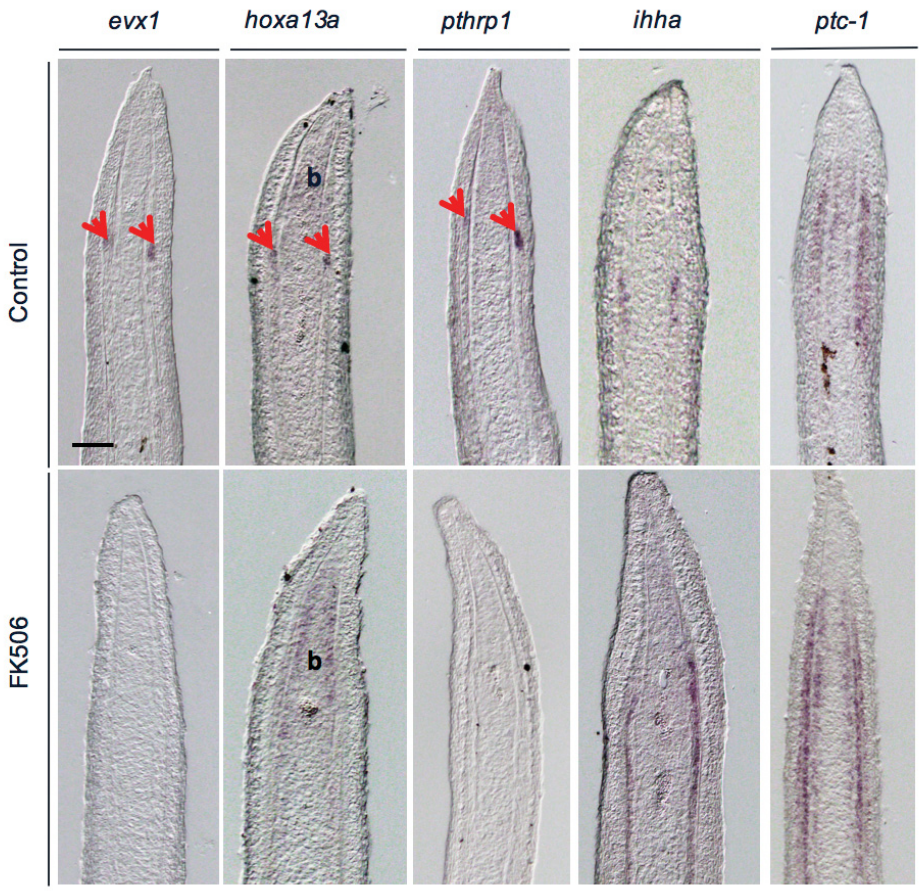

Figure 3.10: Gene expression analysis of 4dpa fin regenerates from FK506 and non-treated control fish. All joint markers (*evx1*, *hoxa13a*, and *pthrp1*) are lost but the expression of bone markers (*ihha, ptc-1)* remain in caudal fin regenerates of FK506 treated fish. *hoxa13a* expression remains in the blastema (b) of FK506 treated fish. No differences were observed in non-treated control fins. Arrows indicate joint forming cells. Scale bar for all images = 100μm.

3.6.6 Joint-Forming Cells Do Not Regenerate Following Laser Ablation

To investigate the regenerative properties of joint-forming cells, a 2-photon laser mediated approach was used to ablate these cells *in vivo*. The *Tg(Hoxa11 MI β-globin: egfp)* transgenic line, which expresses Egfp in the joint cells of the intact and regenerating fin rays was used to visualize the joint cells. Initial experiments were performed to determine the accuracy of the laser in ablating joint-forming cells. Prior to ablation, Egfp positive joint-forming cells are observed as horizontal lines across the 3dpa regenerating fin rays (Figure 3.11 A, A'). Following laser ablation, Egfp positive joint-forming cells are replaced with autofluorescent bubbles produced by the laser (Figure 3.11 B, B'). The presence of bubbles following ablation is a sign of optimal laser power (Roeser and Baier, 2003). Laser ablations were performed on joint-forming cells of a single hemiray and immediately collected to observe any damage. Double immunohistochemistry indicates that Zns5 and GFP positive joint cells were present on the control hemiray and absent on the ablated hemiray (Figure 3.11 C, C'). In some cases, damage to the epidermis was observed (Figure 3.11 D, D'). However, in a previous study, laser ablations targeting the basal epidermal layer adjacent to joint forming cells did not induce any joint defects (Zhang *et al*., 2012; data not shown), indicating epidermal damage does not influence joint formation.

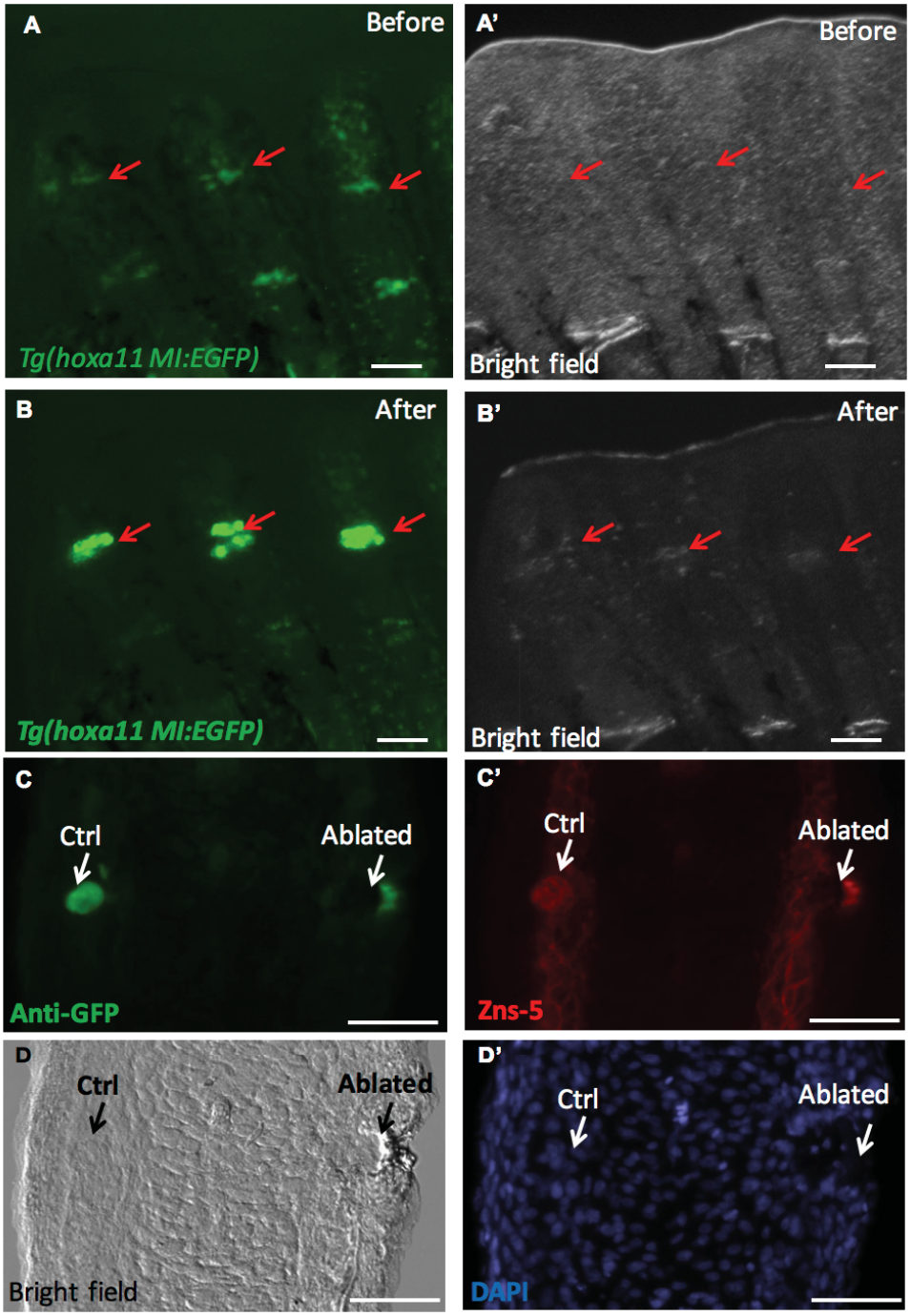

Figure 3.11: Control experiments for joint cell laser ablations. (A, A') *Tg(Hoxa11 MI Bg: egfp)* line illustrating Egfp positive joint cells in the caudal fin regenerate (red arrows). (B, B') Following laser ablation, autofluorescence is observed in lieu of Egfp positive joint cells (red arrows). (C-C') Following ablation Egfp (C) and Zns5 (C') positive joint cells are absent (Ablated) compared to non-ablated control (Ctrl) joint cells on the adjacent hemiray. (D-D') Brightfield (D) and DAPI counterstains illustrate some damage to the ablated side of the fin ray (Ablated) when compared to controls (Ctrl). Scale bars = A-A', B-B' = 100μm; C-C', D-D' = 50μm.

To examine the effects of laser ablation of joint-forming cells, live imaging was performed. 8 dpa/5 days post laser ablation (dpl), 100% of laser ablated joint cells resulted in joint defects (n = 10) (Figure 3.12). The severity of the joint defects was variable. Therefore, the resulting defects were rated as severe if no joint formed (Figure 3.12 A), mild if a partial joint formed (Figure 3.12 B), and none if the ray formed a normal joint. As a result, 60% of ablated joint cells were rated with a severe phenotype and 40% with a mild phenotype (Figure 3.12). No rays formed normal joints following the laser ablation of joint-forming cells 8dpa/5dpl (Figure 3.12). Joints continue to be absent 13dpa/21dpl (data not shown). Overall, these results indicate that joint-forming cells do not regenerate following laser cell ablation.

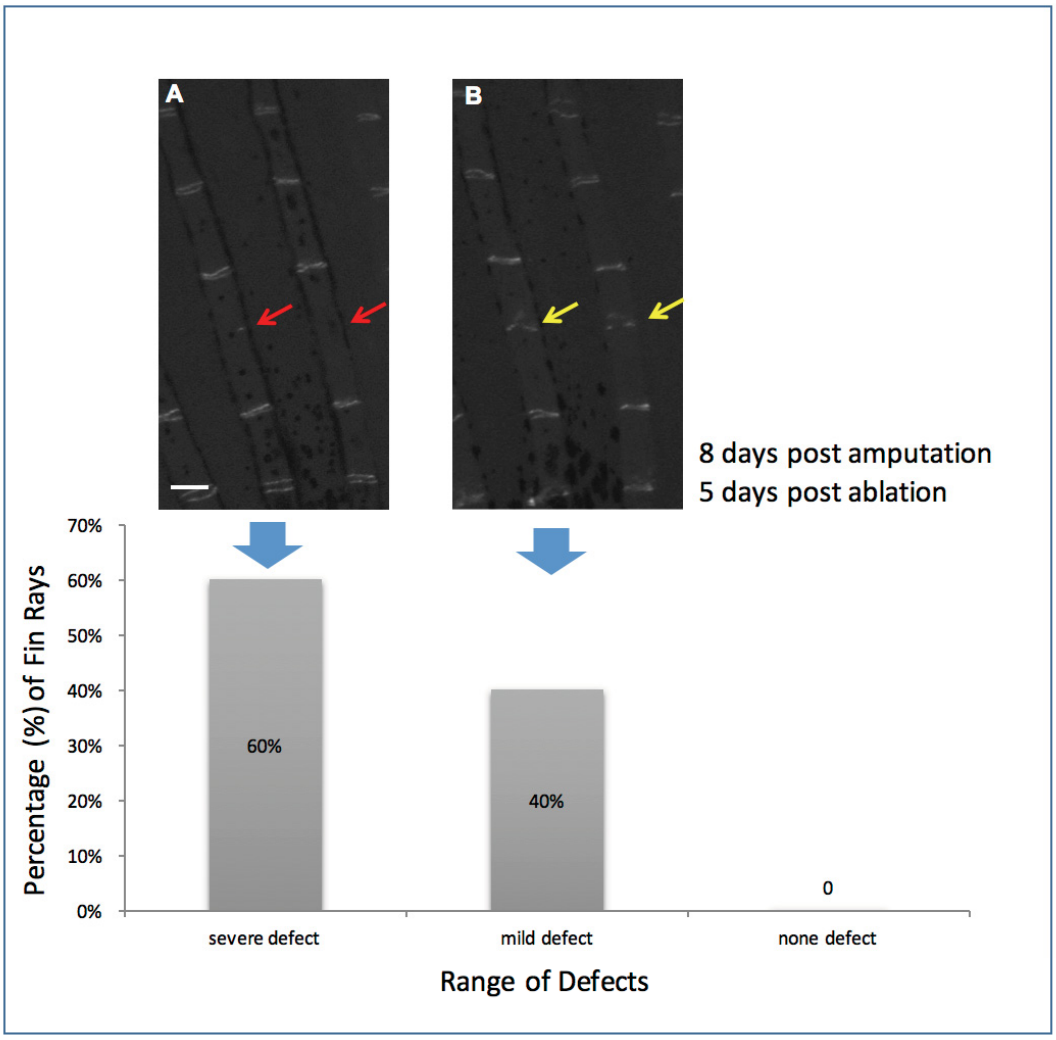

Figure 3.12: Laser ablation of joint cells. 8 dpa/5 days post laser ablation, 100% of laser ablated joint cells resulted in joint defects. (A) 60% of laser ablations resulted in severe defects, illustrated as a complete absence of joints (red arrows). (B) 40% of laser ablations resulted in mild defects, illustrated as the formation of a partial joint (yellow arrows). n = 10 joints. Scale bars for all images on A = 100μm.

3.7 Discussion

The investigation of the joint formation outlines various genetic and molecular mechanisms in which these structures are formed and maintained in the caudal fin rays. Using gene expression and functional analyses, the following regulatory mechanism of joint cell specification and differentiation during fin regeneration has been elucidated. During caudal fin regeneration, calcineurin activity regulates the position of *hoxa13a* expressing presumptive joint cells in the fin regenerate. Presumptive joint cells that express *runx2a, runx2b* and *hoxa13a* are specified to become joint cells, but possess the ability to differentiate into osteoblasts. As regeneration progresses, presumptive joint cells commit and differentiate into joint-forming cells that express *evx1*, *hoxa13a*, and *pthrp1*. During joint cell differentiation *evx1* occurs downstream or parallel to *hoxa13a,* but upstream of *pthrp1*. The expression of *pthrp1* may negatively regulate *ihha* expression in joint-forming cells to inhibit osteoblast commitment and induce a joint cell fate. In the absence of *evx1*, *pthrp1* is not expressed and *hoxa13a* expressing presumptive joint cells are committed to an osteoblast cell fate in the fin regenerate. Furthermore, joint cells do not regenerate following laser ablation, suggesting that joint cell differentiation occurs only at specific intervals during fin regeneration.

3.7.1 Presumptive Joint Cells are Bi-potential and Can Differentiate into Osteoblasts

Initial genetic analysis of 4dpa fin regenerates indicate that presumptive joint cells initially express early osteoblast markers *runx2a* and *runx2b*, but not later osteoblast markers (*osx*, *col10a1a*, *osc*). In mice, it has been shown that *Runx2*-expressing pre-osteoblasts are bipotential cells that can differentiate into either osteoblasts or chondrocytes. However, upon expression of *osx,* cells are committed to an osteoblast cell

fate (Nakashima *et al*., 2002). Conversely, a loss of *osx* in the long bones of mice causes ectopic cartilage formation, potentially due to a fate switch of osteoblast progenitors to chondrocytes (Nakashima *et al.* 2002). Therefore, we propose that the presumptive joint cells of the fin regenerate are also bi-potential cells that could differentiate into osteoblasts in the event *osx* is expressed.

During caudal fin regeneration cells de-differentiate and proliferate as they migrate from the amputation site to form the blastema. Subsequently, cells leave the blastema and re-differentiate into the various cell types to reform the lost fin (Tu and Johnson, 2011; Knopf *et al*., 2012). Previous studies have shown that the fate of many cell types, including osteoblasts, remain restricted to the same lineage (Tu and Johnson, 2011; Knopf *et al*., 2012). However, using transposon-based clonal analysis, it has been suggested that osteoblasts may contribute to joint cell lineage (Tu and Johnson, 2011). Another study showed that upon ablation of osteoblasts, the fin rays regenerate normally (Singh *et al.,* 2012), suggesting a potential transdifferentiation mechanism through an unknown source. Our data suggest that osteoblasts and joint-forming cells originate from a common cell lineage as they both express *runx2a* and *runx2b.* Furthermore, a loss of Evx1 results in a switch from a joint cell to an osteoblast differentiation pathway. Overall, assuming a common cell origin, osteoblasts and joint-forming cells could potentially commit to the alternative cell type during regeneration. These findings suggest an alternative source of osteoblasts during fin regeneration, potentially through transdifferentiation. The ability of presumptive joint cells to differentiate into osteoblasts suggests that these cells may be the elusive potential alternative source of osteoblasts that has been hypothesized in the study by Singh *et al* (2012). Cell lineage tracing of joint cells following osteoblast ablation during

regeneration should test this hypothesis.

3.7.2 Joint Cells Express *pthrp1:* A Potential Inhibitor of Osteoblast Differentiation

Joint-forming cells express *pthrp1,* but do not appear to express *col10a1a* or *ihha* through double FISH. However, *pthrp1*-expressing joint cells do express *patched-1 (ptc-1)*, indicating that hedgehog signaling is still active in these cells. Currently, due to the lack of efficient MO knockdowns (see Appendix I), the specific roles of *pthrp1* are unknown. However, during endochondral ossification in mouse and chick, it has been shown that IHH activates the expression of *Pthrp,* which subsequently signals through PTHR1 to inhibit chondrocyte differentiation and to suppress *Ihh* expression (Lanske *et al*., 1996; St-Jacques *et al.,* 1999; Vortkamp *et al*., 1996). Furthermore, IHH promotes chondrocyte hypertrophy (Mak *et al.,* 2008), and stimulates osteoblast differentiation of the mesenchymal cells surrounding the cartilage (Karp *et al*., 2000; Long *et al.,* 2004; St-Jacques *et al.,* 1999). Similarly, during intramembranous ossification in chick, *Pthrp* is suggested to inhibit osteoblast differentiation (Abzhanov *et al*., 2007). In the zebrafish *evx1*$^{-/-}$ mutant, *pthrp1* expression is lost in joint-forming cells and *ihha, bmp2b,* and *col10a1a* expression is increased in surrounding osteoblasts. Considering the previously established roles for IHH and PTHrP during endochondral and intramembranous ossification in mouse and chick, it is possible that in zebrafish *pthrp1* negatively regulates *ihha* expression in joint-forming cells and surrounding osteoblasts to induce a joint cell fate and regulate osteoblast differentiation. Furthermore, since Hedgehog signaling is active in joint forming cells it is possible that Ihha may signal joint-forming cells to promote *pthrp1* expression similar to what has been observed during endochondral bone ossification in mouse and chick (Lanske *et al*., 1996; St-Jacques *et al.,* 1999; Vortkamp *et*

al., 1996). However, because Shha is expressed adjacent to *ptc-1* expressing joint cells (Laforest *et al*., 1998; Quint *et al*., 2002; Smith *et al*., 2006), one cannot discount the possibility that Shha also contributes to joint formation in an as of yet unknown mechanism.

Analysis of the homozygous *evx1*$^{-/-}$ mutant shows that presumptive joint-forming cells express *osx* and therefore, are likely committed to an osteoblast cell fate. Since *pthrp1* expression is lost in *evx1* mutants, one can speculate that *pthrp1* may act in an autocrine fashion to inhibit osteoblast differentiation in joint-forming cells. Therefore, the loss of *pthrp1* in the *evx1*$^{-/-}$ mutant may result in the commitment of joint-forming cells to an osteoblast cell fate. However, overall the speculative roles of *ihha* and *pthrp1* in the fin regenerate have yet to be confirmed.

3.7.3 *hoxa13a* is Involved in Joint Formation

Gene expression analysis indicates that *hoxa13a* occurs upstream or parallel to *evx1* and likely plays a role in joint formation. Consistent with these results, research in mouse and chick have demonstrated that the *Hox* genes of the A and D clusters play a role in joint formation in the autopod (hand/foot, including palm/sole, thumb, and fingers/toes). Gene expression analysis indicates *Hoxd-13, Hoxd-11,* and *Hoxa-13* are expressed at the sites of future joints (Suzuki and Kuroiwa, 2002). Furthermore, mutations in *Hoxa-13*, *Hoxd-11* or *Hoxd-13* has been shown to disrupt proper joint formation (Dollé *et al*. 1993; Small and Potter 1993; Davis and Capecchi, 1994; Davis *et al*. 1995; Favier *et al*. 1994; Fromental-Ramain *et al.* 1996). More specifically, *Hoxd11* mouse mutants possess a few fused carpals and phalanges (Davis and Capecchi, 1994; Favier *et al*., 1994). *Hoxd13* mouse mutants possess a few metacarpals that are fused to phalanges and some fused carpal bones (Dollé

et al., 1993). *Hoxa13* mutants possess forelimbs in which the phalanges are occasionally fused (Fromental-Ramain *et al.,* 1996). Due to potential redundancy, mutations in two of these factors at any given time, i.e. *Hoxd13*$^{-/-}$*; Hoxa13*$^{+/-}$mutants, results in more severe joint defects in which most of the metatarsal and phalangeal cartilages are fused (Fromental-Ramain *et al*., 1996; Villavicencio-Lorini *et al*., 2010). In humans, mutations in these factors result in various genetic diseases. In humans, *HOXD13* mutations can lead to a variety of diseases such as Syndactyly type V, VACTERL (vertebral defects, anal atresia, cardiac defects, tracheo-esophageal fistula, renal anomalies, and limb abnormalities) association, and Brachydactyly type E (Quinonez and Innis, 2014; Imagawa *et al*., 2014; Klopocki *et al*., 2010). All of these genetic diseases result in the fusion of some joints in the autopod. Interestingly, Brachydactyly type E is also associated with missense mutations in the human *PTHRP* (Klopocki *et al*., 2010). In cases of *PTHRP* mutations, fusion of the phalanges has been observed (Klopocki *et al*., 2010). Our results in zebrafish suggest that *hoxa13a* plays a role in joint formation in the fin regenerate. Interestingly, *hoxd13a*, is expressed in the distal fin regenerate in a region that may overlap with the *hoxa13a* positive joint cells (data not shown). The potential co-expression of the two paralogs indicates there is potential for redundancy, similar to that observed during limb patterning (Suzuki and Kuroiwa, 2002; Fromental-Ramain *et al*., 1996). Future research will determine the roles of *hoxa13a* and *hoxd13a* and explore the potential of redundancy between these paralogs in joint formation of the caudal fin regenerate.

Gene expression analysis also illustrates *hoxa13a, pthrp1*, and *evx1* expression is maintained in mature joint cells. The continued expression suggests that these factors may be required for joint maintenance. Previously, it has been shown that the maintenance of

synovial joint articular cartilage depends on the inhibition of differentiation in chondrocytes (Bohme, *et al*., 1993; Lotz *et al*., 1999; Serra *et al*., 1997; Serra, *et al*., 1999; Drissi *et al*., 2005). The loss of mechanisms associated with the arrest of articular cartilage differentiation have been associated with degenerative joint diseases such as osteoarthritis. Therefore, it is possible that these factors are required in mature joint cells to inhibit osteoblast differentiation. The continued lack of osteoblasts surrounding the joints likely inhibits the deposition of bone matrix and consequently, the fusion of adjacent segments. Future work will aim to confirm the roles of these factors (*pthrp1, evx1,* and *hoxa13a*) in joint maintenance.

3.7.4 A Disruption of Positional Information Inhibits Joint Formation

Fish treated with FK506 do not express joint cell markers (*hoxa13a, evx1,* and *pthrp1*) and joints are not formed, indicating that calcineurin activity is required for joint formation in the fin regenerate. Previous studies indicate that the treatment of fish with FK506 results in a proximalization of the fin regenerate (Kujawski *et al.,* 2014). Furthermore, the authors suggest that the loss in positional information may be through the direct or indirect regulation of RA signaling (Kujawski *et al.,* 2014). FK506 treatments indicate that calcineurin signaling, through RA signaling, may establish the position of joints through the induction of *hoxa13a* expression in the presumptive joint cells of the caudal fin regenerate. Consistent with this data, it has been shown that RA signaling plays a major role in patterning the AP axis by controlling *Hox* gene expression directly through retinoic acid response elements (RAREs) or indirectly through other factors (Maden *et al*., 1996; Maden, 2002). However, it has also been shown that other factors in the Fibrobast growth factor (Fgf) and Wnt signaling pathways were upregulated in fin regenerates of

FK506 treated fish (Kujawski *et al.,* 2014). These pathways (RA, Fgf, and Wnt) have all been shown to interact during fin regeneration (Blum and Begemann, 2012). Furthermore, these pathways have all been implicated in establishing *Hox* gene expression during both hindbrain and axial patterning (Dubrulle *et al.* 2001; Zakany *et al.* 2001; Gavalas, 2002; Gavalas and Krumlauf 2000; Kessel and Gruss, 1991). Therefore, it is possible that calcineurin signaling in the fin regenerate may act through any of these pathways to establish the position of joints through the induction of *hoxa13a* expression in the presumptive joint cells of the caudal fin regenerate.

3.7.5 Joint-Forming Cells Do Not Regenerate Following Laser Ablation

Finally, we show that joint-forming cells do not regenerate following laser cell ablation. However, joint cells can regenerate in the context of fin regeneration. These data suggest that upon laser cell ablation, *osx*-expressing osteoblasts surrounding the laser ablated joint forming cells have already committed to an osteoblast cell fate, and therefore cannot readily de-differentiate to recontribute the joint cell lineage. Alternatively, *cx43,* a gap junction protein that is expressed in the blastema and a subpopulation of osteoblasts surrounding both newly forming and mature joints, has been suggested to control segment length via the suppression of joint formation (Iovine *et al.*, 2005). Therefore, upon laser ablation, it is possible that surrounding cells cannot regenerate joint cells due to the surrounding suppressive action of *cx43*.

Chapter 4: Analysis of Breeding Tubercles on Zebrafish Pectoral Fins.

4.1 Summary:

In an attempt to further elucidate the roles of Hedgehog signaling during fin regeneration, the roles of *shha* in the formation and regeneration of breeding tubercles, multicellular epidermal structures, was explored in the male intact and regenerating pectoral fins. Unfortunately, no differences in the expression of *shha* were observed in the intact or regenerating male and female pectoral fins. However, differences in regenerative capabilities and vascularization were observed between male and female pectoral fins. Consequently, these observations prompted us to perform a detailed analysis of the Breeding Tubercles (BT), sexually dimorphic keratinized epidermal structures on the male pectoral fins. This work led to two publications. The first publication characterizes these BT clusters on male pectoral fins, and subsequently describes the requirement of androgens and two waves of vascularization for their regeneration. The second publication discusses the use of BTs on male pectoral fins in determining zebrafish sex.

Manuscript #1: Regeneration of breeding tubercles on zebrafish pectoral fins requires androgens and two waves of re-vascularization.

Stephanie C. McMillan[ab], Zhe T. Xu, Jing Zhang[b], Cathleen Teh[c], Vladimir Korzh[c], Vance L. Trudeau[bd], Marie-Andrée Akimenko[bd].

[a] Department of Cellular and Molecular Medicine, University of Ottawa, ON, K1N 6N5 Canada
[b] CAREG, 30 Marie Curie, University of Ottawa, ON, K1N 6N5 Canada
[c] Department of Biological Sciences, National University of Singapore, 117543 Singapore.
[d] Department of Biology, 30 Marie Curie, University of Ottawa, ON, K1N 6N5 Canada

E-mail addresses:

Stephanie C. McMillan:
Jing Zhang:
Tim Xu:
Cathleen Teh:
Vladimir Korzh:
Vance L. Trudeau:
Marie-Andrée Akimenko

Corresponding author: Marie-Andrée Akimenko
Department of Biology
University of Ottawa
30, Marie Curie
Ottawa, ON, K1N 6N5
Canada

Running Title: Zebrafish Breeding Tubercle Regeneration

Key Words: Breeding Tubercles, Fin Regeneration, Blood vessels

Grant Sponsor: Canadian Institute of Health Research (MAA) and Natural Sciences and Engineering Research Council (VLT).

Published in: ***Development.*** **2013 Oct 2; 140(21):4323-34**

4.2 Author Contributions:

Stephanie C. McMillan: Performed the majority of the experiments in this publication and wrote the majority of the manuscript.

Zhe T. Xu: Tim performed initial Mallory stains on transverse sections of a BT keratinized cap (Figure 4.1 K) and took initial pictures of BT clusters on the bottom of breeding tanks (Figure 4.1 N, N'). Furthermore, although not published in this manuscript, Tim performed initial imaging of the highly vascularized BTs using *Tg(KR21)* and *Tg(fli1a:EGFP)* lines and performed some of the initial hormone treatments.

Jing Zhang: Performed important initial studies including picrosirius red staining and DAPI staining (Figure 4.1 L, M). Jing also helped edit the final images.

Cathleen Teh. and Vlademir Korzh Postdoctoral fellow and Professor in the Department of Biological Sciences at National University of Singapore, 117543 Singapore: Generated the *Et(kr4:GAP-KillerRed)sqKR21* transgenic line.

Dr. Vance Trudeau, Professor at the University of Ottawa, Department of Biology: Assisted in the design of the hormone treatments and provided critical reading of the manuscript.

Marie-Andrée Akimenko: Supervised the project and helped write the manuscript.

4.3 Abstract

Sexually dimorphic breeding tubercles (BTs) are keratinized epidermal structures that form clusters on the dorsal surface of the anterior rays of the zebrafish male pectoral fins. BTs appear during sexual maturation and are maintained through regular shedding and renewal of the keratinized surface. Following pectoral fin amputation, BT clusters regenerate after the initiation of re-vascularization, but concomitantly with a second wave of angiogenesis. This second wave of regeneration forms a web-like blood vessel network that penetrates the supportive epidermis of BTs. Upon analyzing the effects of sex steroids and their inhibitors, we show that androgens induce and estrogens inhibit BT cluster formation in intact and regenerating pectoral fins. Androgen-induced BT formation in females is accompanied by the formation of a male-like blood vessel network. Treatment of females with both androgens and an angiogenesis inhibitor results in the formation of undersized BT clusters when compared to females treated with androgens alone. Overall, the growth and regeneration of large BTs requires a hormonal stimulus and the presence of an additional blood vessel network naturally found in males.

4.4 Introduction:

Breeding tubercles (BTs) are multicellular epidermal structures that often support a conical keratin cap (Wiley and Collette, 1970). In most teleosts, BTs are present only in males or are more developed in males than in females (Wiley and Collette, 1970). Although all BTs share the same structure, their size, shape, number, and location can vary within and between species (Wiley and Collette, 1970). In *Phoxinus,* different morphotypes of BTs have been identified that, depending on location, appear isolated or grouped together to form clusters. In some species of *Phoxinus,* large BTs have been found to form clusters on the dorsal surface of the central to more anterior pectoral fin rays (Chen and Arratia, 1996). In addition, isolated BTs have been observed in various areas including: the head, body, and fins (Chen and Arratia, 1996).

Since BTs are present on multiple areas of contact between males and females, they are believed to serve various roles such as maintaining body contact during spawning or as a fitness indicator during sexual selection (Wiley and Collette, 1970; Kortet *et al*., 2003). Other roles have been suggested for BTs including defense against mechanical injuries, microorganisms, and parasites. BTs have also been implicated in the protection of nests and territories (Ahnelt and Keickis, 1994; Chen and Arriata, 1996; Kortet *et al.,* 2003). In some species, an increase in the number and size of BTs is correlated with a higher level of aggressive behavior. It has been speculated that an increase in dominance occurs along with the presence of larger and more numerous BTs, both of which are correlated with high circulating concentrations of androgens (Kortet *et al*., 2004; Borg, 1994; Kortet *et al*., 2003). Androgens have been shown to induce the formation of BTs (Ramaswami and Hasler, 1955; Egami, 1954; Arai, 1967; Wiley and Collette, 1970). In addition, a reduction in testosterone following castration results in the regression of BTs in medaka (Nagata,

1934; Yamamoto and Egami, 1974). Overall, there appears to be a correlation between the presence of androgens and the development of BTs in many different fish species.

Vascularization of large BTs has been observed in some fish species (Wiley and Collette, 1970). Although not experimentally tested, blood vessels are suggested to play a role in the maintenance of BTs in these species during long periods of spawning (Wiley and Collette, 1970). Recently, studies done in human endothelial cell culture and in mice suggested that androgens have sex-specific pro-angiogenic effects (Sieveking *et al*., 2010). More specifically, androgens, acting through the androgen receptor (AR), increase the downstream expression of genes that promote processes related to angiogenesis, such as migration and proliferation (Death *et al*., 2004; Ng *et al.,* 2003; Ruohola *et al.,* 1999; Sieveking *et al*., 2010).

These studies indicate a correlation between the presence of BTs and androgens, and raise an interesting possibility that androgens in male teleosts stimulate angiogenesis, which is necessary for BT formation and maintenance. However, such a relationship has not yet been explored. In this report, we use two zebrafish transgenic lines, *Tg*(*fli1a:EGFP*) and *Tg(KR21),* to investigate the relationship between sex hormones, vascularization, and the presence of BT clusters on the intact, and regenerating pectoral fins of zebrafish. Using these transgenic lines, a second wave of blood vessel growth is observed in regenerating BTs. Furthermore, we show that androgens promote the formation of BTs and additional blood vessels in intact and regenerating fins. Inhibiting additional blood vessel formation reduces the ability of androgens to induce BT formation in females. We conclude that the growth of large BT clusters in intact and regenerating pectoral fin depends on the presence of androgens and the formation of a unique pattern of blood vessels.

4.5 Materials and Methods

4.5.1 Animals

Fish were maintained at 28.5°C with a photoperiod of 14 hours of light and 10 hours of darkness, and fed regularly (Westerfield, 1995). *Et(krt4:GAP-KillerRed)sqKR21*, or [*Tg(KR21)*], is an enhancer trap line similar to other killer red (KR) lines (Korzh *et al,* 2011). KR is a membrane-tagged dimeric red fluorescent protein that acts as a photosensitizer (Korzh *et al*., 2011; Bulina *et al*., 2006; Serebrovskaya *et al.,* 2009). Photobleaching of *Tg(KR21)* adults on confocal and widefield microscopes has not been determined. However, our exposure times (< 500ms) are far below that required to photobleach embryos using similar membrane-tagged KR lines (Teh *et al.,* 2010). The KR21 insertion site is unknown: http://plover.imcb.a-star.edu.sg/webpages/memKR1.html. The *Tg(fli1a-EGFP)* line was a gift from Brant M. Weinstein (Lawson and Weinstein, 2002).

4.5.2 Fin Amputation

Zebrafish were anesthetized by immersion in system water containing 0.17 mg/ml tricaine (ethyl-aminobenzoate; Westerfield, 1995). Caudal and pectoral fins were amputated using a scalpel and a small pair of scissors, respectively.

4.5.3 Imaging

For brightfield and fluorescence imaging, fish were anesthetized and placed ventral side up on an agarose plate with the pectoral fins spread out. The plate was then inverted and images were taken using a Leica MZ FLIII dissection microscope, an AxioCam HSm digital camera and AxioVision AC software (Carl Zeiss). For confocal imaging, samples were mounted using Aqua-Poly/Mount (Polysciences). Images were captured using a Zeiss

LSM 510/AxioVert 200 confocal and zen2009 software. All images were processed using ImageJ (NIH) and Adobe Photoshop.

4.5.4 Histochemical Procedures

Mallory staining was performed according to Cason (1950). DAPI staining was performed by adding one drop of Vectashield Mounting Medium containing DAPI onto each slide. PAS staining was performed as per the manufacturer's protocol (Sigma-Aldrich). Picrosirius red staining was performed as previously described (Smith *et al*, 2008).

4.5.5 Chemical Treatments

17β-estradiol (E2), 5α-dihydrotestosterone (DHT) and testosterone (T) (all Sigma-Aldrich) were dissolved in ethanol and added to system water at 1 µg/l; this concentration was chosen based on our preliminary studies (DHT and T) and on published data (Miles-Richardson *et al*., 1999) (E2). An end point of 3 weeks for E2 treatments was chosen to ensure that BT absence was not due to a delay in regeneration. Flutamide (Sigma-Aldrich), in our hands, is effective at 2 mg/l when dissolved in ethanol and added to system water. Fadrozole was dissolved in system water at 50 µg/l (Ankley *et al*., 2002; Zhang *et al.,* 2009). PTK787 (Selleck Chemicals) was dissolved in system water at an effective final concentration of 500 nM (Bayliss *et al.,* 2006). Zebrafish were kept in glass tanks throughout treatments. Control tanks contained either the same percentage of ethanol or system water alone.

4.5.6 Immunohistochemistry

Samples were fixed in 4% paraformaldehyde overnight at 4°C and cryosectioned (Smith *et al*., 2008). For Pcna immunohistochemistry, sections were submerged in 10mM

sodium citrate, pH 6.0, 0.05% tween-20, at 98°C for 20 minutes, and cooled to room temperature. A mouse anti-Pcna antibody (Clone PC10, Dako Cat#M0879) was used at 1:250 along with a rabbit anti-GFP (Molecular Probes) at 1:500. Fluorescently labeled secondary antibodies (Alexa Fluor® 488 Goat Anti-mouse IgG (H + L) and AlexaFluor 594 Goat anti-rabbit-IgG (H + L); Invitrogen A11001 and A-11012) were used at 1:500. Slides were counterstained with DAPI and mounted.

4.5.7 Quantitative RT-PCR (qRT-PCR)

Total RNA was extracted from ten caudal fins using Trizol according to the manufacturer's protocol (Invitrogen). Total RNA was checked for purity (Nanodrop) and integrity (agarose gel analysis). Total RNA (2 μg) was reverse transcribed with SuperScript II reverse transcriptase (Invitrogen) using oligo(dT). Quantitative PCR was performed using the Eco Real-Time PCR System (Illumina) and a SYBR Green labeling system (Bio-Rad, 170-8880). Primers flanking a single intron of *ar* were used: forward, 5′-ATGACCCTGGGAGCCCGCAA-3′; reverse, 5′-GTGGTGAACGCCGGCCATGA-3′. Primers used to amplify the *ef1α* (*eef1a1l1*) control also flank a single intron: forward, 5′-CAAACATGGGCTGGTTCAAG-3′; reverse, 5′-AGTGGTTACATTGGCAGGG-3′. Four biological samples were run in triplicate per experiment, with no-template controls. Ct values, extracted from a standard curve, were taken from the Eco Real-Time PCR System program. A two-tailed Student's *t*-test at a 95% confidence level ($P<0.05$) was performed to determine the significance of gene expression values in female versus male pectoral fins.

4.5.8 Calculation of Average BT Width

The average BT width was obtained by dividing a standard distance (285μm) by the number of BTs in a single line within that standard distance using ImageJ software (http://rsb.info.nih.gov/ij/). A 1-tailed Student's t-test at a 95% confidence level ($p<0.05$) was performed to determine the significance of any increase in BT width.

4.6 Results

4.6.1 Breeding Tubercle Distribution in Male and Female Zebrafish

We first analyzed the distribution of BTs on adult (> 6 months old) male and female zebrafish using *Tg(KR21)*, an enhancer trap line that ubiquitously expresses the membrane-tagged fluorescent reporter, killer red (KR), in the epidermis. Fluorescence in *Tg(KR21)* fish appears more intense in BTs (Figure 4.1A-I), most likely because of the increased thickness caused by epidermal aggregates, and/or the differential cellular distribution of the KR protein in BTs versus the rest of the epidermis. Longitudinal sections of *Tg(KR21)* pectoral fins show that KR expression in the superficial cones of BTs is localized only at the cell membrane. In the underlying epidermis, KR appears to be distributed equally between the Golgi, where it is synthesized, and the cell membrane (data not shown). The intracellular distribution pattern of KR between the Golgi apparatus and the cell membrane is consistent with that in other transgenic lines using the same membrane-tagged KR (Korzh *et al*., 2011).

Using *Tg(KR21)* zebrafish, we observed that BTs are present in both sexes, but are more prominent in males. Both sexes display a small cluster and a single row of BTs on each side of the head and isolated BTs on the ventral surface of the head (Supplementary Figure II.1). The presence of BTs on the dorsal surface of the head, barbels, and along the

fin rays of dorsal, anal, and pelvic fins in males is sexually dimorphic (Figures. 4.1, Supplementary Figure II.1). On male pectoral fins, isolated BTs are observed from the second branching point to the distal tip of the second to fifth/sixth fin rays and along the entire anteriormost ray (fin ray 1 being the most anterior and ray 11 the most posterior) (Figure 4.1 A, B). In addition, male zebrafish display BT clusters along the dorsal surface of the second to fifth/sixth pectoral fin rays (Figure 4.1 A-F; Supplementary Figure II.1 A). We verified that only males, identified by the presence of testes upon dissection, had BT clusters on their pectoral fins (n = 13). The length of these clusters is proportional to the length of the ray, with the longest clusters on the third to fifth rays and the shortest clusters on the second and sixth rays (Figure 4.1 A, J). *Long fin* mutants, named after their long fin rays, possess longer BT clusters than wildtypes (Supplementary Figure II.1C). Individual BTs within each cluster are conical, and have a single pointed tip with a broad base (Figure 4.1 G-I). Although these BTs are larger, their morphology is similar to isolated BTs elsewhere on zebrafish (Figure 4.1 A-F, Supplementary Figure II.1 D-R). We focused our analysis on the pectoral fin BT clusters.

4.6.2 Pectoral Fin BT Cluster Development in Male Zebrafish

The earliest developmental stage at which pectoral BT clusters appear in male zebrafish is 1.3 cm standard length and at least 2.5 months old (n = 122) (Supplementary Figure II.2), which correlates with sexual maturation (Westerfield, 2000). Random sampling of fish of 2.5 months to 1 year indicates that BTs develop progressively over time. In the earliest stages, a single line of small BTs is observed along the fin rays. Afterwards, a cluster of small BTs develops that progressively enlarges over time (Supplementary Figure II.2).

4.6.3 Pectoral Fin Breeding Tubercle Clusters Are Epidermal Structures Covered with a Renewable Keratin Cap

BT structure was analyzed on pectoral fin transverse sections. The superficial cap of BTs is conical in shape with a hollow center (Figure 4.1 K-M) and is made of keratin, as shown in red following Mallory staining (Figure 4.1 K). These caps are not stained following picrosirius red staining, indicating the absence of collagen (Figure 4.1 L). Underlying each keratin cap is a raised, supportive epidermis that consists of small aggregates of epidermal cells that stain blue with Mallory staining (Figure 4.1 K). More specifically, the epidermis stains light blue along the base and progressively darkens as the keratinization process continues upwards. The progressive darkening during Mallory stains has been suggested to reflect epidermal differentiation during the process of keratinization (Wiley and Collette, 1970). Furthermore, the last two layers of epidermal cells are hypertrophied, likely due to the large keratin content. In addition, nuclei in the epidermis, as shown by DAPI staining, are displaced towards the basal surface of each cell (Figure 4.1 M). Interestingly, the outer keratin cap of each cluster is periodically shed, but males in our fish facility always have BT clusters on their pectoral fins (Figure 4.1 N,N'). Thus, it is likely that the second keratin-containing cell layer replaces the outer keratin cap once it is shed. Cell proliferation analysis by proliferating cell nuclear antigen (Pcna) immunohistochemistry indicates that only cells in the deepest layers of the epidermis are proliferating (Figure 4.1 O). The more superficial cells do not proliferate (Figure 4.1 O). This profile suggests that BT formation involves the proliferation of progenitors within the deepest layers of the epidermis. As these cells progress towards the upper layers, they exit the cell cycle and differentiate into keratin-producing cells.

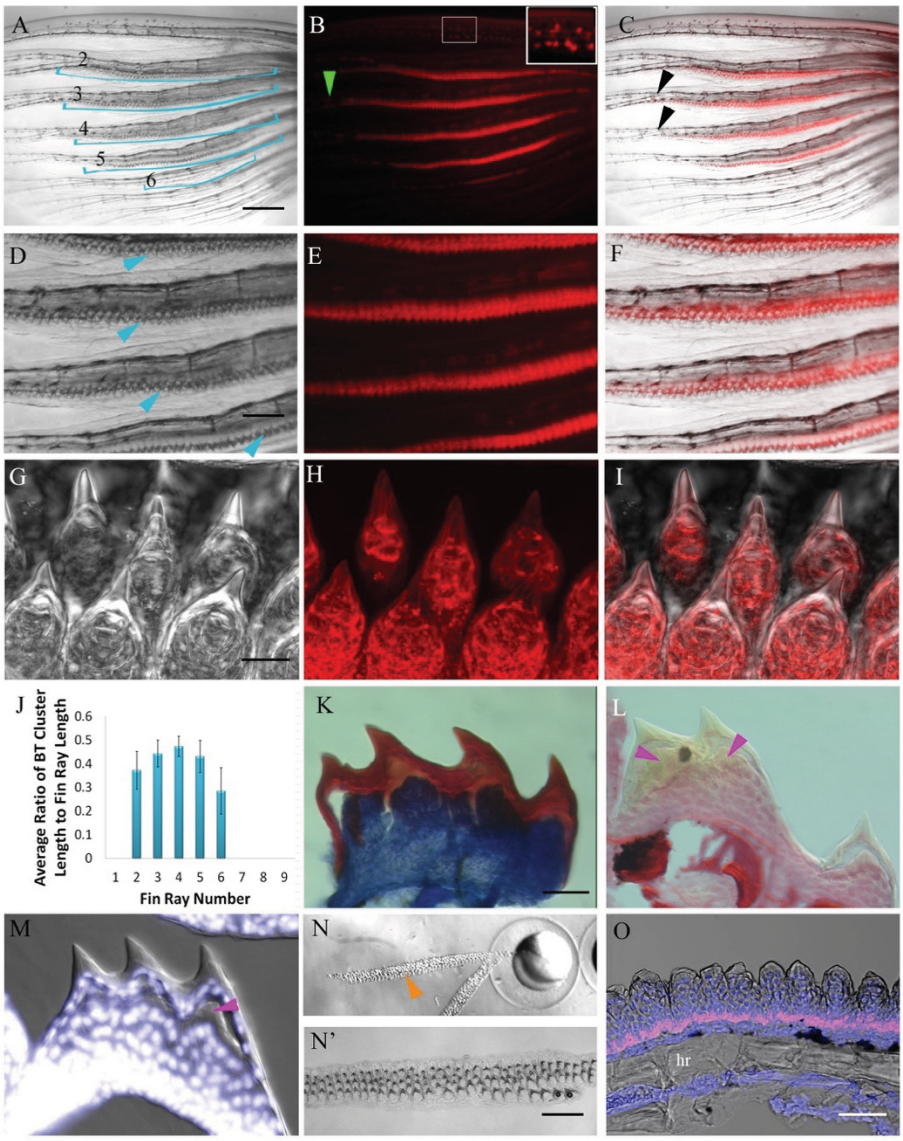

Figure 4.1: Characterization of male zebrafish pectoral fin BTs. (A-F) Brightfield and fluorescent (red) images of BTs (indicated by blue arrowheads in D and lines in A) on *Tg(KR21)* male pectoral fins. (B,C) Isolated BTs on fin ray 1 (inset in B) and on the distal tips (green arrowhead in B, black arrowheads in C) of rays 2-6. (D-F) Higher magnifications of A-C. (G-I) DIC images with confocal acquisition of *Tg(KR21)* BTs. (G) DIC image of BTs. (H) Red fluorescent image of BTs. (I) Merged image of G and H. (J) Length of the BT cluster correlates with the length of the fin ray. Error bars indicate s.d. (K) Mallory stains on a transverse section of a BT keratinized cap (red) and underlying epidermis (blue). (L) Picrosirius Red stain indicates that there is no collagen in BTs. (M) Nuclei are present in all epidermal layers, including the keratin cap of BTs (DAPI stain). (L,M) A second keratin layer is observed underneath the most superficial keratin layer (pink arrowheads). (N,N') Shed BT clusters (orange arrowhead; magnified in N') alongside an embryo. (O) Pcna immunohistochemistry (red) and DAPI staining (blue/white) on longitudinal sections indicates epidermal proliferation. hr, hemiray. Scale bars: 200 μm in A-C; 100 μm in D-F; 25 μm in G-I,K-M; 500 μm in N,N; 50 μm in O.

4.6.4 Breeding Tubercle Clusters Possess a Secondary Blood Vessel Network

The examination of blood vessel networks in *Tg*(*fli1a:EGFP*) fish, expressing EGFP in all endothelial cells (Lawson and Weinstein, 2002), reveals a qualitative increase in vascularisation in regions of male pectoral fins containing BTs in males as compared with females (Figure 4.2). The overall fin vasculature in females is similar to that described in caudal fins (Huang *et al.,* 2003). One artery runs down the center of each ray and two veins run along the external border of the rays. Within and between rays, intervessel commissures and interray vessels connect the arteries to veins and veins to veins, respectively (Figure 4.2 A-C, G-I). In males, regions of pectoral fins devoid of BTs present a vasculature similar to that of females (Fig. 4.2D). By contrast, BT clusters are highly vascularized (Figure 4.2 D-L, P-R). Confocal analysis of *Tg(fli1a:EGFP)* male pectoral fin longitudinal sections reveals a web of blood vessels, which overlies the artery and intervessel commissures/interray vessels and penetrates into the epidermis of BT clusters (Figure 4.2 P-R). Longitudinal sections through the most proximal portion of the male pectoral fin suggests that these additional vessels are derived from the central blood vessels between the two hemirays (Supplementary Figure II.3). Upon reaching the epidermis, the vessel travels in parallel to the hemirays, periodically forming connections with the central blood vessels (Supplementary Figure II.3). In females, no vessels are observed in the epidermis overlying the fin rays (Figure 4.2 M-O).

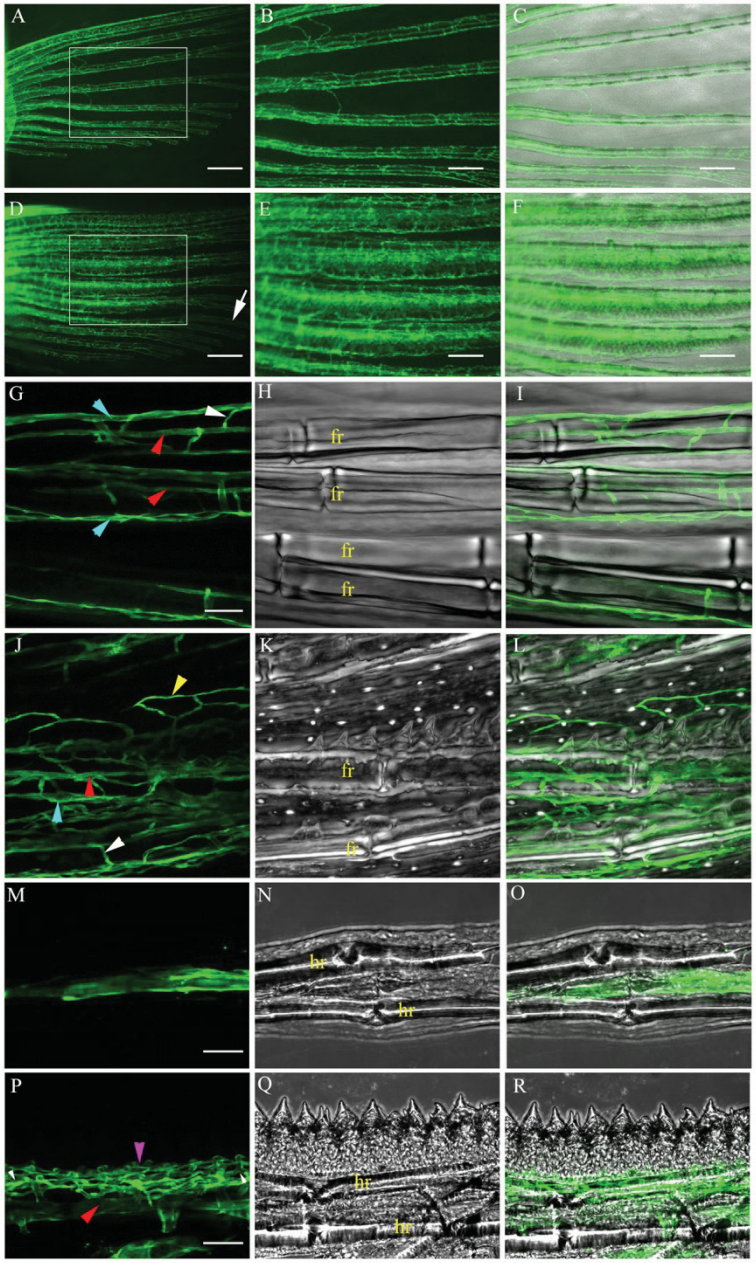

Figure 4.2: Vasculature in *Tg(fli1a:EGFP)* pectoral fins. (A-C) Blood vessels (EGFP, green) in female zebrafish. (D-F) BT clusters in males are highly vascularized (boxed in D), but not in surrounding areas (arrow in D). (B, C, E, F) Higher magnification of the boxed regions in A,D. (C,F) Merged brightfield and fluorescent images. (G-R) Confocal micrographs. (G-I) Female with a single artery (red arrowheads), two veins (blue arrowheads) and intervessel commissures (white arrowhead). (J-L) Male with vascularized BTs, an artery (red arrowhead), intervessel commissures (white arrowhead), interray vessels (yellow arrowhead) and veins (blue arrowhead). (M-R) Longitudinal sections. (M-O) Female showing blood vessels that lie between the two hemirays. (P-R) Male showing blood vessels present in a web-like pattern (pink arrowhead) in the epidermis and above the artery (red arrowhead). fr, fin ray; hr, hemiray. Scale bars: 200 μm in A,D; 100 μm in B,C,E,F; 50 μm in G-L; 25 μm in M-O; 50 μm in P-R.

4.6.5 Pectoral Fin Breeding Tubercle and Blood Vessel Regeneration

To investigate the regenerative properties of BTs, pectoral fins of males (n = 15) and females (n = 15) were amputated and regeneration was observed for 15 days post amputation (dpa) (Figure 4.3). Following amputation, BTs are progressively re-established in a proximal to distal manner over the regenerating tissue. A keratin layer first appears in the regenerate adjacent to the stump between 4 and 5 dpa (Figure 4.3 C, D). Concomitantly, the underlying epidermis progressively thickens (Figure 4.3 C-E) and regenerating BTs reacquire a mature structure with keratin caps and a tooth-like shape at 7 dpa (Figure 4.3 E). By contrast, the female 7 dpa pectoral fin regenerate is not keratinized and the epidermis appears thinner than in males (Figure 4.3 F). Furthermore, PAS staining of regenerating and intact female pectoral fins reveals goblet cells along the dorsal and ventral surfaces. Goblet cells are not observed in male fins containing mature or regenerating BTs (Supplementary Figure II.4). In over half the fish examined (19 out of 30), BT clusters of 15 dpa regenerating fins appear on both the dorsal and ventral sides (Figures 4.5 J, Supplementary Figure II.5 O, S, W). The other 11 pectoral fins reformed BTs on only the dorsal surface of the rays.

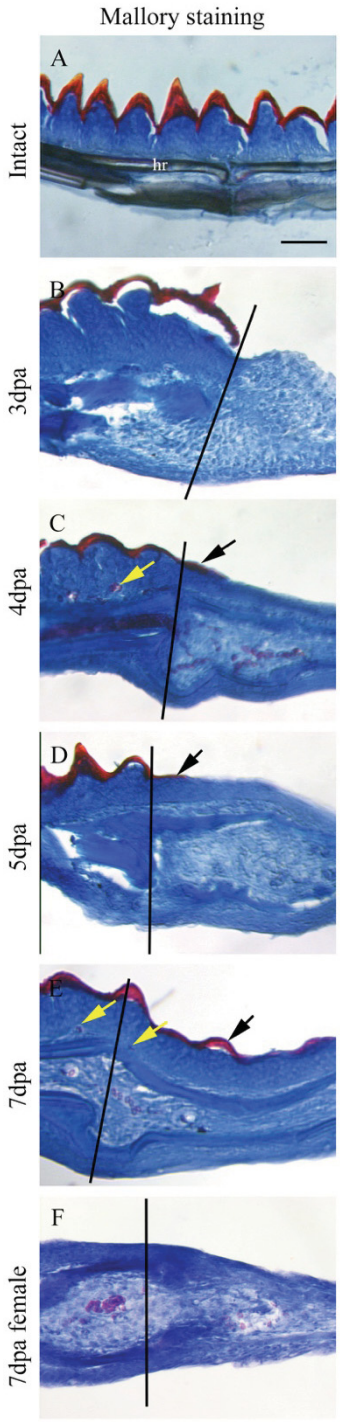

Figure 4.3: Male pectoral fin BT regeneration. Mallory stain of intact (A) and regenerating (B-F) pectoral fin longitudinal sections. (A, B) Keratinized caps (red) and underlying epidermis (blue) are observed on intact fins (A) but are lost in 3-dpa regenerates (B). (C, D) At 4-5 dpa, a layer of keratin is deposited in the proximal regenerate (black arrows). (E) At 7 dpa, BTs (black arrow) are observed in the fin regenerate. (F) Females do not possess BTs. Yellow arrows indicate blood cells. Black lines (B-F) indicate the amputation plane. dpa, days post-amputation. hr, hemiray. Scale bar: 50 μm.

Using *Tg(fli1a:EGFP)* zebrafish, we examined BT regeneration in relation to pectoral fin re-vascularization. In all female fin rays (n = 8) and male posterior fin rays (n = 8), blood vessel regeneration follows a pattern previously observed in caudal fins (Figure 4.4Aa-h, Ba-h, Da-h) (Huang *et al.,* 2003). In contrast, initial plexus formation in the male anterior fin rays appears irregular in shape and is delayed at 3dpa (Figure 4.4 Ab, Cb). From 5 dpa onwards, there is a proximal to distal increase in fluorescence underneath newly forming BTs (Figure 4.4Cd-h).

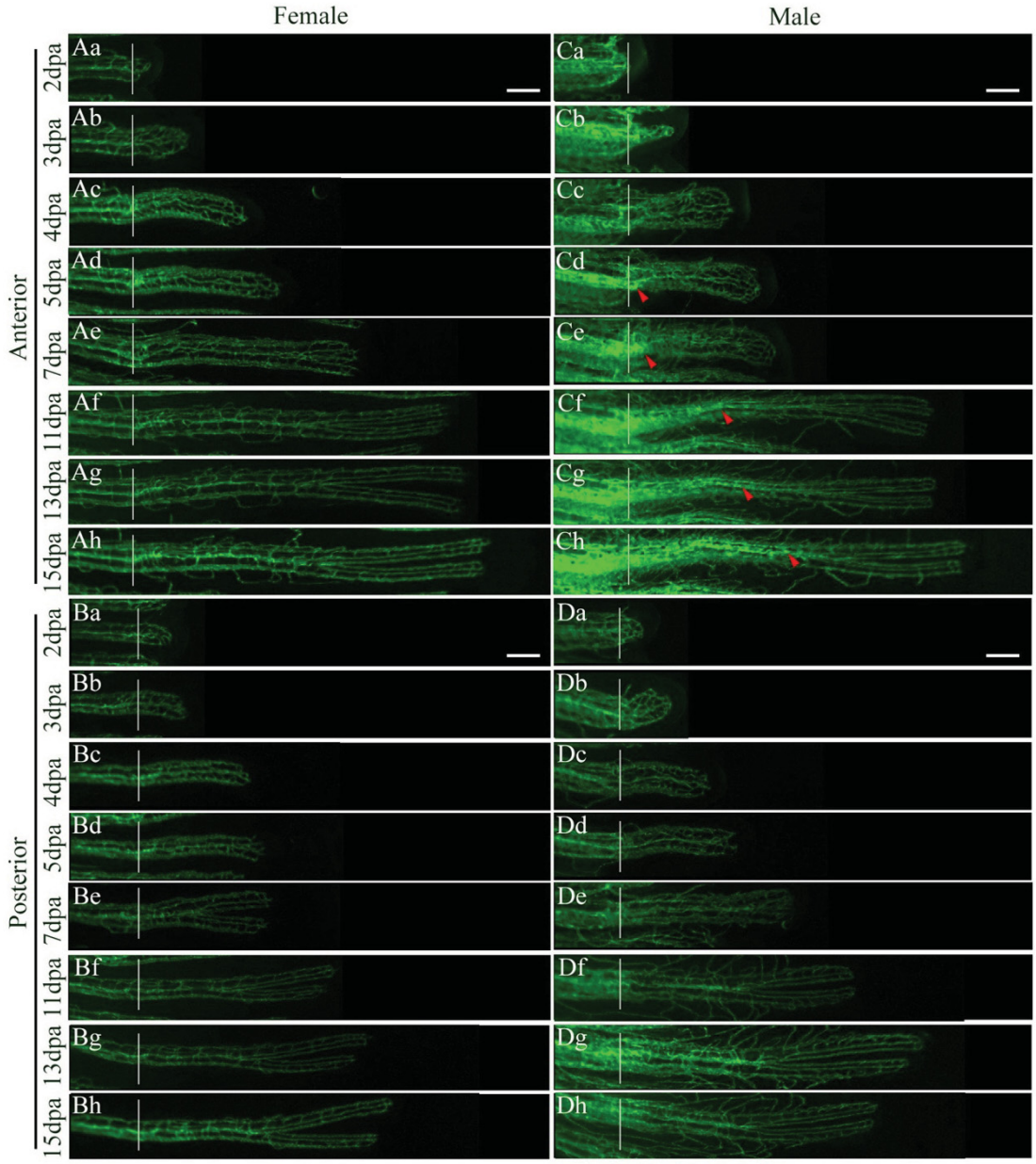

Figure 4.4: Male and female *Tg(fli1a:EGFP)* blood vessel regeneration. (Aa-h, Ba-h, Da-h) Blood vessel regeneration follows similar patterns in the female (A,B) and posterior (D) male rays. (Ca-h) Plexus formation (Cb) is delayed in the male anterior ray compared with females (Ab) and appears irregular in shape. (Cd-h) At 5 dpa, a second wave of neo-angiogenesis occurs underneath new BT formation in the male anterior ray and proceeds in a proximal-to-distal manner (red arrowheads). Anterior, fin ray 4; posterior, fin ray 7. White lines indicate the plane of amputation. Scale bars: 100 μm.

Confocal analysis of longitudinal sections of *Tg(fli1a:EGFP)* female (n = 4) and male (n = 4) anterior pectoral fin regenerates from 4-8 dpa, revealed that the increase in fluorescence in males is due to a second wave of blood vessel regeneration (Figure 4.5). In females, blood vessels regenerate between the two hemirays (Figure 4.5A, C, E, G, I). The same blood vessel pattern is initially observed in males at 4 dpa (Figures 4.4 Cb, Cc, 4.5B). However, by 5 dpa, a second wave of blood vessel regeneration is observed along the base of newly forming BTs (Figures 4.5 D). As BT regeneration proceeds, blood vessels grow in a proximal to distal fashion along the base of the epidermis, reforming the original web of blood vessels (Figures 4.2 P, 4.5 H, J). Furthermore, new vessels periodically sprout from the central blood vessels between hemirays and connect to vessels in the epidermis (Figures 4.5 D, F). Blood cells were often observed in the stump (Figures 4.3 C) and in the regenerate underneath new and forming BTs (Figures 4.3 E). Overall, our data suggest that BT regeneration begins following the initial wave of blood vessel regeneration, but occurs simultaneously with a second wave of neo-angiogenesis.

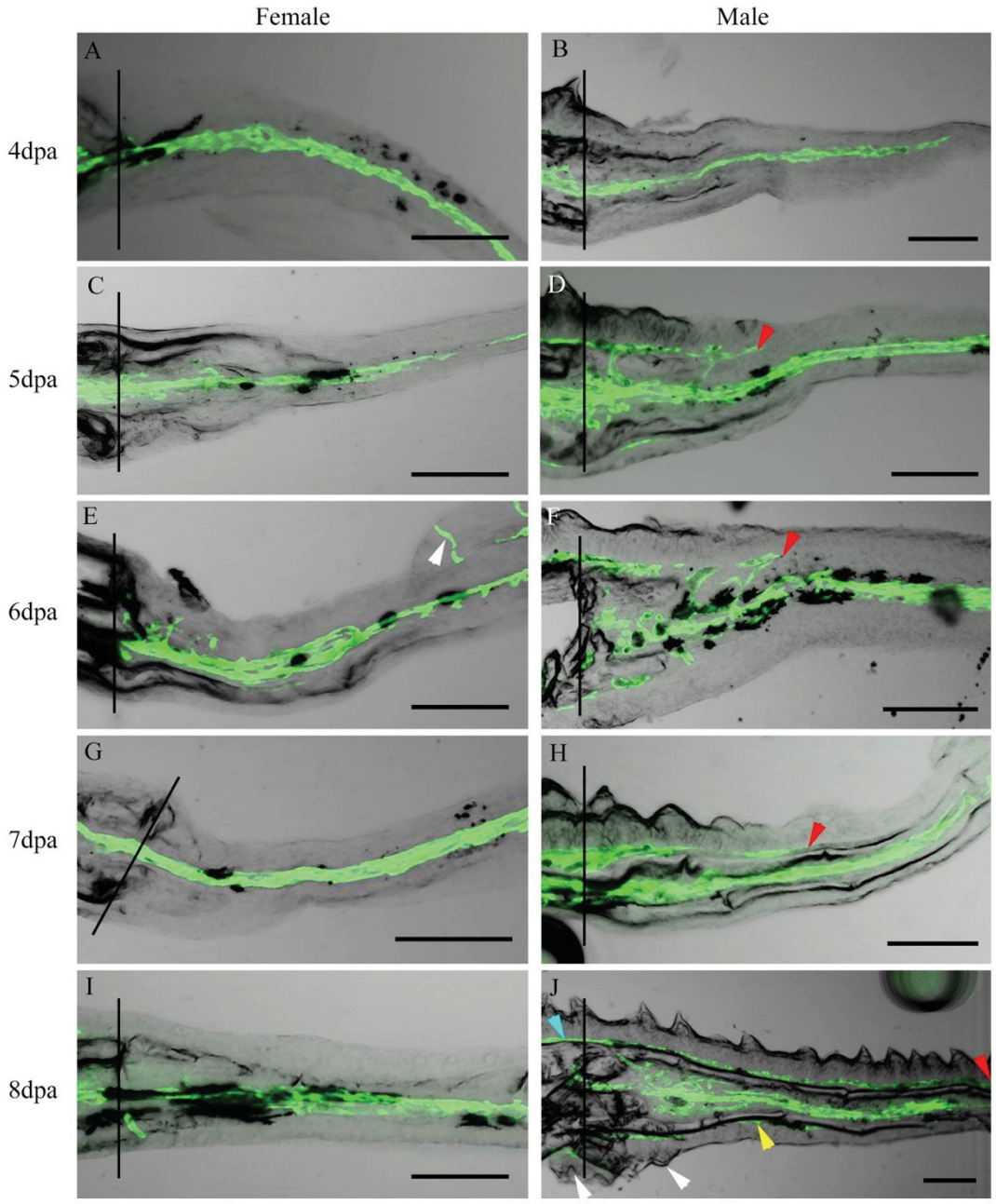

Figure 4.5: BT cluster regeneration occurs alongside a second wave of neo-angiogenesis. Confocal images of longitudinal sections of regenerating male and female pectoral fins. (A, C, E, G, I) Female blood vessels regenerate along the center of the ray. (E) Arrowhead indicates the distal ray folded back on itself. (B) The first wave of male blood vessel regeneration occurs down the center of the ray. (D, F, H, J) At 5-8 dpa, a second wave travels in a proximal-to-distal fashion along the base of the epidermis (red arrowhead). (J) New BTs (white arrowheads) and blood vessels (yellow arrowhead) are observed in the ventral fin regenerate. Blue arrowhead indicates blood vessels along the base of BTs located in the stump. Black vertical lines indicate the amputation plane. Scale bars: 100 μm.

4.6.6 Androgen Treatment Induces BT Formation in Intact and Regenerating Fins

BT development on male pectoral fins coincides with sexual maturation, indicating a potential hormonal contribution. We investigated the role of steroid hormones in BT cluster formation in intact and regenerating adult pectoral fins. In the following experiments, the right pectoral fin of males and females is amputated at the center of the BT cluster and corresponding level, respectively. The left pectoral fin is left intact.

To investigate the role of androgens in BT formation, adult males and females (> 4 months old) were treated for 15 days [days of treatment (dot)] with testosterone (T) (1 μg/L) (n = 6 males and 6 females). T-treated males possess BTs that are larger in intact and regenerating fins than in untreated males (Figures 4.6 A, B, Supplementary Figure II.6). In addition, 4 out of 6 regenerating fins developed BTs on both sides of the ray by 15 dpa (Supplementary Figure II.6 B). In females, T induces BT cluster formation on both intact fins and stumps of regenerating fins after 4 dot (Supplementary Figure II.7 A, B). By 6 dot, immature BTs are observed on the regenerating tissue (n = 6) (Supplementary Figure II.7F). These BT clusters continue to enlarge until treatments are suspended after 15 days, when BTs appear similar to those of untreated males (Figures 4.6C, D, Supplementary Figure II.7). Ethanol treatments alone (0.000033% EtOH) do not affect BT formation or regeneration (n = 6 males and 6 females) (Figures 4.6 E-H).

Treatments for 23 days with flutamide (2 mg/L), an AR antagonist (Peets *et al*., 1974), does not affect female intact and regenerating fins (n = 6) (Figure 4.6 K, L). Treating males with flutamide reduces the size of BT clusters in intact fins and in the stump of fin regenerates after 14 dot (n = 6) (Supplementary Figure II.5 B, F, J). Since no BTs are observed in regenerates after 14 days (Supplementary Figure II.5D, H, L), treatments were

continued to ensure the lack of BTs was not the result of a delay in regeneration (Fig. 4.6 I-L). At 23 dot, only a few small BTs are observed in the regenerate close to the stump in only one of two males examined (Figure 4.6 I) and BTs on the intact fin appear reduced (Figure 4.6 J). Ethanol treatments alone (n = 6 males and 6 females treated with 0.000042% ethanol) appear similar to system water controls (Figure 4.6 E-H). To exclude the possibility that the above effects are the result of aromatization of T into 17β-estradiol (E2), females (n = 12) were treated with 5α-dihydrotestosterone (DHT) (1 μg/L), a non-aromatizable androgen that binds to ARs (Goldstein and Wilson, 1972; Hillier *et al*., 1980). Similar to T, DHT induces BT formation in both intact and regenerate stumps of female pectoral fins after 4 dot (data not shown). BTs are initially observed on fin regenerates after 6 dot (data not shown). These BTs continue to enlarge until the cessation of treatments after 15 days (Figure 4.6 O, P). Similar to T treatment, BTs in DHT-treated males are slightly larger than non-treated BTs and all regenerating fins possess clusters that cover both sides of the ray (Figures 4.6 M, N, Supplementary Figure II.6). In two out of six males examined, the anterior rays in the pectoral fins failed to regenerate. This regeneration failure is similar to that recently described (Nachtrab *et al*., 2011). Mallory staining of 15 day T- and DHT-treated fins indicates keratinized BTs are present on all fins except the caudal fin (data not shown).

To further test the effect of T aromatization on BT formation, males and females were treated with fadrozole (50 μg/L), an aromatase inhibitor. As expected, fadrozole does not affect males (n = 6) (Fig. 4.6 Q, R). However, BTs are observed in fadrozole-treated females (n = 7) after 7dot (3/7), 10dot (4/7), and 14dot (7/7) in the intact fin (Figure 4.6 T).

Similarly, BTs are observed at 7dot (3/7), and at 10dot (7/7) in fadrozole-treated female fin regenerates (Figure 4.6 S).

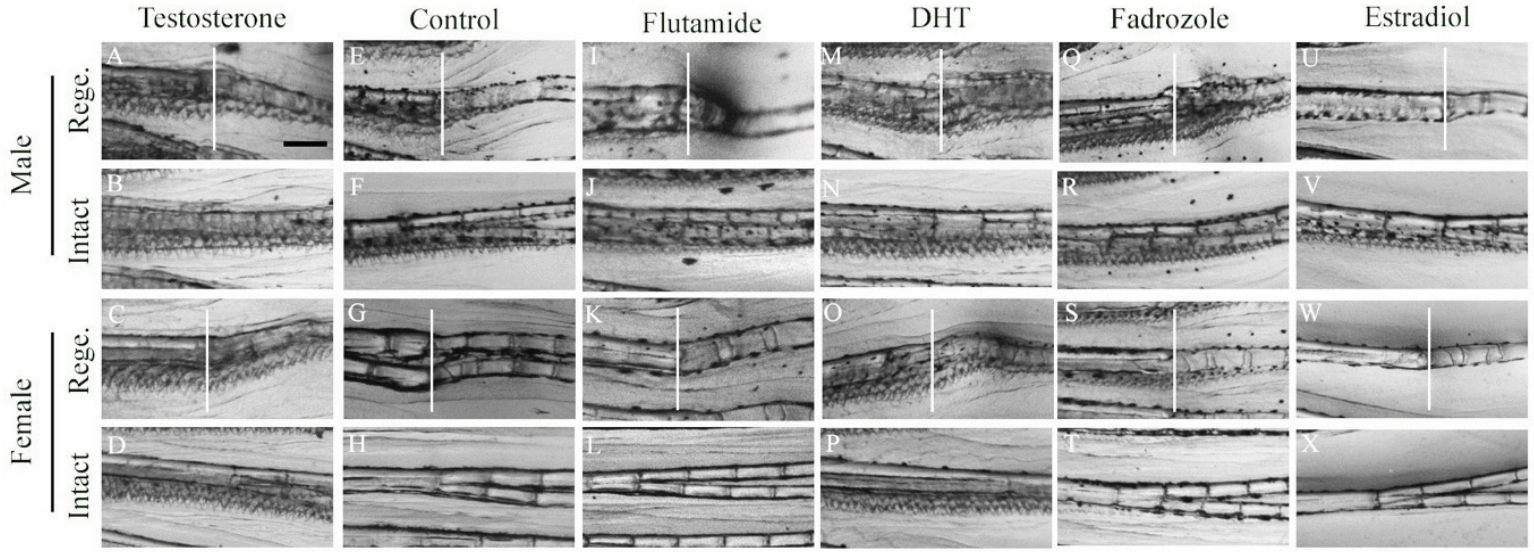

Figure 4.6: Androgens induce and estrogens inhibit pectoral fin BT formation. BTs are observed in male regenerate and intact fins treated with testosterone (T) (1 μg/l) (A, B), 5α-dihydrotestosterone (DHT) (1 μg/l) (M, N) and fadrozole (50 μg/l) (Q, R). Treatment with testosterone (T) (1 μg/l) (C, D), 5α-dihydrotestosterone (DHT) (1 μg/l) (O, P) and fadrozole (50 μg/l) (S,T) for 15 days induces BT formation in the regenerating and intact female fin. Flutamide treatment (2 mg/l) (23 dot) (I, J) and 17β-estradiol (E2) (1 μg/l) (16 dot) (U,V) inhibit and reduce BT formation in the male regenerate and intact fin, respectively. Flutamide (K, L) and E2 (W, X) treatments do not affect females. Controls (E-H). dot, days of treatment. Scale bar: 100 μm.

Following cessation of treatments with fadrozole, females were kept in system water to determine whether BT clusters disappear. 58 days post cessation of treatments [days post treatment (dpt)], BT clusters are completely absent in all females (4/4) (Figure 4.7 A-F). Similarly, DHT-treated females display highly reduced BTs that are barely visible at 88 dpt (4/4) (Figure 4.7 G-L). Altogether, our data suggest that pectoral fin BT cluster development and maintenance depends on the presence of androgens acting through the AR. Interestingly, qRT-PCR data indicate approximately equal levels of the *AR* mRNA in non-treated, male and female pectoral fins (Supplementary Figure II.8).

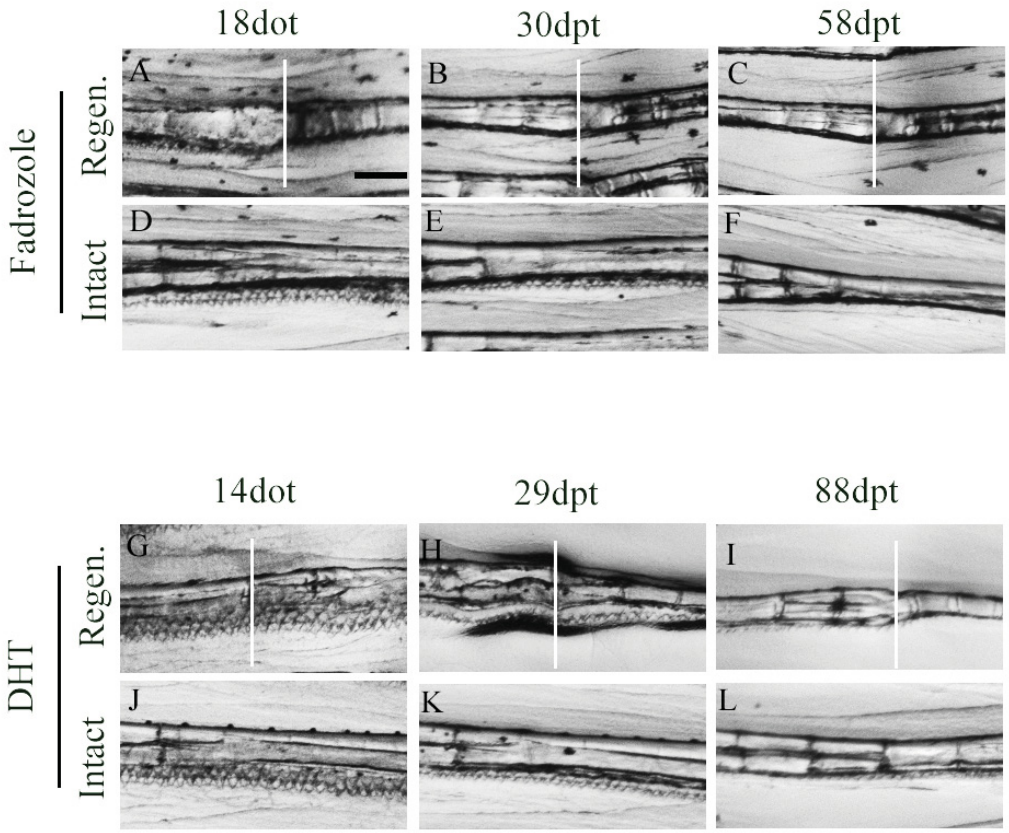

Figure 4.7: Pectoral fin BTs regress following cessation of chemical treatments in females. (A-F) Regenerating (A) and intact (D) fins treated for 18 days with fadrozole. (B, E) At 30 dpt, BTs appear reduced. (C, F) At 58 dpt, BTs have disappeared. (G, J) Female regenerate (G) and intact fins (J) following 14 dot with DHT. (H,K) At 29 dpt, BTs appear. (I, L) At 88 dpt, BTs are barely visible. White vertical line indicates the amputation plane. dpt, days post-treatment. Scale bar: 100 μm.

We next investigated the effects of estrogens on BT formation. Males and females were treated with E2 (1 μg/L), which binds to all zebrafish estrogen receptors (Menuet *et al.,* 2004). After 16 dot, no changes are observed in the intact and regenerating female pectoral fins (n = 6) (Figure 4.6 W, X). In contrast, after 16 dot, BTs do not form in the male pectoral fin regenerates (n = 6)(Figure 4.6 U). Additionally, BT clusters on the male intact fin and stump appear smaller (Figure 4.6 U, V). After 18 and 21 dot BTs are still absent in the male fin regenerate (Supplementary Figure II.5N,P,R,T,V,X). Although there is a variable delay in regeneration, these fins are able to regenerate to the point where BTs should be observed. These treatments are also lethal in 50% of male fish by 7 dot (n = 6). Ethanol treatments alone (0.000033% EtOH) (n = 6 males and 6 females) appear similar to system water controls (Figs. 4.6E-H, Supplementary Figure II.5 M, O, Q, S, U, W). Overall, our data suggest that androgens induce and estrogens inhibit BT formation in zebrafish.

4.6.7 Androgen Treatment Induces Blood Vessel Growth and BT Cluster Formation in the Anterior Rays of Female Pectoral Fins

To investigate the relationship between blood vessels and BT formation, *Tg(fli1a:EGFP)* female pectoral fin vascularization was examined during androgen treatments. Following 14 dot with T (1 μg/L) or with DHT (1 μg/L), all female intact (n = 6) and regenerating (n = 6) rays develop a male-like blood vessel pattern in the region of BT formation (Figure 4.8 A-F, I, J, P, T). Further analysis of longitudinal sections (n = 12) of *Tg(fli1a:EGFP)* T-treated female intact and regenerating pectoral fins, confirmed that T-induced BT formation occurs in conjunction with neo-angiogenesis (Figures 4.8 B', D', Supplementary Figure II.7). More specifically, in T-treated females, BT cluster formation occurs after 4 dot and vascularization is observed along the epidermis after 5 dot

(Supplementary Figure II.7 A, C). In T-treated female fin regenerates, blood vessel regeneration occurs in two waves as observed in males: the central blood vessels regenerate first, followed by the vascularization of maturing BTs (Supplementary Figure II.7 B, D, F, H, J). Interestingly, male pectoral fin regenerates (n = 6) treated for 14 days with flutamide (2 mg/L) are devoid of BTs (Supplementary Figure II.5D, H, L), have a female-like blood vessel network (Figure 4.8 G, H), and no second wave of neo-angiogenesis.

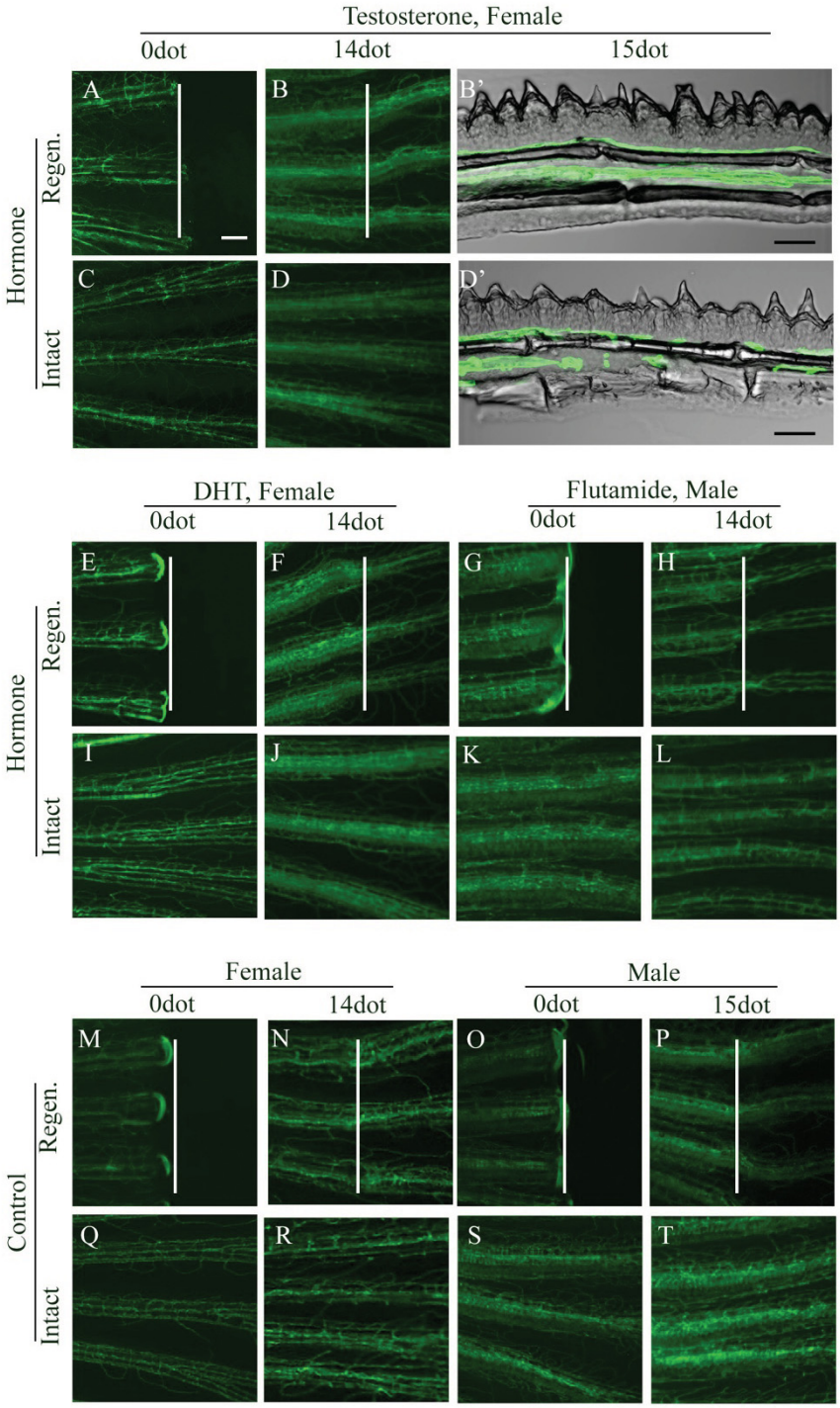

Figure 4.8: Androgens induce neo-angiogenesis in intact and regenerating pectoral fins. (A-D) Intact and regenerating fins of T- (14 dot) (B, B', D, D') and DHT- treated (14 dot) females (F,J) develop vascularized BTs not observed at 0 dot (A,C,E,I). (G, H, K, L) Blood vessels of flutamide-treated (14 dot) male intact and regenerating fins acquire a female-like appearance. (O, S, P, T) Control non-treated males. (M, N, Q, R) Control non-treated females. Amputation site (White vertical lines). Scale bar for all fluorescent images = 100μm (shown in A). Scale bar for confocal images (B',D') = 50μm.

4.6.8 Endothelial and Epidermal Cells Proliferate Upon Testosterone Treatment

To examine changes in cell proliferation that are associated with BT formation in T-treated females, double fluorescent immunohistochemistry for Pcna and EGFP was performed on intact pectoral fins of 5 day T-treated *Tg(fli1a:EGFP)* females. Anterior rays of non-treated female pectoral fins show a few proliferating cells in the epidermis (Figure 4.9 A). However, similar to males, cells in the deepest layers of the epidermis are proliferating in 5-day T-treated females (Figure 4.1 O, 4.9 B, C). Furthermore, endothelial cells between the hemirays of 5-day T-treated females are proliferating, suggesting a potential origin for the blood vessels that vascularize these BTs (Figure 4.9 C).

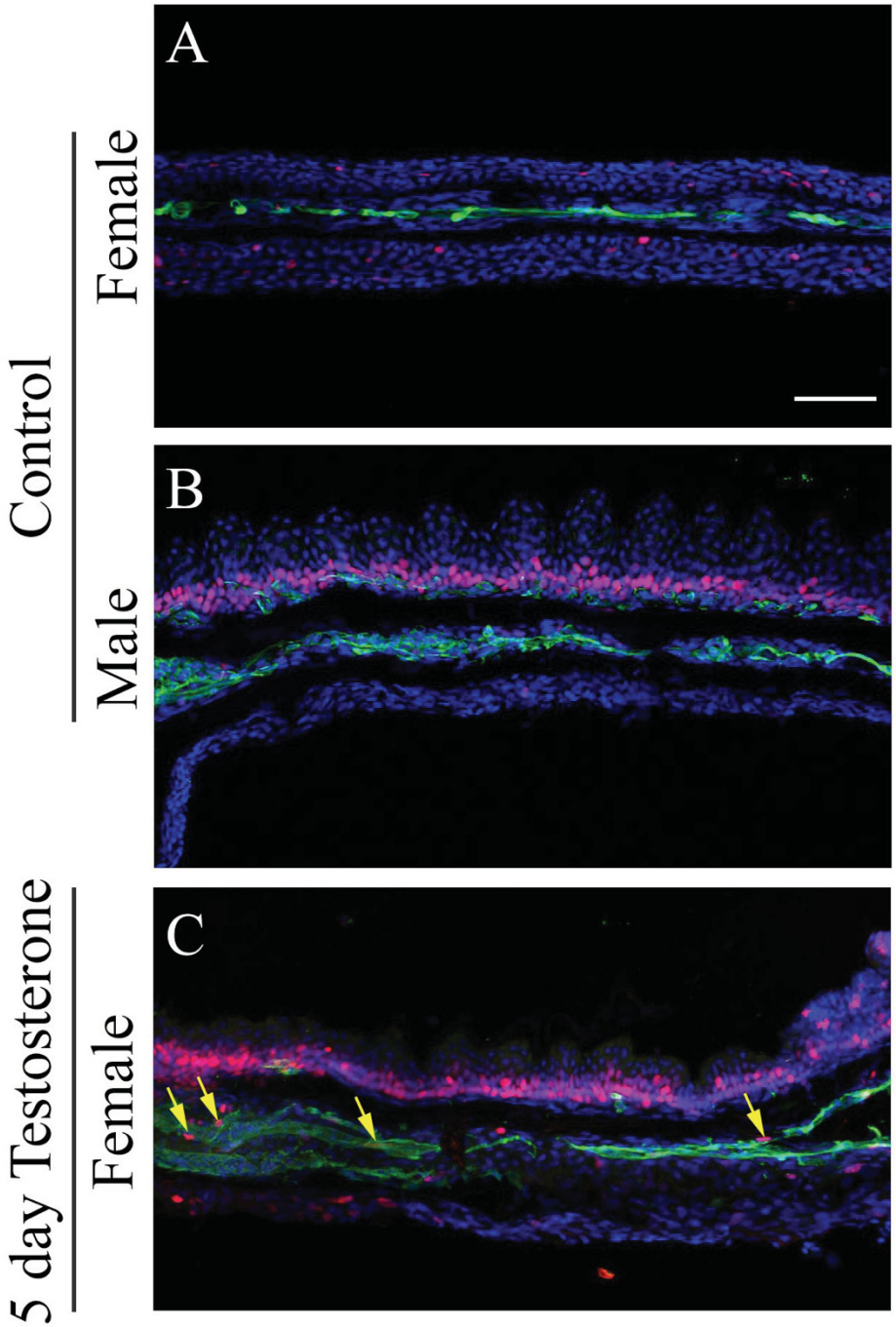

Figure 4.9: Pectoral fin endothelial and epidermal cells proliferate upon testosterone treatment. Pcna (red) and DAPI (blue) staining of *Tg(fli1a:EGFP)* intact fin longitudinal sections. (A) Females display few proliferating cells. (B) Males present many proliferating cells deep in the epidermis. (C) T-treated females (5 dot) develop a proliferation profile similar to that of males in the epidermis. Endothelial cell proliferation is induced (arrows). Scale bar: 50 μm.

4.6.9 BT Cluster Formation Depends on the Development of an Additional Blood Vessel Network

To determine whether an additional blood vessel network was required for BT formation, *Tg(KR21; fli1a:EGFP*) females were treated with T (1 μg/L) and PTK787 (500 nM), an inhibitor of vascular endothelial growth factor receptor tyrosine kinases that effectively inhibits regenerative angiogenesis in the zebrafish caudal fin (Wood *et al.,* 2000; Bayliss *et al*., 2006). Immediately following pectoral fin amputation, PTK787 treatments were initiated. Females were treated for two days with PTK787 prior to T treatment to ensure PTK787 had time to take effect. At 6 dpa, a single row of BTs is observed on PTK787/T-treated female intact fins and the stump of regenerating pectoral fins. No BTs are visible in the regenerate (Figures 4.10Aa-Ca, Supplementary Figure II.9 Aa, Ba). At 8 dpa, BTs on the intact fin have grown slightly and isolated BTs are observed on PTK787/T-treated fin regenerates (Figure 4.10 Ea, Fa, Supplementary Figure II.9 Ca, Da). At 14 dpa, a small BT cluster has formed in the proximal PTK787/T-treated fin regenerate (Figures 4.10 Ga-Ha, Supplementary Figure II.9 Ea). In contrast to PTK787/T-treated females, T-treated females (4 dot) quickly develop large BTs on intact and regenerating fins (Figures 4.10 Ab-Cb, Supplementary Figure II.9 Ab, Bb). These clusters continue to grow until treatments are suspended 12 days later (Figures 4.10 Eb-Ib, Supplementary Figure II.9 Cb-Fb). Finally, all PTK787 treatments, including PTK787/T treatments, efficiently inhibit neo-angiogenesis in the intact and regenerating pectoral fins, limiting the distance of tissue regeneration (Figure 4.10 Aa-Ja, Ac-Jc). Control females that received PTK787 alone or system water did not form BTs (Figure 4.10 Hc, d, Ic, d).

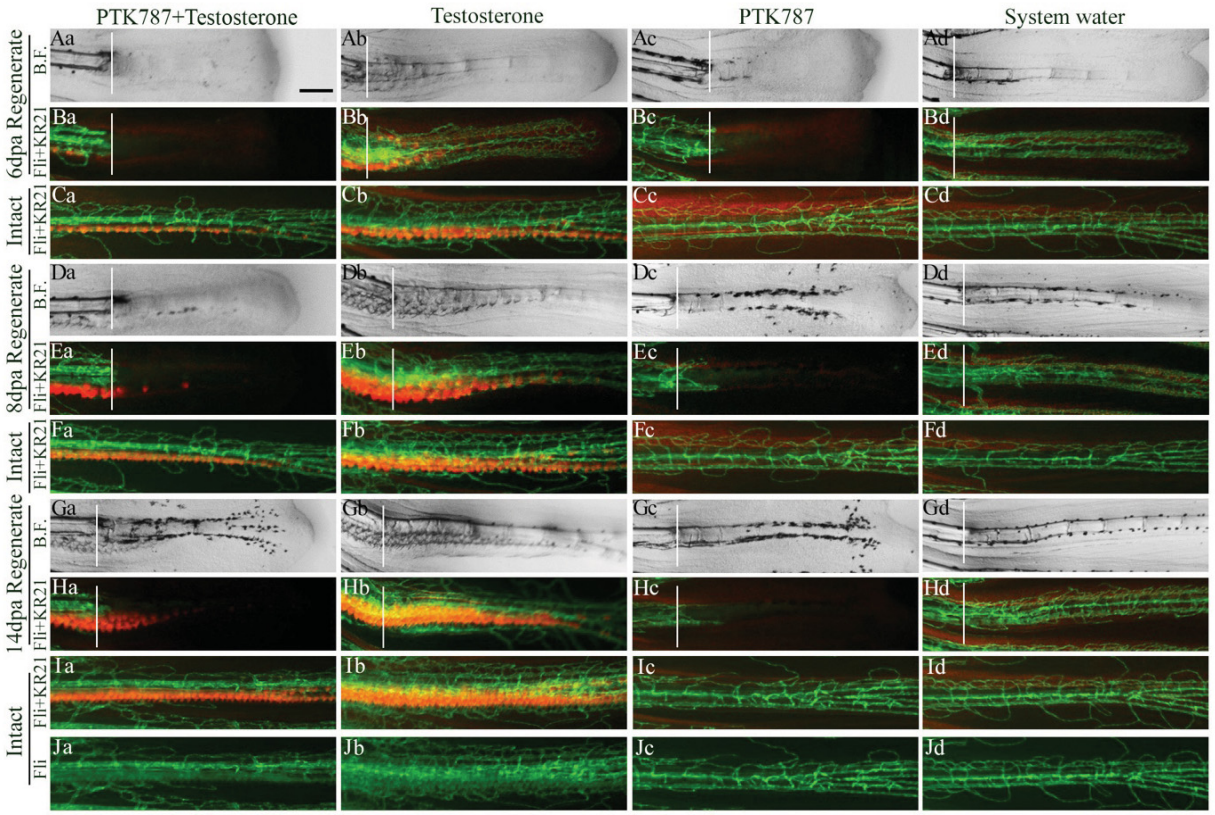

Figure 4.10: Inhibition of neo-angiogenesis affects T-induced BT growth in the female pectoral fin. (Aa-Ja) A single row of BTs on the intact fin and stump after 6-14 dot with PTK787 and 4-12 dot with T. Small BTs appear in the fin regenerate after 8 dot with PTK787 and 6 dot with T (Da, Ea). A small BT cluster appears on the regenerate after 14 dot with PTK787 and 12 dot with T (Ga, Ha). (Ab-Jb) After 4 dot with T, BTs develop on the regenerate, stump and intact fin and continue to grow from 6-12 dot. (Jb) After 12 dot, the blood vessel network of T-treated females is similar to that of males. (Ac-Jc) PTK787-treated females do not possess BTs. (Aa-Ja, Ac-Jc) Neo-angiogenesis and regenerative outgrowth are inhibited in all PTK787-treated females. (Ad-Jd) System water controls regenerate normally and do not grow BTs. B.F., brightfield. Fli, *fli1a:EGFP* (green). KR21 (red) outlines the BTs. White vertical lines indicate the amputation plane. Scale bar: 100μm

4.7 Discussion

The investigation of large, sexually dimorphic, BT clusters in intact and regenerating male pectoral fins outlines a mechanism by which these structures are formed, maintained, and regenerated (Figure 4.11). BT cluster regeneration occurs alongside a second wave of neo-angiogenesis, which forms the web-like blood vessel network of BT clusters. Androgen-induced BT formation occurs through ARs. Concomitantly, androgens induce angiogenesis to promote BT formation. Although the inhibition of neo-angiogenesis using PTK787 does not fully block androgen-induced BT formation, it is likely that blood vessels already present in the fin are sufficient for the growth of small BTs. We propose that the additional blood vessels in males and androgen-treated females are required to promote the formation of large BT clusters. However, we cannot exclude the possibility that BTs themselves may play a role in the induction of angiogenesis. Finally, since BT formation is inhibited by E2-induced activation of estrogen receptors, we suggest that it is the balance between these two sex steroids that determines the presence or absence of BT clusters in zebrafish.

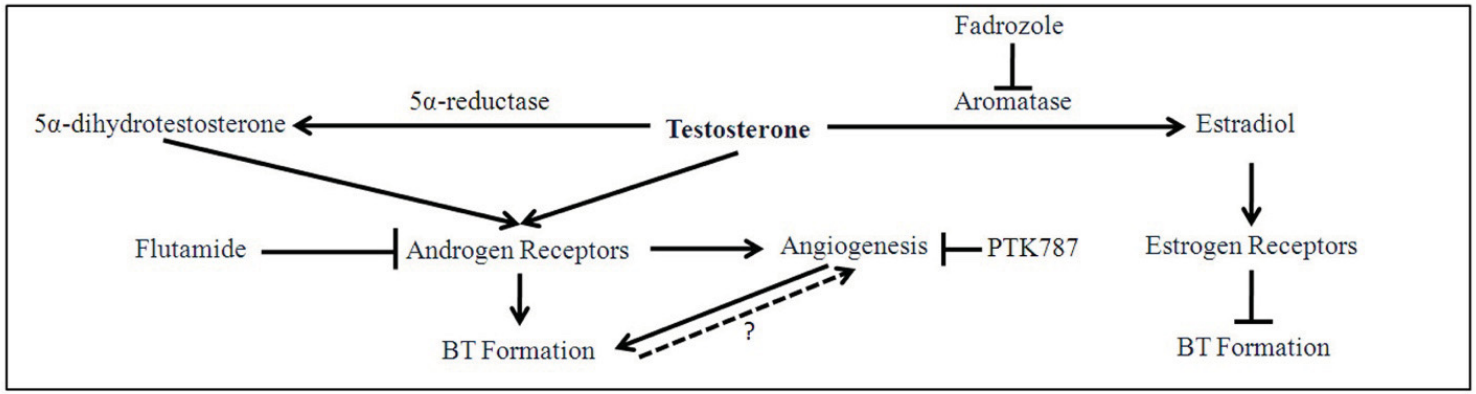

Figure 4.11: A model for BT formation. BTs are induced by androgens 5α-dihydrotestosterone (DHT) and testosterone (T) through androgen receptors (ARs). Receptor blocking via flutamide inhibits BT formation. Androgen-induced neo-angiogenesis through the AR is necessary for BT formation, as PTK787 inhibits BT formation. Inhibition of T conversion to 17β-estradiol (E2) by fadrozole induces BT formation. Estradiol inhibits BT formation through the activation of estrogen receptors. BT formation itself might induce angiogenesis through an as yet unknown mechanism (dashed arrow).

Initial comparisons between male and female zebrafish demonstrate that BTs in males are more prominent than in females. In males, sexually dimorphic BTs appear on all fins except the caudal fin, with the largest BTs clusters occurring along the anterior pectoral fin rays. These BT clusters are present year round, which is consistent with studies in *Oryzias latipes* (medaka) (Okada and Yamashita, 1944; Yamamoto and Egami, 1974). However, this observation contrasts with previous studies of BTs in other species such as *Carassius auratus* (goldfish), *Pimephales promelas* (fathead minnow), *Stenodus leucichthys* (freshwater whitefish), and *Osmeridae* (smelt), which have BTs that appear before the spawning season and gradually disappear over time (Smith 1978; Berg, 1948; Wiley and Collette, 1970). These authors suggest that the presence of BTs depends on temperature, light, and breeding season. We observed the persistent presence of BTs in zebrafish that were kept at a constant temperature of 28.5°C with a photoperiod of 14 hours of light and 10 hours of darkness (Westerfield, 1995). Since temperature, light cycles, and nutrition are variable in the natural habitat of zebrafish (Spence *et al.,* 2008), it is possible that wild zebrafish may lose BTs when seasons change. Furthermore, wild zebrafish breed between April and August (Engeszer *et al*., 2007), while zebrafish in captivity mate year round. The function of BTs in zebrafish is still unknown, but previous studies in other species have implicated roles in mate recognition and body contact maintenance during spawning (Kortet *et al.,* 2003; Wiley and Collette, 1970). If BTs are necessary for zebrafish mating, the constant presence of BTs on the dorsal surface of pectoral fins may be necessary for year-round breeding in laboratory facilities. However, the requirement for BTs during breeding in zebrafish has yet to be determined.

Despite the fact that pectoral fin BT clusters are consistently observed on laboratory zebrafish, the superficial keratin-caps are regularly shed. The proliferation of cells in the deepest layers of the epidermis allows the continual production of new progenitors that differentiate and mature into keratin-producing cells and assures the efficient replacement of shedding keratin-caps. To our knowledge, the mechanisms responsible for this renewal have not been described in any fish species.

Since BT clusters are large, it is suggested that blood vessels are required to efficiently form and maintain these structures over long periods of time. Initial examination of the male zebrafish pectoral fins revealed BT clusters are highly vascularized. Analysis of BT regeneration in relation to blood vessel re-vascularization shows that BT formation correlates with a second wave of neo-angiogenesis in pectoral fin regenerates. This second wave likely derives from vessels set down in the first wave, which supports tissue regeneration. Thus, the delay in the first wave of blood vessel regeneration in males compared to females could be due to an added requirement of BT vascularization. Consequently, we suggest the possibility that the overall delay in male pectoral fin regeneration observed by Nachtrab *et al.,* (2011) may result from BT cluster formation that limits the availability of factors (ie. blood vessels) required for fin regeneration. Overall, these results indicate that the BT cluster formation and growth may benefit from additional blood vessels, but that this might be costly in terms of regeneration.

In other teleost species, the size, number, and appearance of BTs correlate with circulating concentrations of androgens (Borg, 1994; Kortet *et al*., 2003). Furthermore, previous studies have shown that androgens induce and estrogens reduce the formation of BTs, respectively (Smith, 1974; Smith and Smith, 1986; Ramaswami and Hasler 1955;

Pawlowski *et al*., 2004). Here we show that androgens (T and DHT) and an aromatase inhibitor (fadrozole) induce the formation of BTs in both intact and regenerating pectoral fins of female zebrafish. Fadrozole can effectively decrease serum levels of E2, leading to differentially expressed estrogen responsive genes and impaired ovarian development in female goldfish (Zhang *et al.,* 2009). Similarly, fadrozole reduces serum levels of E2 in female fathead minnows, whereas androgen serum levels remain stable (Ankley *et al*., 2002). Since E2 inhibits BT formation in the fin regenerate and reduces the appearance of BTs in intact fins, the presence of BTs in fadrozole-treated female zebrafish is likely the result of an absence of E2 inhibition, not an increase in androgens. Although, Ramaswami and Hasler (Ramaswami and Hasler, 1955) suggest that E2 does not prevent BT formation in developing male *Hyborhynchus,* it is possible that the effects of E2 treatments in the Ramaswami study are not sufficient to overcome androgen-induced BT formation in developing males (1955). In support of our results, Miles-Richardson *et al.* (1999) found a significant reduction in BT size in male fathead minnows treated with E2.

Using flutamide, an AR antagonist (Peets *et al*., 1974), BT formation was inhibited and reduced in the fin regenerate and intact fins, respectively. A few small BTs are observed in the proximal regenerate in a single male after 21 dot. Zebrafish treated with vinclozolin, another competitive AR inhibitor, up-regulate *ar* gene transcription as a compensatory mechanism (Smolinsky *et al*., 2010). Therefore, the inability of flutamide to completely inhibit BT regeneration in all males may result from an increase in *ar* expression in response to treatments. Initial qRT-PCR experiments indicate that *ar* mRNA are not differentially expressed between non-treated male and female intact pectoral fins, suggesting that the *ar* expression levels do not naturally influence BT formation. We

propose that endogenous levels of circulating androgens and estrogens may determine the presence or absence of BTs.

Androgen-treated females develop a male-like blood vessel network surrounding newly formed BTs. These new vessels likely originate from the proliferation of endothelial cells in the central vessels between the hemirays. Overall, these data are consistent with recent *in vitro* and *in vivo* mouse studies, demonstrating the sex-specific pro-angiogenic effects of androgens in males (Sieveking *et al*., 2010). More specifically, in cell culture and in mice, androgens increase the expression of genes (i.e. *Vegf*, and *Vcam1*) and promote processes related to angiogenesis (Death *et al.,* 2004; Ruohola *et al.,* 1999; Sieveking *et al*., 2010). Our data indicate that females treated with androgens experience the same pro-angiogenic effects, resulting in male-like vascularised BTs. However, we cannot exclude the possibility that the increase in tissue thickness associated with BT growth may also play a role in the induction of angiogenesis. Furthermore, the absence of a second wave of blood vessel formation in flutamide-treated zebrafish is consistent with data that indicate endothelial cell proliferation induced via androgens is reduced through the effects of flutamide (Williams *et al.,* 2004). The absence of BTs in flutamide-treated males is likely due to the general inhibition of the AR and/or the absence of a second wave of blood vessel growth. Overall, the presence and absence of the vascularized BT clusters upon androgen and flutamide treatments, respectively, suggest that additional vascularization in non-treated males and androgen-treated females is required for BT formation.

The angiogenesis inhibitor, PTK787 (Wood *et al*., 2000), successfully inhibited neo-angiogenesis and reduced BT growth in intact and regenerating pectoral fins of T-

treated females. Previous data indicate that regeneration can occur up to 1mm away from an intact blood supply (Bayliss *et al*., 2006). Therefore, although treatment with both PTK787 and T did not completely inhibit BT formation, we suggest that the blood vessels already present in the intact fin and stump of females are sufficient to allow the formation of undersized BT clusters. However, when exogenous androgens are provided, the quick growth of large BT clusters in intact and regenerate fins depends on the induction of a blood vessel network similar to that observed naturally in males.

4.8 Acknowledgements

The work summarized here benefited from the assistance of Natasha Bougie, Louai Naddaf and Thinh N'Guyen. We thank Vishal Saxena for help with fish husbandry and Dr. Marc Ekker for discussion and critical reading of the manuscript. Funding from CIHR (MAA) and NSERC (VLT) is acknowledged with appreciation.

Manuscript #2: Pectoral Fin Breeding Tubercle Clusters: A Method to Determine Zebrafish Sex

Stephanie. C. McMillan[a, b]; Jacqueline Géraudie[c] Marie-Andrée Akimenko[b, d]

[a] Department of Cellular and Molecular Medicine, University of Ottawa, ON K1N 6N5, Canada.

[b] CAREG, 30 Marie Curie, University of Ottawa, ON K1N 6N5, Canada.

[c] University of Paris 7, 2 place Jussieu Paris, 75251, France (retired).

[d] Department of Biology, 30 Marie Curie, University of Ottawa, ON K1N 6N5, Canada.

Published in: *Zebrafish* 2015 Jan 20; 12(1): 121-123.

4.9 Author Contributions

Stephanie. McMillan: Wrote the manuscript.

Jacqueline Géraudie, Professor at the Université Paris 6, Jussieu, Paris, France (retired): Initially observed BTs on the pectoral fins of male zebrafish and informed Dr. Marie-Andrée Akimenko about these BTs.

Marie-Andrée Akimenko : Supervised the project and provided critical reading of the manuscript.

4.10 Pectoral Fin Breeding Tubercle Clusters: A Method to Determine Zebrafish Sex

Large breeding tubercle (BT) clusters, spike-like keratinized epidermal structures, have been identified along the mid-dorsal surface of wild-type (AB, Ekkwill, Wik, Tuebingen) and *long fin* mutant male zebrafish pectoral fin rays (McMillan *et al*., 2013; Kang *et al.,* 2013; Fischer *et al*., 2014; Géraudie *et al*., 1994). The androgen-dependent growth of BT clusters occurs only in males and appears around the time of sexual maturation (McMillan *et al*., 2013). Once present, these structures are maintained through the continuous renewal of the most superficial keratinized layer for the entire life of the fish, playing an essential role in stimulating egg release during spawning (Kang *et al.,* 2013). The constant presence of these easily visualized structures only in males allows for the quick distinction of sex. Current guidelines available for distinguishing males from females rely on differences in the color, shape, and behavior of these fish. Generally, males appear pinkish-gold, possess a streamlined body, and chase females prior to mating. Females appear blueish-white and possess a protruding egg-filled abdomen (Avdesh *et al.*, 2012; Parichy *et al*., 2009; Westerfield *et al*., 1995). These guidelines have been proven subjective. For example, not all females possess an obvious distended abdomen and there are reports of similar coloring in males and females (Spence *et al*., 2006). Although females are distinguishable from males via the presence of genital papilla (Yossa *et al*., 2013), these ventrally located structures are small and difficult to observe in non-anesthetized fish. Overall, the ambiguities of previously set guidelines make the determination of zebrafish sex difficult, particularly for new students and staff members. Here we report the use of sexually dimorphic pectoral fin BTs as a means to facilitate in the identification of male and female zebrafish.

The determination of sex using BTs requires that zebrafish are placed in a small fish tank that sits on a light-colored background. Examination of the dorsal surface of each spread pectoral fin will reveal the presence or absence of BTs. BTs are clearly visible from above as brown lines along the central fin rays of males (Figure 4.12 A). Females lack BTs, thus their pectoral fins are translucent (Figure 4.12 B). Together, these characteristics allow for the immediate distinction of zebrafish sex (Figure 4.12 C). BTs are easily visible in adult (AB, Ekkwill, Wik, Tuebingen and *long fin* mutant) zebrafish without any microscopic aids. However, a stereomicroscope can be used to identify small BTs on young, lightly anesthetized, fish as small as 1.3cm or 2.5 months (McMillan *et al*., 2013). A small bowl of 0.17mg/ml of tricaine (ethyl-aminobenzoate) can be placed directly under the stereomicroscope (Westerfield *et al*., 1995). Fish immersed in tricaine solution are immobilized in seconds, spreading their pectoral fins laterally, enabling an immediate unobstructed view of the fin rays. Under the stereomicroscope, the spike-like BT structures are easily identifiable along the central fin rays (McMillan *et al*., 2013) (Figure 4.12 D-G). Fish exposed to tricaine will eventually flip upside-down; however, dorsally located BTs are still visible from the ventral surface of pectoral fins due to inter-ray tissue transparency. Given the ease at which BTs are observed under the stereomicroscope, the determination of sex should take a maximum of 30 seconds.

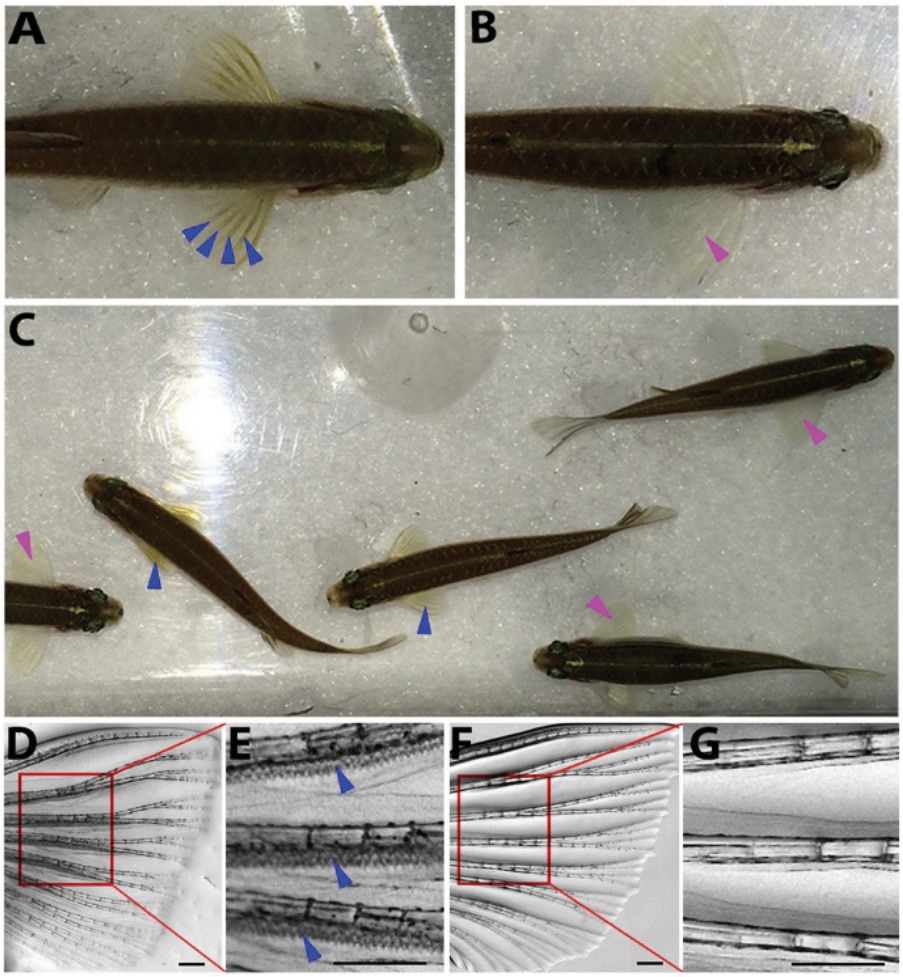

Figure 4.12: Distinguishing male and female zebrafish based on large clusters of breeding tubercles (BTs). (A) Male zebrafish possess BT clusters, observed as brown lines, along the central pectoral fin rays (blue arrowheads). (B) Female pectoral fins are translucent, as they do not possess BT clusters (pink arrowhead). (C) Dorsal view of zebrafish in a standard breeding tank. Female pectoral fins (pink arrowheads) can be distinguished from male pectoral fins (blue arrowheads). (D) Under the stereomicroscope, male zebrafish possess BT clusters that appear as spike-like structures along the central fin rays. (F) These structures are absent on female pectoral fins. (E, G) Higher magnification of the central rays of male (E) and female (G) pectoral fins (red boxes in D, F) highlights the presence (blue arrowheads) and lack of BTs, respectively. All scale bars=200 μm. Photographs (A–C) were taken with an 8-megapixel camera on an iPhone 5S.

Chapter 5: General Discussion

Regeneration, a process in which structures that have been lost or injured are replaced (Morgan *et al.,* 1901; Sunderland, 2010), is highly variable among organisms. Since all organisms are prone to injury, there exists a strong desire to identify strategies to regenerate tissues that do innately possess ability to do so. In order to develop such strategies, one must first understand the basic principles of regeneration. The overall goal of this study was to contribute to a greater understanding of the basic underlying mechanisms that lead to fin regeneration in zebrafish (*Danio rerio*).

Previous work in our lab has been focused on the role of Sonic hedgehog a (Shha) signaling during fin regeneration. Results stemming from this work indicates that *shha*-expressing cells in the basal epidermal layer play an essential role in bone patterning and branching morphogenesis. In tetrapods, Shh has been shown to play a critical role in branching of the lungs (Affolter *et al*., 2009; Chuang *et al.,* 2003; Gjorevski *et al*., 2010; Miller *et al*., 2004; Pepicelli *et al.,* 1998), prostate (Freestone *et al*., 2003; Pu *et al.,* 2004; Thomson and Marker, 2006) and salivary glands (Harunaga *et al.,* 2011; Jaskoll *et al*., 2004). Branching morphogenesis of these structures depends on epithelial and mesenchymal cell interactions (Affolter *et al*., 2009, Gjorevski and Nelson, 2010, Gray *et al.,* 2010 and Harunaga *et al*., 2011). Furthermore, mutations in the human *SHH* gene results in an array of severe congenital defects (Belloni *et al*., 1996; Bertolacini *et al*., 2010; Nanni *et al.,* 1999). In zebrafish, *shha*-expressing cells in the basal epidermal layer have been shown to similarly play a role in patterning the regenerating fin rays via interactions with adjacent osteoblasts (Zhang *et al.,* 2012). Therefore, the zebrafish fin offers a simple model system to better understand the various mechanisms controlling branching

morphogenesis. A greater understanding of these mechanisms could result in the development of novel diagnostic methods or treatments for congenital defects associated with a failure in branching morphogenesis.

One of the outstanding questions in fin regenerates is the mechanism by which the expression domain of *shha* splits and is maintained at the same proximal-distal location in the fin regenerate. Furthermore, we do not know to what extent the descendants of the *shha*-expressing cells contribute to the epidermis of the regenerate. To answer these questions, an inducible genetic fate-mapping approach was attempted to identify the contributions of the derivatives of *shha*-expressing cells to the epidermis of fin regenerates (Figure 5.1). However, determining the cell fate of *shha*-expressing cells was unsuccessful due to a lack of sufficient *cre* expression in *shha*-expressing cells of the *Tg(shha: ERT2CreERT2:ABC; Insulator; cmlc2:EGFP)* transgenic lines during caudal fin regeneration. Future work will involve creating a line that expresses *cre* more strongly in the basal epidermal cells of the adult caudal fin regenerate.

Adjacent to the *shha*-expressing cells, *indian hedgehog a* (*ihha*) is expressed in differentiating osteoblasts that form the regenerating fin rays. Currently, the role of *ihha* in osteoblast differentiation during fin regeneration is unknown. However, *Ihh* has been well described as a major factor regulating endochondral ossification in tetrapods (Bitgood and McMahon,1995; Vortkamp *et al.,*1996). More specifically, it has been shown that a negative feedback mechanism occurs between Ihh and Parathyroid related Protein (PTHrP) to allow the precise control over the amount of chondrocyte proliferation and differentiation during endochondral ossification in long bones (Long *et al.,* 2004). Gene expression analysis indicates that *pthrp1,* the homolog of the mammalian *Pthrp* is

expressed in joint cells of the caudal fin regenerate (Figure 5.1). Consequently, the regenerating dermal fin rays were used as a model to further elucidate the mechanisms underlying intramembranous ossification and joint formation.

During joint formation, it is suggested in this thesis that joint cells express early *runt related transcription factor 2a* and *2b* (*runx2a/runx2b*) pre-osteoblast markers, but do not express the osteoblast commitment marker *sp7* (also known as *osterix, osx*), intermediate stage bone marker *collagen, type X, alpha 1a* (*col10a1a*) (Avaron *et al.,* 2006), or late osteoblast marker *osteocalcin* (*Bgp, osc*) (Sousa *et al*., 2011) (Figure 5.1). Since immature joint cells initially express early osteoblast markers, but not later osteoblast markers it is suggested that these cells may initially retain the ability to differentiate into osteoblast cells. Similar to the caudal fin regenerate, in mouse it has been shown that *Runx2*-expressing pre-osteoblasts are bipotential cells that can differentiate into either osteoblasts or chondrocytes (Nakashima *et al.,* 2002). However, upon expression of *osx* cells must differentiate into osteoblasts (Nakashima *et al.,* 2002). Therefore, future work could focus on using the conserved regulatory modules of human *RUNX2* (Knopf *et al*., 2011), and the cre-loxP system, to drive the expression of *osx* specifically in pre-osteoblasts of the regenerating fin rays. The forced expression of *osx* in joint cells should result in the differentiation of these joint cells into osteoblast cells, illustrated as a complete lack of joints in the fin regenerate.

Furthermore, recent lineage-tracing studies have shown that the dermal fin rays regenerate through the de-differentiation and re-differentiation of spared osteoblasts (Knopf *et al.,* 2011). However, upon ablation of osteoblasts, the fin rays regenerate normally (Singh *et al.,* 2012). These findings suggest an alternative source of osteoblasts

during fin regeneration. The ability of joint cells to potentially differentiate into osteoblasts suggests that these cells are a potential alternative source of osteoblasts during fin regeneration. Currently, the intergenic region between *evx1* and *hoxa13a* is being cloned upstream of an EGFP reporter. It is hoped that this will allow the generation of a transgenic line that will recapitulates *evx1* and/or *hoxa13a* expression in the fin regenerate. If this line successfully recapitulates *evx1* and/or *hoxa13a* expression, we will use these regulatory elements to create a line that expresses *cre* in joint forming cells. Once created, this line could be crossed to *Tg*(*ubi:loxP-GFP-loxP-mCherry*), a reporter line that ubiquitously expresses GFP, but switches to express mCherry permanently following the Cre catalyzed excision of GFP at the LoxP sites (Mosimann *et al*., 2011). Consequently, the fate of joint cells can then be mapped, allowing the contribution of joint cells to the osteoblast lineage to be determined following ablation of intact osteoblasts.

We showed that joint cell differentiation can be separated into three cell types: Presumptive joint cells, joint-forming cells, and mature joint cells. Presumptive joint cells correspond to the most distal *hoxa13a* expression domain (Figure 5.1). The more mature joint-forming cells correspond to a group of cells in the most distal domain that co-expresses *hoxa13a, evx1, and pthrp1* (Figure 5.1). The mature joint cells correspond to any group of joint cells proximal to joint forming cells, including the cells of the intact stump that co-express all three of the above mentioned factors. In the absence of Evx1, presumptive joint cells are committed to an osteoblast cell fate. Furthermore, using the *evx1*$^{-/-}$ homozygous loss of function mutant and the calcineurin inhibitor FK506, a pathway has been discovered in which calcineurin activity regulates the position of *hoxa13a* expressing presumptive joint cells in the fin regenerate (Figure 5.1). Furthermore, as joint

cells differentiate, *evx1* occurs downstream or parallel to *hoxa13a*, but upstream of *pthrp1* (Figure 5.1).

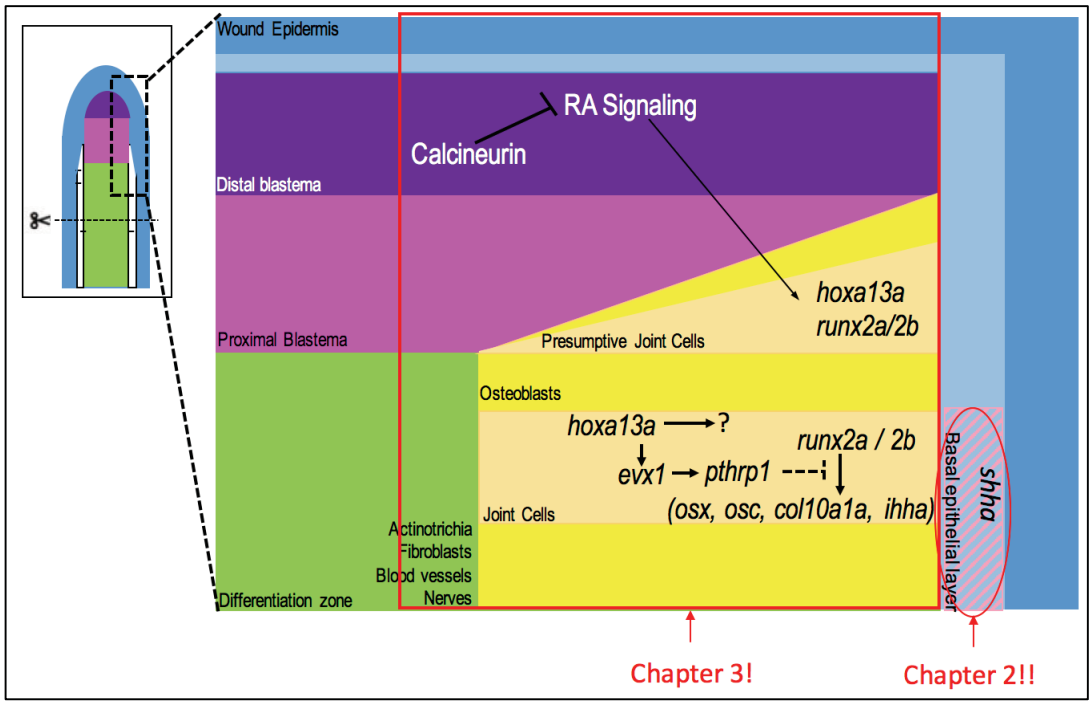

Figure 5.1 Summary of chapters 2 and 3. In chapter 2: Genetic fate-mapping was used to identify the contributions of the derivatives of *shha*-expressing cells to the epidermis of caudal fin regenerates. In chapter 3 the regenerating dermal caudal fin rays calcineurin may act upstream of retinoic acid to regulate the position of presumptive joint cells. These presumptive joint cells express *hoxa13a* and *runx2a/b*. As presumptive joint cells mature into joint forming cells *evx1* is expressed downstream or parallel to *hoxa13a* and upstream of *pthrp1*. *pthrp1* may act to inhibit osteoblast differentiation.

In the fin regenerate, RA signaling is required for blastema formation and proliferation. However, RA signaling inhibits osteoblast de-differentiation and re-differentiation (Blum and Begemann, 2015). To circumvent this issue, mature osteoblasts in the stump de-differentiate and contribute to the blastema through the upregulation of *cyp26b1* (Blum and Begemann, 2015). In the distal blastema, re-differentiation of pre-osteoblasts is suppressed through high RA levels (Blum and Begemann, 2015). However, as pre-osteoblasts enter the more proximal regenerate, *cyp26b1* positive fibroblast cells serve as a sink, reducing RA levels (Blum and Begemann, 2015). Consequently, pre-osteoblasts are able to differentiate into osteoblasts.

In vertebrates, a correlation between *Hox* gene patterning and RA signaling has been observed in regulating the specification of positional identities of the hindbrain during development (Gavalas, 2002; Gavalas and Krumlauf 2000; Maden, 2002; Hernandez *et al*. 2007). In the hindbrain, RA forms a gradient with the highest concentration caudally that decreases in rostral directions. As the hindbrain develops, and new somites are added, the source of RA synthesis shifts posteriorly (Abu-Abed *et al*., 2001; Sakai *et al*., 2001; Alexander *et al*., 2009). Concurrently, various Cyp26 family members, RA degrading enzymes, are dynamically expressed in the anterior hindbrain during embryonic development restricting access of the developing hindbrain to RA (Abu-Abed *et al*., 2001; Sakai *et al*. 2001). Through the opposing action of RA availability and members of the Cyp26 family, *Hox* gene expression domains are specified, either directly or indirectly, in an anterior to posterior manner (Hernandez *et al*. 2007).

Similar to vertebrate hindbrain patterning, it is suggested that the opposing action of RA signaling and Cyp26 family members specifies the domain of *hoxa13a* gene

expression in the zebrafish fin regenerate. Furthermore, since calcineurin appears to regulate RA signaling (Kujawski *et al*., 2014), FK506 treatments may disrupt the opposing actions of these two factors, inhibiting the expression of the *hoxa13a* domain in the presumptive joint cells. In the absence of *hoxa13a*, joint cell identity is not specified and no joints are formed. To substantiate this hypothesis, future work will entail gene expression analysis of Cyp26 family members (*cyp26a1, cyp26c1*, and *cyp26b1)* in joint cells. Furthermore, we will evaluate the effect of FK506 on the expression of the Cyp26 family members in the caudal fin regenerate. Further experiments will also be performed to knockdown the Cyp26 family members and disrupt RA signaling. It is hoped that the misregulation of these two factors will result in the disruption of joint formation.

The zebrafish dermal caudal fin rays are periodically segmented along the proximal distal axis by joints that are comparable to fibrous joints that are typically found between skull bones, or cranial sutures (Borday *et al*., 2001). In humans, cranial sutures undergo intramembranous ossification, eventually closing around the end of adolescence (Madeline and Elster, 1995). However, increased Hedgehog activity results in craniosynostosis, the premature fusion of one or more joints between the bones of the skull (Jenkins *et al*., 2007; for review see Pan *et al.,* 2013). Craniosyntosis inhibits bone growth, resulting in a number of clinical impairments including: increased intracranial pressure (Bristol *et al*., 2004), learning disabilities (Kapp-Simon, 1998; Panchal *et al*., 2001), craniofacial abnormalities, and impaired eyesight (Macintosh *et al.,* 2012). Similarly, studies in chick and mouse have shown that an absence of Ihh results in widened sutures (Lenton *et al*., 2011; Abzhanov *et al.,* 2007). However, these studies have revealed conflicting mechanisms by which Ihh signaling at osteogenic fronts regulate intramembranous bone ossification during cranial

suture formation. Similar to cranial sutures, the regenerating zebrafish fin rays are a great model to study intramembranous ossification. It is hoped that studying intramembranous ossification in zebrafish will provide a useful framework for future studies that are relevant to cranial intramembranous bone development.

In an attempt to further elucidate the roles of Hedgehog signaling during fin regeneration, the roles of *shha* in the formation and regeneration of breeding tubercles was explored in the male intact and regenerating pectoral fins. Unfortunately, no differences in the expression of *shha* were observed in the intact or regenerating male and female pectoral fins. However, differences in regenerative capabilities and vascularization were observed in regions of BT clusters between males and females. These observations lead to a more detailed analysis of Breeding Tubercles on the developing and regenerating pectoral fins and two publications. The first publication characterizes these BT clusters on male pectoral fins, and subsequently describes the requirement of androgens and two waves of vascularization for their regeneration.

Regeneration studies on the pectoral fins indicate BTs regenerate following the initiation of revascularization, but concomitantly with a novel second wave of angiogenesis that ultimately vascularizes each BT (McMillan *et al.,* 2013). Furthermore, since BT clusters on the pectoral fins are sexually dimorphic and form during sexual maturation (McMillan *et al.,* 2013), the effects of sex steroids on BT growth was investigated. Our analysis indicated that androgens induce and estrogens inhibit BT formation in the intact and regenerating pectoral fins (Figure 5.2) (McMillan *et al.,* 2013). Interestingly, similar to males, androgen treated females experience the same pro-angiogenic effects in the intact and regenerating fins, resulting in male-like vascularized BTs (McMillan *et al.,* 2013).

Furthermore, we showed that the observed androgen-induced neo-angiogenesis is necessary for the rapid growth of large BT clusters (Figure 5.2) (McMillan *et al.,* 2013). Overall, BT growth and regeneration in pectoral fins requires androgens and the presence of a blood vessel network similar to that naturally found in males (McMillan *et al.,* 2013).

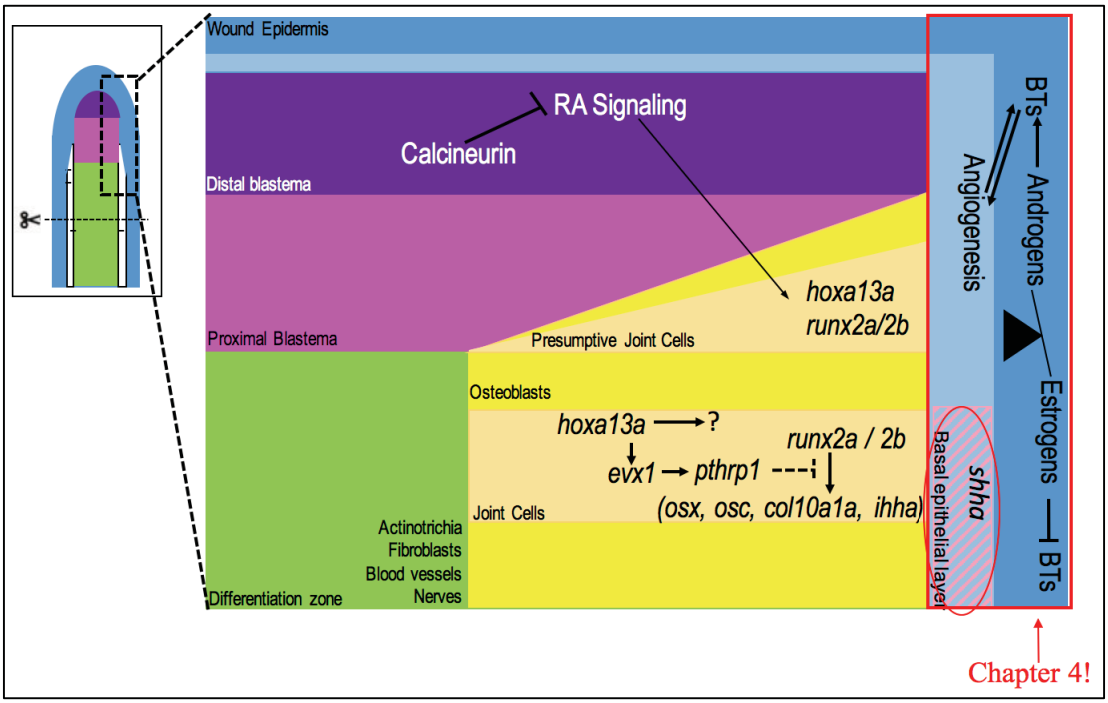

Figure 5.2: Summary of chapter 4. BT formation and regeneration are induced by androgens and inhibited by estrogens. Androgen-induced neo-angiogenesis through androgen receptors is necessary for the rapid growth of large BT clusters. However, BT formation may itself induce angiogenesis through an as of yet unknown mechanism.

Subsequent to our studies another group confirmed that androgens induced, and flutamide inhibits BT cluster formation on the pectoral fins (Kang *et al*., 2013). In addition, it was discovered that the strict regulation of Wnt signaling is critical for both pectoral fin regeneration and BT formation (Kang *et al*., 2013). Further confirmation of our studies was later observed in another study that focused on the BTs of the male and female lower jaws (Fischer *et al.,* 2014; McMillan *et al.,* 2013). Similar to pectoral fin BT clusters, the basal epidermal layers of BTs of the lower jaw are highly proliferative, possessed nuclei in the most superficial layers, and are regularly shed and renewed (Fischer *et al.,* 2014).

Furthermore, in our publication, the roles of BT clusters on the zebrafish pectoral fins were unknown. Consequently, we outlined the various postulated roles of BTs described in other fish (McMillan *et al.,* 2013). These roles included: maintaining body contact during spawning, fitness indicators during sexual selection (Wiley and Collette, 1970; Kortet *et al.,* 2003), defense against mechanical injury, microorganisms and parasites and the protection of nests and territories (Ahnelt and Keckeis, 1994; Chen and Arratia, 1996; Kortet *et al*., 2003). Subsequent to our publication, it was shown that BT clusters, appearing on male zebrafish pectoral fins during sexual maturation, play an essential role in stimulating egg release during spawning (Kang *et al*., 2013). In addition, we also showed that the BT clusters on the pectoral fins are maintained throughout the life of the male zebrafish in animal facilities (McMillan *et al*., 2013). The constant presence of these large structures enable the easy distinction between males from females, which led to our second publication (McMillan *et al.,* 2014).

The analysis of lower jaw BT clusters illustrates the existence of a genetic pathway that is required for the proliferation and differentiation of keratinocytes in the basal and

upper BT layers, respectively (Fischer *et al*., 2014). More specifically it was shown that TAp63 and p53, promote Notch signaling, which activates caspase 3 in the upper BT layers, promoting differentiation (Fischer *et al*., 2014). Furthermore, it was suggested that this pathway enhances proliferation in the lower BT layers potentially in a paracrine fashion through an unknown secreted factor (Fischer *et al*., 2014). Differentiation is suppressed in the basal layers of BTs by ΔNp63, an inhibitory competitor of TAp63, blocking differentiation and promoting proliferation (Fischer *et al*., 2014). Since these experiments were performed on BTs of jaws that appear in both males and females, it would be of interest to determine whether this pathway is also observed in sexually dimorphic BTs on the male pectoral fin. Already it has been suggested that TAp63 and p53 mutants also possess a reduction in the number and sizes of BTs in the male pectoral fin (Fischer *et al*., 2014), indicating a similar pathway is likely involved. However, further studies should be performed to confirm the roles of Notch Signaling and Caspase-3 activity in sexually dimorphic BTs of the pectoral fin.

Overall, this thesis contributes to a greater understanding of the basic underlying mechanisms that lead to fin regeneration in zebrafish (*Danio rerio*). Furthermore, this work has shown that the zebrafish fin rays are a great model for studying intramembranous bone ossification and joint formation. It is hoped that this knowledge will provide a useful framework for future studies surrounding intramembranous bone development, joint formation and regeneration in other model organisms.

Appendix I

I.1 Materials and Methods:

I.1.1 Morpholino knockdowns

Injection and electroporation experiments were performed as described previously (Hyde *et al*., 2012). However, for the experiments outlined here, fins are electroporated using the spectra 360 electrode gel rather than electroporation through system water. Briefly, 0.028ul/ray of *pthrp1* or *ihha* splice-blocking morpholinos (MO) were injected into the blastema of six 3dpa fin ray regenerates. Similar quantities of standard control MOs were injected into the six complementary rays. Entry of MO into the cells of the fin rays were determined through live imaging 1-day post injection. Efficiency of splice-blocking MOs were determined by RT-PCR. The MO sequences were as follows: *ihha* splice blocking MO 5'-GTTTCTCAGTGAA-CGGCGAGCTGTG-3'; *ihha* translation blocking MO 5'-GGGAGACGCATTCCACCC-CAAGCGG-3'; *pthrp1* splice blocking MO 5'-TGGACCTGAAGGAAAACACCCAAA-T-3'; *pthrp1* translation-blocking MO 5'-CCCGTCTGCAACACAACATCCTCAT-3'. Effects of the MOs were determined by comparing the % average bone growth and average length of 4 segments (following the formation of the first segment) in experimental and control regenerating fin rays. Significance was calculated by performing a one-tailed student t-test ($p \leq 0.05$).

I.1.2 Alizarin Red and Alcian Blue Staining

Alcian blue and alizarin red staining on fixed caudal fins were performed, with some modifications, as previously described (Javidan and Schiling, 2004). Fins were collected in 4% PFA and incubated overnight at 4°C. fins were then washed in PBS (3 x 10min). Fins were stained in alcian blue solution (Sigma) (0.1% w/v in 70% EtOH:30%

AcOH) for six hours at room temperature. Following staining, fins were dehydrated in a series of 25 minute washes (70% ethanol in PBS, 95% ethanol in PBS, and 100% ethanol). Fins were then placed in 100% ethanol overnight at 4°C. The next day, the fins were removed from ethanol and rehydrated in a series of 45 minute washes (80% ethanol in PBS, 50% ethanol in PBS, 30% ethanol in PBS). Fins were then washed for one hour in water. The fins were then stained in alizarin red (Sigma) solution (0.5% w/v in KOH) for 5 hours. After staining, the fins were rinsed overnight in water.

I.2 Results:

I.2.1 The Roles of Ihha and PTHrP during Dermal Fin Ray Regeneration

Previous results in the lab indicated that *pthrp1* was expressed in a small group of *evx1*-expressing presumptive joint cells. Furthermore, although the *runx2a/runx2b* positive presumptive joint cells were aligned with newly differentiating osteoblasts, they did not express *ihha*.

The expression of *ihha* in osteoblasts and *pthrp1* in adjacent joint-forming cells indicates that these factors are potentially involved in controlling ossification of the bone segments, similar to both endochondral and intramembranous ossification of other bone structures (Lenton *et al.,* 2011; Abzhanov *et al.,* 2007; Lanske *et al.,* 1996; St-Jacques *et al.,* 1999; Vortkamp *et al*., 1996). Therefore, morpholino (MO) knockdowns were performed to elucidate the roles of *pthrp1* and *ihha* in segmentation and bone growth. Initially, translation-blocking MOs were injected into the blastemas of 2dpa caudal fin rays (Supplementary Figure I.1). Following MO knockdowns, live imaging was performed daily for 7 days to observe the effect of the knockdowns on bone growth, segmentation, and branching (Supplementary Figure I.1). Additionally, fins were collected 4 days post

injection (4dpi) (6dpa) and stained for alizarin red/alcian Blue to observe bone growth (Supplementary Figure I.1). Analyses of the *pthrp1* and *ihha* knockdowns indicated that there is no obvious decrease in bone growth, or segment formation in the fin regenerates when compared to controls (data not shown). However, it was possible that the absence of any significant effects on the fin regenerate could be due to an ineffective MO knockdown. Unfortunately, it was not possible to assess the efficiency of the translation blocking MO using western blots due to the lack of appropriate antibodies that can cross-react with the zebrafish *ihha* and *pthrp1*. To circumvent this problem, new splice-blocking MOs for *pthrp1* and *ihha* were designed, enabling the observation of successful splice-modifications through RT-PCR as sizes change in the PCR product band on a gel. To test the newly designed splice-blocking MOs, 1-cell stage zebrafish embryos were injected with 1.0–2.0 nl of a 3.0 mg/ml *pthrp1*-MO or *ihha*-MO. Three days post fertilization (dpf), RT-PCR was performed on non-injected controls and pooled (*pthrp1* or *ihha*) MO-injected embryos. In both cases, RT-PCR following knockdowns in embryos demonstrates the MO is effective through the decrease in the product band size by 262bp and 124bp for *ihha* and *pthrp1*, respectively (Supplementary Figure I.1E). The observed decrease in product band sizes are consistent with the designed splice-blocking MO induced loss of exon2 for both *pthrp1* and *ihha.*

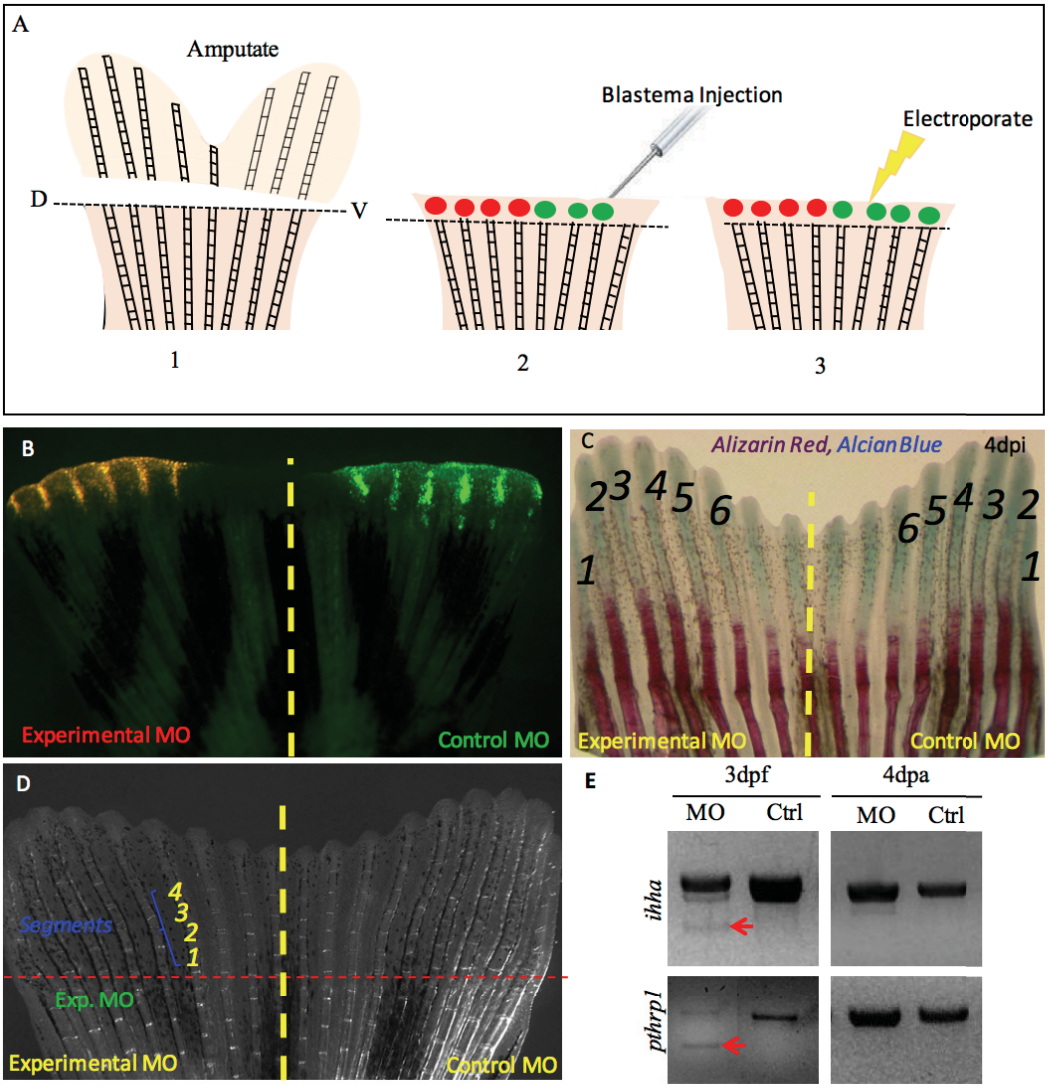

Supplementary Figure I.1: Techniques used in morpholino electroporation and subsequent analysis of the caudal fin regenerate. (A) Schematic illustrating the three steps involved in morpholino electroporation. (1) Amputate caudal fin rays. (2) 2-3dpa inject the six most dorsal blastemas with experimental morpholino tagged with lissamine (red) and the six most ventral blastemas standard control morpholino tagged with fluorescein (green). (3) Following injections, fins are immediately electroporated and fish are returned to water for recovery. (B) Fins were imaged 1day post injection (dpi)/4dpa to ensure morpholinos (red and green) were successfully electroporated into the blastema. (C) Fins were collected 3dpi/6dpa and stained with alizarin red/alcian blue to observed bone growth. Control rays were compared only to corresponding experimental rays. (D) Live imaging of fins enabled daily observations of joint formation. The length of 4 segments were measured following the formation of the first joint. 4 segment lengths were compared between experimental and control morpholinos following the formation of the first formed joint. (E) RT-PCR of 3dpf embryos illustrate a loss of an exon consistent with morpholino splice-blocking in both *pthrp1-MO* and *ihha-MO* (red arrow). In 4dpa fin regenerates, no exon loss was observed for either morpholino when compared to controls. (Image A adapted from Hyde *et al.,* 2012).

Once validated in embryos, 238ng of *pthrp1* or 247 ng of *ihha* splice-blocking MO were injected followed by electroporation into the blastema of 2dpa fin regenerates. Bone formation measurements following alizarin red and alcian blue staining 6dpa indicates that *pthrp1* (n = 12) and *ihha* (n = 12) MO knockdowns result in significant increases (*pthrp1*-MO, ray 4) and decreases (*ihha*-MO, rays 1, 2, and 4) in the bone growth ($p \leq 0.05$) (Supplementary Figure I.2).

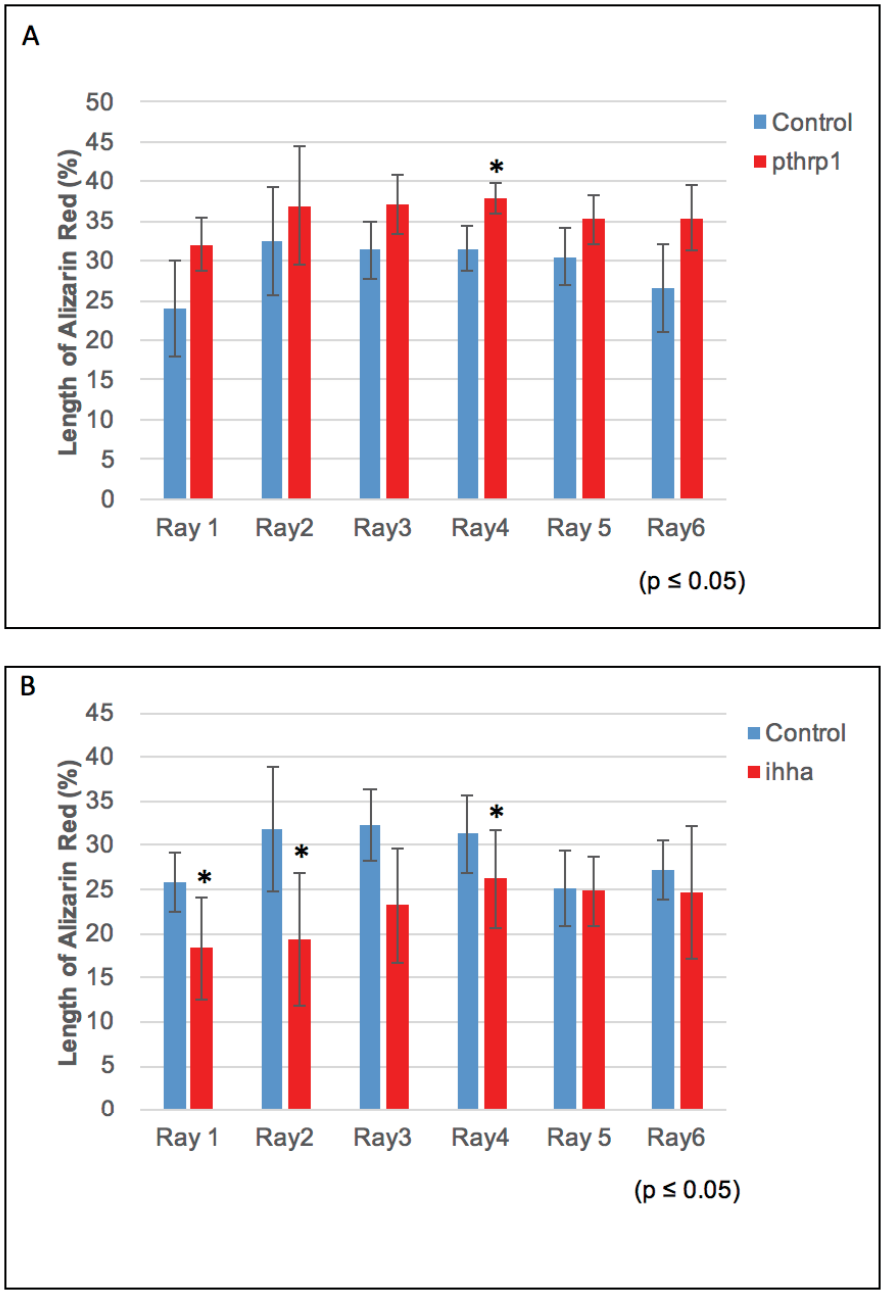

Supplementary Figure I.2: Calculation of the average bone growth percentage per fin ray for *ihha-MO* and *pthrp1-MO* fin regenerates. (A) Injections of *pthrp1* MO resulted in a significant increase in bone growth on ray#4. (B) Injections of *ihha* resulted in significant decreases in bone growth in ray 1, 2, and 4. Significance is based on a paired 1-tailed students T-Test ($p \leq 0.05$). Significant differences are marked with an asterisk. Experimental MOs (red) and Standard control MOs (blue).

However, *pthrp1 (n* = 12) and *ihha* (n = 12) MO knockdowns did not significantly affect joint formation as observed through measurements of segment length ($p \leq 0.05$) (measurement from 1 joint to the next) (Supplementary Figure I.3). Since only moderate effects were observed on bone growth and no effects were observed in segment length RT-PCR was performed to test effectiveness of the MO knockdown in the fin regenerate. RT-PCR analysis of the MO knockdowns of the fin regenerates indicates that there was no exon-loss, indicating that the MO are potentially not efficiently targeting the genes of interest (Supplementary Figure I.1 E). Overall, this data indicates that *pthrp1* and *ihha* may play a role in bone growth. However, future work must confirm the efficiency and specificity of the MO knockdowns in the fin regenerate.

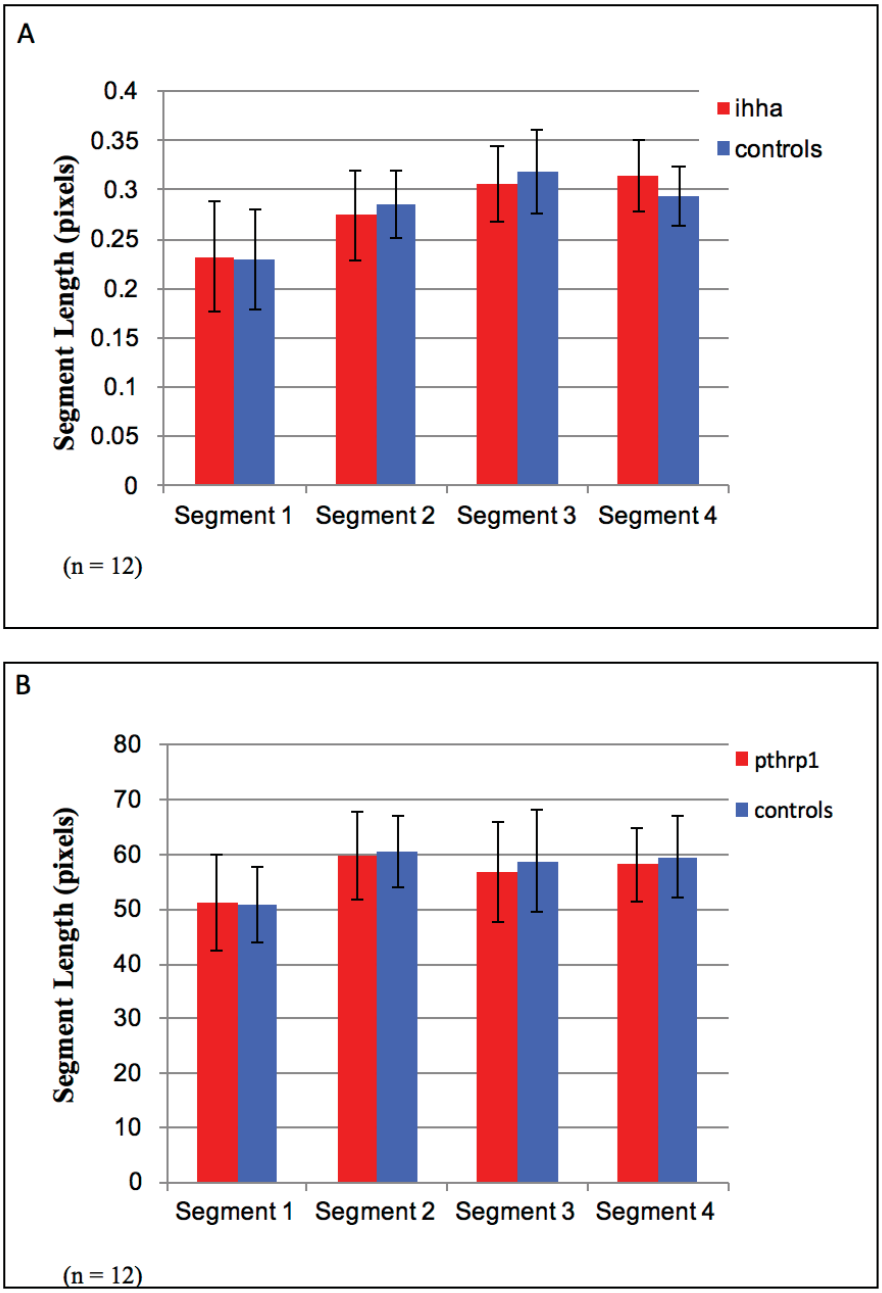

Supplementary Figure I.3: Calculation of average segment length for *ihha-MO* and *pthrp1-MO* fin regenerates. No differences were observed in the average length of 4 segments in regenerating caudal fins 7dpa/4dpi injected with MOs for *ihha* (A) or *pthrp1* (B) when compared to controls (n =12). Significance is based on a paired 1-tailed students T-Test ($p \leq 0.05$). Experimental MOs (red) and Standard control MOs (blue).

I.3 Discussion

Although RT-PCR is an effective tool to check for splice-blocking activity, one cannot predict whether a splice-blocking MO will cause an exon deletion, intron insertion, or activation of a cryptic splice site (partial insertion/deletion). Although no exon loss was observed, future work could include sequencing the resulting PCR fragment to determine the presence of a cryptic splice site that cannot be resolved on a gel, and re-designing PCR primers to look for intron insertions. It is also possible that the MO resulted in nonsense mediated decay. To determine if this is the case, qRT-PCR could be performed to evaluate a reduction in transcripts. In the event that a targeted knockdown is observed, future work would still have to determine whether the observed moderate effects on bone growth were specific or non-specific. Traditionally, 3 controls are used to limit the possibility of off target effects. First, two MOs against the same target gene should be tested independently and simultaneously to ensure a similar phenotype is observed. Second, RNA rescue experiments should be performed to determine whether the phenotype is ameliorated when rescued with the wildtype mRNA sequence. Third, control MO should always be used (ie. standard control MO, a MO that affects a gene that is not expressed in the cells of interest, or a 5-base pair mismatch MO) (Blum *et al*., 2015). Although these methods limit the possibility of off target effects, there are there are many examples in literature in which defects previously associated with MO knockdowns of a specific gene are not being observed following the subsequent generation of a mutant line (Aranguren *et al*., 2011; Swift *et al*., 2014; van Impel *et al.,* 2014; Chapman *et al*., 2013; Fleisch *et al*., 2013; Nourizadeh-Lillabadi *et al*., 2010; Vettori *et al*., 2011; Kikuta *et al.,* 2003; Su *et al*., 2014; Aman *et al*., 2011). These recent observations in addition to the implementation of new

techniques, such as Clustered Regularly-Interspaced Short Palindromic Repeats (CRISPRs) (Schulte-Merker and Stainier, 2014) have caused the zebrafish community to minimize the use of MO. However, in many cases MOs remain advantageous. For example, many mutants are embryonic lethal, and cannot be used to evaluate function in adult structures, such as the fin regenerate. Furthermore, a high degree of redundancy has been observed in the zebrafish genome, excluding the use of chemicals as means to affect specific factors. Literature suggests that the *ihha*^{hu2131} null mutant is viable up to at least 30dpf (Hammond and Schulte-Merker, 2009). Therefore, it may be possible to perform studies on the caudal fin of *ihha*^{hu2131} null mutants. Unfortunately, due to the presence of *shha* in the basal epidermal layer adjacent to *ihha* expressing osteoblasts, there is the possibility of redundancy in the fin regenerate. Therefore, chemical inhibition/activation of the Hedgehog signaling pathway will not provide details on the specific roles of these factors. Currently, it is unknown whether a *pthrp1* mutant would be embryonic lethal. Therefore, it is possible that the creation of a mutant may also enable the observation of a loss of *pthrp1* in the fin regenerate.

Appendix II

II.1 Manuscript #1 Supplementary Figures:

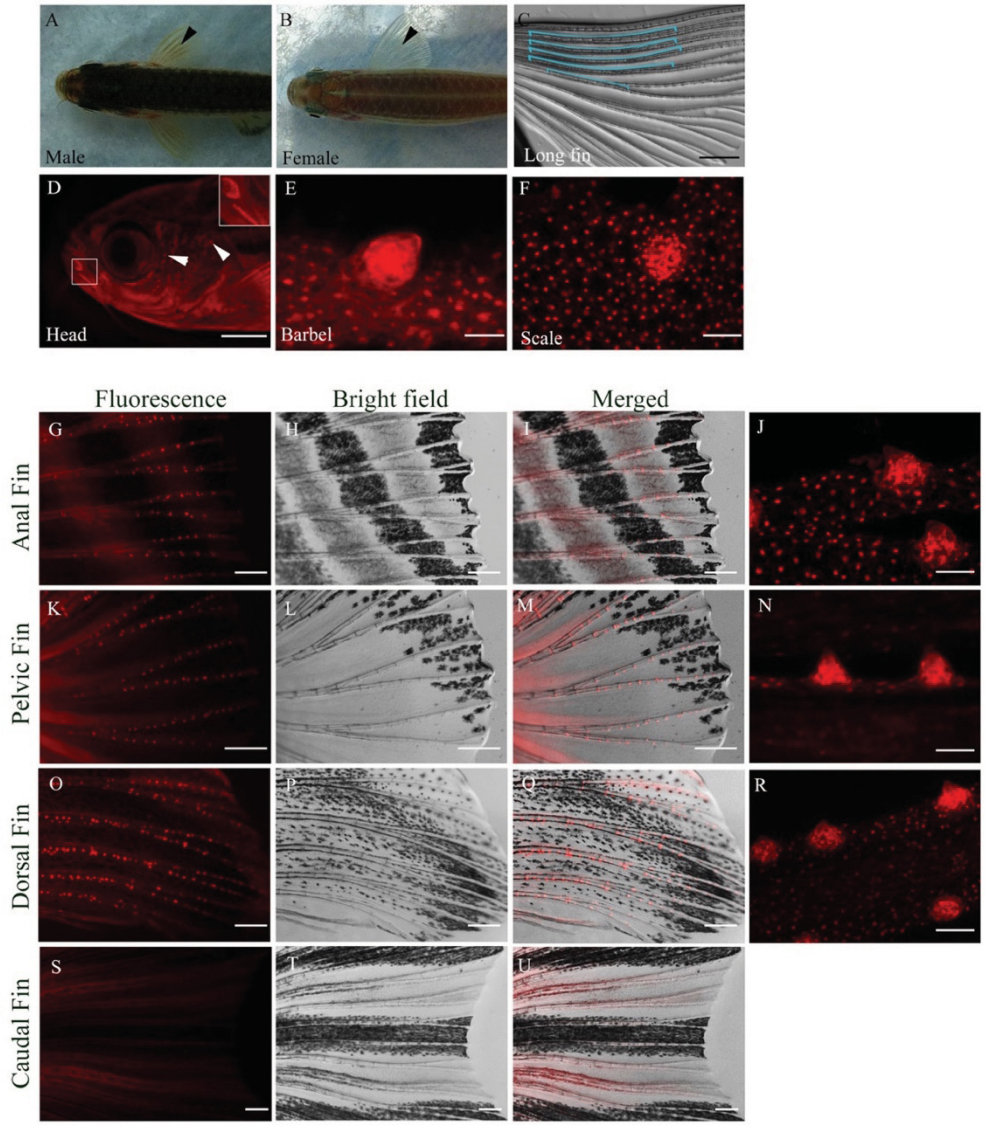

Supplementary Figure II.1: Distribution and morphology of BTs in male zebrafish. (A) Dorsal view of a male zebrafish with pectoral fin BTs (black arrowhead). (B) Dorsal view of a female zebrafish with no BTs and translucent fins (black arrowhead). (C) Pectoral fin of a male *longfin* mutant with long BT clusters (outlined in blue). (D) Grouped BTs in a line/semi circle (white box) and isolated BTs (white arrowheads) on the side of a male zebrafish head. (E) BT on a barbel. (F) A BT on a scale pulled from the body surface. (G-J) BTs distributed along the anal fin rays. (K-N) BTs along the pelvic fin rays. (O-R) BTs along the dorsal fin rays. (S-U) No BTs are observed on the caudal fin. Fluorescence *Tg(KR21)* images (red), Merged (*Tg(KR21)* + Brightfield) images. Scale bar for C = 200µm; D = 400µm; E = 12.5µm; J, N, R, F = 25µm; G-I, K-M, O-Q, S-U = 200µm.

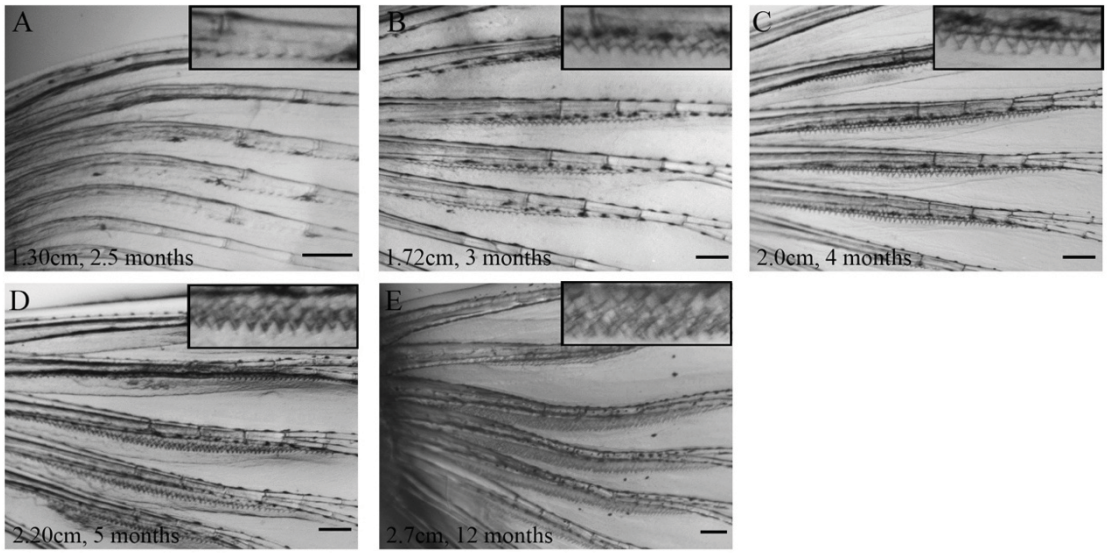

Supplementary Figure II.2: Development of BTs in male zebrafish. (A) BTs are observed as a single row beginning at 1.30 cm standard length or 2.5 months post fertilization. (B) Individual BTs grow larger and form clusters 1.72 cm standard length or 3 months post fertilization. (C, D, E) BT clusters grow until zebrafish reach 1 year of age. Scale bars for all panels = 100μm.

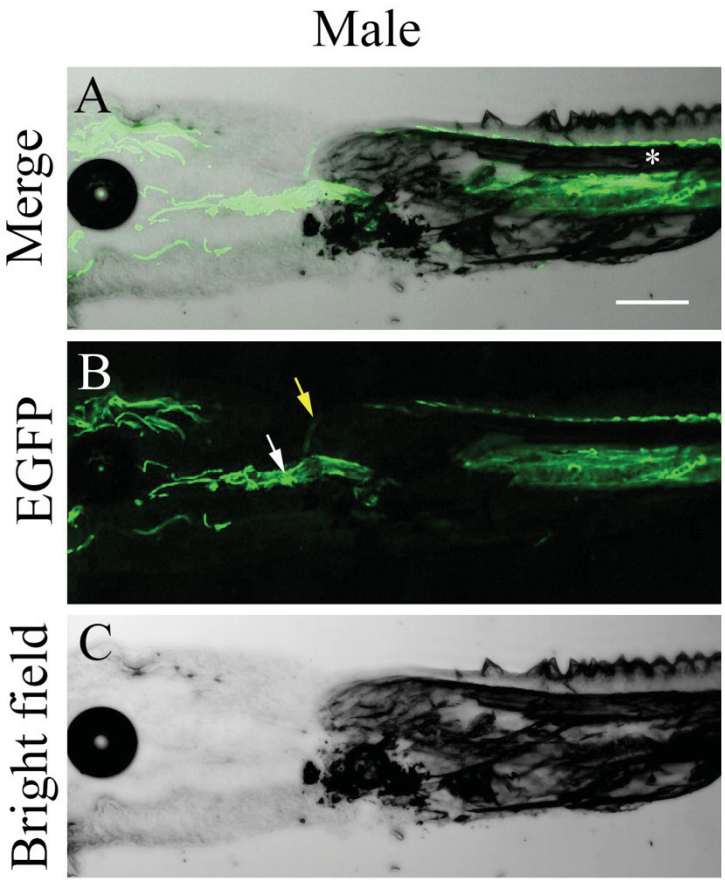

Supplementary Figure II.3: Origin of BT vascularization. Longitudinal sections of the area connecting the body to the pectoral fin of males (A-C) of the *Tg(fli1a:EGFP)* fish. A blood vessel (yellow arrow) is observed sprouting from the central artery (white arrow) and projecting parallel to the hemiray (white asterisk). (A) Merge = Brightfield + GFP; (B) GFP fluorescence; (C) Brightfield. Scale bars = 100µm (shown in A).

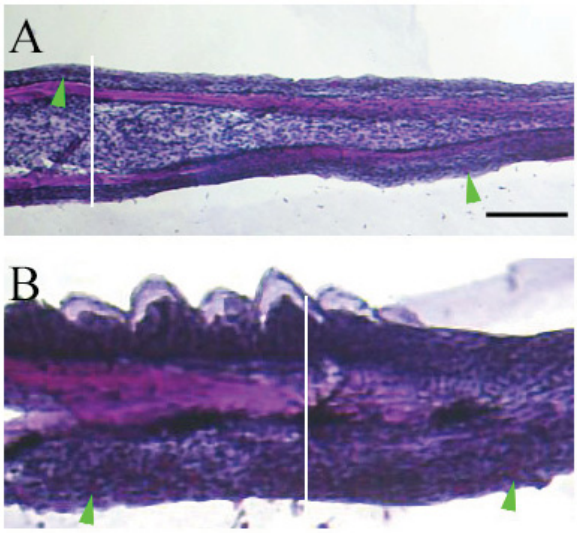

Supplementary Figure II.4: PAS stain on 7 dpa pectoral fin regenerate longitudinal sections. (A) Goblet cells (green arrowheads) in the intact and regenerating dorsal and ventral surfaces of the females. (B) In males, goblet cells (green arrowheads) are present only in regions where BTs are absent. Amputation plane (white vertical lines). Scale bars for both panels = 25μm (shown in A).

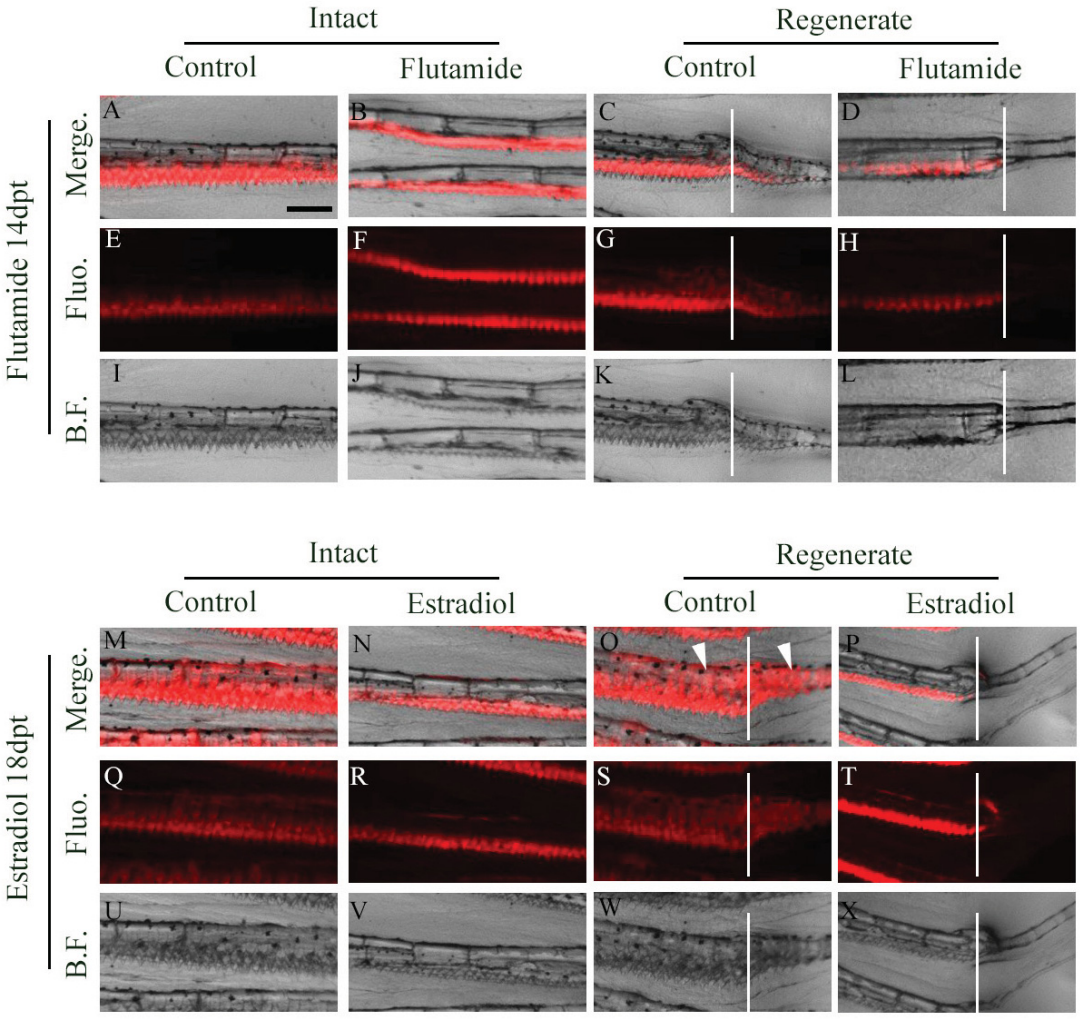

Supplementary Figure II.5: Estradiol and flutamide inhibit BT regeneration and growth in the male pectoral fins. (A, C, E, G, I, K, M, O, Q, U, S, W) BTs along the anterior rays of control intact and regenerating fins. In some cases, BT clusters are observed on dorsal and ventral surfaces of the fin rays (white arrowheads in (O)). (B, D, F, H, J, L) Treatment with flutamide (14 dot) results in smaller BTs on the intact fin/stump and no BTs on the fin regenerate. (N, P, R, T, V, X) E2 treatment (18 dot) results in BTs that are reduced in size in the intact fin and regenerate stump and no BTs in the regenerate. White vertical lines indicate amputation plane. Scale bar for all panels = 100μm (shown in A). B.F. = Brightfield; Fluo = KR21/RFP; Merge = Brightfield +KR21/RFP.

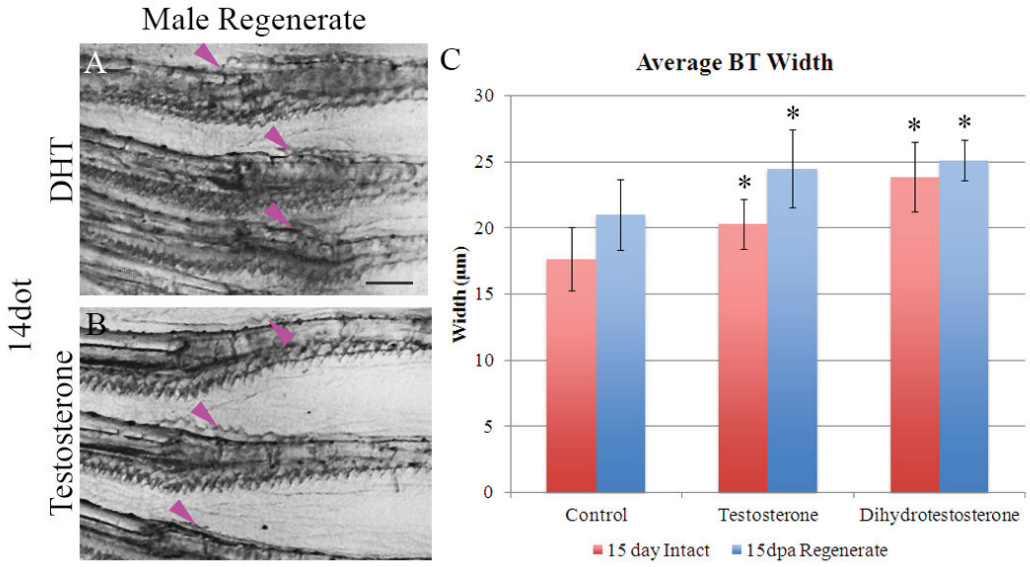

Supplementary Figure II.6: Treatment with androgens increases BT width in males. (A-B) Androgen- treated (DHT and T) males (14 dot) displaying BT clusters that cover both dorsal and ventral sides of the regenerate rays (pink arrows). (C) Graph illustrating the average width of each BT. When compared to non-treated controls, T and DHT-treated anterior regenerating and intact fins possess BTs that are significantly wider in width (asterisk). ($p < 0.05$ via Student's T-test analysis) Error bars = s.d. Scale bars = 100 µm (shown in A).

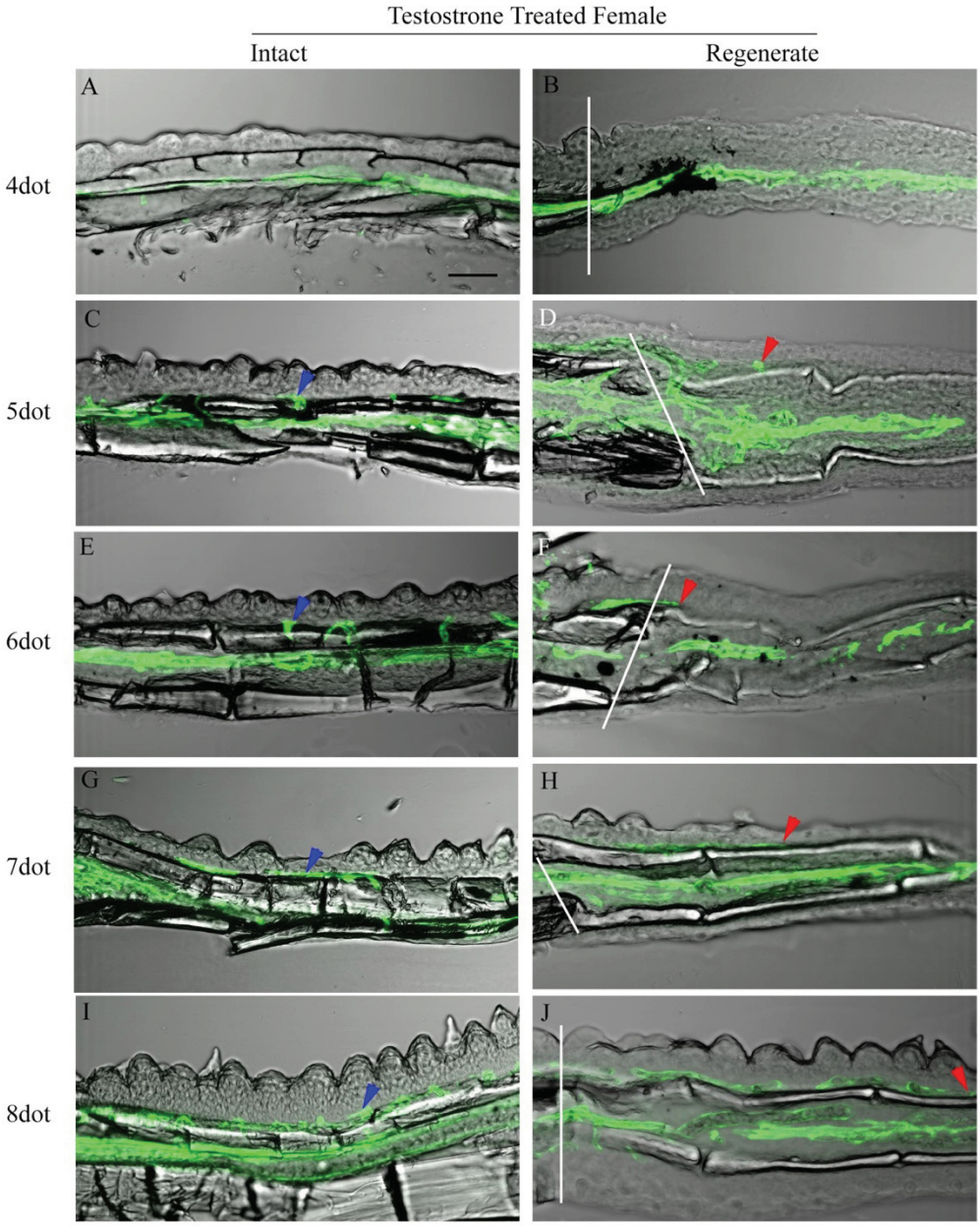

Supplementary Figure II.7: Androgens induce angiogenesis in intact and regenerating female pectoral fins. (A, C, E, G, I) Intact fins of T-treated females develop BTs following 4 dot (A). BTs are vascularized 5 dot (blue arrowhead) (C). (E, G, I) 6-8dot, BTs mature and appear similar to 2 males. (B, D, F, H, J) Regenerating pectoral fins of T-treated females undergo two waves of blood vessel regeneration. (B) The central artery located between the hemirays regenerates in the first wave. (D, F, H, J) Initiated at 5 dpa, the second wave of angiogenesis travels in a proximal-distal fashion parallel to the hemiray (red arrowheads), occurring alongside BT regeneration. Amputation plane is indicated by white vertical lines. Scale bars= 50μm (shown in A).

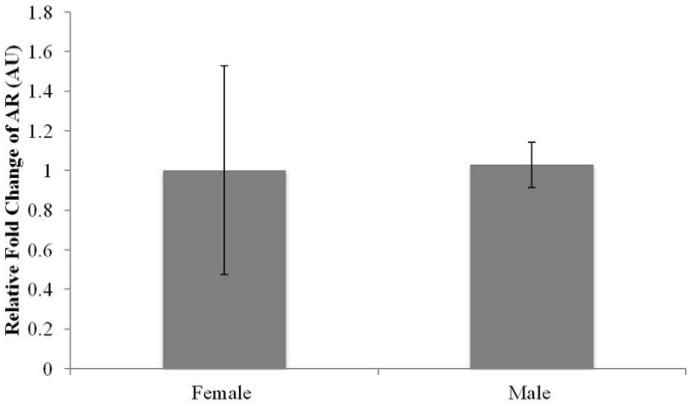

Supplementary Figure II.8: Quantitative RT-PCR for *AR* mRNA in male and female pectoral fins. Expression data indicate the relative expression levels for the *ar* mRNA are not significant between male and female pectoral fins (p = 0.91 via Student's T-test analysis) AU = arbitrary units. *ar* expression was normalized to *ef1α.* Four biological samples were performed per experiment and each biological sample was run in triplicate. Error bars = s.d.

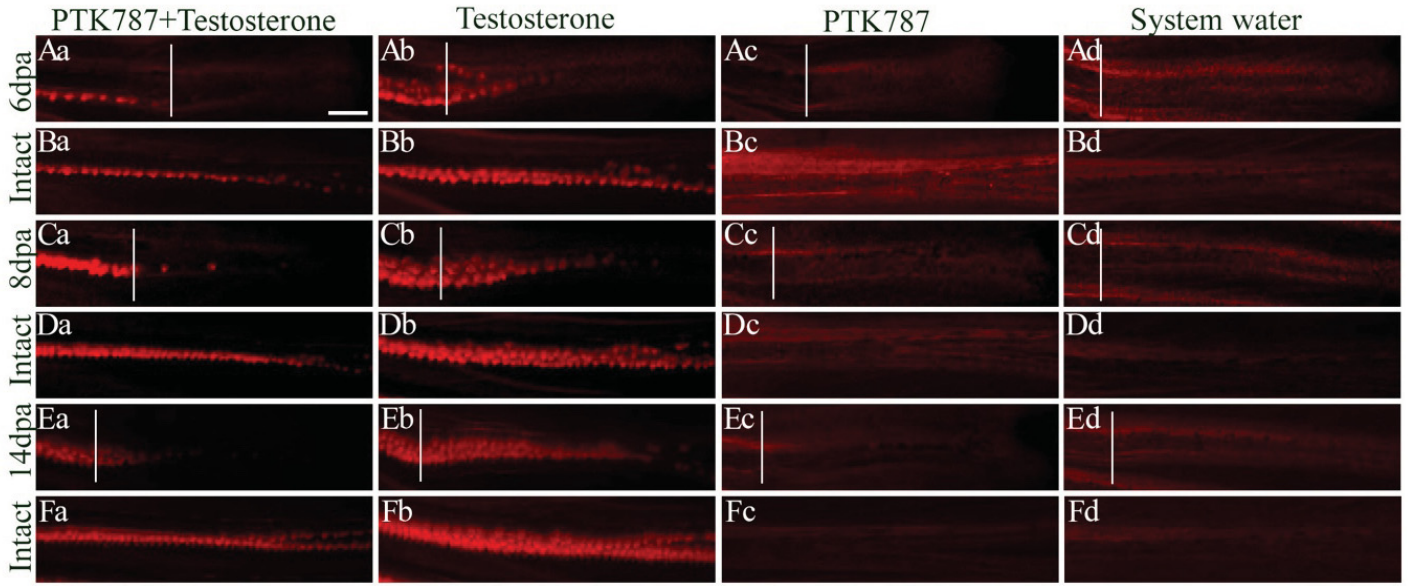

Supplementary Figure II.9: Female pectoral fin BT growth is affected by PTK787. (Aa, Ba) A single row of BTs on the intact fin, and 6dpa regenerate stump after 6 dot with PTK787 and 4 dot testosterone. No BTs were visible in the regenerate (Aa). (Ca, Da) Small individual BTs appear in the fin regenerate after 8 dot with PTK787 and 6 dot with testosterone. BTs are visible on the intact fin and stump. (Ea, Fa) Small BT cluster on the regenerate 14 dot with PTK787 and 12 dot with T. Small BTs on the intact fin and stump. (Ab, Bb) After 4 dot, T-treated females develop BT clusters on the regenerate, stump, and intact fin. (Cb-Fb) BT clusters continue to grow on the intact fin, stump, and regenerate from 6-12 dot with T. (Ac-Fc, Ad-Fd) No BT growth in the intact and regenerating fins with PTK787 treatments or system water controls. White vertical lines indicate the amputation plane. Scale bars for all panels = 100μm

References

Abad V, Meyers JL, Weise M, Gafni RI, Barnes KM, Nilsson O, Bacher JD, Baron J. 2002. The role of the resting zone in growth plate chondrogenesis. Endocrinology 143(5):1851-7.

Abu-Abed S, Dolle P, Metzger D, Beckett B, Chambon P, Petkovich M. 2001. The retinoic acid-metabolizing enzyme, CYP26A1, is essential for normal hindbrain patterning, vertebral identity, and development of posterior structures. Genes Dev 15(2):226-40.

Abzhanov A, Rodda SJ, McMahon AP, Tabin CJ. 2007. Regulation of skeletogenic differentiation in cranial dermal bone. Development 134(17):3133-44.

Affolter M, Zeller R, Caussinus E. 2009. Tissue remodelling through branching morphogenesis. Nat Rev Mol Cell Biol 10(12):831-42.

Ahn D and Ho RK. 2008. Tri-phasic expression of posterior hox genes during development of pectoral fins in zebrafish: Implications for the evolution of vertebrate paired appendages. Dev Biol 322(1):220-33.

Ahnelt H and Keckeis H. 1994. Breeding tubercles and spawning behaviour in Chondrostomanasus (Teleostei: Cyprinidea): a correlation? Ichtyol. Explor. Freshw. 5:321-330.

Akimenko MA, Johnson SL, Westerfield M, Ekker M. 1995. Differential induction of four msx homeobox genes during fin development and regeneration in zebrafish. Development 121(2):347-57.

Akimenko MA, Mari-Beffa M, Becerra J, Geraudie J. 2003. Old questions, new tools, and some answers to the mystery of fin regeneration. Dev Dyn 226(2):190-201.

Alexander T, Nolte C, Krumlauf R. 2009. Hox genes and segmentation of the hindbrain and axial skeleton. Annu Rev Cell Dev Biol 25:431-56.

Alonso M, Tabata YA, Rigolino MG, Tsukamoto RY. 2000. Effect of induced triploidy on fin regeneration of juvenile rainbow trout, oncorhynchus mykiss. J Exp Zool 287(7):493-502.

Aman A, Nguyen M, Piotrowski T. 2011. Wnt/beta-catenin dependent cell proliferation underlies segmented lateral line morphogenesis. Dev Biol 349(2):470-82.

Andersson ER and Lendahl U. 2009. Regenerative medicine: A 2009 overview. J Intern Med 266(4):303-10.

Ankley GT, Kahl MD, Jensen KM, Hornung MW, Korte JJ, Makynen EA, Leino RL. 2002. Evaluation of the aromatase inhibitor fadrozole in a short-term reproduction assay with the fathead minnow (pimephales promelas). Toxicol Sci 67(1):121-30.

Apschner A, Schulte-Merker S, Witten PE. 2011. Not all bones are created equal - using zebrafish and other teleost species in osteogenesis research. Methods Cell Biol 105:239-55.

Arai R. 1967. Androgenic effects of 11-ketotestosterone on some sexual characteristics in the teleost, Oryzias latipes. Annot. Zool. Japonenses. 40:1-5.

Aranguren XL, Beerens M, Vandevelde W, Dewerchin M, Carmeliet P, Luttun A. 2011. Transcription factor COUP-TFII is indispensable for venous and lymphatic development in zebrafish and xenopus laevis. Biochem Biophys Res Commun 410(1):121-6.

Atwood SX, Li M, Lee A, Tang JY, Oro AE. 2013. GLI activation by atypical protein kinase C iota/lambda regulates the growth of basal cell carcinomas. Nature 494(7438):484-8.

Avaron F, Hoffman L, Guay D, Akimenko MA. 2006. Characterization of two new zebrafish members of the hedgehog family: Atypical expression of a zebrafish indian hedgehog gene in skeletal elements of both endochondral and dermal origins. Dev Dyn 235(2):478-89.

Avdesh A, Chen M, Martin-Iverson MT, Mondal A, Ong D, Rainey-Smith S, Taddei K, Lardelli M, Groth DM, Verdile G, et al. 2012. Regular care and maintenance of a zebrafish (danio rerio) laboratory: An introduction. J Vis Exp (69):e4196. doi(69):e4196.

Aza-Blanc P, Lin HY, Ruiz i Altaba A, Kornberg TB. 2000. Expression of the vertebrate gli proteins in drosophila reveals a distribution of activator and repressor activities. Development 127(19):4293-301.

Azevedo AS, Grotek B, Jacinto A, Weidinger G, Saude L. 2011. The regenerative capacity of the zebrafish caudal fin is not affected by repeated amputations. PLoS One 6(7):e22820.

Bayliss PE, Bellavance KL, Whitehead GG, Abrams JM, Aegerter S, Robbins HS, Cowan DB, Keating MT, O'Reilly T, Wood JM, et al. 2006. Chemical modulation of receptor signaling inhibits regenerative angiogenesis in adult zebrafish. Nat Chem Biol 2(5):265-73.

Becerra J, Junqueira LC, Bechara IJ, Montes GS. 1996. Regeneration of fin rays in teleosts: A histochemical, radioautographic, and ultrastructural study. Arch Histol Cytol 59(1):15-35.

Beil J, Fairbairn L, Pelczar P, Buch T. 2012. Is BAC transgenesis obsolete? state of the art in the era of designer nucleases. J Biomed Biotechnol 2012:308414.

Belloni E, Muenke M, Roessler E, Traverso G, Siegel-Bartelt J, Frumkin A, Mitchell HF, Donis-Keller H, Helms C, Hing AV, et al. 1996. Identification of sonic hedgehog as a candidate gene responsible for holoprosencephaly. Nat Genet 14(3):353-6.

Berg LS. 1948. Freshwater fishes of the U.S.S.R. and adjacent countries. Zool. Inst. Akad. Nauk. S.S.S.R. 3:1381.

Bertolacini CD, Richieri-Costa A, Ribeiro-Bicudo LA. 2010. Sonic hedgehog (SHH) mutation in patients within the spectrum of holoprosencephaly. Brain Dev 32(3):217-22.

Bessa J, Tena JJ, de la Calle-Mustienes E, Fernandez-Minan A, Naranjo S, Fernandez A, Montoliu L, Akalin A, Lenhard B, Casares F, et al. 2009. Zebrafish enhancer detection (ZED) vector: A new tool to facilitate transgenesis and the functional analysis of cis-regulatory regions in zebrafish. Dev Dyn 238(9):2409-17.

Bhatia S, Gordon CT, Foster RG, Melin L, Abadie V, Baujat G, Vazquez MP, Amiel J, Lyonnet S, van Heyningen V, et al. 2015. Functional assessment of disease-associated regulatory variants in vivo using a versatile dual colour transgenesis strategy in zebrafish. PLoS Genet 11(6):e1005193.

Bitgood MJ and McMahon AP. 1995. Hedgehog and bmp genes are coexpressed at many diverse sites of cell-cell interaction in the mouse embryo. Dev Biol 172(1):126-38.

Blum M, De Robertis EM, Wallingford JB, Niehrs C. 2015. Morpholinos: Antisense and sensibility. Dev Cell 35(2):145-9.

Blum N and Begemann G. 2012. Retinoic acid signaling controls the formation, proliferation and survival of the blastema during adult zebrafish fin regeneration. Development 139(1):107-16.

Blum N and Begemann G. 2015. Osteoblast de- and redifferentiation are controlled by a dynamic response to retinoic acid during zebrafish fin regeneration. Development 142(17):2894-903.

Bockelmann PK, Ochandio BS, Bechara IJ. 2010. Histological study of the dynamics in epidermis regeneration of the carp tail fin (cyprinus carpio, linnaeus, 1758). Braz J Biol 70(1):217-23.

Bohme K, Winterhalter KH, Bruckner P. 1995. Terminal differentiation of chondrocytes in culture is a spontaneous process and is arrested by transforming growth factor-beta 2 and basic fibroblast growth factor in synergy. Exp Cell Res 216(1):191-8.

Boniface EJ, Lu J, Victoroff T, Zhu M, Chen W. 2009. FlEx-based transgenic reporter lines for visualization of cre and flp activity in live zebrafish. Genesis 47(7):484-91.

Boras-Granic K, Chang H, Grosschedl R, Hamel PA. 2006. Lef1 is required for the transition of wnt signaling from mesenchymal to epithelial cells in the mouse embryonic mammary gland. Dev Biol 295(1):219-31.

Borday V, Thaeron C, Avaron F, Brulfert A, Casane D, Laurenti P, Geraudie J. 2001. Evx1 transcription in bony fin rays segment boundaries leads to a reiterated pattern during zebrafish fin development and regeneration. Dev Dyn 220(2):91-8.

Borg B. 1994. Androgens in teleost fishes. Comp. Biochem. Physiol. 109C:219–245.

Borgens RB. 1982. Mice regrow the tips of their foretoes. Science 217(4561):747-50.
Briscoe J and Therond PP. 2013. The mechanisms of hedgehog signalling and its roles in development and disease. Nat Rev Mol Cell Biol 14(7):416-29.

Bristol RE, Lekovic GP, Rekate HL. 2004. The effects of craniosynostosis on the brain with respect to intracranial pressure. Semin Pediatr Neurol 11(4):262-7.

Brockes JP and Kumar A. 2002. Plasticity and reprogramming of differentiated cells in amphibian regeneration. Nat Rev Mol Cell Biol 3(8):566-74.

Broussonet M. 1786. Observations sur la regeneration de quelques parties du corps des Poissons. Hist de l'Acad Roy des Sciences.

Brown AM, Fisher S, Iovine MK. 2009. Osteoblast maturation occurs in overlapping proximal-distal compartments during fin regeneration in zebrafish. Dev Dyn 238(11):2922-8.

Bruder SP and Caplan AI. 1989. Cellular and molecular events during embryonic bone development. Connect Tissue Res 20(1-4):65-71.

Bryant PJ. 1971. Regeneration and duplication following operations in situ on the imaginal discs of drosophila melanogaster. Dev Biol 26(4):637-51.

Bulina ME, Lukyanov KA, Britanova OV, Onichtchouk D, Lukyanov S, Chudakov DM. 2006. Chromophore-assisted light inactivation (CALI) using the phototoxic fluorescent protein KillerRed. Nat Protoc 1(2):947-53.

Burke R, Nellen D, Bellotto M, Hafen E, Senti KA, Dickson BJ, Basler K. 1999. Dispatched, a novel sterol-sensing domain protein dedicated to the release of cholesterol-modified hedgehog from signaling cells. Cell 99(7):803-15

Cason JE. 1950. A rapid one-step mallory-heidenhain stain for connective tissue. Stain Technol 25(4):225-6.

Chamoun Z, Mann RK, Nellen D, von Kessler DP, Bellotto M, Beachy PA, Basler K. 2001. Skinny hedgehog, an acyltransferase required for palmitoylation and activity of the hedgehog signal. Science 293(5537):2080-4.

Chapman AL, Bennett EJ, Ramesh TM, De Vos KJ, Grierson AJ. 2013. Axonal transport defects in a mitofusin 2 loss of function model of charcot-marie-tooth disease in zebrafish.

PLoS One 8(6):e67276.

Chen X, Arratia G. 1996. Breeding Tubercles of Phoxinus (Teleostei: Cyprinidae): Morphology, Distribution, and Phylogenetic Implications. Journal of Morphology. 228:127-144.

Chen MH, Li YJ, Kawakami T, Xu SM, Chuang PT. 2004. Palmitoylation is required for the production of a soluble multimeric hedgehog protein complex and long-range signaling in vertebrates. Genes Dev 18(6):641-59.

Chen Y and Struhl G. 1996. Dual roles for patched in sequestering and transducing hedgehog. Cell 87(3):553-63.

Cheng SY and Bishop JM. 2002. Suppressor of fused represses gli-mediated transcription by recruiting the SAP18-mSin3 corepressor complex. Proc Natl Acad Sci U S A 99(8):5442-7.

Chien C., 2007. The Tol2 Kit Blog. Dept Neurobiology & Anatomy, University of Utah, Salt Lake City, UT, USA. http://tol2kit.blogspot.ca/2010/04/questions-on-tol2kit-3610-onwards.html.

Chuang PT and McMahon AP. 2003. Branching morphogenesis of the lung: New molecular insights into an old problem. Trends Cell Biol 13(2):86-91.

Chuang PT and McMahon AP. 1999. Vertebrate hedgehog signalling modulated by induction of a hedgehog-binding protein. Nature 397(6720):617-21.

Clift RA, Thomas ED, Seattle Marrow Transplant Team. 2004. Follow-up 26 years after treatment for acute myelogenous leukemia. N Engl J Med 351(23):2456-7.

Colnot C, Lu C, Hu D, Helms JA. 2004. Distinguishing the contributions of the perichondrium, cartilage, and vascular endothelium to skeletal development. Dev Biol 269(1):55-69.

Concordet JP, Lewis KE, Moore JW, Goodrich LV, Johnson RL, Scott MP, Ingham PW. 1996. Spatial regulation of a zebrafish patched homologue reflects the roles of sonic hedgehog and protein kinase A in neural tube and somite patterning. Development 122(9):2835-46.

Cox BC, Liu Z, Lagarde MM, Zuo J. 2012. Conditional gene expression in the mouse inner ear using cre-loxP. J Assoc Res Otolaryngol 13(3):295-322.

Cuervo R, Hernandez-Martinez R, Chimal-Monroy J, Merchant-Larios H, Covarrubias L. 2012. Full regeneration of the tribasal polypterus fin. Proc Natl Acad Sci U S A 109(10):3838-43.

Cuny GD, Yu PB, Laha JK, Xing X, Liu JF, Lai CS, Deng DY, Sachidanandan C, Bloch KD, Peterson RT. 2008. Structure-activity relationship study of bone morphogenetic protein (BMP) signaling inhibitors. Bioorg Med Chem Lett 18(15):4388-92.

Currie PD and Ingham PW. 1996. Induction of a specific muscle cell type by a hedgehog-like protein in zebrafish. Nature 382(6590):452-5.

Davis AP and Capecchi MR. 1994. Axial homeosis and appendicular skeleton defects in mice with a targeted disruption of hoxd-11. Development 120(8):2187-98.

Davis AP, Witte DP, Hsieh-Li HM, Potter SS, Capecchi MR. 1995. Absence of radius and ulna in mice lacking hoxa-11 and hoxd-11. Nature 375(6534):791-5.

Death AK, McGrath KC, Sader MA, Nakhla S, Jessup W, Handelsman DJ, Celermajer DS. 2004. Dihydrotestosterone promotes vascular cell adhesion molecule-1 expression in male human endothelial cells via a nuclear factor-kappaB-dependent pathway. Endocrinology 145(4):1889-97.

Dollé P, Dierich A, LeMeur M, Schimmang T, Schuhbaur B, Chambon P, Duboule D. 1993. Disruption of the hoxd-13 gene induces localized heterochrony leading to mice with neotenic limbs. Cell 75(3):431-41.

Dor Y, Brown J, Martinez OI, Melton DA. 2004. Adult pancreatic beta-cells are formed by self-duplication rather than stem-cell differentiation. Nature 429(6987):41-6.

Drissi H, Zuscik M, Rosier R, O'Keefe R. 2005. Transcriptional regulation of chondrocyte maturation: Potential involvement of transcription factors in OA pathogenesis. Mol Aspects Med 26(3):169-79.

Dubrulle J, McGrew MJ, Pourquie O. 2001. FGF signaling controls somite boundary position and regulates segmentation clock control of spatiotemporal hox gene activation. Cell 106(2):219-32.

Eames BF, de la Fuente L, Helms JA. 2003. Molecular ontogeny of the skeleton. Birth Defects Res C Embryo Today 69(2):93-101.

Egami, N. (1954). Effects of hormonic steroids on the formation of male characteristics in females of the fish, Oryzias latipes, kept in water containing testosterone propionate. Annot. Zool. Japonenses, 27, 122-127.

Ekker SC, McGrew LL, Lai CJ, Lee JJ, von Kessler DP, Moon RT, Beachy PA. 1995. Distinct expression and shared activities of members of the hedgehog gene family of xenopus laevis. Development 121(8):2337-47.

Ekker SC, Ungar AR, Greenstein P, von Kessler DP, Porter JA, Moon RT, Beachy PA. 1995. Patterning activities of vertebrate hedgehog proteins in the developing eye and brain. Curr Biol 5(8):944-55.

Engeszer RE, Patterson LB, Rao AA, Parichy DM. 2007. Zebrafish in the wild: A review of natural history and new notes from the field. Zebrafish 4(1):21-40.

Erlebacher A, Filvaroff EH, Gitelman SE, Derynck R. 1995. Toward a molecular understanding of skeletal development. Cell 80(3):371-8.

Ertzer R, Muller F, Hadzhiev Y, Rathnam S, Fischer N, Rastegar S, Strahle U. 2007. Cooperation of sonic hedgehog enhancers in midline expression. Dev Biol 301(2):578-89.

Eugster C, Panakova D, Mahmoud A, Eaton S. 2007. Lipoprotein-heparan sulfate interactions in the hh pathway. Dev Cell 13(1):57-71.

Faiella A, D'Esposito M, Rambaldi M, Acampora D, Balsofiore S, Stornaiuolo A, Mallamaci A, Migliaccio E, Gulisano M, Simeone A. 1991. Isolation and mapping of EVX1, a human homeobox gene homologous to even-skipped, localized at the 5' end of HOX1 locus on chromosome 7. Nucleic Acids Res 19(23):6541-5.

Favier B, Le Meur M, Chambon P, Dolle P. 1995. Axial skeleton homeosis and forelimb malformations in hoxd-11 mutant mice. Proc Natl Acad Sci U S A 92(1):310-4.

Feil R, Brocard J, Mascrez B, LeMeur M, Metzger D, Chambon P. 1996. Ligand-activated site-specific recombination in mice. Proc Natl Acad Sci U S A 93(20):10887-90.

Fischer B, Metzger M, Richardson R, Knyphausen P, Ramezani T, Franzen R, Schmelzer E, Bloch W, Carney TJ, Hammerschmidt M. 2014. p53 and TAp63 promote keratinocyte proliferation and differentiation in breeding tubercles of the zebrafish. PLoS Genet 10(1):e1004048.

Fleisch VC, Leighton PL, Wang H, Pillay LM, Ritzel RG, Bhinder G, Roy B, Tierney KB, Ali DW, Waskiewicz AJ, et al. 2013. Targeted mutation of the gene encoding prion protein in zebrafish reveals a conserved role in neuron excitability. Neurobiol Dis 55:11-25.

Freestone SH, Marker P, Grace OC, Tomlinson DC, Cunha GR, Harnden P, Thomson AA. 2003. Sonic hedgehog regulates prostatic growth and epithelial differentiation. Dev Biol 264(2):352-62.

Fujimori S, Novak H, Weissenbock M, Jussila M, Goncalves A, Zeller R, Galloway J, Thesleff I, Hartmann C. 2010. Wnt/beta-catenin signaling in the dental mesenchyme regulates incisor development by regulating Bmp4. Dev Biol 348(1):97-106.

Fumoto K, Hoogenraad CC, Kikuchi A. 2006. GSK-3beta-regulated interaction of BICD with dynein is involved in microtubule anchorage at centrosome. Embo j 25(24):5670-82.

Fromental-Ramain C, Warot X, Messadecq N, LeMeur M, Dolle P, Chambon P. 1996. Hoxa-13 and hoxd-13 play a crucial role in the patterning of the limb autopod. Development 122(10):2997-3011.

Gallet A and Therond PP. 2005. Temporal modulation of the hedgehog morphogen gradient by a patched-dependent targeting to lysosomal compartment. Dev Biol 277(1):51-62.

Gavaia PJ, Simes DC, Ortiz-Delgado JB, Viegas CS, Pinto JP, Kelsh RN, Sarasquete MC, Cancela ML. 2006. Osteocalcin and matrix gla protein in zebrafish (danio rerio) and senegal sole (solea senegalensis): Comparative gene and protein expression during larval development through adulthood. Gene Expr Patterns 6(6):637-52.

Gavalas A and Krumlauf R. 2000. Retinoid signaling and hindbrain patterning. Curr Opin Genet Dev 10(4):380-6.

Gavalas A. 2002. ArRAnging the hindbrain. Trends Neurosci 25(2):61-4.

Géraudie J and Ferretti P. 1998. Gene expression during amphibian limb regeneration. Int Rev Cytol 180:1-50.

Géraudie J, Brulfert A, Monnot MJ, Ferretti P. 1994. Teratogenic and morphogenetic effects of retinoic acid on the regenerating pectoral fin in Zebrafish.

Gjorevski N and Nelson CM. 2010. The mechanics of development: Models and methods for tissue morphogenesis. Birth Defects Res C Embryo Today 90(3):193-202.

Goldsmith MI, Fisher S, Waterman R, Johnson SL. 2003. Saltatory control of isometric growth in the zebrafish caudal fin is disrupted in long fin and rapunzel mutants. Dev Biol 259(2):303-17.

Goldstein JL and Wilson JD. 1972. Studies on the pathogenesis of the pseudohermaphroditism in the mouse with testicular feminization. J Clin Invest 51(7):1647-58.

Goss RJ. 1969. Regeneration in fishes. In: GossRJ, editor. Principles of regeneration. New York: Academic Press Inc. p 113–139.

Grabher C and Wittbrodt J. 2007. Meganuclease and transposon mediated transgenesis in medaka. Genome Biol 8 Suppl 1:S10.

Grajevskaja V, Balciuniene J, Balciunas D. 2013. Chicken beta-globin insulators fail to shield the nkx2.5 promoter from integration site effects in zebrafish. Mol Genet Genomics 288(12):717-25.

Gray RS, Cheung KJ, Ewald AJ. 2010. Cellular mechanisms regulating epithelial morphogenesis and cancer invasion. Curr Opin Cell Biol 22(5):640-50.

Hall BK and Miyake T. 2000. All for one and one for all: Condensations and the initiation of skeletal development. Bioessays 22(2):138-47.

Hammerschmidt M, Pelegri F, Mullins MC, Kane DA, van Eeden FJ, Granato M, Brand M, Furutani-Seiki M, Haffter P, Heisenberg CP, et al. 1996. Dino and mercedes, two genes regulating dorsal development in the zebrafish embryo. Development 123:95-102.

Hammond CL and Schulte-Merker S. 2009. Two populations of endochondral osteoblasts with differential sensitivity to hedgehog signalling. Development 136(23):3991-4000.

Hammond KL and Whitfield TT. 2009. Expression of zebrafish hip: Response to hedgehog signalling, comparison with ptc1 expression, and possible role in otic patterning. Gene Expr Patterns 9(6):391-6.

Han C, Belenkaya TY, Wang B, Lin X. 2004. Drosophila glypicans control the cell-to-cell movement of hedgehog by a dynamin-independent process. Development 131(3):601-11.
Han M, Yang X, Taylor G, Burdsal CA, Anderson RA, Muneoka K. 2005. Limb regeneration in higher vertebrates: Developing a roadmap. Anat Rec B New Anat 287(1):14-24.

Harunaga J, Hsu JC, Yamada KM. 2011. Dynamics of salivary gland morphogenesis. J Dent Res 90(9):1070-7.

Hata S, Namae M, Nishina H. 2007. Liver development and regeneration: From laboratory study to clinical therapy. Dev Growth Differ 49(2):163-70.

Hayashi S and McMahon AP. 2002. Efficient recombination in diverse tissues by a tamoxifen-inducible form of cre: A tool for temporally regulated gene activation/inactivation in the mouse. Dev Biol 244(2):305-18.

Hellemans J, Mortier G, De Paepe A, Speleman F, Vandesompele J. 2007. qBase relative quantification framework and software for management and automated analysis of real-time quantitative PCR data. Genome Biol 8(2):R19.

Hernandez RE, Putzke AP, Myers JP, Margaretha L, Moens CB. 2007. Cyp26 enzymes generate the retinoic acid response pattern necessary for hindbrain development. Development 134(1):177-87.

Hillier SG, van den Boogaard AM, Reichert LE,Jr, van Hall EV. 1980. Alterations in granulosa cell aromatase activity accompanying preovulatory follicular development in the rat ovary with evidence that 5alpha-reduced C19 steroids inhibit the aromatase reaction in vitro. J Endocrinol 84(3):409-19.

Ho L and Alman B. 2010. Protecting the hedgerow: P53 and hedgehog pathway interactions. Cell Cycle 9(3):506-11.

Hoptak-Solga AD, Nielsen S, Jain I, Thummel R, Hyde DR, Iovine MK. 2008. Connexin43 (GJA1) is required in the population of dividing cells during fin regeneration. Dev Biol 317(2):541-8.

Howlett CR. 1979. The fine structure of the proximal growth plate of the avian tibia. J Anat 128(Pt 2):377-99.

Huang CC, Lawson ND, Weinstein BM, Johnson SL. 2003. Reg6 is required for branching morphogenesis during blood vessel regeneration in zebrafish caudal fins. Dev Biol 264(1):263-74.

Hulsey CD, Fraser GJ, Streelman JT. 2005. Evolution and development of complex biomechanical systems: 300 million years of fish jaws. Zebrafish 2(4):243-57.

Hunziker EB. 1994. Mechanism of longitudinal bone growth and its regulation by growth plate chondrocytes. Microsc Res Tech 28(6):505-19.

Huycke TR, Eames BF, Kimmel CB. 2012. Hedgehog-dependent proliferation drives modular growth during morphogenesis of a dermal bone. Development 139(13):2371-80.

Huysseune, A. 2000. Skeletal system. *In* "The Laboratory Fish. Part 4 Microscopic Functional Anatomy" pp. 307-317. Academic Press, San Diego.

Hyde DR, Godwin AR, Thummel R. 2012. In vivo electroporation of morpholinos into the regenerating adult zebrafish tail fin. J Vis Exp (61). pii: 3632. doi(61):10.3791/3632.
Hynes M, Stone DM, Dowd M, Pitts-Meek S, Goddard A, Gurney A, Rosenthal A. 1997. Control of cell pattern in the neural tube by the zinc finger transcription factor and oncogene gli-1. Neuron 19(1):15-26.

Imagawa E, Kayserili H, Nishimura G, Nakashima M, Tsurusaki Y, Saitsu H, Ikegawa S, Matsumoto N, Miyake N. 2014. Severe manifestations of hand-foot-genital syndrome associated with a novel HOXA13 mutation. Am J Med Genet A 164A(9):2398-402.

Incardona JP, Lee JH, Robertson CP, Enga K, Kapur RP, Roelink H. 2000. Receptor-mediated endocytosis of soluble and membrane-tethered sonic hedgehog by patched-1. Proc Natl Acad Sci U S A 97(22):12044-9.

Indra AK, Warot X, Brocard J, Bornert JM, Xiao JH, Chambon P, Metzger D. 1999. Temporally-controlled site-specific mutagenesis in the basal layer of the epidermis: Comparison of the recombinase activity of the tamoxifen-inducible cre-ER(T) and cre-ER(T2) recombinases. Nucleic Acids Res 27(22):4324-7.

Iovine MK. 2007. Conserved mechanisms regulate outgrowth in zebrafish fins. Nat Chem

Biol 3(10):613-8.

Iovine MK and Johnson SL. 2000. Genetic analysis of isometric growth control mechanisms in the zebrafish caudal fin. Genetics 155(3):1321-9.

Iovine MK, Higgins EP, Hindes A, Coblitz B, Johnson SL. 2005. Mutations in connexin43 (GJA1) perturb bone growth in zebrafish fins. Dev Biol 278(1):208-19.

Jaenisch R, Jahner D, Nobis P, Simon I, Lohler J, Harbers K, Grotkopp D. 1981. Chromosomal position and activation of retroviral genomes inserted into the germ line of mice. Cell 24(2):519-29.

Jaskoll T, Leo T, Witcher D, Ormestad M, Astorga J, Bringas P,Jr, Carlsson P, Melnick M. 2004. Sonic hedgehog signaling plays an essential role during embryonic salivary gland epithelial branching morphogenesis. Dev Dyn 229(4):722-32.

Javidan Y and Schilling TF. 2004. Development of cartilage and bone. Methods Cell Biol 76:415-36.

Jenkins D, Seelow D, Jehee FS, Perlyn CA, Alonso LG, Bueno DF, Donnai D, Josifova D, Mathijssen IM, Morton JE, et al. 2007. RAB23 mutations in carpenter syndrome imply an unexpected role for hedgehog signaling in cranial-suture development and obesity. Am J Hum Genet 80(6):1162-70.

Jeong J and McMahon AP. 2005. Growth and pattern of the mammalian neural tube are governed by partially overlapping feedback activities of the hedgehog antagonists patched 1 and Hhip1. Development 132(1):143-54.

Jessen JR, Meng A, McFarlane RJ, Paw BH, Zon LI, Smith GR, Lin S. 1998. Modification of bacterial artificial chromosomes through chi-stimulated homologous recombination and its application in zebrafish transgenesis. Proc Natl Acad Sci U S A 95(9):5121-6.

Johnson SL and Bennett P. 1999. Growth control in the ontogenetic and regenerating zebrafish fin. Methods Cell Biol 59:301-11.

Johnson SL and Weston JA. 1995. Temperature-sensitive mutations that cause stage-specific defects in zebrafish fin regeneration. Genetics 141(4):1583-95.

Kaesler S, Luscher B, Ruther U. 2000. Transcriptional activity of GLI1 is negatively regulated by protein kinase A. Biol Chem 381(7):545-51.

Kague E, Gallagher M, Burke S, Parsons M, Franz-Odendaal T, Fisher S. 2012. Skeletogenic fate of zebrafish cranial and trunk neural crest. PLoS One 7(11):e47394.

Kang J, Nachtrab G, Poss KD. 2013. Local Dkk1 crosstalk from breeding ornaments impedes regeneration of injured male zebrafish fins. Dev Cell 27(1):19-31.

Kapp-Simon KA. 1998. Mental development and learning disorders in children with single suture craniosynostosis. Cleft Palate Craniofac J 35(3):197-203.

Karlstrom RO, Tyurina OV, Kawakami A, Nishioka N, Talbot WS, Sasaki H, Schier AF. 2003. Genetic analysis of zebrafish gli1 and gli2 reveals divergent requirements for gli genes in vertebrate development. Development 130(8):1549-64.

Karp SJ, Schipani E, St-Jacques B, Hunzelman J, Kronenberg H, McMahon AP. 2000. Indian hedgehog coordinates endochondral bone growth and morphogenesis via parathyroid hormone related-protein-dependent and -independent pathways. Development 127(3):543-8.

Katogi R, Nakatani Y, Shin-i T, Kohara Y, Inohaya K, Kudo A. 2004. Large-scale analysis of the genes involved in fin regeneration and blastema formation in the medaka, oryzias latipes. Mech Dev 121(7-8):861-72.

Kawakami K. 2007. Tol2: A versatile gene transfer vector in vertebrates. Genome Biol 8 Suppl 1:S7.

Kemp NE and Park JH. 1970. Regeneration of lepidotrichia and actinotrichia in the tailfin of the teleost tilapia mossambica. Dev Biol 22(2):321-42.

Ke Z, Emelyanov A, Lim SE, Korzh V, Gong Z. 2005. Expression of a novel zebrafish zinc finger gene, gli2b, is affected in hedgehog and notch signaling related mutants during embryonic development. Dev Dyn 232(2):479-86.

Kessel M and Gruss P. 1991. Homeotic transformations of murine vertebrae and concomitant alteration of hox codes induced by retinoic acid. Cell 67(1):89-104.

Kikuta H, Kanai M, Ito Y, Yamasu K. 2003. gbx2 homeobox gene is required for the maintenance of the isthmic region in the zebrafish embryonic brain. Dev Dyn 228(3):433-50.

Klee CB and Haiech J. 1980. Concerted role of calmodulin and calcineurin in calcium regulation. Ann N Y Acad Sci 356:43-54.

Klopocki E, Hennig BP, Dathe K, Koll R, de Ravel T, Baten E, Blom E, Gillerot Y, Weigel JF, Kruger G, et al. 2010. Deletion and point mutations of PTHLH cause brachydactyly type E. Am J Hum Genet 86(3):434-9.

Knopf F, Hammond C, Chekuru A, Kurth T, Hans S, Weber CW, Mahatma G, Fisher S, Brand M, Schulte-Merker S, et al. 2011. Bone regenerates via dedifferentiation of osteoblasts in the zebrafish fin. Dev Cell 20(5):713-24.

Knowles HJ, Moskovsky L, Thompson MS, Grunhen J, Cheng X, Kashima TG, Athanasou

NA. 2012. Chondroclasts are mature osteoclasts which are capable of cartilage matrix resorption. Virchows Arch 461(2):205-10.

Kobayashi T, Chung UI, Schipani E, Starbuck M, Karsenty G, Katagiri T, Goad DL, Lanske B, Kronenberg HM. 2002. PTHrP and indian hedgehog control differentiation of growth plate chondrocytes at multiple steps. Development 129(12):2977-86.

Kogerman P, Grimm T, Kogerman L, Krause D, Unden AB, Sandstedt B, Toftgard R, Zaphiropoulos PG. 1999. Mammalian suppressor-of-fused modulates nuclear-cytoplasmic shuttling of gli-1. Nat Cell Biol 1(5):312-9.

Komori T, Yagi H, Nomura S, Yamaguchi A, Sasaki K, Deguchi K, Shimizu Y, Bronson RT, Gao YH, Inada M, et al. 1997. Targeted disruption of Cbfa1 results in a complete lack of bone formation owing to maturational arrest of osteoblasts. Cell 89(5):755-64.

Kortet R, Taskinen J, Vainikka A, Ylönen H. 2004. Breeding Tubercles, Papillomatosis and Dominance Behaviour of Male Roach (Rutilus rutilus) During the Spawning Period. Ethology. 110:591-601.

Kortet R, Vainikka A, Rantala MJ, Jokinen I, Taskinen J. 2003. Sexual ornamentation, androgens and papillomatosis in male roach (Rutilus rutilus). Evolutionary Ecology Research. 5:411-419.

Korzh V, Teh C, Kondrychyn I, Chudakov DM, Lukyanov, S. 2011. Visualizing Compound Transgenic Zebrafish in Development: A Tale of Green Fluorescent Protein and KillerRed. Zebrafish 8:23-29.

Krauss S, Concordet JP, Ingham PW. 1993. A functionally conserved homolog of the drosophila segment polarity gene hh is expressed in tissues with polarizing activity in zebrafish embryos. Cell 75(7):1431-44.

Kronenberg HM. 2003. Developmental regulation of the growth plate. Nature 423(6937):332-6.

Kujawski S, Lin W, Kitte F, Bormel M, Fuchs S, Arulmozhivarman G, Vogt S, Theil D, Zhang Y, Antos CL. 2014. Calcineurin regulates coordinated outgrowth of zebrafish regenerating fins. Dev Cell 28(5):573-87.

Laforest L, Brown CW, Poleo G, Geraudie J, Tada M, Ekker M, Akimenko MA. 1998. Involvement of the sonic hedgehog, patched 1 and bmp2 genes in patterning of the zebrafish dermal fin rays. Development 125(21):4175-84.

Lanske B, Karaplis AC, Lee K, Luz A, Vortkamp A, Pirro A, Karperien M, Defize LH, Ho C, Mulligan RC, et al. 1996. PTH/PTHrP receptor in early development and indian hedgehog-regulated bone growth. Science 273(5275):663-6.

Lawson ND and Weinstein BM. 2002. In vivo imaging of embryonic vascular development using transgenic zebrafish. Dev Biol 248(2):307-18.

Lee Y, Grill S, Sanchez A, Murphy-Ryan M, Poss KD. 2005. Fgf signaling instructs position-dependent growth rate during zebrafish fin regeneration. Development 132(23):5173-83.

Lee Y, Hami D, De Val S, Kagermeier-Schenk B, Wills AA, Black BL, Weidinger G, Poss KD. 2009. Maintenance of blastemal proliferation by functionally diverse epidermis in regenerating zebrafish fins. Dev Biol 331(2):270-80.

Lenton K, James AW, Manu A, Brugmann SA, Birker D, Nelson ER, Leucht P, Helms JA, Longaker MT. 2011. Indian hedgehog positively regulates calvarial ossification and modulates bone morphogenetic protein signaling. Genesis 49(10):784-96.

Lettice LA, Horikoshi T, Heaney SJ, van Baren MJ, van der Linde HC, Breedveld GJ, Joosse M, Akarsu N, Oostra BA, Endo N, et al. 2002. Disruption of a long-range cis-acting regulator for shh causes preaxial polydactyly. Proc Natl Acad Sci U S A 99(11):7548-53.

Li N, Felber K, Elks P, Croucher P, Roehl HH. 2009. Tracking gene expression during zebrafish osteoblast differentiation. Dev Dyn 238(2):459-66.

Lin, M. 2013. Functional Analysis of the Zebrafish Caudal Fin Regeneration. Masters Thesis, University of Ottawa, Ottawa, Canada. Retrieved from https://www.ruor.uottawa.ca/handle/10393/26202.

Long F, Chung UI, Ohba S, McMahon J, Kronenberg HM, McMahon AP. 2004. Ihh signaling is directly required for the osteoblast lineage in the endochondral skeleton. Development 131(6):1309-18.

Lotz M, Hashimoto S, Kuhn K. 1999. Mechanisms of chondrocyte apoptosis. Osteoarthritis Cartilage 7(4):389-91.

Ma Y, Erkner A, Gong R, Yao S, Taipale J, Basler K, Beachy PA. 2002. Hedgehog-mediated patterning of the mammalian embryo requires transporter-like function of dispatched. Cell 111(1):63-75.

Macintosh C, Wells R, Johnson D, Wall S. 2011. What are the effects of metopic synostosis on visual function? J Craniofac Surg 22(4):1280-3.

Mackay EW, Apschner A, Schulte-Merker S. 2014. A bone to pick with zebrafish. Bonekey Rep 2:445.

Mackie EJ, Tatarczuch L, Mirams M. 2011. The skeleton: A multi-functional complex organ: The growth plate chondrocyte and endochondral ossification. J Endocrinol 211(2):109-21.

Mackie EJ, Ahmed YA, Tatarczuch L, Chen KS, Mirams M. 2008. Endochondral ossification: How cartilage is converted into bone in the developing skeleton. Int J Biochem Cell Biol 40(1):46-62.

Maden M. 1982. Vitamin A and pattern formation in the regenerating limb. Nature 295(5851):672-5.

Maden M, Gale E, Kostetskii I, Zile M. 1996. Vitamin A-deficient quail embryos have half a hindbrain and other neural defects. Curr Biol 6(4):417-26.

Maden M. 2002. Retinoid signaling in the development of the central nervous system. Nat Rev Neurosci 3(11):843-53.

Mak KK, Bi Y, Wan C, Chuang PT, Clemens T, Young M, Yang Y. 2008a. Hedgehog signaling in mature osteoblasts regulates bone formation and resorption by controlling PTHrP and RANKL expression. Dev Cell 14(5):674-88.

Mak KK, Kronenberg HM, Chuang PT, Mackem S, Yang Y. 2008. Indian hedgehog signals independently of PTHrP to promote chondrocyte hypertrophy. Development 135(11):1947-56.

Mari-Beffa M and Murciano C. 2010. Dermoskeleton morphogenesis in zebrafish fins. Dev Dyn 239(11):2779-94.

Mari-Beffa M, Mateos I, Palmqvist P, Becerra J. 1996. Cell to cell interactions during teleosts fin regeneration. Int J Dev Biol Suppl 1:179S-80S.

Markeson D, Pleat JM, Sharpe JR, Harris AL, Seifalian AM, Watt SM. 2015. Scarring, stem cells, scaffolds and skin repair. J Tissue Eng Regen Med 9(6):649-68.

Matsuda T and Cepko CL. 2007. Controlled expression of transgenes introduced by in vivo electroporation. Proc Natl Acad Sci U S A 104(3):1027-32.

McMillan SC, Géraudie J, Akimenko MA. 2015. Pectoral fin breeding tubercle clusters: A method to determine zebrafish sex. Zebrafish 12(1):121-3.

McMillan SC, Xu ZT, Zhang J, Teh C, Korzh V, Trudeau VL, Akimenko MA. 2013. Regeneration of breeding tubercles on zebrafish pectoral fins requires androgens and two waves of revascularization. Development 140(21):4323-34.

Menuet A, Le Page Y, Torres O, Kern L, Kah O, Pakdel F. 2004. Analysis of the estrogen regulation of the zebrafish estrogen receptor (ER) reveals distinct effects of ERalpha, ERbeta1 and ERbeta2. J Mol Endocrinol 32(3):975-86.

Meunier, FJ. 1989. The acellularisation process in osteichthyan bone. Prog. Zool.

35:443–445.

Miles-Richardson SR, Kramer VJ, Fitzgerald SD, Render JA, Behzad Y, Barbee, SJ, Giesy JP. 1999. Effects of waterborne exposure of 17 b-estradiol on secondary sex characteristics and gonads of fathead minnows (Pimephales promelas). Aquat Toxicol. 47:129-145.

Miller LA, Wert SE, Clark JC, Xu Y, Perl AK, Whitsett JA. 2004. Role of sonic hedgehog in patterning of tracheal-bronchial cartilage and the peripheral lung. Dev Dyn 231(1):57-71.

Moreau J and Jeannotte L. 2002. Sequence analysis of a Hoxa4-Hoxa5 intergenic region including shared regulatory elements. DNA Seq 13(4):203-9.

Morgan TH. 1901. Regeneration and liability to injury. Science 14(346):235-48.

Moro E, Ozhan-Kizil G, Mongera A, Beis D, Wierzbicki C, Young RM, Bournele D, Domenichini A, Valdivia LE, Lum L, et al. 2012. In vivo wnt signaling tracing through a transgenic biosensor fish reveals novel activity domains. Dev Biol 366(2):327-40.

Mosimann C, Kaufman CK, Li P, Pugach EK, Tamplin OJ, Zon LI. 2011. Ubiquitous transgene expression and cre-based recombination driven by the ubiquitin promoter in zebrafish. Development 138(1):169-77.

Munch J, Gonzalez-Rajal A, de la Pompa JL. 2013. Notch regulates blastema proliferation and prevents differentiation during adult zebrafish fin regeneration. Development 140(7):1402-11.

Murciano C, Fernandez TD, Duran I, Maseda D, Ruiz-Sanchez J, Becerra J, Akimenko MA, Mari-Beffa M. 2002. Ray-interray interactions during fin regeneration of danio rerio. Dev Biol 252(2):214-24.

Muyrers JP, Zhang Y, Stewart AF. 2001. Techniques: Recombinogenic engineering--new options for cloning and manipulating DNA. Trends Biochem Sci 26(5):325-31.

Muyrers JP, Zhang Y, Stewart AF. 2000. ET-cloning: Think recombination first. Genet Eng (N Y) 22:77-98.

Nabrit SM. 1929. The role of the fin rays in the regeneration in the tail fins of fishes (in Fundulus and goldfish). Biol Bull 56: 235–266.

Nabrit SM. 1931. The role of the basal of the tail in regeneration in the tail-fins of fishes (Fundulus and Carassius). Biol Bull 60:60 – 63.

Nachtrab G, Czerwinski M, Poss KD. 2011. Sexually dimorphic fin regeneration in zebrafish controlled by Androgen/GSK3 signaling. Curr Biol 21(22):1912-7.

Nagata Y. 1934. Gonadectomy in Oryzias latipes. Zool. Mag. 46:293-294.

Nakashima K, Zhou X, Kunkel G, Zhang Z, Deng JM, Behringer RR, de Crombrugghe B. 2002. The novel zinc finger-containing transcription factor osterix is required for osteoblast differentiation and bone formation. Cell 108(1):17-29.

Nechiporuk A and Keating MT. 2002. A proliferation gradient between proximal and msxb-expressing distal blastema directs zebrafish fin regeneration. Development 129(11):2607-17.

Niazi IA and Saxena S. 1978. Abnormal hind limb regeneration in tadpoles of the toad, bufo andersoni, exposed to excess vitamin A. Folia Biol (Krakow) 26(1):3-8.

Ng MK, Quinn CM, McCrohon JA, Nakhla S, Jessup W, Handelsman DJ, Celermajer DS, Death AK. 2003. Androgens up-regulate atherosclerosis-related genes in macrophages from males but not females: molecular insights into gender differences in atherosclerosis. J. Am. Coll. Cardiol. 42:1306–1313.

Nikaido M, Tada M, Saji T, Ueno N. 1997. Conservation of BMP signaling in zebrafish mesoderm patterning. Mech Dev 61(1-2):75-88.

Nishio Y, Dong Y, Paris M, O'Keefe RJ, Schwarz EM, Drissi H. 2006. Runx2-mediated regulation of the zinc finger Osterix/Sp7 gene. Gene 372:62-70.

Nourizadeh-Lillabadi R, Seilo Torgersen J, Vestrheim O, Konig M, Alestrom P, Syed M. 2010. Early embryonic gene expression profiling of zebrafish prion protein (Prp2) morphants. PLoS One 5(10):e13573.

Okada YK, Yamashita H. 1944. Experimental investigation of the manifestation of secondary sexual characters in fish, using the medaka, Oryzias latipes. Jour. Fac. Sci. Imp. Univ. Tokyo. 6:383-437.

Ornitz DM and Marie PJ. 2002. FGF signaling pathways in endochondral and intramembranous bone development and human genetic disease. Genes Dev 16(12):1446-65.

Paces-Fessy M, Boucher D, Petit E, Paute-Briand S, Blanchet-Tournier MF. 2004. The negative regulator of gli, suppressor of fused (sufu), interacts with SAP18, Galectin3 and other nuclear proteins. Biochem J 378(Pt 2):353-62.

Pacifici M, Koyama E, Shibukawa Y, Wu C, Tamamura Y, Enomoto-Iwamoto M, Iwamoto M. 2006. Cellular and molecular mechanisms of synovial joint and articular cartilage formation. Ann N Y Acad Sci 1068:74-86.

Padhi BK, Joly L, Tellis P, Smith A, Nanjappa P, Chevrette M, Ekker M, Akimenko MA. 2004. Screen for genes differentially expressed during regeneration of the zebrafish caudal fin. Dev Dyn 231(3):527-41.

Pan A, Chang L, Nguyen A, James AW. 2013. A review of hedgehog signaling in cranial bone development. Front Physiol 4:61.

Panakova D, Sprong H, Marois E, Thiele C, Eaton S. 2005. Lipoprotein particles are required for hedgehog and wingless signalling. Nature 435(7038):58-65.

Panchal J, Amirsheybani H, Gurwitch R, Cook V, Francel P, Neas B, Levine N. 2001. Neurodevelopment in children with single-suture craniosynostosis and plagiocephaly without synostosis. Plast Reconstr Surg 108(6):1492,8; discussion 1499-500.

Parichy DM, Elizondo MR, Mills MG, Gordon TN, Engeszer RE. 2009. Normal table of postembryonic zebrafish development: Staging by externally visible anatomy of the living fish. Dev Dyn 238(12):2975-3015.

Pawlowski S, van Aerle R, Tyler CR, Braunbeck T. 2004. Effects of 17alpha-ethinylestradiol in a fathead minnow (pimephales promelas) gonadal recrudescence assay. Ecotoxicol Environ Saf 57(3):330-45.

Peets EA, Henson MF, Neri R. 1974. On the mechanism of the anti-androgenic action of flutamide (alpha-alpha-alpha-trifluoro-2-methyl-4'-nitro-m-propionotoluidide) in the rat. Endocrinology 94(2):532-40.

Pepicelli CV, Lewis PM, McMahon AP. 1998. Sonic hedgehog regulates branching morphogenesis in the mammalian lung. Curr Biol 8(19):1083-6.

Pepinsky RB, Zeng C, Wen D, Rayhorn P, Baker DP, Williams KP, Bixler SA, Ambrose CM, Garber EA, Miatkowski K, et al. 1998. Identification of a palmitic acid-modified form of human sonic hedgehog. J Biol Chem 273(22):14037-45.

Perathoner S, Daane JM, Henrion U, Seebohm G, Higdon CW, Johnson SL, Nusslein-Volhard C, Harris MP. 2014. Bioelectric signaling regulates size in zebrafish fins. PLoS Genet 10(1):e1004080.

Poleo G, Brown CW, Laforest L, Akimenko MA. 2001. Cell proliferation and movement during early fin regeneration in zebrafish. Dev Dyn 221(4):380-90.

Porter JA, Young KE, Beachy PA. 1996. Cholesterol modification of hedgehog signaling proteins in animal development. Science 274(5285):255-9.

Poss KD, Keating MT, Nechiporuk A. 2003. Tales of regeneration in zebrafish. Dev Dyn 226(2):202-10.

Poss KD, Shen J, Nechiporuk A, McMahon G, Thisse B, Thisse C, Keating MT. 2000. Roles for fgf signaling during zebrafish fin regeneration. Dev Biol 222(2):347-58.

Pu Y, Huang L, Prins GS. 2004. Sonic hedgehog-patched gli signaling in the developing rat prostate gland: Lobe-specific suppression by neonatal estrogens reduces ductal growth and branching. Dev Biol 273(2):257-75.

Quinonez SC and Innis JW. 2014. Human HOX gene disorders. Mol Genet Metab 111(1):4-15.

Quint E, Smith A, Avaron F, Laforest L, Miles J, Gaffield W, Akimenko MA. 2002. Bone patterning is altered in the regenerating zebrafish caudal fin after ectopic expression of sonic hedgehog and bmp2b or exposure to cyclopamine. Proc Natl Acad Sci U S A 99(13):8713-8.

Ramaswami LS, Hasler AD. 1955. Hormones and secondary sex characters in the minnow, Hyborhynchus. Physiol. Zool. 28:62-68.

Roberts JA, Miguel-Escalada I, Slovik KJ, Walsh KT, Hadzhiev Y, Sanges R, Stupka E, Marsh EK, Balciuniene J, Balciunas D, et al. 2014. Targeted transgene integration overcomes variability of position effects in zebrafish. Development 141(3):715-24.

Roelink H, Augsburger A, Heemskerk J, Korzh V, Norlin S, Ruiz i Altaba A, Tanabe Y, Placzek M, Edlund T, Jessell TM. 1994. Floor plate and motor neuron induction by vhh-1, a vertebrate homolog of hedgehog expressed by the notochord. Cell 76(4):761-75.

Roeser T and Baier H. 2003. Visuomotor behaviors in larval zebrafish after GFP-guided laser ablation of the optic tectum. J Neurosci 23(9):3726-34.

Rossant J, Nutter LM, Gertsenstein M. 2011. Engineering the embryo. Proc Natl Acad Sci U S A 108(19):7659-60.

Ruohola JK, Valve EM, Karkkainen MJ, Joukov V, Alitalo K, Harkonen PL. 1999. Vascular endothelial growth factors are differentially regulated by steroid hormones and antiestrogens in breast cancer cells. Mol Cell Endocrinol 149(1-2):29-40.

Sakai Y, Meno C, Fujii H, Nishino J, Shiratori H, Saijoh Y, Rossant J, Hamada H. 2001. The retinoic acid-inactivating enzyme CYP26 is essential for establishing an uneven distribution of retinoic acid along the anterio-posterior axis within the mouse embryo. Genes Dev 15(2):213-25.

Santamaria JA and Becerra J. 1991. Tail fin regeneration in teleosts: Cell-extracellular matrix interaction in blastemal differentiation. J Anat 176:9-21.

Santamaria JA, Mari-Beffa M, Becerra J. 1992. Interactions of the lepidotrichial matrix components during tail fin regeneration in teleosts. Differentiation 49(3):143-50.

Santamaria JA, Mari-Beffa M, Santos-Ruiz L, Becerra J. 1996. Incorporation of bromodeoxyuridine in regenerating fin tissue of the goldfish carassius auratus. J Exp Zool 275(4):300-7.

Santos-Ruiz L, Santamaria JA, Ruiz-Sanchez J, Becerra J. 2002. Cell proliferation during blastema formation in the regenerating teleost fin. Dev Dyn 223(2):262-72.

Schulte CJ, Allen C, England SJ, Juarez-Morales JL, Lewis KE. 2011. Evx1 is required for joint formation in zebrafish fin dermoskeleton. Dev Dyn 240(5):1240-8.

Schulte-Merker S and Stainier DY. 2014. Out with the old, in with the new: Reassessing morpholino knockdowns in light of genome editing technology. Development 141(16):3103-4.

Serebrovskaya EO, Edelweiss EF, Stremovskiy OA, Lukyanov KA, Chudakov DM, Deyev SM. 2009. Targeting cancer cells by using an antireceptor antibody-photosensitizer fusion protein. Proc Natl Acad Sci U S A 106(23):9221-5.

Serra R, Johnson M, Filvaroff EH, LaBorde J, Sheehan DM, Derynck R, Moses HL. 1997. Expression of a truncated, kinase-defective TGF-beta type II receptor in mouse skeletal tissue promotes terminal chondrocyte differentiation and osteoarthritis. J Cell Biol 139(2):541-52.

Serra R, Karaplis A, Sohn P. 1999. Parathyroid hormone-related peptide (PTHrP)-dependent and -independent effects of transforming growth factor beta (TGF-beta) on endochondral bone formation. J Cell Biol 145(4):783-94.

Shao J, Qian X, Zhang C, Xu Z. 2009. Fin regeneration from tail segment with musculature, endoskeleton, and scales. J Exp Zool B Mol Dev Evol 312(7):762-9.

Shkumatava A, Fischer S, Muller F, Strahle U, Neumann CJ. 2004. Sonic hedgehog, secreted by amacrine cells, acts as a short-range signal to direct differentiation and lamination in the zebrafish retina. Development 131(16):3849-58.

Sieveking DP, Chow RW, Ng MK. 2010. Androgens, angiogenesis and cardiovascular regeneration. Curr Opin Endocrinol Diabetes Obes 17(3):277-83.

Sillibourne JE, Milne DM, Takahashi M, Ono Y, Meek DW. 2002. Centrosomal anchoring of the protein kinase CK1delta mediated by attachment to the large, coiled-coil scaffolding protein CG-NAP/AKAP450. J Mol Biol 322(4):785-97.

Sims K,Jr, Eble DM, Iovine MK. 2009. Connexin43 regulates joint location in zebrafish fins. Dev Biol 327(2):410-8.

Singh SP, Holdway JE, Poss KD. 2012. Regeneration of amputated zebrafish fin rays from de novo osteoblasts. Dev Cell 22(4):879-86.

Small KM and Potter SS. 1993. Homeotic transformations and limb defects in hox A11 mutant mice. Genes Dev 7(12A):2318-28.

Smith A, Avaron F, Guay D, Padhi BK, Akimenko MA. 2006. Inhibition of BMP signaling during zebrafish fin regeneration disrupts fin growth and scleroblasts differentiation and function. Dev Biol 299(2):438-54.

Smith A, Zhang J, Guay D, Quint E, Johnson A, Akimenko MA. 2008. Gene expression analysis on sections of zebrafish regenerating fins reveals limitations in the whole-mount in situ hybridization method. Dev Dyn 237(2):417-25.

Smith JD, Smith RJF. 1986. Effect of hormone treatments on alarm substance cell counts in the pearl dace, Semotilus margarita. Can. J. Zool. 64:29 1-295.

Smith RJ. 1974. Effects of 17 alpha-methyltestosterone on the dorsal pad and tubercles of fathead minnows (pimephales promelas). Can J Zool 52(8):1031-8.

Smith RJF. 1978. Seasonal changes in the histology of the gonads and dorsal skin of the fathead minnow, Pimephales promelas. Can. J. Zool. 56:103-109.

Smolinsky AN, Doughman JM, Kratzke LT, Lassiter CS. 2010. Zebrafish (Danio Rerio) Androgen Receptor: Sequence Homology and Up-Regulation by the Fungicide Vinclozolin. Comp. Biochem. Physiol. C. Toxicol. Pharmacol. 151:161-166.

Sousa S, Afonso N, Bensimon-Brito A, Fonseca M, Simoes M, Leon J, Roehl H, Cancela ML, Jacinto A. 2011. Differentiated skeletal cells contribute to blastema formation during zebrafish fin regeneration. Development 138(18):3897-905.

Spence R, Fatema MK, Reichard M, Huqk KA, Wahab MA, Ahmed ZF, et al. The distribution and habitat preferences of the zebrafish in Bangladesh. J Fish Biol 2006; 69:1435–1448.

Spence R, Gerlach G, Lawrence C, Smith, C. 2008. The Behaviour and Ecology of the Zebrafish, Danio Rerio. Biol. Rev. Camb. Philos. Soc. 83:13-34.

Stewart S, Gomez AW, Armstrong BE, Henner A, Stankunas K. 2014. Sequential and opposing activities of wnt and BMP coordinate zebrafish bone regeneration. Cell Rep 6(3):482-98.

St-Jacques B, Hammerschmidt M, McMahon AP. 1999. Indian hedgehog signaling regulates proliferation and differentiation of chondrocytes and is essential for bone formation. Genes Dev 13(16):2072-86.

Stoick-Cooper CL, Weidinger G, Riehle KJ, Hubbert C, Major MB, Fausto N, Moon RT. 2007. Distinct wnt signaling pathways have opposing roles in appendage regeneration. Development 134(3):479-89.

Su CY, Kemp HA, Moens CB. 2014. Cerebellar development in the absence of gbx function in zebrafish. Dev Biol 386(1):181-90.

Sunderland ME. 2010. Regeneration: Thomas hunt morgan's window into development. J Hist Biol 43(2):325-61.

Sustar A and Schubiger G. 2005. A transient cell cycle shift in drosophila imaginal disc cells precedes multipotency. Cell 120(3):383-93.

Suster ML, Kikuta H, Urasaki A, Asakawa K, Kawakami K. 2009. Transgenesis in zebrafish with the tol2 transposon system. Methods Mol Biol 561:41-63.

Suzuki M and Kuroiwa A. 2002. Transition of hox expression during limb cartilage development. Mech Dev 118(1-2):241-5.

Swift MR, Pham VN, Castranova D, Bell K, Poole RJ, Weinstein BM. 2014. SoxF factors and notch regulate nr2f2 gene expression during venous differentiation in zebrafish. Dev Biol 390(2):116-25.

Teh C, Chudakov DM, Poon KL, Mamedov IZ, Sek JY, Shidlovsky K, Lukyanov S, Korzh V. 2010. Optogenetic in vivo cell manipulation in KillerRed-expressing zebrafish transgenics. BMC Dev Biol 10:110,213X-10-110.

Tenzen T, Allen BL, Cole F, Kang JS, Krauss RS, McMahon AP. 2006. The cell surface membrane proteins cdo and boc are components and targets of the hedgehog signaling pathway and feedback network in mice. Dev Cell 10(5):647-56.

Thaeron C, Avaron F, Casane D, Borday V, Thisse B, Thisse C, Boulekbache H, Laurenti P. 2000. Zebrafish evx1 is dynamically expressed during embryogenesis in subsets of interneurones, posterior gut and urogenital system. Mech Dev 99(1-2):167-72.

Thermes V, Grabher C, Ristoratore F, Bourrat F, Choulika A, Wittbrodt J, Joly JS. 2002. I-SceI meganuclease mediates highly efficient transgenesis in fish. Mech Dev 118(1-2):91-8.

Therond PP. 2012. Release and transportation of hedgehog molecules. Curr Opin Cell Biol 24(2):173-80.

Thisse C and Thisse B. 2008. High-resolution in situ hybridization to whole-mount zebrafish embryos. Nat Protoc 3(1):59-69.

Thoms SD and Stocum DL. 1984. Retinoic acid-induced pattern duplication in

regenerating urodele limbs. Dev Biol 103(2):319-28.

Thomson AA and Marker PC. 2006. Branching morphogenesis in the prostate gland and seminal vesicles. Differentiation 74(7):382-92.

Thomson AW, Bonham CA, Zeevi A. 1995. Mode of action of tacrolimus (FK506): Molecular and cellular mechanisms. Ther Drug Monit 17(6):584-91.

Thorel F, Nepote V, Avril I, Kohno K, Desgraz R, Chera S, Herrera PL. 2010. Conversion of adult pancreatic alpha-cells to beta-cells after extreme beta-cell loss. Nature 464(7292):1149-54.

Tuson M, He M, Anderson KV. 2011. Protein kinase A acts at the basal body of the primary cilium to prevent Gli2 activation and ventralization of the mouse neural tube. Development 138(22):4921-30.

Tyurina OV, Guner B, Popova E, Feng J, Schier AF, Kohtz JD, Karlstrom RO. 2005. Zebrafish Gli3 functions as both an activator and a repressor in hedgehog signaling. Dev Biol 277(2):537-56.

van Genderen C, Okamura RM, Farinas I, Quo RG, Parslow TG, Bruhn L, Grosschedl R. 1994. Development of several organs that require inductive epithelial-mesenchymal interactions is impaired in LEF-1-deficient mice. Genes Dev 8(22):2691-703.

Ton QV and Iovine MK. 2013. Identification of an evx1-dependent joint-formation pathway during FIN regeneration. PLoS One 8(11):e81240.

Tu S and Johnson SL. 2011. Fate restriction in the growing and regenerating zebrafish fin. Dev Cell 20(5):725-32.

Vagefi PA, Parekh J, Ascher NL, Roberts JP, Freise CE. 2011. Outcomes with split liver transplantation in 106 recipients: The university of california, san francisco, experience from 1993 to 2010. Arch Surg 146(9):1052-9.

van Impel A, Zhao Z, Hermkens DM, Roukens MG, Fischer JC, Peterson-Maduro J, Duckers H, Ober EA, Ingham PW, Schulte-Merker S. 2014. Divergence of zebrafish and mouse lymphatic cell fate specification pathways. Development 141(6):1228-38.

Varjosalo M, Li SP, Taipale J. 2006. Divergence of hedgehog signal transduction mechanism between drosophila and mammals. Dev Cell 10(2):177-86.

Vettori A, Bergamin G, Moro E, Vazza G, Polo G, Tiso N, Argenton F, Mostacciuolo ML. 2011. Developmental defects and neuromuscular alterations due to mitofusin 2 gene (MFN2) silencing in zebrafish: A new model for charcot-marie-tooth type 2A neuropathy. Neuromuscul Disord 21(1):58-67.

Villavicencio-Lorini P, Kuss P, Friedrich J, Haupt J, Farooq M, Turkmen S, Duboule D, Hecht J, Mundlos S. 2010. Homeobox genes d11-d13 and a13 control mouse autopod cortical bone and joint formation. J Clin Invest 120(6):1994-2004.

Vortkamp A, Lee K, Lanske B, Segre GV, Kronenberg HM, Tabin CJ. 1996. Regulation of rate of cartilage differentiation by indian hedgehog and PTH-related protein. Science 273(5275):613-22.

Wagner GP and Misof BY. 1992. Evolutionary modification of regenerative capability in vertebrates: A comparative study on teleost pectoral fin regeneration. J Exp Zool 261(1):62-78.

Wehner D and Weidinger G. 2015. Signaling networks organizing regenerative growth of the zebrafish fin. Trends Genet 31(6):336-43.

Wehner D, Cizelsky W, Vasudevaro MD, Ozhan G, Haase C, Kagermeier-Schenk B, Roder A, Dorsky RI, Moro E, Argenton F, et al. 2014. Wnt/beta-catenin signaling defines organizing centers that orchestrate growth and differentiation of the regenerating zebrafish caudal fin. Cell Rep 6(3):467-81.

Welten MC, de Haan SB, van den Boogert N, Noordermeer JN, Lamers GE, Spaink HP, Meijer AH, Verbeek FJ. 2006. ZebraFISH: Fluorescent in situ hybridization protocol and three-dimensional imaging of gene expression patterns. Zebrafish 3(4):465-76.

Westerfield M. 1995. The Zebrafish Book: A Guide for the Laboratory Use of Zebrafish (Brachydanio rerio). Eugene, OR: University of Oregon Press.

Westerfield, M. (2000). The Zebrafish Book: A Guide for the Laboratory Use of Zebrafish (Brachydanio rerio). Univ. of Oregon Press, Eugene, OR

White JA, Boffa MB, Jones B, Petkovich M. 1994. A zebrafish retinoic acid receptor expressed in the regenerating caudal fin. Development 120(7):1861-72.

Whitehead GG, Makino S, Lien CL, Keating MT. 2005. Fgf20 is essential for initiating zebrafish fin regeneration. Science 310(5756):1957-60.

Widelitz RB, Jiang TX, Lu J, Chuong CM. 2000. Beta-catenin in epithelial morphogenesis: Conversion of part of avian foot scales into feather buds with a mutated beta-catenin. Dev Biol 219(1):98-114.

Wiley ML, Collette BB. 1970. Breeding tubercles and contact organs in fishes: Their occurrence, structure, and significance. Bull. h e r . Mus. Nat. Hist. 143, 147-216.

Williams MR, Dawood T, Ling S, Dai A, Lew R, Myles K, Funder JW, Sudhir K, Komesaroff PA. 2004. Dehydroepiandrosterone increases endothelial cell proliferation in

vitro and improves endothelial function in vivo by mechanisms independent of androgen and estrogen receptors. J Clin Endocrinol Metab 89(9):4708-15.

Wilson C, Bellen HJ, Gehring WJ. 1990. Position effects on eukaryotic gene expression. Annu Rev Cell Biol 6:679-714.

Wood JM, Bold G, Buchdunger E, Cozens R, Ferrari S, Frei J, Hofmann F, Mestan J, Mett H, O'Reilly T, et al. 2000. PTK787/ZK 222584, a novel and potent inhibitor of vascular endothelial growth factor receptor tyrosine kinases, impairs vascular endothelial growth factor-induced responses and tumor growth after oral administration. Cancer Res 60(8):2178-89.

Yamamoto T and Kajishima T. 1968. Sex hormone induction of sex reversal in the goldfish and evidence for male heterogamity. J Exp Zool 168(2):215-21.

Yan YL, Bhattacharya P, He XJ, Ponugoti B, Marquardt B, Layman J, Grunloh M, Postlethwait JH, Rubin DA. 2012. Duplicated zebrafish co-orthologs of parathyroid hormone-related peptide (PTHrP, pthlh) play different roles in craniofacial skeletogenesis. J Endocrinol 214(3):421-35.

Yanik MF, Cinar H, Cinar HN, Chisholm AD, Jin Y, Ben-Yakar A. 2004. Neurosurgery: Functional regeneration after laser axotomy. Nature 432(7019):822.

Yates A, Akanni W, Amode MR, Barrell D, Billis K, Carvalho-Silva D, Cummins C, Clapham P, Fitzgerald S, et al. Ensembl 2016. Nucleic Acids Res. 2016 44 Database issue: D710-6. PubMed PMID: 26687719; PubMed CentralPMCID: PMC4702834.

Yokoyama Ho, Wilson Me, Tsuboi Kk, Stowell Re. 1953. Regeneration of mouse liver after partial hepatectomy. Cancer Res 13(1):80-5.

Yoshizato K. 2007. Growth potential of adult hepatocytes in mammals: Highly replicative small hepatocytes with liver progenitor-like traits. Dev Growth Differ 49(2):171-84.

Yossa R, Sarker PK, Proulx E, Saxena V, Ekker M, Vandenberg GW. A practical approach for sexing zebrafish, Danio rerio. J Appl Aquacult 2013;25:148–153.

Zakany J, Kmita M, Alarcon P, de la Pompa JL, Duboule D. 2001. Localized and transient transcription of hox genes suggests a link between patterning and the segmentation clock. Cell 106(2):207-17.

Zerucha T, Stuhmer T, Hatch G, Park BK, Long Q, Yu G, Gambarotta A, Schultz JR, Rubenstein JL, Ekker M. 2000. A highly conserved enhancer in the Dlx5/Dlx6 intergenic region is the site of cross-regulatory interactions between dlx genes in the embryonic forebrain. J Neurosci 20(2):709-21.

Zhang J, Jeradi S, Strahle U, Akimenko MA. 2012. Laser ablation of the sonic hedgehog-a-expressing cells during fin regeneration affects ray branching morphogenesis. Dev Biol 365(2):424-33.

Zhang Y, Buchholz F, Muyrers JP, Stewart AF. 1998. A new logic for DNA engineering using recombination in escherichia coli. Nat Genet 20(2):123-8.

Zhang D, Popesku JT, Martyniuk CJ, Xiong H, Duarte-Guterman P, Yao L, Xia X, Trudeau VL. 2009. Profiling neuroendocrine gene expression changes following fadrozole-induced estrogen decline in the female goldfish. Physiol Genomics 38(3):351-61.

Zhang J, Wagh P, Guay D, Sanchez-Pulido L, Padhi BK, Korzh V, Andrade-Navarro MA, Akimenko MA. 2010. Loss of fish actinotrichia proteins and the fin-to-limb transition. Nature 466(7303):234-7.

Zhao Q, Brauer PR, Xiao L, McGuire MH, Yee JA. 2002. Expression of parathyroid hormone-related peptide (PthrP) and its receptor (PTH1R) during the histogenesis of cartilage and bone in the chicken mandibular process. J Anat 201(2):137-51.

Zhu X, Ling J, Zhang L, Pi W, Wu M, Tuan D. 2007. A facilitated tracking and transcription mechanism of long-range enhancer function. Nucleic Acids Res 35(16):5532-44.